
Supplementary information

Geminal-atom catalysis for cross-coupling

In the format provided by the
authors and unedited

Supplementary information for

Geminal atom catalysis for cross-coupling

Xiao Hai^{1,10}, Yang Zheng^{1,10}, Qi Yu^{2,10}, Na Guo^{3,4,10}, Shibo Xi^{5}, Xiaoxu Zhao⁶, Sharon Mitchell⁷, Xiaohua Luo¹, Victor Tulus⁷, Mu Wang¹, Xiaoyu Sheng¹, Longbin Ren¹, Xiangdong Long¹, Jing Li¹, Peng He¹, Huihui Lin¹, Yige Cui¹, Xinnan Peng¹, Jiwei Shi¹, Jie Wu¹, Chun Zhang^{1,3,4}, Ruqiang Zou⁶, Gonzalo Guillén-Gosálbez⁷, Javier Pérez-Ramírez^{7*}, Ming Joo Koh^{1*}, Ye Zhu^{1*}, Jun Li^{8,9*} and Jiong Lu^{1*}*

¹Department of Chemistry, National University of Singapore, 3 Science Drive 3, Singapore 117543, Singapore.

²School of Materials Science and Engineering and Shaanxi Key Laboratory of Catalysis, Shaanxi University of Technology, Hanzhong 723001, China.

³National University of Singapore Chongqing Research Institute, Chongqing 401123, China.

⁴Department of Physics, National University of Singapore, 2 Science Drive 3, Singapore 117551, Singapore.

⁵Institute of Sustainability for Chemicals, Energy and Environment (ISCE2), Agency for Science, Technology and Research (A*STAR), 1 Pesek Road Jurong Island, Singapore 627833, Singapore.

⁶School of Materials Science and Engineering, Peking University, Beijing 100871, China.

⁷Institute for Chemical and Bioengineering, Department of Chemistry and Applied Biosciences, ETH Zurich, Zurich, Switzerland.

⁸Department of Chemistry and Engineering Research Center of Advanced Rare-Earth Materials of Ministry of Education, Tsinghua University, Beijing 100084, China.

⁹Department of Chemistry and Guangdong Provincial Key Laboratory of Catalytic Chemistry, Southern University of Science and Technology, Shenzhen 518055, China.

¹⁰These authors contributed equally: Xiao Hai, Yang Zheng, Qi Yu, Na Guo.

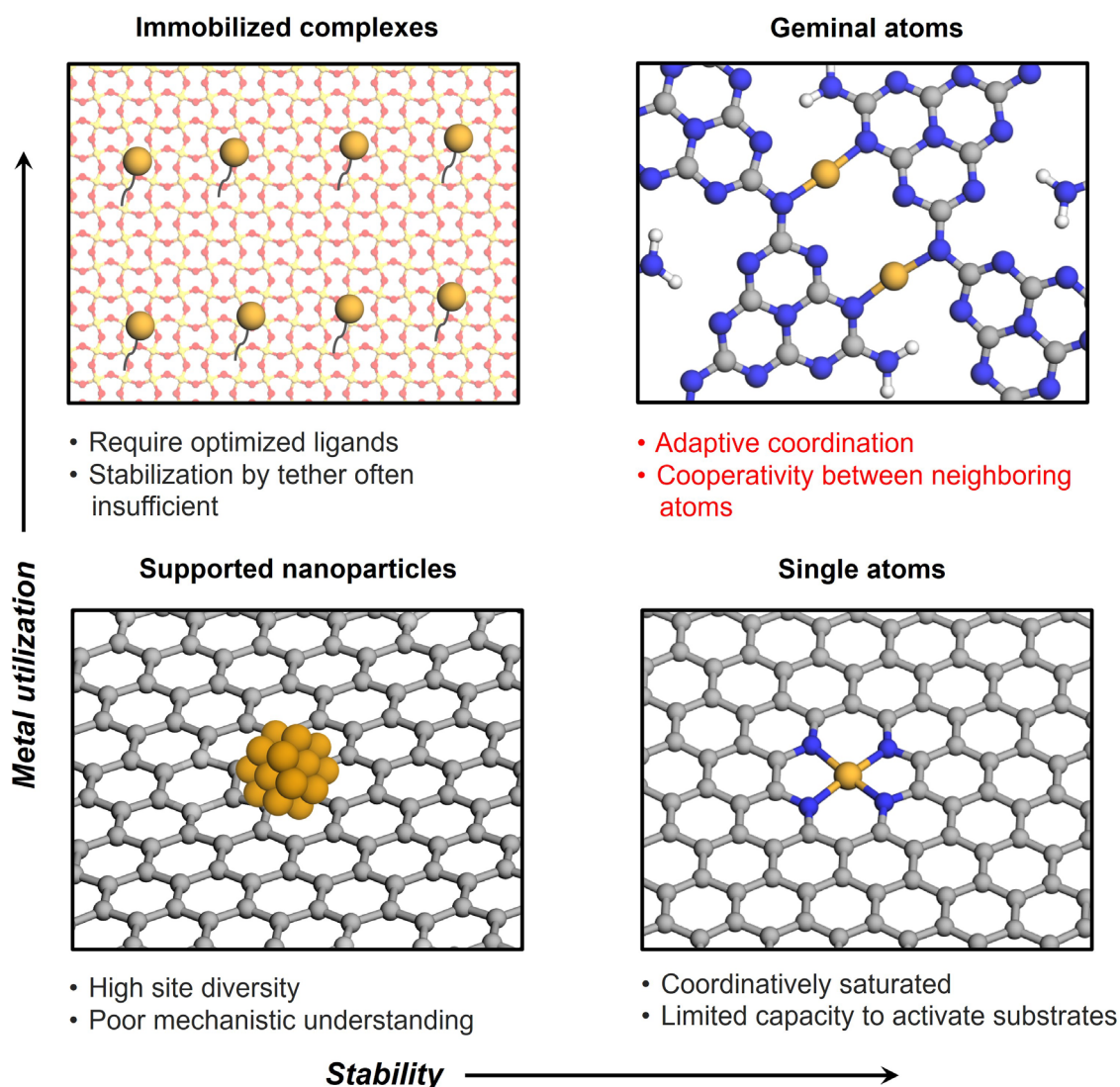
*Corresponding author. Email: xi_shibo@partner.nus.edu.sg; jpr@chem.ethz.ch; chmkmj@nus.edu.sg; chmzhu@nus.edu.sg; junli@tsinghua.edu.cn; chmluj@nus.edu.sg

Table of Contents

Supplementary Figures 1-23

Supplementary Tables 1-7

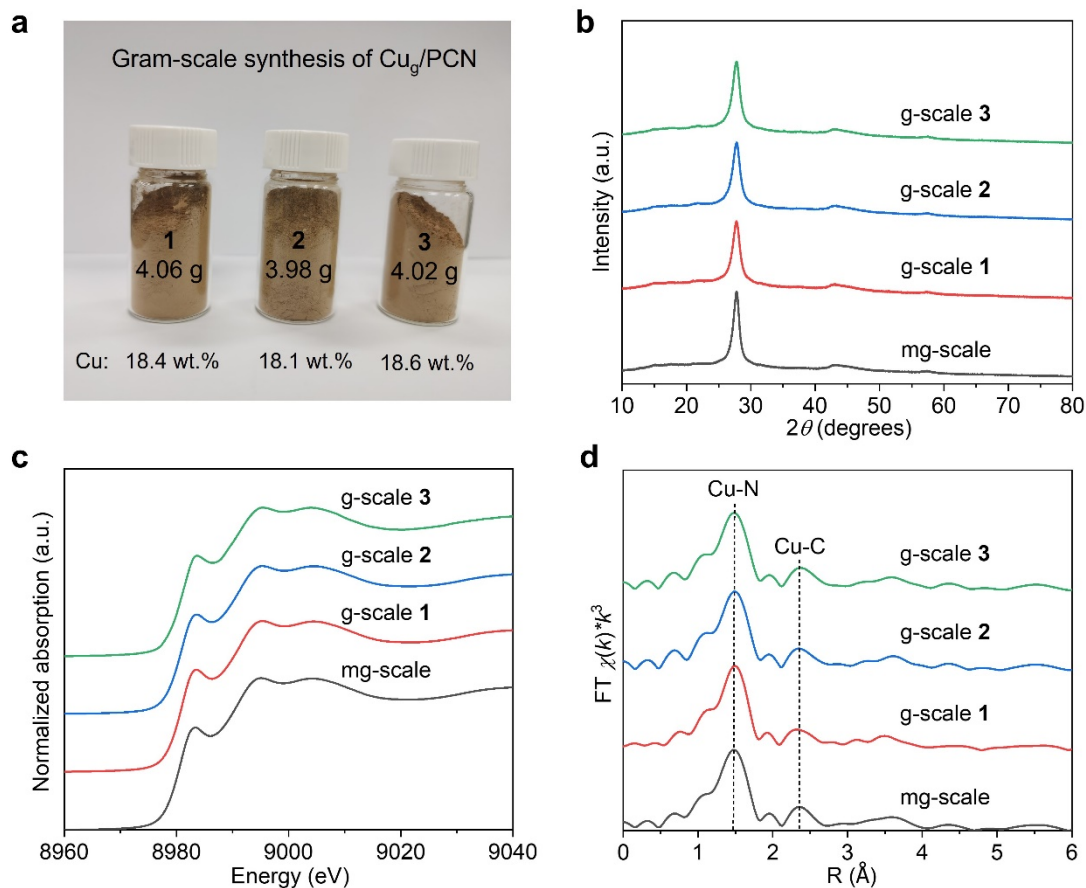
NMR data



Supplementary Fig. 1 | Design principles of geminal-atom catalysis, illustrating how they overcome the limitations of previously reported heterogeneous copper catalysts for organic synthesis to deliver high specific metal utilization and stability.

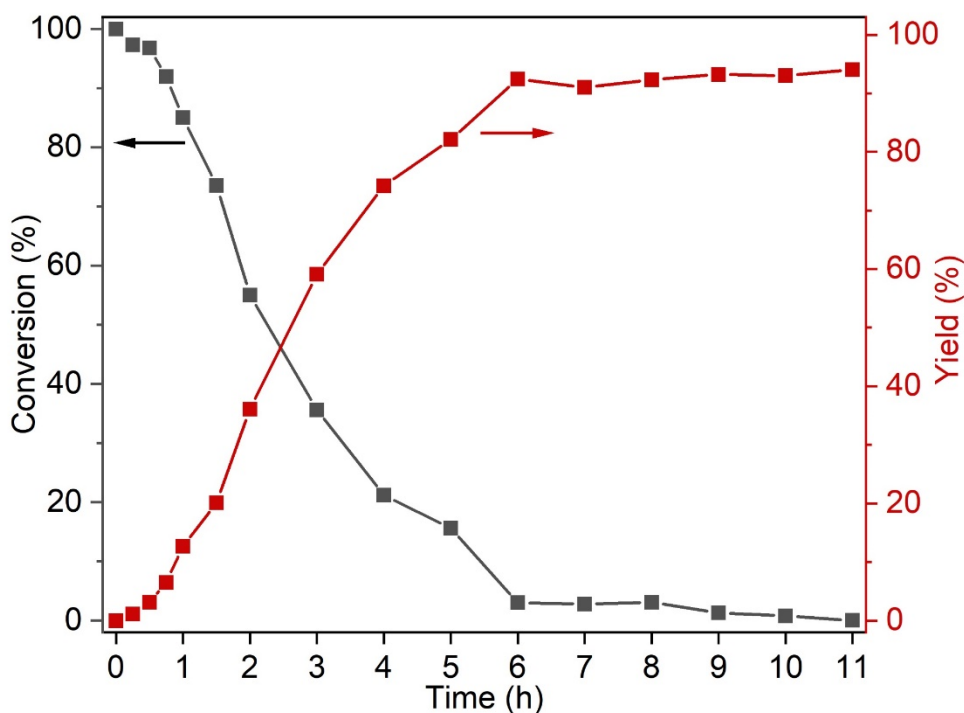
Due to the potential operational and sustainability advances that could be achieved using heterogeneous catalytic systems, many researchers have studied the performance of nanostructured copper catalysts (e.g., supported metallic or oxidic Cu clusters or nanoparticles, immobilized Cu complexes, and Cu-containing metal-organic frameworks (MOFs) or zeolites) in cross-coupling applications¹⁻¹¹. However, despite the fact that some materials have been commercialized, all of these classes of catalyst have intrinsic limitations that hinder their broad industrial application¹². Specifically, supported Cu-based clusters or nanoparticles may contain

inaccessible metal atoms in the bulk of the structure leading to poor metal utilization, furthermore the lack of atomic control in their structure and resulting diversity of active sites limits their selectivity and also makes it very challenging to understand the reaction mechanism. Since Cu atoms in extended metal surfaces may strongly interact with reaction intermediates and ligands in coupling applications high levels of metal leaching are common, which has triggered extensive debate over whether the observed performance is heterogeneously or homogeneously catalysed. Cu-based MOFs and zeolites have intrinsic problems associated with poor accessibility of active sites within microporous channels, high costs of the support materials, and strong adsorption of organic components in the case of zeolites and poor structural stability in the case of MOFs. Immobilized metal complexes operate under a similar principle to organometallic complexes, meaning that the ligands in the structure are removed and replaced during the catalytic cycle. This implies that the metal centres can have a very low coordination number to the solid carrier and therefore a high tendency to leach into the reaction mixture. Heterogeneous single-atom catalysts (SACs) with well-defined metal sites have attracted growing attention due to their potential to bridge homogeneous and heterogeneous catalysis for fine chemical production^{13,14}. While the strong interaction between single-metal centres and the carrier necessary to prevent metal detachment or aggregation typically require high coordination numbers, rendering them inactive because of their limited capacity to activate multiple substrates simultaneously. These limitations call for technology innovation in the design and synthesis of new efficient heterogeneous catalysts that are active enough but also stable against leaching for organic coupling reactions. Toward this goal, a new class of heterogeneous geminal-atom catalysts (GACs), consisting of pairs of regularly separated low-valence single-atom metal sites was developed, aims to provide a powerful, economically-vital generalized platform to solve the longstanding reactivity challenge beyond conventional cross-coupling protocols, enabling us to implement environmentally benign organic synthesis by adjusting the nature and combination of the geminal metals to promote industrially-crucial coupling reactions.



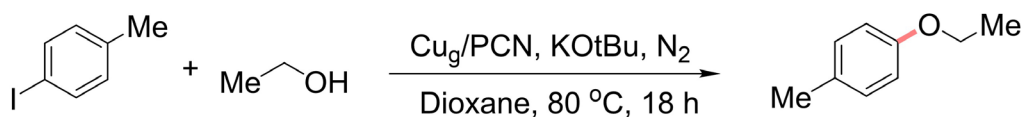
Supplementary Fig. 2 | Photos (a), XRD patterns (b), Cu K-edge XANES (c) and Fourier-transformed EXAFS spectra (d) of three independent batches of Cu_g/PCN prepared in gram scale.

Experimental procedure for each batch of preparation conditions: CuCl₂ (3.2 g) and PCN (3.5 g) were dispersed in 1000 ml formamide, sonicated for 10 min then stirred in an oil bath (120 °C) for 12 h, following centrifugation and washing thoroughly by ethanol several times. The oven-dried powder (80 °C) was subsequently heated to 500 °C with a heating rate of 2 °C min⁻¹ and kept for 5 h with the protection of N₂ flow.



Supplementary Fig. 3 | Reaction profile of Cu_g/PCN catalyzed C-O bonding formation.

In a nitrogen-filled glovebox, 11 oven-dried screw-top reaction tubes were equipped with a magnetic stir bar. 4-Iodotoluene (0.2 mmol × 11, 479.7 mg), *n*-butanol (0.4 mmol × 11, 326.1 mg), Potassium tert-butoxide (KO^tBu, 0.3 mmol × 11, 370.3mg), decane (0.2 mmol × 11, 313.0 mg) and anhydrous dioxane (2.0 mL × 11) were sequentially added. Then shaking the mixture to make the homogeneous solution. Subsequently, Cu_g/PCN (4.0 mg) was weighed individually for every single tube. After that, we used the injector to transfer the aforementioned homogeneous solution to the 11 reaction tubes with 2 mL amount for each one. The reaction tubes were sealed with a Teflon-lined screw cap, removed from the glovebox, placed in an oil bath preheated to 80 °C for the indicated time. After cooling to rt, the reaction cap was removed. An aliquot of the solution was transferred into a GC vial and diluted with EtOAc. GC analysis was used for determination of the conversion and yield.



120 mmol scale, 87% yield

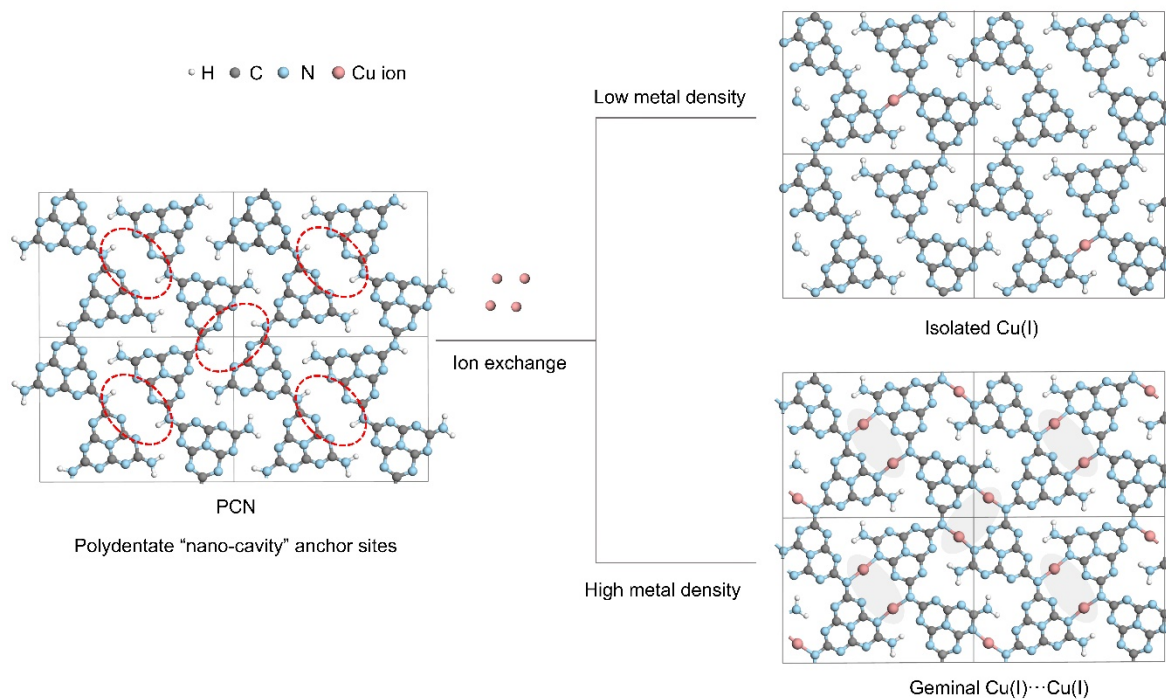
4-iodotoluene (120 mmol), ethanol (240 mmol), Cu_g/PCN (600 mg), KOtBu (180 mmol), anhydrous dioxane (1200 mL), 80 °C, 18 h.



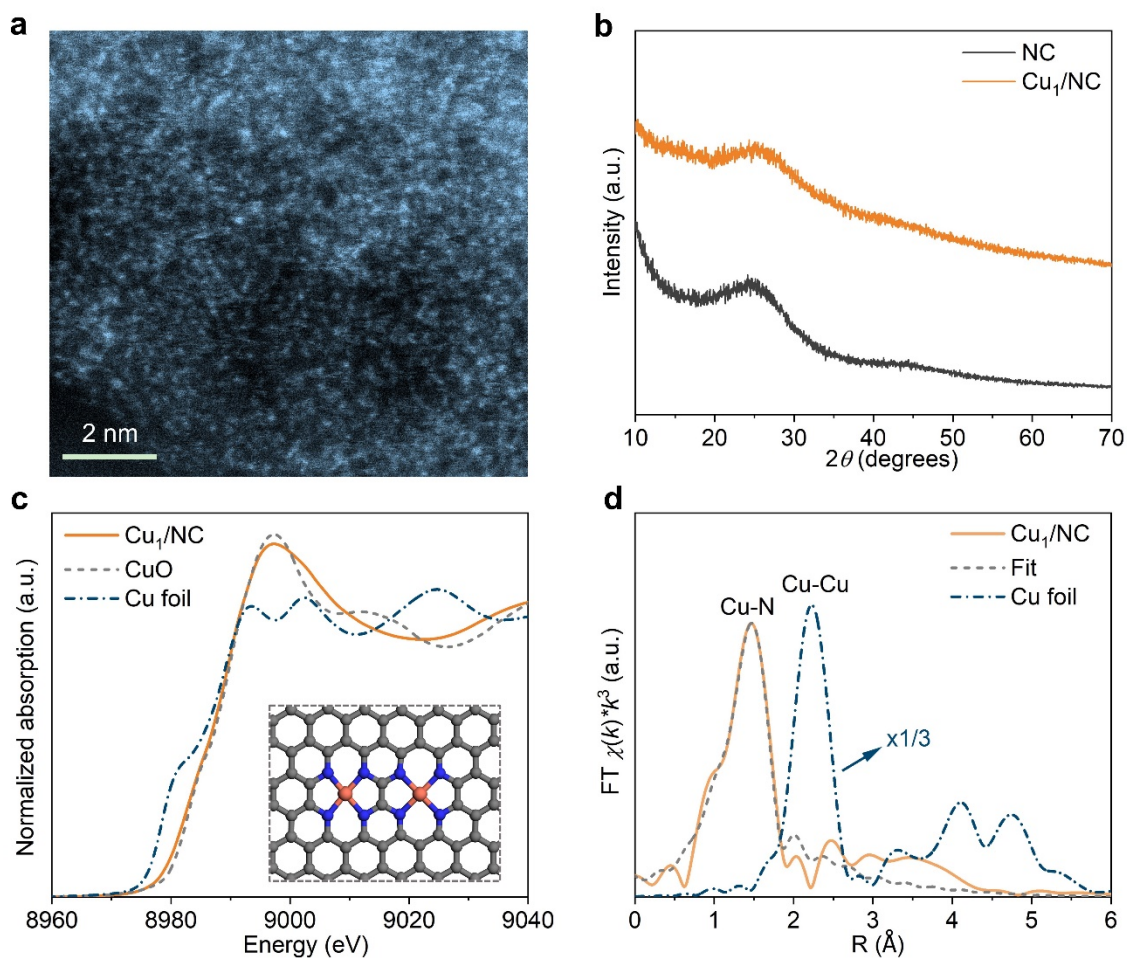
14.20 g
p-ethoxytoluene

Supplementary Fig. 4 | Cu_g/PCN catalyzed *p*-ethoxytoluene synthesis in multi-gram scale.

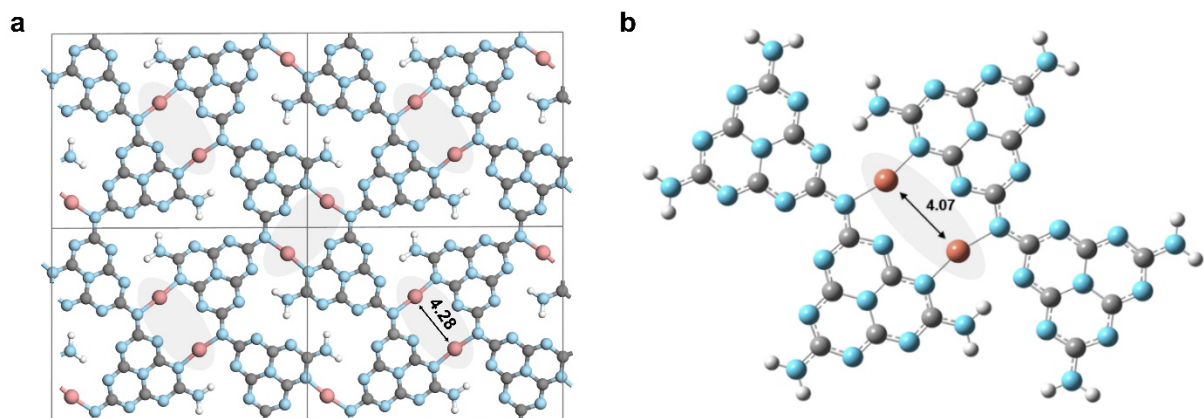
Experimental procedure for multi-gram synthesis of *p*-ethoxytoluene: In a nitrogen-filled glovebox, the aryl iodide (120 mmol), alcohol (240 mmol), Cu_g/PCN (600 mg, 1.4 mol% Cu), KOtBu (180 mmol) and anhydrous dioxane (1200 mL) were sequentially added to an oven-dried screw-top reaction bottle equipped with a stir bar. The reaction bottle was sealed with a Teflon-lined screw cap, removed from the glovebox, placed in an oil bath preheated to 80 °C and stirred for 18 h. After cooling to room temperature (rt), the cap was removed, and the reaction mixture was concentrated in vacuo with the aid of a rotary evaporator. The resulting residue was then purified by silica gel column chromatography to obtain the pure product.



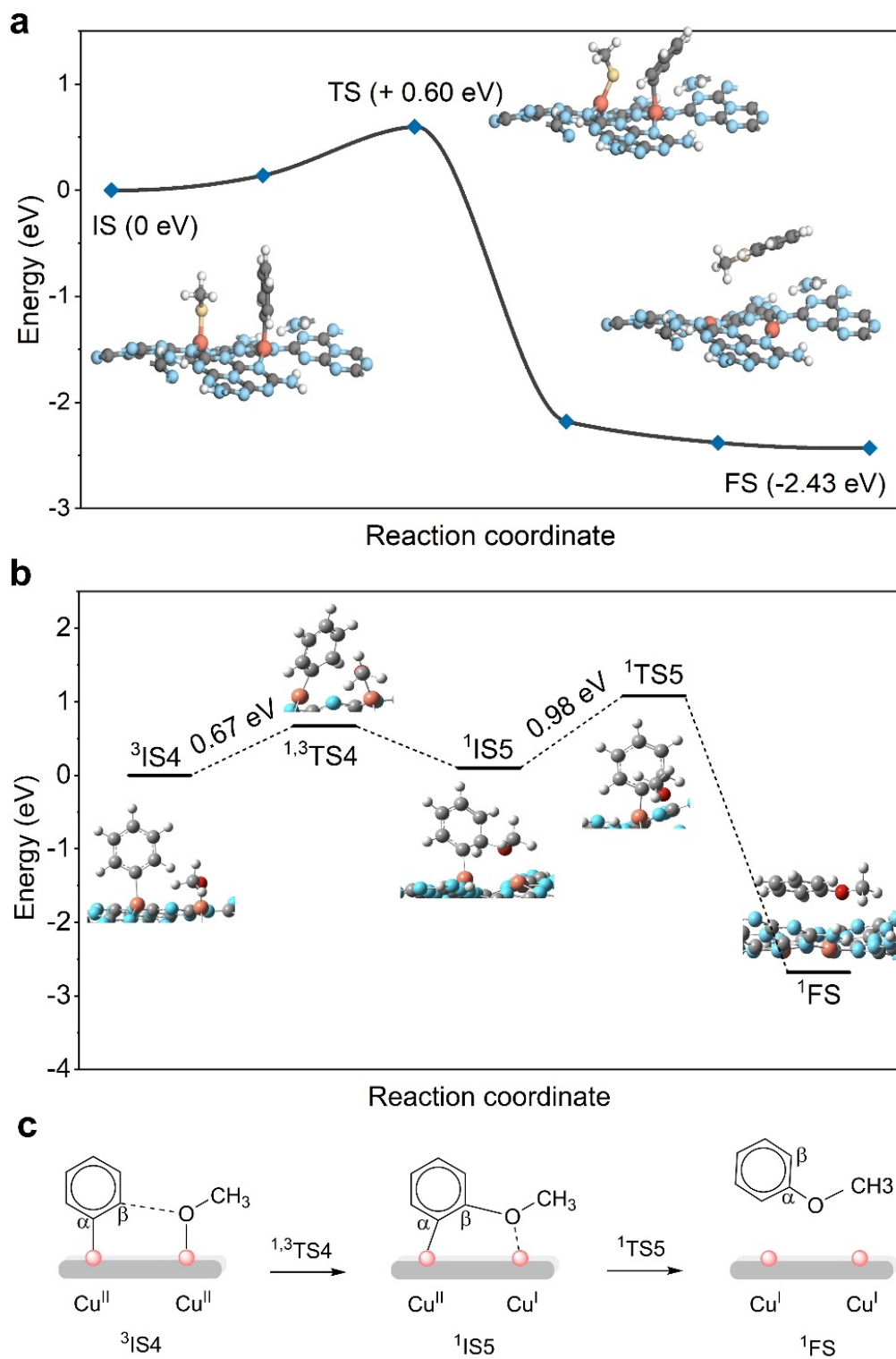
Supplementary Fig. 5 | Strategy for preparing Cu_1/PCN (SACs) and Cu_g/PCN (GACs) based on the periodic crystal structure of the PCN host.



Supplementary Fig. 6 | Characterization of ultra-high-density Cu_1/NC . **a**, ADF-STEM image evidences the high density of Cu single atoms. **b**, XRD patterns of NC and Cu_1/NC . Cu K-edge **c**, Cu K-edge XANES (the atomic structure is shown inset, colour code: C, grey; N, blue; Cu, orange.) and **d**, Fourier-transformed EXAFS spectra of Cu_1/NC . Cu_1/NC was synthesized following our previously developed two-step annealing method (*Nat. Nanotechnol.* **17**, 174-181 (2022)).

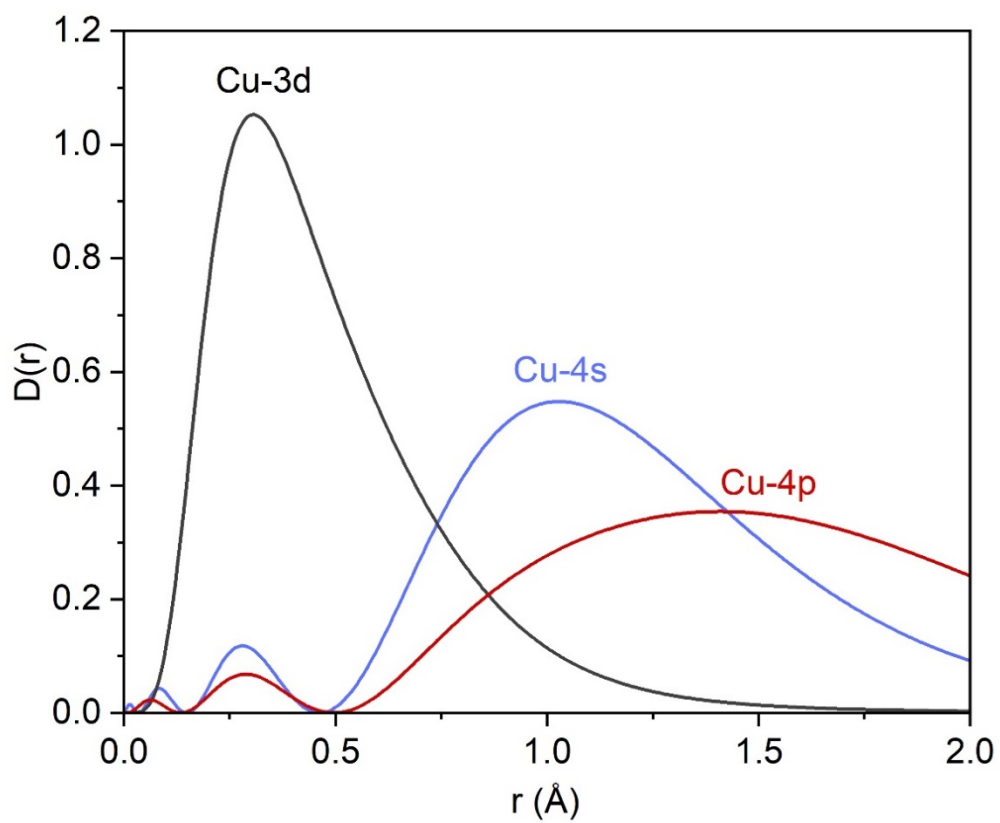


Supplementary Fig. 7 | The geometric structure of the Cu_g/PCN. **a**, The periodic structure optimized from VASP code. **b**, The cluster model used in the molecular DFT calculations. Colour code: Cu, orange; C, grey; N, blue; H, white.

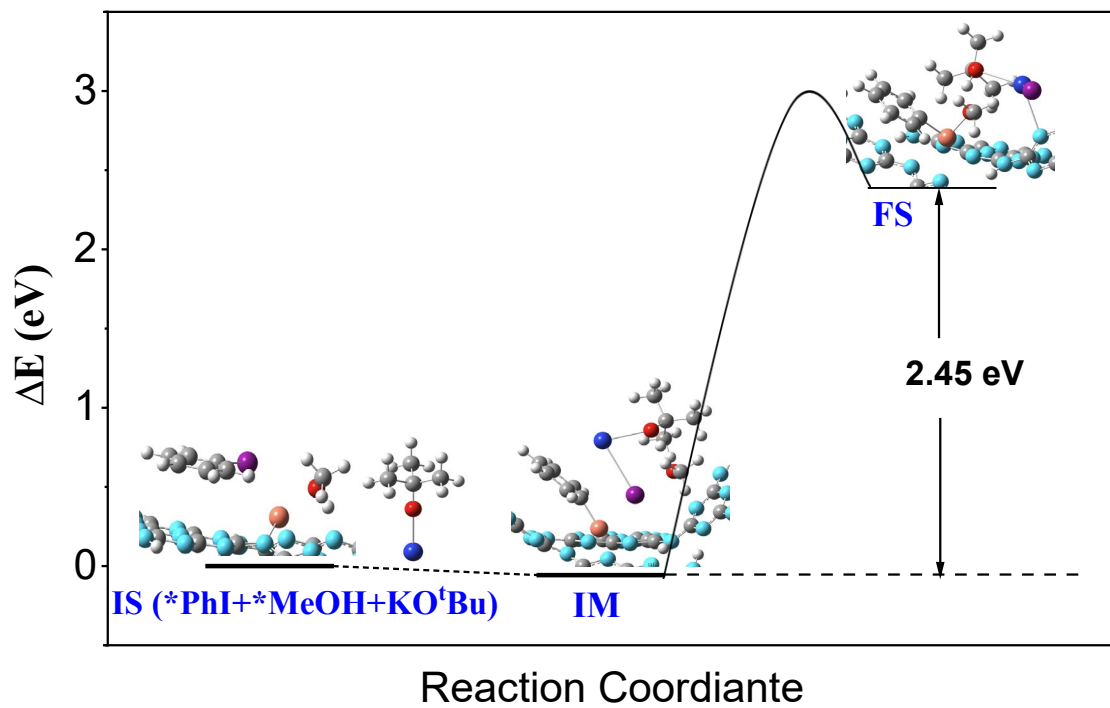


Supplementary Fig. 8 | Indirect C-O coupling of CH_3O and C_6H_5 to form $C_6H_5OCH_3$ by periodic (a) and molecular (b) DFT modelling over Cu_g/PCN with the corresponding schematic structures of the intermediates (c).

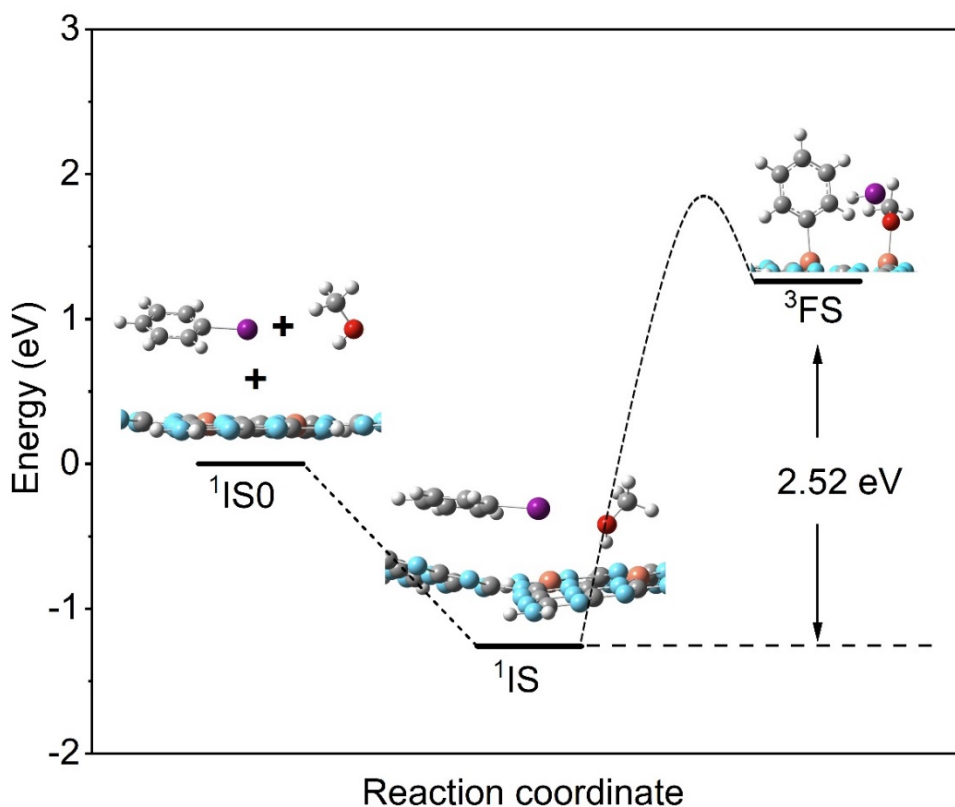
As the Cu...Cu distance is almost 4 Å, direct C-O coupling is unlikely due to the large separation of *OCH₃ and *C₆H₅. Therefore, an indirect C-O coupling pathway was initially considered. In this pathway, the OCH₃ bonded with Cu_B will approach the near-by β-position carbon atom of *C₆H₅, and it will then migrate to the α-position carbon atom. Here α-position carbon atom denotes the carbon atom of *C₆H₅ directly bonded with Cu_A(II), and the β-position carbon atom is its nearest-neighbour in the benzene ring. It turns out that this indirect pathway is rather difficult because it involves a spin-forbidden reaction (³IS₄ → ¹IS₅) and a high barrier for ¹IS₅ → ¹TS₅ (0.98 eV).



Supplementary Fig. 9 |The radial distribution probability density ($D(r) = r^2R(r)^2$) of Cu (II) atomic orbitals (AOs).

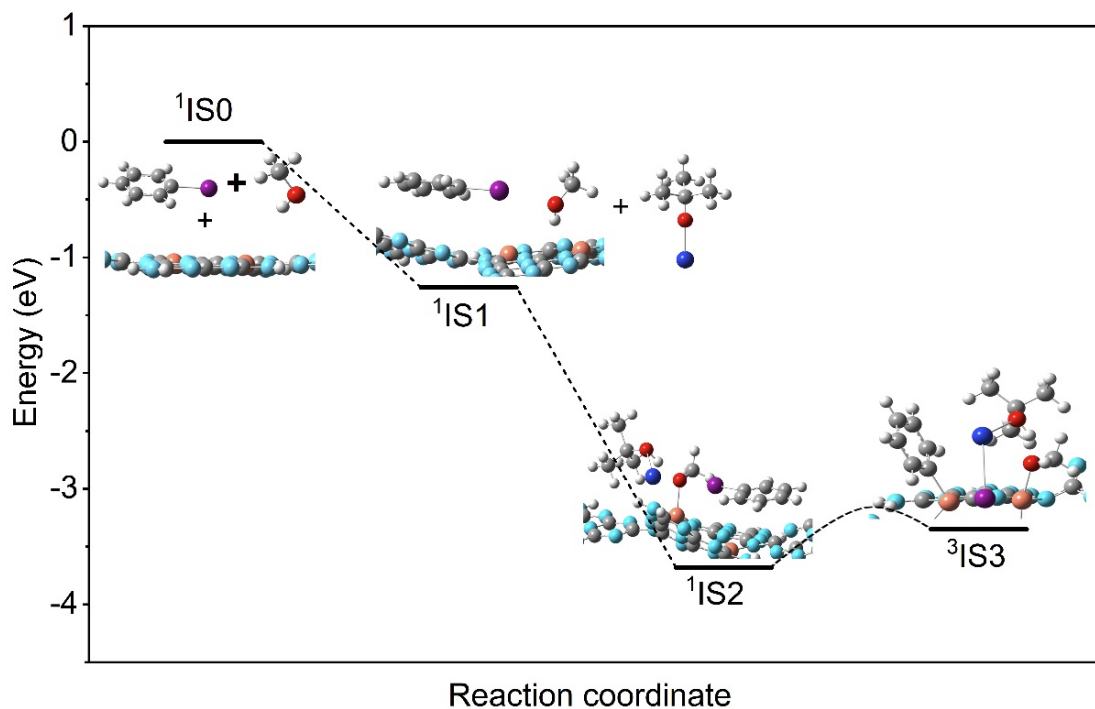


Supplementary Fig. 10 | The calculated energy profiles for C-O bond formation catalyzed by isolated single-atom. Colour code: C, grey; N, cyan; Cu, orange; O, red; H, white; I, purple.



Supplementary Fig. 11 | Reaction energy profile for direct dehalogenation and dehydrogenation of C₆H₅I and CH₃OH into *C₆H₅ + CH₃O* + HI without assistance of the base. Colour code: C, grey; N, cyan; Cu, orange; O, red; H, white; I, purple.

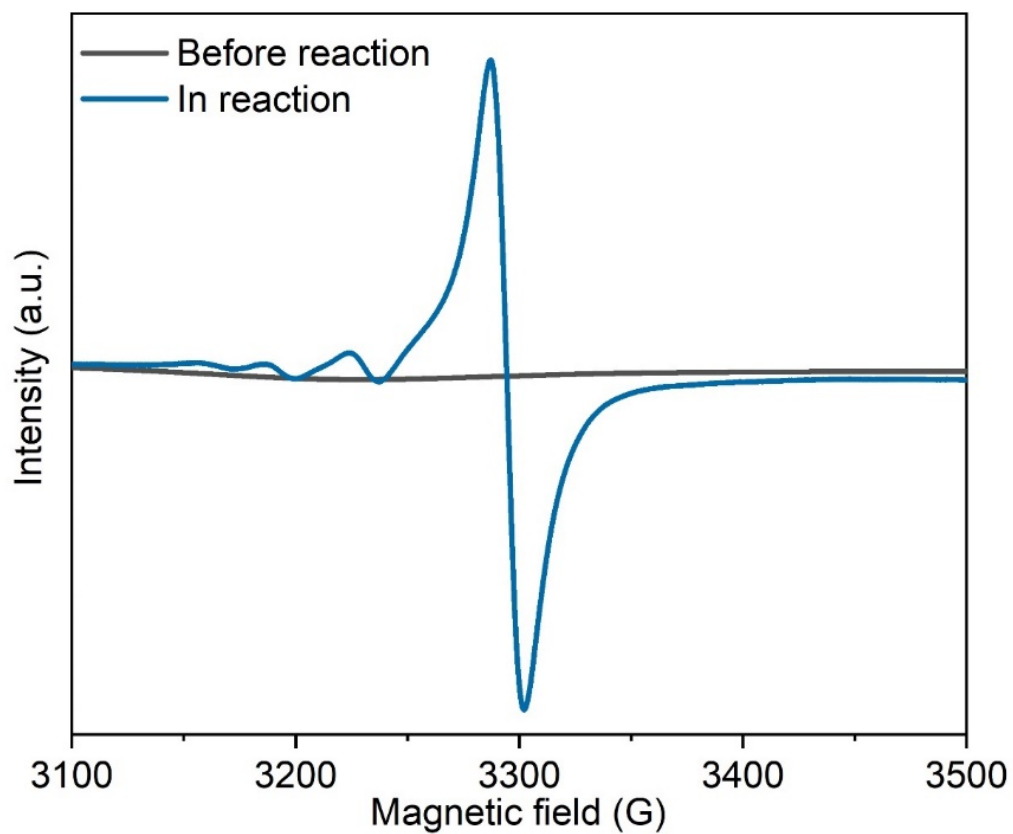
The calculations show that the co-adsorption of C₆H₅I and CH₃OH on two Cu(I) atoms has an adsorption energy of -1.27 eV (singlet $^1IS_0 \rightarrow$ singlet 1IS). However, the direct dehalogenation of C₆H₅I and dehydrogenation of CH₃OH to form HI and adsorbed *C₆H₅ and CH₃O* species on Cu(II) sites of the surface are strongly endothermic (2.52 eV), implying that it would have much higher reaction barrier. Note with direct bonding between C₆H₅ and CH₃O with copper, the Cu(I, d¹⁰)···Cu(I, d¹⁰) sites are converted into oxidized Cu(II, d⁹)···Cu(II, d⁹) sites. Therefore, the direct dehalogenation and dehydrogenation reaction from singlet 1IS to triplet 3FS_0 is a spin-forbidden reaction, and no attempt is made to determine its reaction barrier. This result agrees with the experimental fact that the reaction cannot occur without addition of strong base.



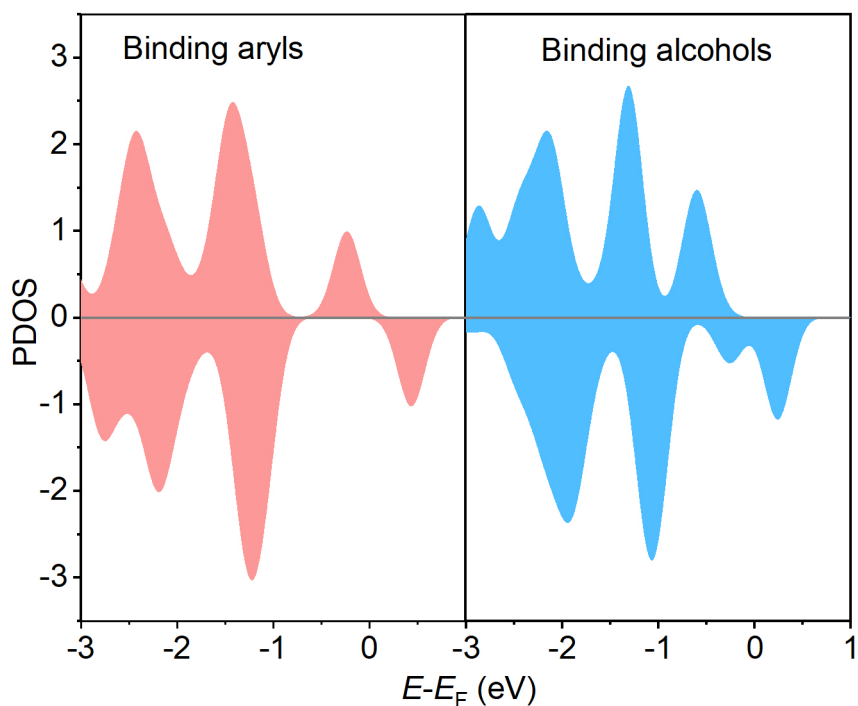
Supplementary Fig. 12 | Reaction energy profile for direct dehydrogenation CH_3OH by KO^tBu and subsequent dehalogenation of $\text{C}_6\text{H}_5\text{I}$ to form $\text{Cu(II)}^*\text{C}_6\text{H}_5 + \text{CH}_3\text{O}^*\text{Cu(II)}$ over Cu_g/PCN , with releasing KI and HO^tBu in solution. Colour code: C, grey; N, cyan; Cu, orange; O, red; H, white; I, purple; K, blue.

When a strong base like KO^tBu is added to the system, it will immediately deprotonate CH_3OH to form K^+OCH_3 and HO^tBu (singlet $^1\text{IS}_1 \rightarrow$ singlet $^1\text{IS}_2$), with an exothermicity of -2.41 eV. This process is rather easy because of the higher pKa of HO^tBu (17.0) compared to CH_3OH (15.5). The reaction between K^+OCH_3 and weakly adsorbed $\text{C}_6\text{H}_5\text{I}$ to form the KI salt and adsorbed $^*\text{C}_6\text{H}_5$ and CH_3O^* species on Cu(II) sites of the surface will be difficult again, as it involves another spin-forbidden reaction to form $\text{C}_6\text{H}_5\text{-Cu(II, } d^9)$ and $\text{Cu(II, } d^9)\text{-OCH}_3$. Although this process (singlet $^1\text{IS}_2 \rightarrow$ triplet $^3\text{IS}_3$) is only slightly endothermic (-0.33 eV), the reaction rate of this spin-forbidden reaction will be very low because singlet-to-triplet spin crossing is necessary via a relatively small spin-orbit coupling, which makes this process the rate-determining step (RDS) of the whole reaction. Indeed, experimentally, EPR measurements identified the formation of Cu(II) during the reaction. In addition, the crucial role of strong

base of KO^tBu and the experimentally observed reaction time of C₆H₅I < C₆H₅Br << C₆H₅Cl agrees with this computational result. It is worth mentioning that upon nucleation, the KI molecules will form KI solid deposit to drive the chemical equilibrium toward formation of triplet ³I₃ product.

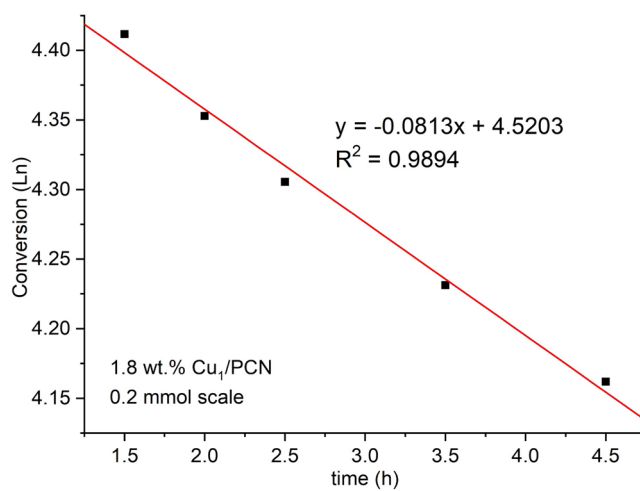
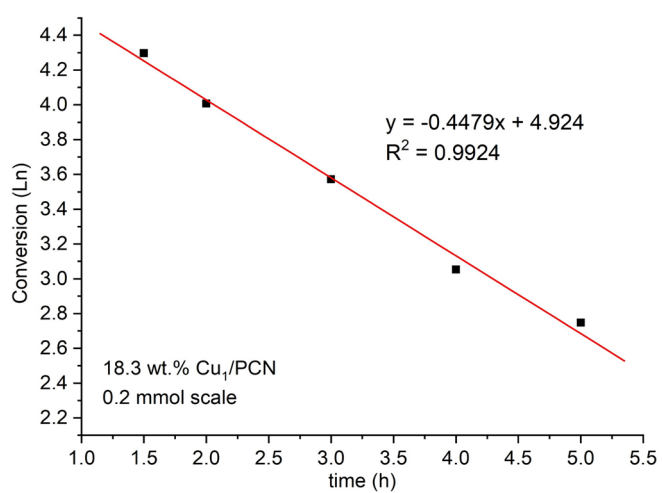
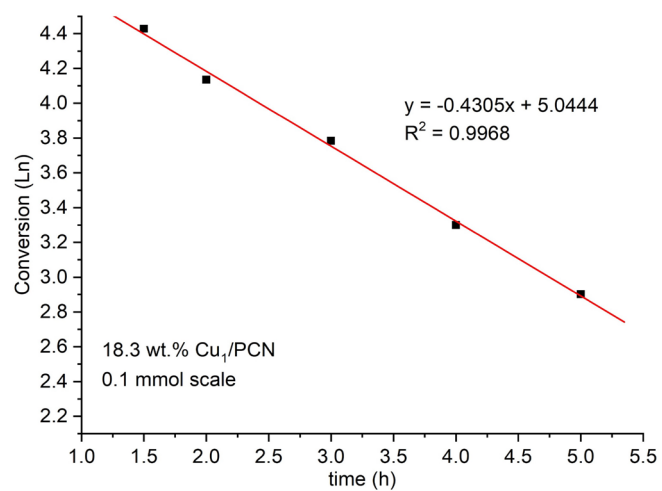


Supplementary Fig. 13 | EPR spectra of Cu_g/PCN measured under C-O coupling reaction conditions.



Supplementary Fig. 14 | Calculated PDOS of Cu sites in Cu_g/PCN bonding with aryl halide (4-iodobenzene) and alcohol (methanol), respectively.

Briefly, comparison of the PDOS in Cu_g/PCN before (**Extended Data Fig. 5d**) and after (**Supplementary Figure 14**) reactant adsorption indicates that the interaction with the reactants shifts the PDOS of the copper centres to higher energies, crossing the Fermi energy (E_F). This is because the copper atoms lose more electrons to the adsorbed reactants, as supported by the Bader charge analysis (**Supplementary Table 4**). Furthermore, the adsorption changed the non-spin polarized electronic states of copper to spin-polarized with an average magnetic momentum of $1 \mu_B/\text{Cu}$.

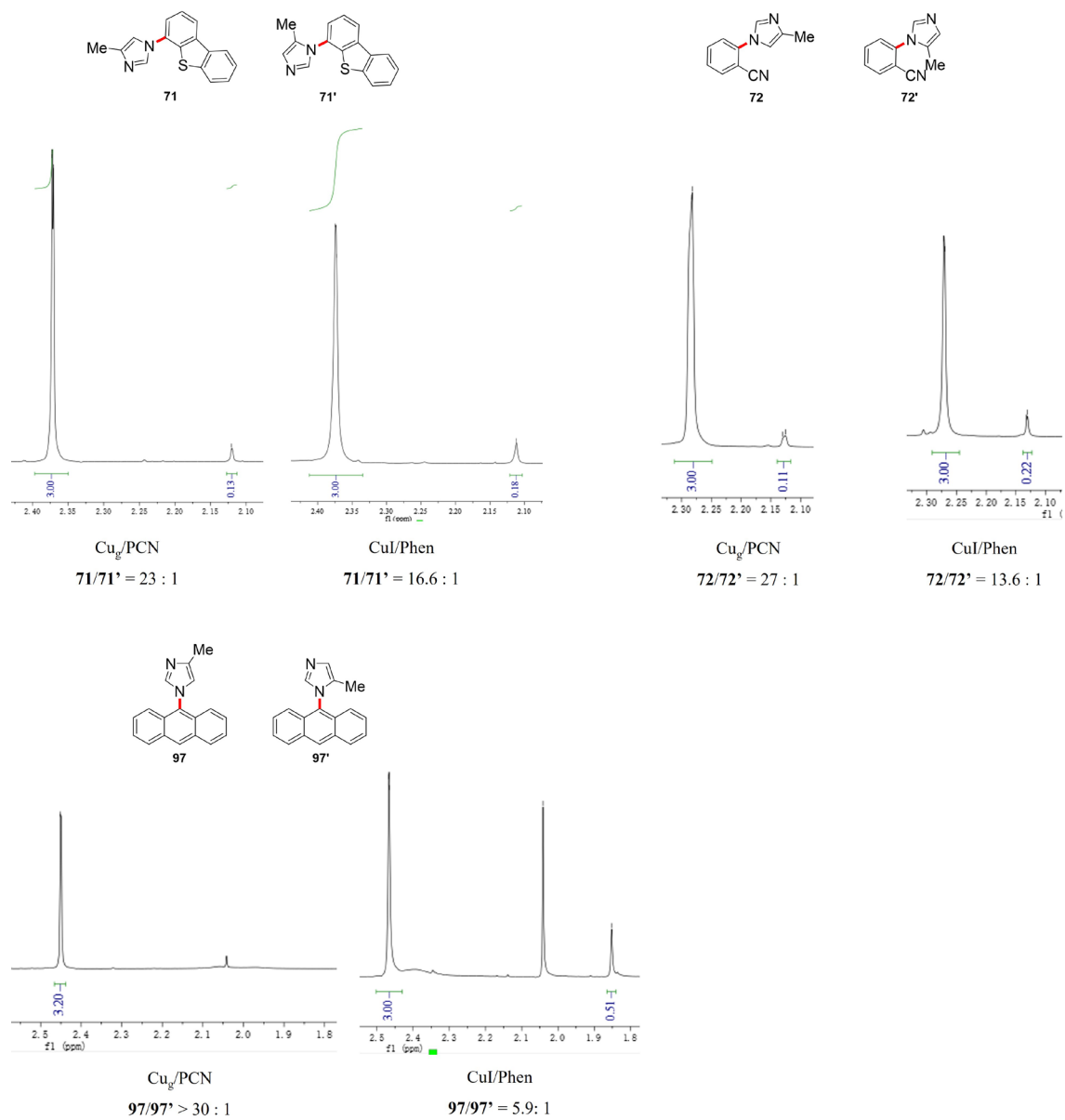


Supplementary Fig. 15 | Kinetic studies of Cu_I/PCN containing 18.3 wt.% (GAC) or 1.8 wt.% (SAC) Cu catalysed C-O bonding formation. The plots of the natural logarithm of the

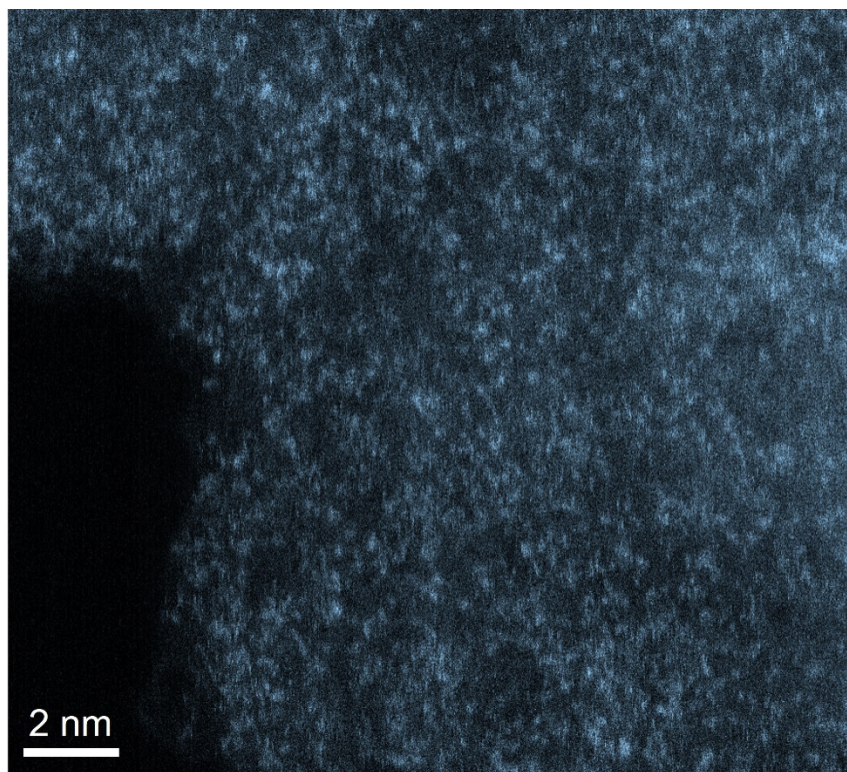
concentration of aryl halide versus time: initial concentration of aryl halide $C_0 = 0.05$ M (top left), $C_0 = 0.1$ M (top right and bottom). All reactions were conducted with 1.4 mol% Cu.

Experimental procedure: In an N_2 -filled glovebox, 1.4 mol.% of Cu_1/PCN (corresponding to 1.0 mg for 18.3 wt.% Cu_1/PCN or 10 mg for 1.8 wt.% Cu_1/PCN) was added to each of five oven-dried screw-top reaction tubes equipped with stir bars. Subsequently, a premixed stock solution containing 0.1 mmol ($C_0 = 0.05$ M) or 0.2 mmol ($C_0 = 0.1$ M) of 4-iodotoluene, 0.4 mmol *n*-butanol, 0.3 mmol KO t Bu, and 0.2 mmol decane (internal standard for GC analysis) in anhydrous dioxane (2.0 mL) was added to each reaction tube. The reaction tubes were sealed with Teflon-lined screw caps, removed from the glovebox, and placed in an oil bath preheated to 80 °C for the desired time (1-5 h). After cooling to rt, the reaction cap was removed. An aliquot of the solution was transferred into a vial, diluted with EtOAc, and the reactant conversion was analysed by gas chromatography.

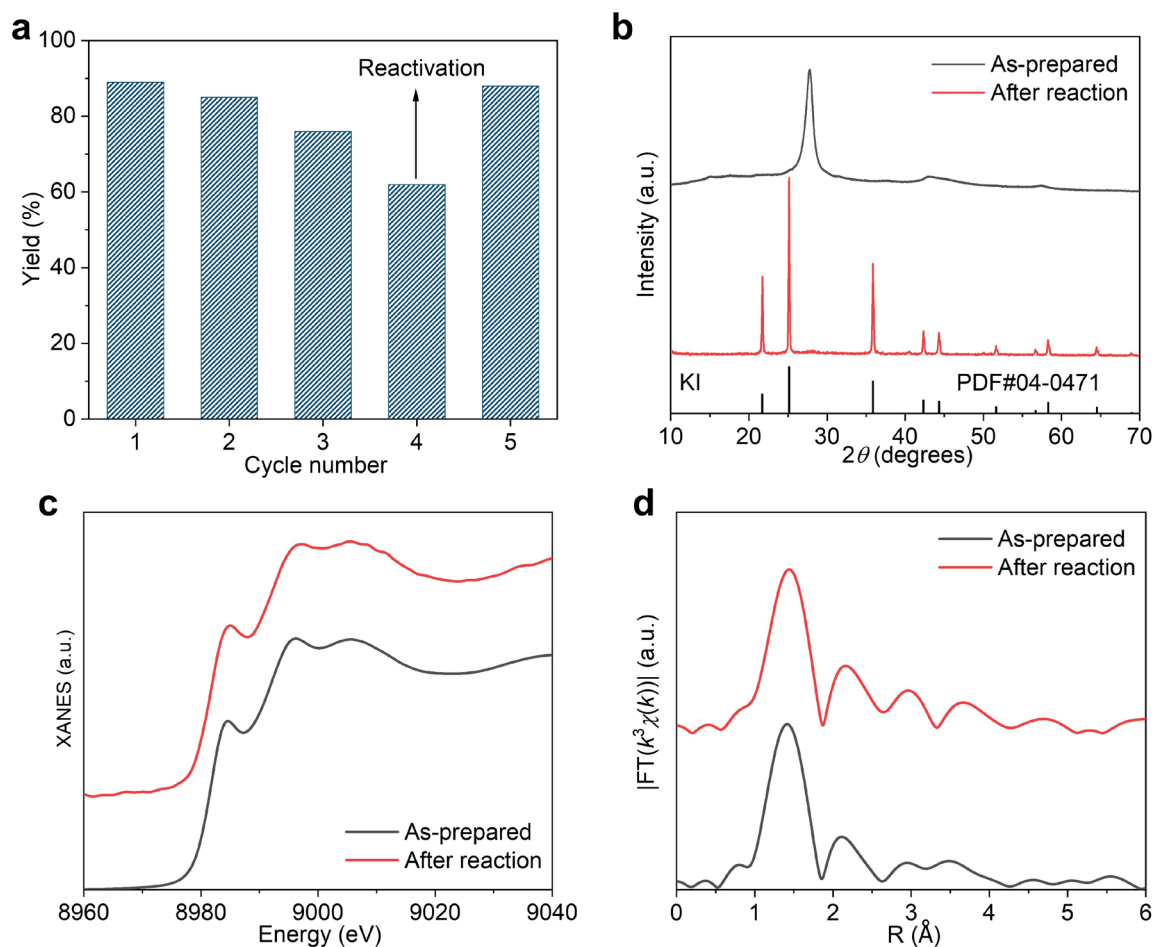
Under the optimized reaction conditions, the natural logarithm of the concentration of aryl halide versus time evidences a straight line, indicating that the reaction is first order in aryl halide. Consistently, the first-order rate constants ($-\text{slop}$, h^{-1}) at initial concentrations of 0.05 M or 0.1 M are very similar ($0.431 h^{-1}$ or $0.448 h^{-1}$, respectively) on a 1.4 mol% Cu basis over the Cu_g/PCN catalyst with 18.3 wt.% metal content. Therefore, the aryl halide likely participates in the rate-limiting step. This finding agrees with the computational studies, which predict the activation of 4-iodobenzene (from IS2 to IS3, see **Fig. 3c**) to be rate-limiting. In contrast, the reaction using the 1.8 wt.% Cu_1/PCN catalyst proceeded significantly slower than the 18.3 wt.% Cu_g/PCN catalyst, despite the equivalent amount of copper introduced in the reaction (1.4 mol%). Comparatively, the first-order rate constant was 5.5 times higher over the material containing 18.3 wt.% copper, consistent with the higher yield observed over this catalyst.



Supplementary Fig. 16 | Product Analysis in Ullmann type coupling over Cu_g/PCN by NMR.

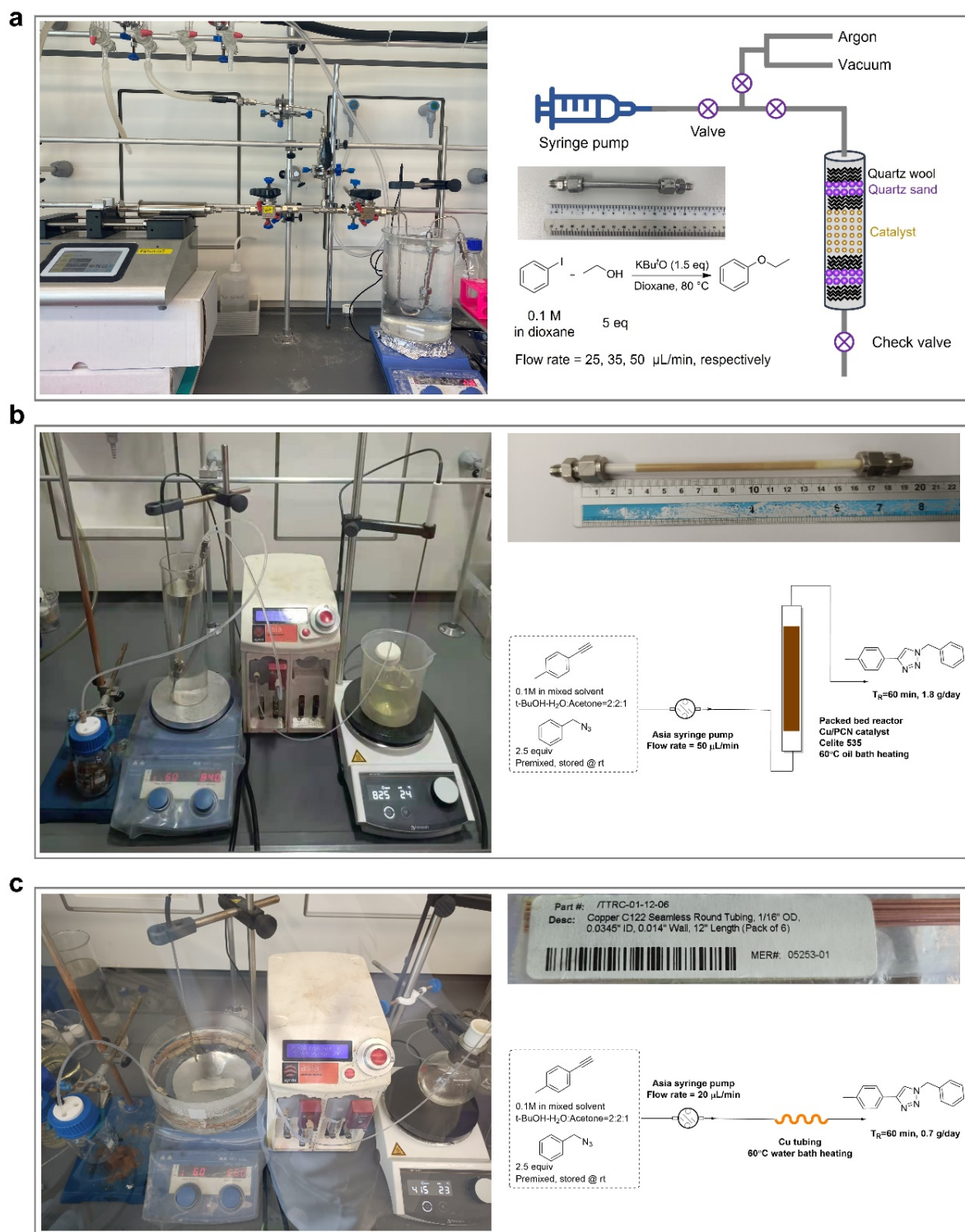


Supplementary Fig. 17 | ADF-STEM image of the used Cu_g/PCN catalyst in C-O coupling reaction.

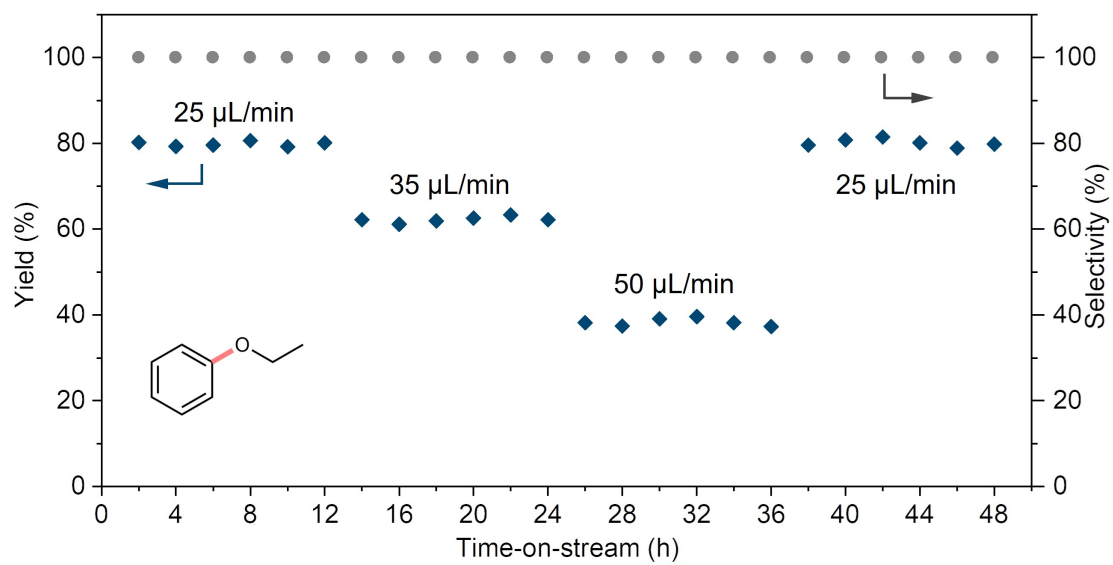


Supplementary Fig. 18 | **a**, Cycling test for the coupling of 4-iodotoluene with ethanol to form C-O bond over Cu_g/PCN . **b-d**, **b**, XRD pattern, **c**, Cu K-edge XANES and **d**, Fourier-transformed EXAFS spectra of the as-prepared Cu_g/PCN and the catalyst after four reaction cycles. For the first four cycles, the catalyst was washed with dioxane before use in the next cycle reaction. For reactivation, the catalyst was carefully cleaned with ethanol and water to remove KI before it was used in the fifth reaction cycle.

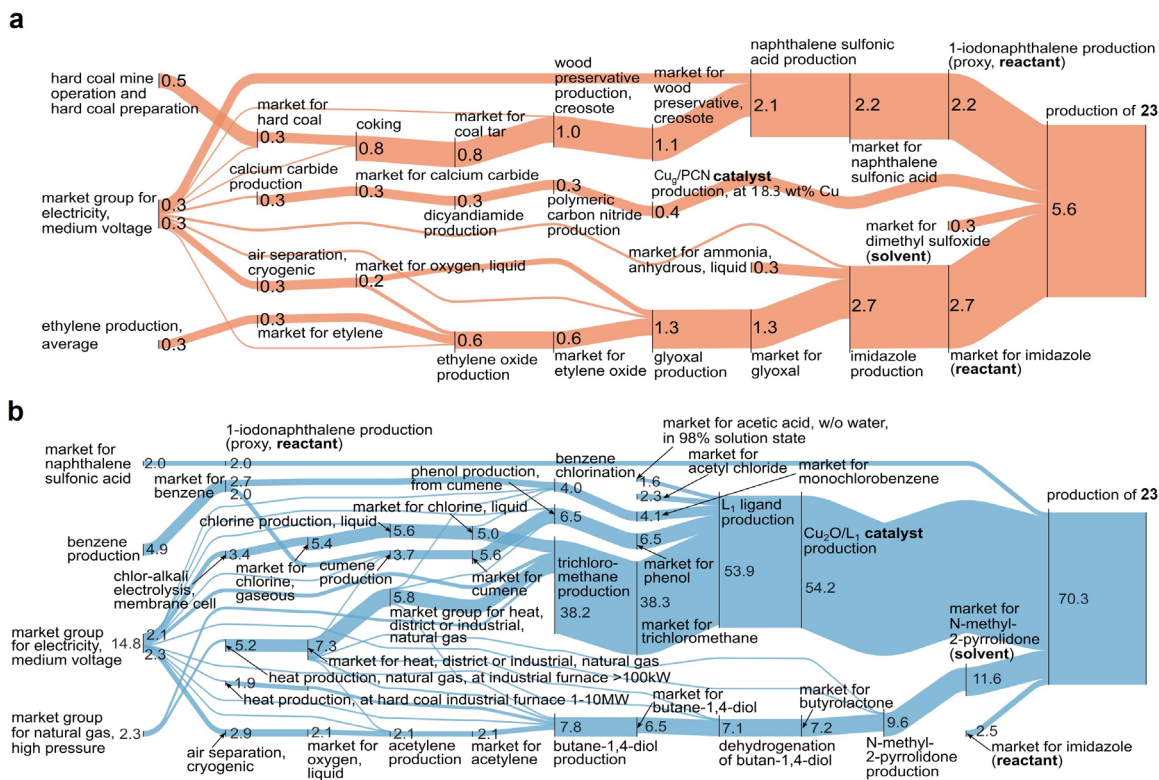
The deposited insoluble KI salts can be clearly seen from the XRD pattern, where a complete set of peaks belonging to KI crystals appeared in the used catalyst. At the same time, Cu K-edge Fourier-transformed EXAFS and XANES spectroscopy showed that the coordination and electronic structure of the copper atoms were identical before and after the reaction, meaning that the deposited KI salts were only physically covered on the surface of the catalyst, rather than chemically bound to the copper sites.



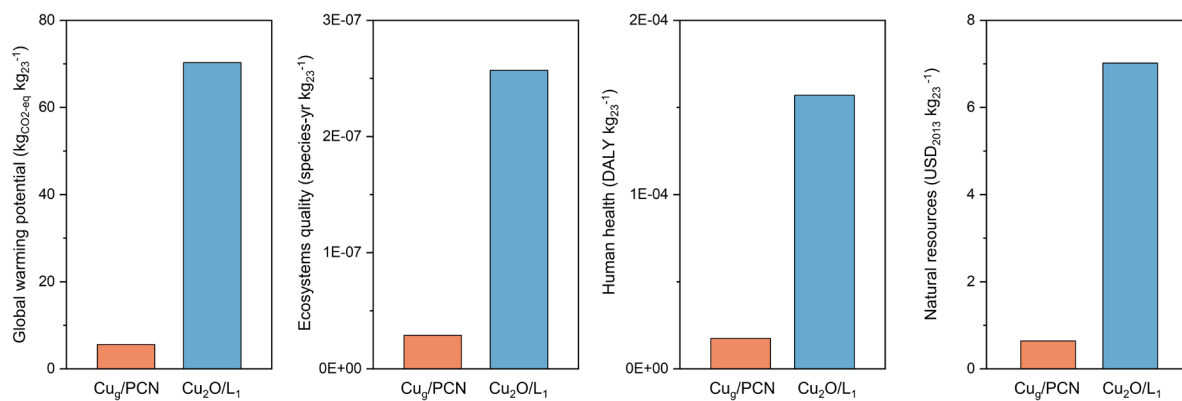
Supplementary Fig. 19 | The continuous flow setup used to evaluate the catalytic performance. **a**, Cu_g/PCN catalyzed C-O bonding formation. **b**, Cu_g/PCN catalyzed azide-alkyne cycloaddition. **c**, Cu tube catalyzed azide-alkyne cycloaddition.



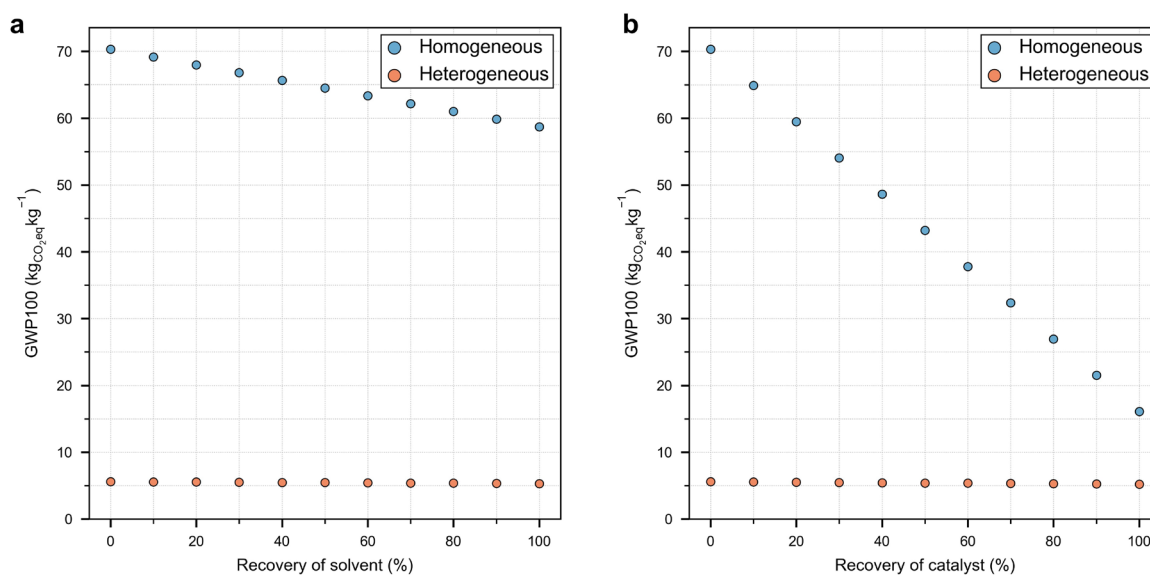
Supplementary Fig. 20 | Continuous flow synthesis of ethoxybenzene over Cu_g/PCN under various flow rates.



Supplementary Fig. 21 | Sankey diagram of embodied GWP flows for homogeneously and heterogeneously catalyzed C-N coupling. Impact contributions are based on the performance of **a** Cu₆/PCN (Fig. 2) and **b** Cu₂O+L₁ (Supplementary Table 2, Entry 2) in the synthesis of product 1, expressed in kilogram of CO₂ equivalent per kilogram of product according to the IPCC 2021 definition. The analysis considers the optimized conditions reported for both systems. For simplicity, only contributions above a 3% cut-off are shown.



Supplementary Fig. 22 | Comparative impact derived from an ex-ante LCA of using a homogeneous or heterogeneous catalysts in one of the studied C-N coupling reactions based on four sustainability metrics: the midpoint global warming potential, ecosystems quality, endpoints human health, and resources. The base case considers a single use of the catalytic system. Reported values are per kg of product 1. DALY = daily adjusted life years.



Supplementary Fig. 23 | Sensitivity analysis on solvent (a) and catalyst (b) recyclability of the reaction mixture for the homogeneous and heterogeneous catalytic systems in the C-N coupling reaction. We repeated the LCA calculations considering that both the catalyst (Cu_g/PCN or Cu₂O/L₁) and solvent could be re-used multiple times by recovering them from the reaction media without any energy penalty, assuming 1% loss of catalyst and solvent in each cycle and neglecting potential catalyst deactivation. Hence, the sensitivity analysis, which complements the evaluation of the two catalytic systems presented in the main manuscript, covers the performance of a wide range of more efficient homogenous and heterogeneous systems with different catalyst and solvent requirements. In the heterogeneous case, recycling does not significantly affect the total impact because this is given mostly by the reactants. In contrast, the carbon footprint of the homogenous system decreases with the recyclability level, first sharply and later with a milder slope as the bottleneck starts to shift to the reactants. The heterogeneous system would still outperform the homogenous system after re-using the catalyst and solvent 100 times under these ideal conditions. Hence, the results suggest that it would be highly unlikely to find a homogenous system outperforming the heterogeneous counterpart substantially.

Assumptions and limitations of the LCA approach. Our LCA relies on a set of assumptions, described below, which we believe would not affect the main conclusions.

1. We omitted the utilities required in the reaction steps in the foreground system. Exothermic reactions would likely require cooling water to control the reactor temperature, whose impact tends to be negligible (particularly when cooling water is recycled), while endothermic reactions would need steam. We also note that heat integration is very challenging in batch processes, which would be most likely the preferred choice for this reaction system. Hence, it would be hard to use the heat generated in exothermic reactions to obtain environmental credits, omitted in our analysis.
2. We further assume that the final product could be easily separated from the reaction mixture without any energy penalty. In practice, we should scale up the separation step using suitable unit operations. However, this separation was not attempted at the lab scale, so we lack an experimental basis for the scale-up calculations. We note that both routes would require such a separation step, so it is likely that the associated impacts would be similar and the comparative assessment would lead to the same conclusions. Moreover, the homogenous system may require an additional step to separate the catalyst from the reaction mixture, which is also omitted, thereby further underestimating its impact.
3. Similarly, we omitted the separations needed in the different synthesis steps for the catalyst components and the 1-iodonaphthalene in the foreground system. Note that we adopted the same simplification, i.e., impacts of separations are omitted, in the synthesis of both catalytic systems, underestimating the impact in both cases.
4. We consider that the data in the background system retrieved from ecoinvent accurately describe the life cycle activities linked to the catalytic systems. To this end, we selected global markets representing average data worldwide. This is a common assumption in many studies that adopt the same temporal and technological level of representation as in the database.

Overall, we provide a lower bound on the total impact for each case (i.e., an optimistic estimate), since some impact contributions were neglected, e.g., utilities and impacts of the separation steps. However, we expect that the estimates will be close to the actual total impacts, since

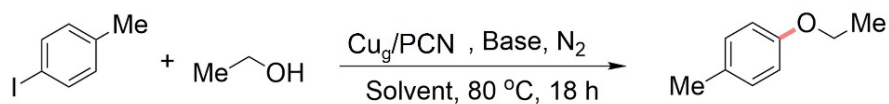
these are often dominated by the raw materials (explicitly considered in our LCA), as occurs in the heterogeneous case, while the other contributions tend to be significantly lower¹⁵. Moreover, the same assumptions were applied in both catalytic systems, so the potential errors of the approximations may cancel out, thereby leading to similar relative performance.

Supplementary Table 1 | Results of EXAFS fits of Cu_g/PCN and Cu₁/NC.

Sample	Shell	N	R (Å)	σ^2 (10^{-3}Å^2)	R factor
Cu _g /PCN	Cu-N	2.5	1.90	0.0069	0.005
Cu ₁ /NC	Cu-N	4.2	1.95	0.0053	0.003

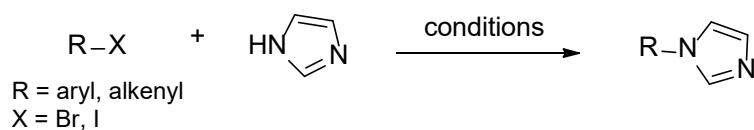
N , coordination number; R , distance between absorbing and backscattering atoms; σ^2 , Debye-Waller factor to account for thermal and structural disorders; R factor as a measure of the goodness of fit. The fitted coordination environment of Cu_g/PCN, and Cu₁/NC coincides well with the proposed structures from DFT.

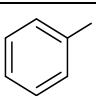
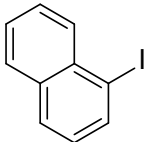
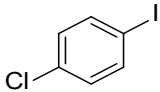
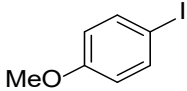
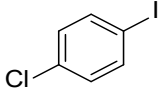
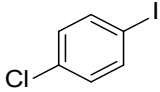
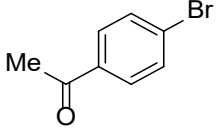
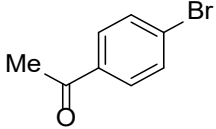
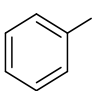
Supplementary Table 2 | Optimization of the reaction conditions for C-O coupling. Reactions were carried out under an N₂ atmosphere. Conditions: 4-iodotoluene (1.0 equiv.), ethanol (2.0 equiv.), Cu_g/PCN Catalyst (1 mg), base (1.5 equiv.), solvent (2 ml), 80 °C, 18 h. 0.2 mmol scale.

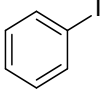
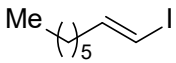
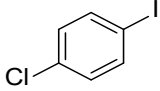
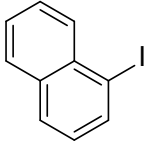
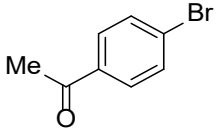


Entry	Base	Solvent	Temp. (°C)	Conversion (%)	Yield (%)
1	KOtBu	dioxane	80	95	90
2	NaOtBu	dioxane	80	19	14
3	LiOtBu	dioxane	80	< 5	1.2
4	K ₃ PO ₄	dioxane	80	1	trace
5	Cs ₂ CO ₃	dioxane	80	< 1	trace
6	K ₂ CO ₃	dioxane	80	< 1	trace
7	KOtBu	Toluene	80	78	< 5
8	KOtBu	CH ₃ CN	80	< 1	trace
9	KOtBu	THF	80	70	60
10	KOtBu	DMF	80	36	28

Supplementary Table 3 | Comparison of the turnover number (TON) reported over copper catalysts in the Ullmann reaction.



Entry ^a	R-X	Catalyst ^b	Reaction mode	TON	Ref.
1		Cu ₂ O + L ₁	homogeneous	36.8	16
2		Cu ₂ O + L ₁	homogeneous	18.6	16
3		CuBr + L ₂	homogeneous	9.1	17
4		CuI + L ₃	homogeneous	49	18
5 ^a		CuCl + L ₄	homogeneous	18.4	19
6		CuI + furfuryl alcohol	homogeneous	80	20
7		Cu ₂ O + L ₁	homogeneous	18.0	16
8		CuI + L ₅	homogeneous	4.7	21
9		Cu ^I -USY	heterogeneous	8.8 (Recycle 5 times)	22

10		CuI/Meso-N-C	heterogeneous	5.9	23
11		sub-nanometric Cu clusters	heterogeneous	413	24
12		Cu _g /PCN	heterogeneous	2352	This work
13		Cu _g /PCN	heterogeneous	1443	This work
14		Cu _g /PCN	heterogeneous	1556	This work

^a Entries 1-10 estimated from reported product yield

^b L₁ = 4,7-Dimethoxy-1,10-phenanthroline; L₂ = β-Keto ester; L₃ = 8-hydroxyquinoline; L₄ = (1E,2E)-oxalaldehyde dioxime; L₅ = per-6-amino-β-cyclodextrin; TON = [mole of converted aryl halides / [mole of Cu catalyst] × 100%.

Supplementary Table 4 | Catalytic performance of Cu₁/PCN with variable copper contents in different reactions.

Cu content (wt.%)	Cat. Amount (mg)	Cu (mol%)	C-N coupling ^a yield (%)	C-O coupling ^b yield (%)	Azide-alkyne cycloaddition ^c yield (%)
18.3	1.4	2	95	92	94
10.8	2.4	2	76	70	83
8.0	3.2	2	56	52	63
1.8	14.2	2	21	31	38
0.9	28.4	2	3	8	12
0.2	128.0	2	0	0	0

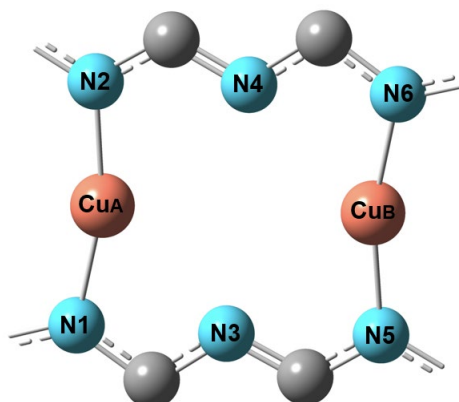
^a1-Chloro-4-iodobenzene (0.2 mmol), imidazole (0.24 mmol), Cu₁/PCN (2 mol% Cu), K₃PO₄ (0.4 mmol), decane (0.2 mmol), anhydrous DMSO (2.0 mL), 110 °C, 28 h.

^b4-iodotoluene (0.2 mmol), ethanol (0.4 mmol), Cu₁/PCN (2 mol% Cu), KO^tBu (0.3 mmol), decane (0.2 mmol), anhydrous dioxane (2.0 mL), 80 °C, 18 h.

^cEthynylbenzene (0.2 mmol), 1-(Azidomethyl)-4-methylbenzene (0.6 mmol), Cu₁/PCN (2 mol% Cu), decane (0.2 mmol), 1:1 water/acetonitrile (3.0 mL), 60 °C, 24 h.

The yield was determined by gas chromatography.

Supplementary Table 5 | Atomic numbering of the active sites as well as the calculated bond distances and Wiberg bond orders for IS5 and IS6 intermediates.

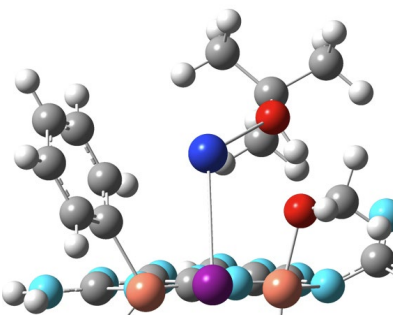
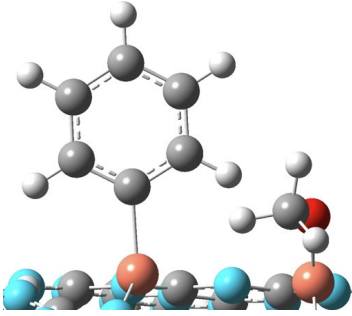


Bond	¹ IS5		¹ IS6	
	Bond distance	Bond order	Bond distance	Bond order
Cu _A -Cu _B	2.46	0.31	2.95	0.11
Cu _A -C ₂	1.93	0.51	1.94	0.53
Cu _A -O	3.13	0.16	1.93	0.41
Cu _B -O	1.84	0.49	2.08	0.25
Cu _A -N ₁	2.18	0.24	2.35	0.19
Cu _A -N ₂	2.20	0.22	2.14	0.25
Cu _A -N ₃	2.01	0.26	2.10	0.24
Cu _B -N ₄	1.95	0.28	2.37	0.11
Cu _B -N ₅	2.34	0.18	2.03	0.25
Cu _B -N ₆	2.35	0.17	2.01	0.28

Supplementary Table 6 | Charge density (ΔQ in e^-) analysis of Cu atoms in Cu_g/PCN at various stages of the C-O coupling reaction. Initial state (IS), transition state (TS) and final state (FS) are defined same as presented in **Supplementary Figure 8a**.

$\Delta Q(e^-)$	Cu (CH_3O^*)	Cu (C_6H_5^*)
Cu_g/PCN	-0.60	-0.60
IS	-0.92	-0.76
TS	-0.92	-0.79
FS	-0.60	-0.60

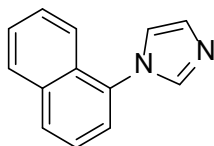
Supplementary Table 7 | Mulliken spin density populations of the open-shell intermediates ${}^3\text{IS3}$ and ${}^3\text{IS4}$.

	${}^3\text{IS3}$	${}^3\text{IS4}$
Atom		
Cu _A	0.39	0.36
Cu _B	0.42	0.40
C ₁	0.29	0.46
O	0.21	0.41

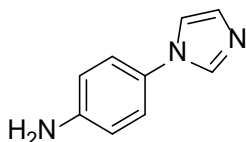
References

- 1 Mondal, J., Borah, P., Modak, A., Zhao, Y. & Bhaumik, A. Cu-grafted functionalized mesoporous SBA-15: a novel heterogeneous catalyst for facile one-pot three-component C-S cross-coupling reaction of aryl halides in water. *Organic Process Research & Development* **18**, 257-265 (2014).
- 2 Sonei, S., Taghavi, F., Khojastehnezhad, A. & Gholizadeh, M. Copper-functionalized silica-coated magnetic nanoparticles for an efficient Suzuki cross-coupling reaction. *ChemistrySelect* **6**, 359-368 (2021).
- 3 Seyedi, N., Shahabi Nejad, M., Saidi, K. & Sheibani, H. Fabrication of nitrogen-enriched graphene oxide/Cu NPs as a highly efficient and recyclable heterogeneous nanocatalyst for the Chan-Lam cross-coupling reaction. *Applied Organometallic Chemistry* **34**, e5307 (2020).
- 4 Muñoz, A., Leo, P., Orcajo, G., Martínez, F. & Calleja, G. URJC-1-MOF as new heterogeneous recyclable catalyst for C-heteroatom coupling reactions. *ChemCatChem* **11**, 3376-3380 (2019).
- 5 Hajipour, A. R., Hosseini, S. M. & Mohammadsaleh, F. DABCO-functionalized silica-copper (I) complex: a novel and recyclable heterogeneous nanocatalyst for palladium-free Sonogashira cross-coupling reactions. *New Journal of Chemistry* **40**, 6939-6945 (2016).
- 6 Frindy, S., el Kadib, A., Lahcini, M., Primo, A. & García, H. Copper nanoparticles stabilized in a porous chitosan aerogel as a heterogeneous catalyst for C-S cross-coupling. *ChemCatChem* **7**, 3307-3315 (2015).
- 7 Anbarasu, G. *et al.* Silica-Supported Azo-linked Schiff base Cu(II) complex as efficient heterogeneous catalysts for Suzuki-Miyaura cross coupling reaction at low catalyst loadings in green media. *Materials Today: Proceedings* **4**, 12416-12425 (2017).
- 8 Nasrollahzadeh, M., Rostami-Vartooni, A., Ehsani, A. & Moghadam, M. Fabrication, characterization and application of nanopolymer supported copper(II) complex as an effective and reusable catalyst for the CN bond cross-coupling reaction of sulfonamides with arylboronic acids in water under aerobic conditions. *Journal of Molecular Catalysis A: Chemical* **387**, 123-129 (2014).
- 9 Ma, P. *et al.* Heterogeneous amorphous Cu-MOF-74 catalyst for C-N coupling reaction. *ChemistrySelect* **3**, 10694-10700 (2018).
- 10 Devarajan, N. & Suresh, P. Framework-copper-catalyzed C-N cross-coupling of arylboronic acids with imidazole: convenient and ligand-free synthesis of N-Arylimidazoles. *ChemCatChem* **8**, 2953-2960 (2016).
- 11 Hemmati, S., Ahany Kamangar, S., Yousefi, M., Hashemi Salehi, M. & Hekmati, M. Cu(I)-anchored polyvinyl alcohol coated-magnetic nanoparticles as heterogeneous nanocatalyst in Ullmann-type C-N coupling reactions. *Applied Organometallic Chemistry* **34**, e5611 (2020).
- 12 Vásquez-Céspedes, S., Betori, R. C., Cismesia, M. A., Kirsch, J. K. & Yang, Q. Heterogeneous catalysis for cross-coupling reactions: an underutilized powerful and

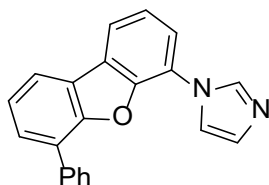
- sustainable tool in the fine chemical industry? *Organic Process Research & Development* **25**, 740-753 (2021).
- 13 Chen, F., Jiang, X., Zhang, L., Lang, R. & Qiao, B. Single-atom catalysis: bridging the homo- and heterogeneous catalysis. *Chinese Journal of Catalysis* **39**, 893-898 (2018).
- 14 Chen, Z., Liu, J., Koh, M. J. & Loh, K. P. Single-atom catalysis: from simple reactions to the synthesis of complex molecules. *Adv. Mater.* **34**, 2103882 (2022).
- 15 Galán-Martín, Á. *et al.* Sustainability footprints of a renewable carbon transition for the petrochemical sector within planetary boundaries. *One Earth* **4**, 565-583 (2021).
- 16 Altman, R. A. & Buchwald, S. L. 4, 7-Dimethoxy-1, 10-phenanthroline: an excellent ligand for the Cu-catalyzed N-arylation of imidazoles. *Organic Letters* **8**, 2779-2782 (2006).
- 17 Lv, X. & Bao, W. A β -keto ester as a novel, efficient, and versatile ligand for copper(I)-catalyzed C-N, C-O, and C-S coupling reactions. *The Journal of organic chemistry* **72**, 3863-3867 (2007).
- 18 Yang, X. *et al.* CuI/8-Hydroxyquinoline Promoted N-arylation of indole and azoles. *Chinese Journal of Chemistry* **30**, 875-880 (2012).
- 19 Li, X., Yang, D., Jiang, Y. & Fu, H. Efficient copper-catalyzed N-arylations of nitrogen-containing heterocycles and aliphatic amines in water. *Green Chemistry* **12**, 1097-1105 (2010).
- 20 Ferlin, F. *et al.* A waste-minimized protocol for copper-catalyzed Ullmann-type reaction in a biomass derived furfuryl alcohol/water azeotrope. *Green Chemistry* **20**, 1634-1639 (2018).
- 21 Suresh, P. & Pitchumani, K. Per-6-amino- β -cyclodextrin as an efficient supramolecular ligand and host for Cu(I)-catalyzed N-arylation of imidazole with aryl bromides. *The Journal of organic chemistry* **73**, 9121-9124 (2008).
- 22 Garnier, T. *et al.* Copper (I)-USY as a ligand-free and recyclable catalyst for Ullmann-type O-, N-, S-, and C-arylation reactions: scope and application to total synthesis. *The Journal of Organic Chemistry* **83**, 6408-6422 (2018).
- 23 Zhang, P. *et al.* Mesoporous nitrogen-doped carbon for copper-mediated Ullmann-type C-O/-N/-S cross-coupling reactions. *RSC advances* **3**, 1890-1895 (2013).
- 24 Oliver-Messeguer, J. *et al.* Stabilized naked sub-nanometric Cu clusters within a polymeric film catalyze C-N, C-C, C-O, C-S, and C-P bond-forming reactions. *J. Am. Chem. Soc.* **137**, 3894-3900 (2015).



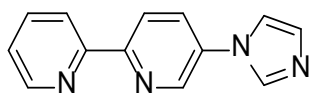
1-(naphthalen-1-yl)-1H-imidazole (1). The compound was prepared in 81% yield. $^1\text{H NMR}$ (500 MHz, Chloroform-*d*) δ [ppm] 7.97 – 7.94 (m, 2H), 7.78 (s, 1H), 7.63 – 7.50 (comp, 4H), 7.47 – 7.45 (m, 1H), 7.31 (s, 1H), 7.27 (s, 1H); $^{13}\text{C NMR}$ (125 MHz, Chloroform-*d*) δ [ppm] 138.5, 134.3, 134.2, 129.6, 129.4, 128.4, 127.7, 127.1, 125.3, 123.8, 122.4, 121.9.



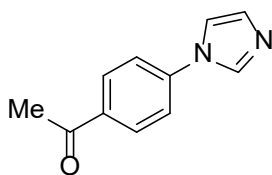
4-(1H-imidazol-1-yl)aniline (2). The compound was prepared in 70% yield. $^1\text{H NMR}$ (500 MHz, Chloroform-*d*) δ [ppm] 7.73 (s, 1H), 7.21 – 7.10 (comp, 4H), 6.74 (d, $J = 8.7$ Hz, 2H), 3.74 (br, 2H); $^{13}\text{C NMR}$ (125 MHz, Chloroform-*d*) δ [ppm] 146.2, 136.0, 129.9, 129.0, 123.5, 119.0, 115.7.



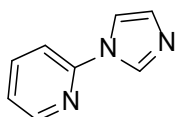
1-(6-phenyldibenzo[*b,d*]furan-4-yl)-1H-imidazole (3). The compound was prepared in 66% yield. $^1\text{H NMR}$ (500 MHz, Chloroform-*d*) δ [ppm] 8.28 (s, 1H), 7.94 (ddd, $J = 13.3, 7.7, 1.1$ Hz, 2H), 7.90 – 7.84 (m, 2H), 7.68 (dd, $J = 7.6, 1.2$ Hz, 1H), 7.62 (s, 1H), 7.54 (t, $J = 8.0$ Hz, 2H), 7.51 – 7.46 (m, 2H), 7.44 (td, $J = 7.6, 1.8$ Hz, 2H), 7.28 (s, 1H); $^{13}\text{C NMR}$ (125 MHz, Chloroform-*d*) δ [ppm] 153.4, 146.8, 136.7, 135.7, 129.9, 128.9, 128.5, 128.1, 127.7, 126.8, 126.3, 124.3, 124.1, 123.8, 122.6, 119.9, 119.2, 119.2, 118.6.



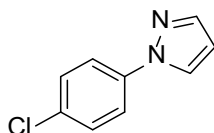
5-(1H-imidazol-1-yl)-2,2'-bipyridine (4). The compound was prepared in 72% yield. $^1\text{H NMR}$ (500 MHz, Chloroform-*d*) δ [ppm] 8.77 (dd, $J = 2.7, 0.7$ Hz, 1H), 8.68 (ddd, $J = 4.8, 1.8, 0.9$ Hz, 1H), 8.55 (dd, $J = 8.6, 0.7$ Hz, 1H), 8.41 (dt, $J = 7.9, 1.1$ Hz, 1H), 7.93 (s, 1H), 7.86 – 7.79 (m, 2H), 7.41 – 7.30 (m, 2H), 7.27 (s, 1H); $^{13}\text{C NMR}$ (125 MHz, Chloroform-*d*) δ [ppm] 155.4, 154.9, 149.4, 141.9, 137.2, 135.6, 133.8, 131.3, 129.5, 124.2, 121.9, 121.2, 118.1.



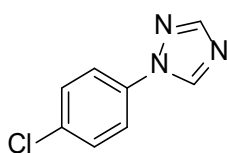
1-[4-(1*H*-imidazol-1-yl)phenyl]ethanone (5). The compound was prepared in 78% yield. ¹H NMR (500 MHz, Chloroform-*d*) δ [ppm] 8.08 (d, J = 8.6 Hz, 2H), 7.95 (s, 1H), 7.50 (d, J = 8.6 Hz, 2H), 7.35 (s, 1H), 7.24 (s, 1H), 2.63 (s, 3H); ¹³C NMR (125 MHz, Chloroform-*d*) δ [ppm] 196.7, 140.8, 135.9, 135.5, 131.3, 130.5, 120.8, 117.9, 26.7.



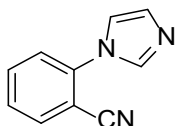
2-(1*H*-imidazol-1-yl)pyridine (6). The compound was prepared in 86% yield. ¹H NMR (500 MHz, Chloroform-*d*) δ [ppm] 8.49 – 8.47 (m, 1H), 8.35 (s, 1H), 7.84 – 7.80 (m, 1H), 7.64 (s, 1H), 7.36 – 7.34 (m, 1H), 7.25 – 7.22 (m, 1H), 7.19 (s, 1H); ¹³C NMR (125 MHz, Chloroform-*d*) δ [ppm] 149.3, 139.1, 135.1, 130.8, 122.1, 116.3, 112.5.



1-(4-methoxyphenyl)-1*H*-imidazole (7). The compound was prepared in 87% yield. ¹H NMR (500 MHz, Chloroform-*d*) δ [ppm] 7.93 – 7.87 (m, 1H), 7.72 (d, J = 1.7 Hz, 1H), 7.64 (d, J = 8.9 Hz, 2H), 7.42 (d, J = 8.9 Hz, 2H), 6.49 – 6.47 (m, 1H); ¹³C NMR (125 MHz, Chloroform-*d*) δ [ppm] 141.5, 138.6, 129.7, 126.8, 120.9, 120.5, 108.1.

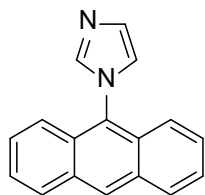


1-(4-methoxyphenyl)-1*H*-imidazole (8). The compound was prepared in 78% yield. ¹H NMR (500 MHz, Chloroform-*d*) δ [ppm] 8.54 (s, 1H), 8.10 (s, 1H), 7.63 (d, J = 8.9 Hz, 2H), 7.49 (d, J = 8.9 Hz, 2H); ¹³C NMR (125 MHz, Chloroform-*d*) δ [ppm] 152.9, 141.0, 135.7, 134.1, 130.1, 121.4.

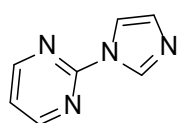


2-(1*H*-imidazol-1-yl)benzonitrile (9). The compound was prepared in 96% yield. ¹H NMR (500 MHz, Chloroform-*d*) δ [ppm] 7.85 (s, 1H), 7.82 (dt, J = 7.8, 1.5 Hz, 1H), 7.74 (tt, J = 7.9, 1.3 Hz, 1H), 7.53

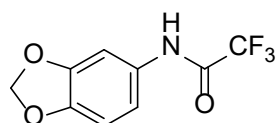
(tt, $J = 7.7, 1.2$ Hz, 1H), 7.49 – 7.44 (m, 1H), 7.35 (s, 1H), 7.26 (s, 1H); ^{13}C NMR (125 MHz, Chloroform-*d*) δ [ppm] 139.4, 136.8, 134.6, 134.4, 130.9, 128.6, 125.8, 119.8, 115.9, 108.2.



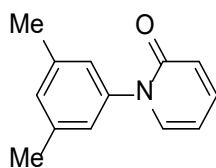
1-(45henanthre-9-yl)-1H-imidazole (10). The compound was prepared in 70% yield. ^1H NMR (500 MHz, Chloroform-*d*) δ [ppm] 8.59 (s, 1H), 8.08 (d, $J = 7.4$ Hz, 2H), 7.78 (s, 1H), 7.55 – 7.43 (comp, 7H), 7.27 (s, 1H); ^{13}C NMR (125 MHz, Chloroform-*d*) δ [ppm] 139.7, 131.4, 129.8, 128.9, 128.6, 128.5, 127.7, 126.0, 122.9, 122.5.



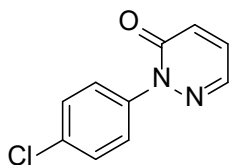
2-(1H-imidazol-1-yl)pyrimidine (11). The compound was prepared in 82% yield. ^1H NMR (500 MHz, Chloroform-*d*) δ [ppm] 8.68 (d, $J = 4.8$ Hz, 2H), 8.61 (s, 1H), 7.88 (s, 1H), 7.19 (t, $J = 4.8$ Hz, 1H), 7.15 (s, 1H); ^{13}C NMR (125 MHz, Chloroform-*d*) δ [ppm] 158.7, 154.8, 136.2, 130.7, 118.9, 116.5.



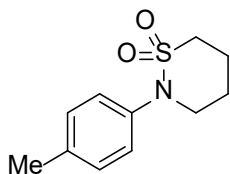
N-(benzo[*d*][1,3]dioxol-5-yl)-2,2,2-trifluoroacetamide (12). The compound was prepared in 65% yield. NaOtBu was used instead of K_3PO_4 . ^1H NMR (500 MHz, Chloroform-*d*) δ 7.79 (br, 1H), 7.23 (d, $J = 2.2$ Hz, 1H), 6.89 (dd, $J = 8.3, 2.2$ Hz, 1H), 6.80 (d, $J = 8.4$ Hz, 1H), 6.00 (s, 2H); ^{13}C NMR (125 MHz, Chloroform-*d*) δ [ppm] 154.8 (d, $J = 37.5$ Hz), 148.3, 146.0, 129.2, 115.9 (q, $J = 286.3$ Hz), 114.2, 108.5, 103.1, 101.9; ^{19}F NMR (471 MHz, Chloroform-*d*) δ [ppm] -75.66.



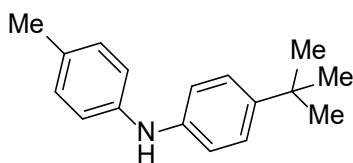
1-(4-methoxyphenyl)-1H-imidazole (13). The compound was prepared in 82% yield. Cs_2CO_3 was used instead of K_3PO_4 . ^1H NMR (500 MHz, Chloroform-*d*) δ [ppm] 7.42 – 7.36 (m, 1H), 7.35 – 7.29 (m, 1H), 7.11 – 7.05 (m, 1H), 7.00 (s, 2H), 6.68 – 6.66 (dt, $J = 9.3, 1.8$ Hz, 1H), 6.25 – 6.21 (m, 1H), 2.38 (s, 6H); ^{13}C NMR (125 MHz, Chloroform-*d*) δ [ppm] 162.7, 1401.0, 139.9, 139.3, 138.3, 130.4, 124.3, 121.9, 105.8, 21.4.



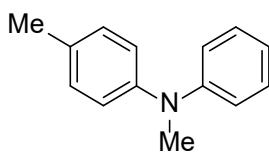
1-(4-methoxyphenyl)-1H-imidazole (14). The compound was prepared in 63% yield. Cs_2CO_3 was used instead of K_3PO_4 . $^1\text{H NMR}$ (500 MHz, Chloroform-*d*) δ [ppm] 7.90 – 7.89 (m, 1H), 7.60 (d, $J = 8.9$ Hz, 2H), 7.44 (d, $J = 8.9$ Hz, 2H), 7.26 – 7.24 (m, 1H), 7.05 (dd, $J = 9.5, 1.7$ Hz, 1H); $^{13}\text{C NMR}$ (125 MHz, Chloroform-*d*) δ [ppm] 165.4, 137.02, 131.55, 131.38, 129.9, 129.06, 126.70, 122.74.



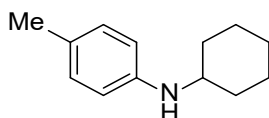
1-(4-methoxyphenyl)-1H-imidazole (15). The compound was prepared in 60% yield. NaOtBu was used instead of K_3PO_4 . $^1\text{H NMR}$ (500 MHz, Chloroform-*d*) δ [ppm] 7.22 (d, $J = 8.4$ Hz, 2H), 7.16 (d, $J = 8.4$ Hz, 2H), 3.72 – 3.63 (m, 2H), 3.17 (td, $J = 6.1, 2.2$ Hz, 2H), 2.33 (s, 3H), 2.32 – 2.25 (m, 2H), 1.94 – 1.82 (m, 2H); $^{13}\text{C NMR}$ (125 MHz, Chloroform-*d*) δ [ppm] 137.9, 137.3, 129.8, 126.9, 53.6, 50.6, 24.5, 24.3, 21.0.



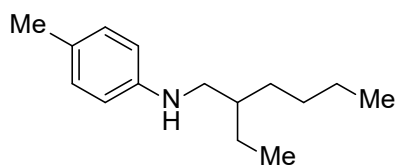
4-(*tert*-butyl)-*N*-(*p*-tolyl)aniline (16). The compound was prepared in 70% yield. $^1\text{H NMR}$ (500 MHz, Chloroform-*d*) δ [ppm] 7.31-7.28 (m, 2H), 7.09 (m, 2H), 7.01-6.99 (m, 4H), 2.32 (s, 3H), 1.33 (s, 9H).



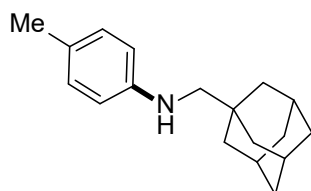
***N*,4-dimethyl-*N*-phenylaniline (17).** The compound was prepared in 83% yield. $^1\text{H NMR}$ (500 MHz, Chloroform-*d*) δ [ppm] 7.25-7.21 (m, 2H), 7.13 (d, $J = 8.3$ Hz, 2H), 7.00 (d, $J = 8.2$ Hz, 2H), 6.93 (d, $J = 8.5$ Hz, 2H), 6.88 (t, $J = 7.4$ Hz, 1H), 3.29 (s, 3H), 2.32 (s, 3H).



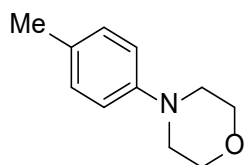
***N*-cyclohexyl-4-methylaniline (18).** The compound was prepared in 65% yield. $^1\text{H NMR}$ (500 MHz, Chloroform-*d*) δ [ppm] 6.98 (d, $J = 8.1$ Hz, 2H), 6.54 (d, $J = 8.1$ Hz, 2H), 3.22 (t, $J = 4.1$ Hz, 1H), 2.23 (s, 1H), 2.06 (d, $J = 13.6$ Hz, 2H), 1.76 (d, $J = 13.6$ Hz, 2H), 1.63 -1.12 (m, 6H).



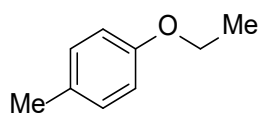
***N*-(2-ethylhexyl)-4-methylaniline (19).** The compound was prepared in 74% yield. $^1\text{H NMR}$ (500 MHz, Chloroform-*d*) δ [ppm] 6.99 (d, $J = 7.9$ Hz, 2H), 6.56 (d, $J = 7.9$ Hz, 2H), 3.00 (d, $J = 6.5$ Hz, 1H), 2.23 (s, 3H), 1.58-1.53 (m, 1H), 1.42-1.30 (m, 8H), 0.92-0.89 (m, 6H).



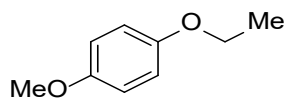
***N*-(1-((1*s*,3*s*)-adamantan-1-yl)methyl)-4-methylaniline (20).** The compound was prepared in 80% yield. $^1\text{H NMR}$ (500 MHz, Chloroform-*d*) δ [ppm] 6.98 (d, $J = 8.0$ Hz, 2H), 6.56 (d, $J = 8.0$ Hz, 2H), 2.77 (s, 2H), 2.22 (s, 3H), 1.99 (s, 3H), 1.75-1.65 (m, 6H), 1.58 (s, 6H).



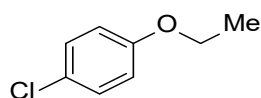
4-(*p*-tolyl)morpholine (21). The compound was prepared in 76% yield. $^1\text{H NMR}$ (500 MHz, Chloroform-*d*) δ [ppm] 7.10 (d, $J = 8.3$ Hz, 2H), 6.85 (d, $J = 8.3$ Hz, 2H), 3.87 (t, $J = 4.8$ Hz, 4H), 3.12 (t, $J = 4.8$ Hz, 4H), 2.28 (s, 3H).



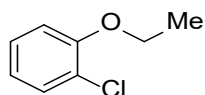
1-ethoxy-4-methylbenzene (22). The compound was prepared in 90% yield. $^1\text{H NMR}$ (500 MHz, Chloroform-*d*) δ [ppm] 7.09 (d, $J = 8.1$ Hz, 2H), 6.82 (d, $J = 8.1$ Hz, 2H), 4.02 (q, $J = 7.0$ Hz, 2H), 2.31 (d, $J = 1.1$ Hz, 3H), 1.42 (t, $J = 7.0$ Hz, 3H); $^{13}\text{C NMR}$ (125 MHz, Chloroform-*d*) δ [ppm] 156.9, 129.9, 129.8, 114.5, 63.5, 20.6, 15.0.



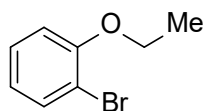
ethoxy-4-methoxybenzene (23). The compound was prepared in 86% yield. $^1\text{H NMR}$ (500 MHz, Chloroform-*d*) δ [ppm] 6.85-6.83 (comp, 4H), 3.99 (q, $J = 7.0$ Hz, 2H), 3.77 (s, 3H), 1.39 (t, $J = 7.0$ Hz, 3H); $^{13}\text{C NMR}$ (125 MHz, Chloroform-*d*) δ [ppm] 153.8, 153.2, 115.6, 114.8, 64.2, 55.9, 15.1.



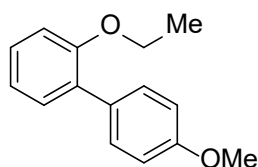
1-chloro-4-ethoxybenzene (24). The compound was prepared in 88% yield. $^1\text{H NMR}$ (500 MHz, Chloroform-*d*) δ [ppm] 7.24–7.20 (m, 2H), 6.84–6.80 (m, 2H), 4.00 (q, $J = 7.0$ Hz, 2H), 1.41 (t, $J = 7.0$ Hz, 3H); $^{13}\text{C NMR}$ (125 MHz, Chloroform-*d*) δ [ppm] 157.7, 129.4, 125.5, 115.9, 63.9, 14.9.



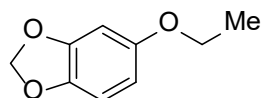
1-chloro-2-ethoxybenzene (25). The compound was prepared in 68% yield. $^1\text{H NMR}$ (500 MHz, Chloroform-*d*) δ [ppm] 7.36 (dd, $J = 7.9, 1.6$ Hz, 1H), 7.21–7.18 (m, 1H), 6.92 (dd, $J = 8.2, 1.4$ Hz, 1H), 6.93–6.86 (m, 1H), 4.11 (q, $J = 7.0$ Hz, 2H), 1.47 (t, $J = 7.0$ Hz, 3H); $^{13}\text{C NMR}$ (125 MHz, Chloroform-*d*) δ [ppm] 154.6, 130.4, 127.8, 121.3, 113.6, 64.8, 14.9.



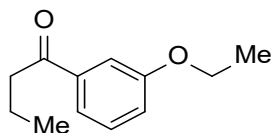
1-bromo-2-ethoxybenzene (26). The compound was prepared in 65% yield. $^1\text{H NMR}$ (500 MHz, Chloroform-*d*) δ [ppm] 7.53 (dd, $J = 7.8, 1.7$ Hz, 1H), 7.26 – 7.22 (m, 1H), 6.89 (dd, $J = 8.2, 1.4$ Hz, 1H), 6.82 (td, $J = 7.6, 1.4$ Hz, 1H), 4.11 (q, $J = 7.0$ Hz, 2H), 1.47 (t, $J = 7.0$ Hz, 3H); $^{13}\text{C NMR}$ (125 MHz, Chloroform-*d*) δ [ppm] 155.5, 133.5, 128.5, 121.8, 113.4, 112.4, 64.9, 14.9.



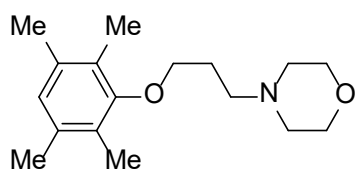
2-ethoxy-4'-methoxy-1,1'-biphenyl (27). The compound was prepared in 72% yield. $^1\text{H NMR}$ (500 MHz, Chloroform-*d*) δ [ppm] 7.52–7.49 (m, 2H), 7.31 (dd, $J = 7.6, 1.8$ Hz, 1H), 7.29–7.26 (m, 1H), 7.00 (td, $J = 7.4, 1.2$ Hz, 1H), 6.97–6.93 (comp, 3H), 4.04 (q, $J = 6.9$ Hz, 2H), 3.85 (s, 3H), 1.36 (t, $J = 7.0$ Hz, 3H); $^{13}\text{C NMR}$ (125 MHz, Chloroform-*d*) δ [ppm] 158.7, 155.9, 131.2, 130.8, 130.8, 130.7, 128.2, 120.9, 113.5, 112.8, 64.2, 55.4, 15.0.



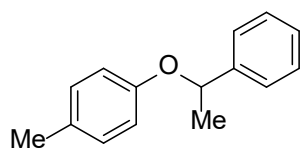
5-ethoxybenzo[d][1,3]dioxole (28). The compound was prepared in 88% yield. $^1\text{H NMR}$ (500 MHz, Chloroform-*d*) δ [ppm] 6.70 (d, $J = 8.5$ Hz, 1H), 6.49 (d, $J = 2.4$ Hz, 1H), 6.32 (dd, $J = 8.5, 2.5$ Hz, 1H), 5.91 (s, 2H), 3.95 (q, $J = 7.0$ Hz, 2H), 1.38 (t, $J = 7.0$ Hz, 3H); $^{13}\text{C NMR}$ (125 MHz, Chloroform-*d*) δ [ppm] 154.6, 148.6, 141.6, 108.1, 105.8, 101.2, 98.2, 64.5, 15.0.



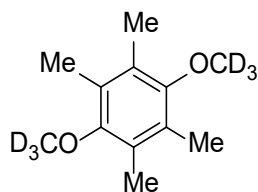
1-(3-ethoxyphenyl)butan-1-one (29). The compound was prepared in 72% yield. $^1\text{H NMR}$ (500 MHz, Chloroform-*d*) δ [ppm] 7.62 (dt, $J = 7.7, 1.3$ Hz, 1H), 7.55 (dd, $J = 2.7, 1.5$ Hz, 1H), 7.33 (t, $J = 7.9$ Hz, 1H), 7.10–7.07 (m, 1H), 4.37 (q, $J = 7.1$ Hz, 2H), 4.08 (q, $J = 7.0$ Hz, 2H), 1.43 (t, $J = 7.0$ Hz, 3H), 1.39 (t, $J = 7.1$ Hz, 3H); $^{13}\text{C NMR}$ (125 MHz, Chloroform-*d*) δ [ppm] 166.6, 158.9, 131.8, 129.3, 121.8, 119.7, 114.7, 63.7, 61.0, 14.8, 14.3.



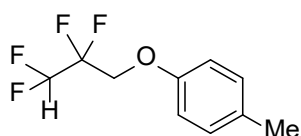
4-[3-(2,3,5,6-tetramethylphenoxy)propyl]morpholine (30). The compound was prepared in 83% yield. $^1\text{H NMR}$ (500 MHz, Chloroform-*d*) δ [ppm] 6.78 (s, 1H), 3.76 (t, $J = 4.9$ Hz, 6H), 2.65 – 2.61 (m, 2H), 2.59 – 2.46 (comp, 4H), 2.23 (s, 6H), 2.18 (s, 6H), 2.06 – 1.99 (m, 2H); $^{13}\text{C NMR}$ (125 MHz, Chloroform-*d*) δ [ppm] 155.6, 134.9, 126.9, 126.7, 70.6, 67.2, 55.7, 53.8, 27.4, 19.9, 12.4.



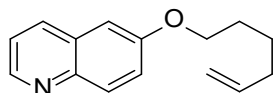
1-methyl-4-(1-phenylethoxy)benzene (31). The compound was prepared in 83% yield. 100 °C was used. $^1\text{H NMR}$ (500 MHz, Chloroform-*d*) δ [ppm] 7.41–7.35 (m, 2H), 7.33–7.30 (m, 2H), 7.26–7.23 (m, 1H), 7.00 (d, $J = 8.5$ Hz, 2H), 6.77 (d, $J = 8.5$ Hz, 2H), 5.27 (q, $J = 6.5$ Hz, 1H), 2.24 (s, 3H), 1.63 (d, $J = 6.5$ Hz, 3H); $^{13}\text{C NMR}$ (125 MHz, Chloroform-*d*) δ [ppm] 155.9, 143.6, 129.9, 129.9, 128.7, 127.5, 125.7, 115.9, 76.2, 24.6, 20.6.



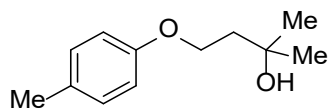
1,4-[α,α,α -2H3]-dimethoxy-2,3,5,6-tetramethylbenzene (32). The compound was prepared in 55% yield. $^1\text{H NMR}$ (400 MHz, Chloroform-*d*) δ [ppm] 2.19 (s, 12H); $^{13}\text{C NMR}$ 152.9, 127.8, 60.1–58.3 (m), 12.8.



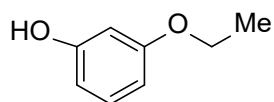
1-methyl-4-(2,2,3,3-tetrafluoropropoxy)benzene (33). The compound was prepared in 92% yield. $^1\text{H NMR}$ (500 MHz, Chloroform-*d*) δ [ppm] 7.13–7.09 (m, 2H), 6.84–6.79 (m, 2H), 6.18–6.59 (m, 1H), 4.31 (tt, $J = 11.8, 1.6$ Hz, 2H), 2.31 (s, 3H); $^{13}\text{C NMR}$ (125 MHz, Chloroform-*d*) δ [ppm] 155.5, 132.0, 130.3, 114.8, 111.4–106.9 (m, 1C), 65.8 (t, $J = 30$ Hz, 1C), 20.6; $^{19}\text{F NMR}$ (377 MHz, Chloroform-*d*) δ -125.38 (d, $J = 4.7$ Hz), -139.73 (t, $J = 4.7$ Hz).



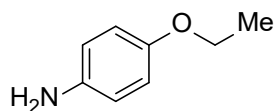
6-(hex-5-en-1-yloxy)quinoline (34). The compound was prepared in 92% yield. $^1\text{H NMR}$ (500 MHz, Chloroform-*d*) δ [ppm] 8.75 (dd, $J = 4.3, 1.7$ Hz, 1H), 8.02 (dd, $J = 8.4, 1.5$ Hz, 1H), 7.99 (d, $J = 9.2$ Hz, 1H), 7.36 (dd, $J = 9.2, 2.8$ Hz, 1H), 7.33 (dd, $J = 8.3, 4.2$ Hz, 1H), 7.05 (d, $J = 2.7$ Hz, 1H), 5.84 (ddt, $J = 16.9, 10.2, 6.7$ Hz, 1H), 5.11 – 4.94 (m, 2H), 4.07 (t, $J = 6.5$ Hz, 2H), 2.15 (tdt, $J = 7.8, 6.6, 1.4$ Hz, 2H), 1.92 – 1.83 (m, 2H), 1.62 (tt, $J = 9.8, 6.4$ Hz, 2H); $^{13}\text{C NMR}$ (125 MHz, Chloroform-*d*) δ [ppm] 157.3, 147.9, 144.4, 138.6, 134.9, 130.9, 129.5, 122.7, 121.4, 115.0, 105.9, 68.2, 33.5, 28.7, 25.5.



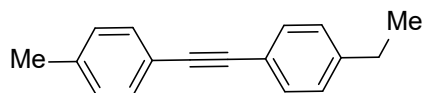
2-methyl-4-(p-tolyloxy)butan-2-ol (35). The compound was prepared in 78% yield. $^1\text{H NMR}$ (500 MHz, Chloroform-*d*) δ [ppm] 7.09 (d, $J = 8.6$ Hz, 2H), 6.81 (d, $J = 8.6$ Hz, 2H), 4.16 (s, 2H), 2.29 (s, 3H), 1.98 (t, $J = 8.0$ Hz, 2H), 1.67 (br, 1H), 1.30 (s, 6H); $^{13}\text{C NMR}$ (125 MHz, Chloroform-*d*) δ [ppm] 130.5, 130.1, 114.5, 114.2, 70.6, 65.5, 41.7, 29.7, 20.6.



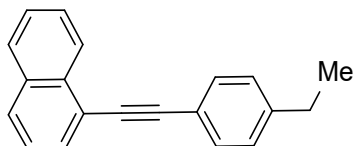
3-ethoxyphenol (36). The compound was prepared in 78% yield. $^1\text{H NMR}$ (500 MHz, Chloroform-*d*) δ [ppm] 7.16–7.06 (m, 1H), 6.51–6.46 (m, 1H), 6.45–6.38 (m, 2H), 4.86 (br, 1H), 4.00 (q, $J = 7.0$ Hz, 2H), 1.40 (t, $J = 7.0$ Hz, 3H); $^{13}\text{C NMR}$ (125 MHz, Chloroform-*d*) δ [ppm] 160.5, 156.8, 130.2, 107.7, 107.2, 102.2, 63.6, 15.0.



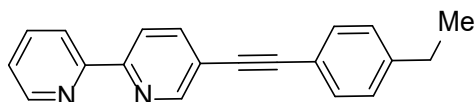
4-ethoxyaniline (37). The compound was prepared in 70% yield. $^1\text{H NMR}$ (500 MHz, Chloroform-*d*) δ [ppm] 7.16–7.06 (m, 1H), 6.51–6.46 (m, 1H), 6.45–6.38 (m, 2H), 4.86 (br, 1H), 4.00 (q, $J = 7.0$ Hz, 2H), 1.40 (t, $J = 7.0$ Hz, 3H); $^{13}\text{C NMR}$ (125 MHz, Chloroform-*d*) δ [ppm] 152.3, 139.9, 116.6, 115.8, 64.2, 15.1.



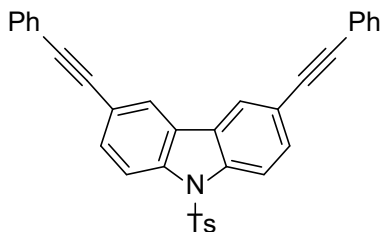
1-ethyl-4-(*p*-tolylethynyl)benzene (38). The compound was prepared in 86% yield. $^1\text{H NMR}$ (500 MHz, Chloroform-*d*) δ [ppm] 7.45-7.41 (m, 4H), 7.18-7.14 (m, 4H), 2.68 (q, $J = 7.7$ Hz, 2H), 2.36 (s, 3H), 1.24 (t, $J = 7.7$ Hz, 3H).



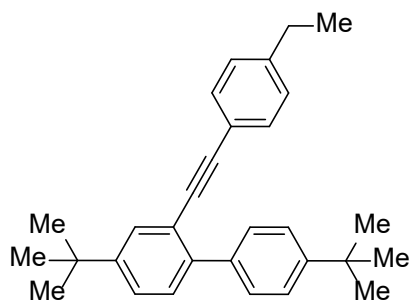
1-((4-ethylphenyl)ethynyl)naphthalene (39). The compound was prepared in 82% yield. $^1\text{H NMR}$ (500 MHz, Chloroform-*d*) δ [ppm] 8.05 (d, $J = 0.8$ Hz, 1H), 7.83-7.80 (m, 3H), 7.58 (dd, $J = 1.6$ Hz, $J = 8.4$ Hz, 1H), 7.51-7.48 (m, 4H), 7.21 (d, $J = 7.6$ Hz, 2H), 2.70 (q, $J = 7.7$ Hz, 2H), 1.27 (t, $J = 7.7$ Hz, 3H).



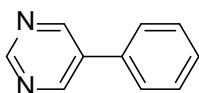
5-((4-ethylphenyl)ethynyl)-2,2'-bipyridine (40). The compound was prepared in 68% yield. $^1\text{H NMR}$ (500 MHz, Chloroform-*d*) δ [ppm] 8.81 (d, $J = 0.8$ Hz, 1H), 8.71 (d, $J = 4.7$ Hz, 1H), 8.46 (d, $J = 8.1$ Hz, 2H), 7.95 (dd, $J = 8.3$ Hz, $J = 2.2$ Hz, 1H), 7.87 (t, $J = 7.8$ Hz, 1H), 7.50 (d, $J = 8.2$ Hz, 2H), 7.36 (t, $J = 6.6$ Hz, 1H), 7.22 (d, $J = 7.8$ Hz, 2H), 2.71 (q, $J = 7.6$ Hz, 2H), 1.27 (t, $J = 7.6$ Hz, 3H).



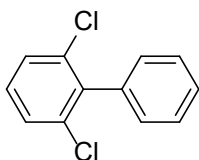
3,6-bis(phenylethynyl)-9-tosyl-9*H*-carbazole (41). The compound was prepared in 69% yield. K_3PO_4 was used instead of $\text{Cs}(\text{OH})_2 \cdot \text{H}_2\text{O}$. $^1\text{H NMR}$ (500 MHz, Chloroform-*d*) δ [ppm] 8.30 (dd, $J = 8.5$, 0.7 Hz, 2H), 8.08 (dd, $J = 1.7$, 0.7 Hz, 2H), 7.72 – 7.64 (m, 4H), 7.61 – 7.52 (m, 4H), 7.41 – 7.32 (comp, 6H), 7.16 – 7.10 (m, 2H), 2.29 (s, 3H); $^{13}\text{C NMR}$ (125 MHz, Chloroform-*d*) δ [ppm] 145.5, 138.4, 134.7, 131.8, 131.4, 130.0, 128.6, 128.5, 126.6, 126.1, 123.6, 123.3, 119.4, 115.4, 89.6, 89.2, 21.7.



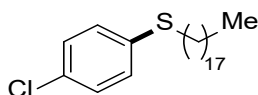
4,4'-di-tert-butyl-2-((4-ethylphenyl)ethynyl)-1,1'-biphenyl (42). The compound was prepared in 72% yield. $^1\text{H NMR}$ (500 MHz, Chloroform-*d*) δ [ppm] 7.68 (d, $J = 2.1$ Hz, 1H), 7.66 (d, $J = 8.2$ Hz, 2H), 7.51 (d, $J = 8.5$ Hz, 2H), 7.45 (dd, $J = 2.0$ Hz, $J = 8.2$ Hz, 1H), 7.41 (d, $J = 8.2$ Hz, 1H), 7.31 (d, $J = 8.1$ Hz, 2H), 7.16 (d, $J = 8.0$ Hz, 2H), 2.69 (q, $J = 7.6$ Hz, 2H), 1.42 (s, 9H), 1.41 (s, 9H), 1.27 (t, $J = 7.6$ Hz, 3H).



5-Phenylpyrimidine (43). The compound was prepared in 48% yield. Pyrimidine (0.5 mmol, 40mg), 4-iodobenzene (0.75 mmol, 153 mg), Cu_2/PCN (10 mg, 5.6 mol% Cu), Et_3COLi (0.75 mmol, 92mg) and anhydrous DMSO: DMPU= 1:1 (0.25 mL), 120 °C 18 h. $^1\text{H NMR}$ (500 MHz, Chloroform-*d*) δ 9.19 (s, 1H), 8.94 (s, 2H), 7.60 – 7.54 (m, 2H), 7.54 – 7.50 (m, 2H), 7.50 – 7.42 (m, 1H).; $^{13}\text{C NMR}$ (125 MHz, Chloroform-*d*) δ [ppm] δ 157.4, 154.8, 134.3, 134.2 129.4, 129.0, 126.9.

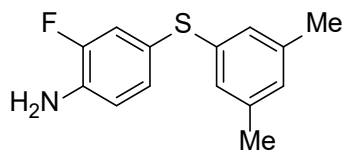


2,6-Dichloro-1,1'-biphenyl (44). The compound was prepared in 62% yield. 1,3-dichlorobenzene (0.5 mmol, 73mg), 4-iodobenzene (0.75 mmol, 153 mg), Cu_2/PCN (10 mg, 5.6 mol% Cu), Et_3COLi (0.75 mmol, 92mg) and anhydrous DMSO: DMPU = 1:1 (0.25 mL), 120 °C 18 h. $^1\text{H NMR}$ (500 MHz, Chloroform-*d*) δ [ppm] 7.49 – 7.42 (m, 3H), 7.41 (d, $J = 8.1$ Hz, 2H), 7.29 – 7.26 (m, 2H), 7.23 (dd, $J = 8.4, 7.7$ Hz, 1H); $^{13}\text{C NMR}$ (125 MHz, Chloroform-*d*) δ [ppm] δ 139.5, 137.0, 135.0, 129.5, 129.0, 128.2, 128.1, 128.0.

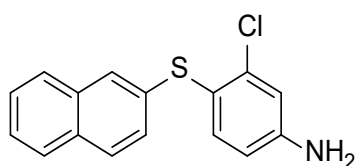


1-(4-methoxyphenyl)-1H-imidazole (45). The compound was prepared in 93% yield. $^1\text{H NMR}$ (500 MHz, Chloroform-*d*) δ [ppm] 7.24 (comp, 4H), 2.92–2.83 (m, 2H), 1.65–1.59 (m, 2H), 1.43–1.37 (m, 2H), 1.31–1.23 (comp, 28H), 0.88 (t, $J = 6.9$ Hz, 3H); $^{13}\text{C NMR}$ (125 MHz, Chloroform-*d*) δ [ppm]

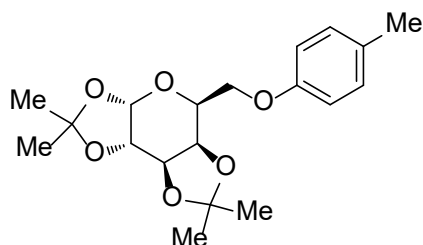
135.7, 131.7, 130.3, 129.1, 34.0, 33.5, 32.1, 29.9, 29.8, 29.8, 29.7, 29.6, 29.5, 29.3, 29.2, 28.9, 29.1, 22.9, 14.3.



4-[(3,5-dimethylphenyl)thio]-2-fluoroaniline (46). The compound was prepared in 74% yield. $^1\text{H NMR}$ (500 MHz, Chloroform-*d*) δ [ppm] 7.20 – 7.08 (m, 2H), 6.89 – 6.75 (comp, 4H), 2.28 (s, 6H); $^{13}\text{C NMR}$ (125 MHz, Chloroform-*d*) δ [ppm] 138.8, 137.7, 130.4 (d, $J = 2.5$ Hz), 128.1, 126.4, 122.5 (d, $J = 6.3$ Hz), 122.2, 120.8, 120.6, 117.3 (d, $J = 3.8$ Hz), 21.4; $^{19}\text{F NMR}$ (471 MHz, Chloroform-*d*) δ [ppm] -133.81.

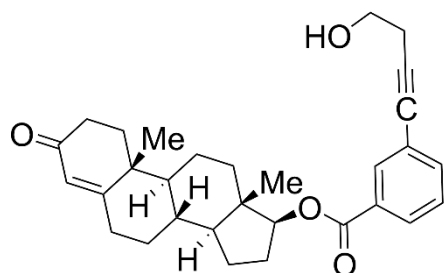


3-chloro-4-(naphthalen-2-ylthio)aniline (47). In a nitrogen-filled glovebox, an oven-dried screw-top reaction tube was equipped with a stir bar. 3-chloro-4-iodoaniline (5.0 mmol, 1.27 g), naphthalene-2-thiol (6.0 mmol, 961.2 mg), Cu_2/PCN (2.0 mg), NaOtBu (1.1 mmol, 123.4 mg) and anhydrous dioxane (40.0 mL) were sequentially added. The reaction tube was sealed with a Teflon-lined screw cap, removed from the glovebox, placed in an oil bath preheated to 100 °C and stirred for 26 h. After cooling to rt, the reaction cap was removed, and the reaction mixture was concentrated in vacuo with the aid of a rotary evaporator. The resulting residue was then purified by silica gel column chromatography to give the pure product **47** in 90% yield. (Bioorganic & medicinal chemistry letters, 14, 5263-5267 (2004).) $^1\text{H NMR}$ (500 MHz, Chloroform-*d*) δ [ppm] 7.79 – 7.75 (m, 1H), 7.72 (d, $J = 8.7$ Hz, 1H), 7.68 (dt, $J = 7.9, 1.0$ Hz, 1H), 7.57 (d, $J = 1.8$ Hz, 1H), 7.47 – 7.38 (m, 2H), 7.33 (d, $J = 8.3$ Hz, 1H), 7.28 (dd, $J = 8.6, 1.9$ Hz, 1H), 6.84 (d, $J = 2.5$ Hz, 1H), 6.56 (dd, $J = 8.4, 2.5$ Hz, 1H), 3.87 (br, 2H); $^{13}\text{C NMR}$ (125 MHz, Chloroform-*d*) δ [ppm] 148.3, 139.3, 137.3, 135.0, 133.9, 131.9, 128.7, 127.8, 127.3, 126.6, 126.4, 126.2, 125.7, 119.8, 116.4, 114.4.



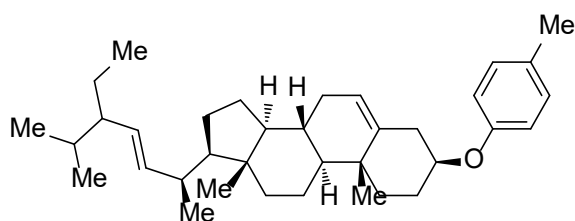
(3a*S*,5*S*,5a*R*,8a*R*,8b*S*)-2,2,7,7-tetramethyl-5-[(*p*-tolylloxy)methyl]tetrahydro-3a*H*-bis([1,3]dioxolo)[4,5-*b*:4',5'-*d*]pyran (48). The compound was prepared in 82% yield. $^1\text{H NMR}$ (500 MHz, Chloroform-*d*) δ [ppm] 7.06 (d, $J = 8.5$ Hz, 2H), 6.84 (d, $J = 8.5$ Hz, 2H), 5.57 (d, $J = 4.9$ Hz, 1H), 4.64 (dd, $J = 7.9, 2.4$ Hz, 1H), 4.51–4.28 (m, 2H), 4.27–4.03 (m, 3H), 2.28 (s, 3H), 1.52 (s, 3H),

1.47 (s, 3H), 1.36 (s, 3H), 1.34 (s, 3H); ^{13}C NMR (125 MHz, Chloroform-*d*) δ [ppm] 156.6, 130.2, 129.9, 114.8, 109.5, 108.8, 96.5, 71.1, 70.8, 70.8, 66.8, 66.3, 26.2, 26.1, 25.1, 24.6, 20.6.



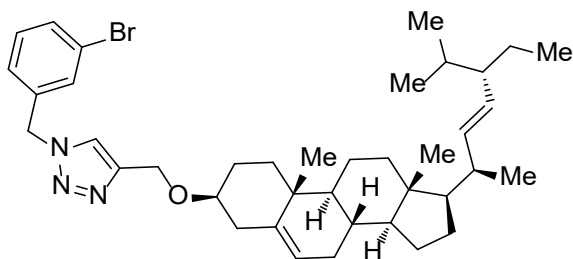
(8R,9S,10R,13S,14S,17S)-10,13-dimethyl-3-oxo-2,3,6,7,8,9,10,11,12,13,14,15,16,17-tetradecahydro-1H-cyclopenta[*a*]henanthrene-17-yl 3-(4-hydroxybut-1-yn-1-yl) benzoate (49).

The compound was prepared in 86% yield. ^1H NMR (500 MHz, Chloroform-*d*) δ [ppm] 8.04 (t, $J = 1.5$ Hz, 1H), 7.94 (dt, $J = 7.9, 1.5$ Hz, 1H), 7.62 – 7.51 (m, 1H), 7.36 (t, $J = 7.8$ Hz, 1H), 5.73 (s, 1H), 4.84 (dd, $J = 9.2, 7.7$ Hz, 1H), 3.83 (t, $J = 6.3$ Hz, 2H), 2.70 (t, $J = 6.3$ Hz, 2H), 2.46 – 2.24 (comp, 5H), 2.01 (ddd, $J = 13.4, 5.0, 3.2$ Hz, 1H), 1.86 (ddt, $J = 10.5, 4.4, 2.1$ Hz, 2H), 1.76 – 1.56 (comp, 5H), 1.48 – 1.37 (m, 2H), 1.30 – 1.22 (m, 1H), 1.19 (s, 3H), 1.16 – 1.11 (m, 1H), 1.10 – 1.01 (m, 1H), 1.00 – 0.92 (comp, 4H); ^{13}C NMR (125 MHz, Chloroform-*d*) δ [ppm] 199.6, 171.0, 165.8, 135.8, 132.6, 130.8, 128.9, 128.4, 123.9, 123.8, 87.6, 83.2, 81.5, 61.1, 53.7, 50.3, 42.9, 38.6, 36.7, 35.7, 35.4, 33.9, 32.8, 31.5, 27.6, 23.8, 23.6, 20.6, 17.4, 12.3.

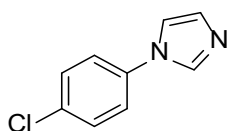


(3S,8S,9S,10R,13R,14S,17R)-17-((2S,E)-5-ethyl-6-methylhept-3-en-2-yl)-10,13-dimethyl-3-(*p*-tolylloxy)-2,3,4,7,8,9,10,11,12,13,14,15,16,17-tetradecahydro-1H-cyclopenta[*a*]phenanthrene (50).

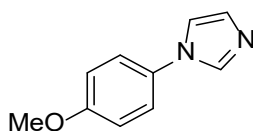
The compound was prepared in 50% yield. 100°C was used. ^1H NMR (500 MHz, Chloroform-*d*) δ [ppm] 7.03 (d, $J = 8.4$ Hz, 2H), 6.73 (d, $J = 8.4$ Hz, 2H), 5.36 – 5.34 (m, 1H), 5.17 – 5.13 (m, 1H), 5.04 – 4.99 (m, 1H), 3.56 – 3.50 (m, 1H), 2.32 – 2.21 (comp, 5H), 2.06 – 1.92 (comp, 3H), 1.89 – 1.78 (m, 2H), 1.74 – 1.67 (m, 2H), 1.57 – 1.49 (comp, 6H), 1.48 – 1.40 (comp, 3H), 1.28 – 1.25 (m, 2H), 1.18 – 1.09 (comp, 3H), 1.02 (d, $J = 6.6$ Hz, 3H), 1.01 (s, 3H), 0.85 (d, $J = 6.4$ Hz, 3H), 0.80 (d, $J = 6.8$ Hz, 6H), 0.70 (s, 3H); ^{13}C NMR (125 MHz, Chloroform-*d*) δ [ppm] 153.4, 140.7, 138.3, 130.0, 129.8, 129.3, 121.8, 115.1, 71.9, 56.9, 55.9, 51.3, 50.2, 42.3, 42.2, 40.5, 39.7, 37.3, 36.5, 31.9, 31.9, 31.7, 28.9, 25.4, 24.4, 21.2, 21.1, 20.5, 19.4, 18.9, 12.3, 12.1.



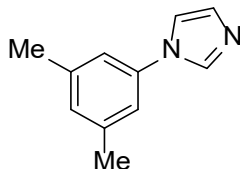
1-(3-bromobenzyl)-4-((((3*S*,8*S*,9*S*,10*R*,13*R*,14*S*,17*R*)-17-((2*R*,5*S*,*E*)-5-ethyl-6-methylhept-3-en-2-yl)-10,13-dimethyl-2,3,4,7,8,9,10,11,12,13,14,15,16,17-tetradecahydro-1*H*-cyclopenta[*a*]henanthrene-3-yl)oxy)methyl)-1*H*-1,2,3-triazole (51). An oven-dried screw-top reaction tube was equipped with a stir bar. 1-(azidomethyl)-3-bromobenzene (0.24 mmol, 50.9 mg), alkyne (0.20 mmol, 90.1 mg), Cu_g/PCN (1.0 mg), and CH₃CN (1.0 mL), H₂O (1.0 mL) were sequentially added. The reaction tube was sealed with a Teflon-lined screw cap, placed in an oil bath preheated to 60 °C and stirred for 12 h. After cooling to rt, the reaction cap was removed. And the reaction mixture was washed with brine, extracted with ethyl acetate (10 mL X 3). Then the organic phase was collected, dry with Na₂SO₄, concentrated in vacuo with the aid of a rotary evaporator. The resulting residue was then purified by silica gel column chromatography to give the pure product **51** in 86% yield. ¹H NMR (500 MHz, Chloroform-*d*) δ [ppm] 7.50 (h, *J* = 1.8 Hz, 2H), 7.44 (d, *J* = 1.8 Hz, 1H), 7.31 – 7.17 (m, 2H), 5.49 (s, 2H), 5.35 (dd, *J* = 4.8, 2.7 Hz, 1H), 5.17 (dd, *J* = 15.2, 8.4 Hz, 1H), 5.03 (dd, *J* = 15.2, 8.4 Hz, 1H), 4.69 (s, 2H), 3.32 (tt, *J* = 11.2, 4.5 Hz, 1H), 2.40 (ddd, *J* = 13.1, 4.8, 2.2 Hz, 1H), 2.32 – 2.17 (m, 1H), 2.12 – 1.83 (comp, 5H), 1.72 (s, 2H), 1.62 – 1.36 (comp, 9H), 1.35 – 1.12 (comp, 5H), 1.07 – 1.03 (comp, 4H), 1.01 (s, 3H), 0.89 – 0.78 (comp, 9H), 0.71 (s, 3H); ¹³C NMR (75 MHz, Chloroform-*d*) δ [ppm] 146.8, 140.7, 138.4, 136.9, 132.0, 131.2, 130.8, 129.4, 126.8, 123.2, 122.3, 122.0, 79.2, 61.8, 57.0, 56.1, 53.5, 51.4, 50.3, 42.3, 40.6, 39.8, 39.1, 37.3, 37.0, 32.03, 32.01, 29.1, 28.4, 25.5, 24.5, 21.4, 21.2, 21.18, 19.5, 19.1, 12.4, 12.2.



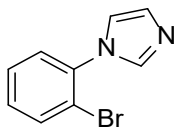
1-(4-chlorophenyl)-1*H*-imidazole (52). The compound was prepared in 95% yield. ¹H NMR (500 MHz, Chloroform-*d*) δ [ppm] 7.81 (s, 1H), 7.43 (d, *J* = 8.7 Hz, 2H), 7.31 (d, *J* = 8.7 Hz, 2H), 7.23 (s, 1H), 7.19 (s, 1H); ¹³C NMR (125 MHz, Chloroform-*d*) δ [ppm] 135.9, 135.6, 133.3, 130.8, 130.1, 122.8, 118.3



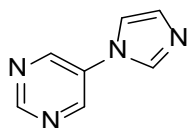
1-(4-methoxyphenyl)-1*H*-imidazole (53). The compound was prepared in 83% yield. ¹H NMR (500 MHz, Chloroform-*d*) δ [ppm] 7.77 (s, 1H), 7.30 (d, *J* = 8.9 Hz, 2H), 7.21 (s, 1H), 7.19 (s, 1H), 6.98 (d, *J* = 8.8 Hz, 2H), 3.85 (s, 3H); ¹³C NMR (125 MHz, Chloroform-*d*) δ [ppm] 159.1, 136.2, 130.9, 130.2, 123.4, 119.0, 115.1, 55.8.



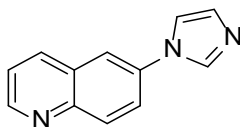
1-(3,5-dimethylphenyl)-1*H*-imidazole (54). The compound was prepared in 90% yield. ¹H NMR (500 MHz, Chloroform-*d*) δ [ppm] 7.83 (s, 1H), 7.26 (s, 1H), 7.18 (s, 1H), 7.00 (s, 3H), 2.38 (s, 6H); ¹³C NMR (125 MHz, Chloroform-*d*) δ [ppm] 139.9, 137.4, 135.8, 130.2, 129.2, 119.5, 118.5, 21.5.



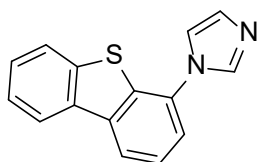
1-(2-bromophenyl)-1*H*-imidazole (55). The compound was prepared in 70% yield. ¹H NMR (500 MHz, Chloroform-*d*) δ [ppm] 7.75 – 7.70 (m, 1H), 7.67 (s, 1H), 7.46 – 7.39 (m, 1H), 7.36 – 7.29 (m, 2H), 7.20 (s, 1H), 7.13 (s, 1H); ¹³C NMR (125 MHz, Chloroform-*d*) δ [ppm] 137.7, 136.9, 134.1, 130.2, 129.5, 128.6, 128.2, 120.7, 120.1.



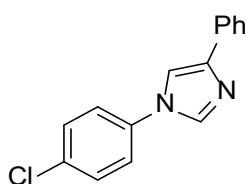
5-(1*H*-imidazol-1-yl)pyrimidine (56). The compound was prepared in 79% yield. ¹H NMR (500 MHz, Chloroform-*d*) δ [ppm] 9.25 (s, 1H), 8.89 (s, 2H), 7.92 (s, 1H), 7.34 (s, 2H); ¹³C NMR (125 MHz, Chloroform-*d*) δ [ppm] 157.6, 149.7, 135.5, 132.1, 117.9, 109.5.



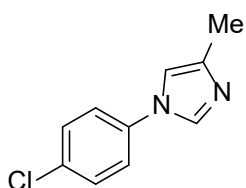
6-(1*H*-imidazol-1-yl)quinoline (57). The compound was prepared in 93% yield. ¹H NMR (500 MHz, Chloroform-*d*) δ [ppm] 8.95 (dd, *J* = 4.2, 1.7 Hz, 1H), 8.27 – 8.16 (comp, 2H), 7.99 (s, 1H), 7.83 – 7.74 (m, 2H), 7.48 (dd, *J* = 8.3, 4.2 Hz, 1H), 7.41 (t, *J* = 1.4 Hz, 1H), 7.26 (s, 1H); ¹³C NMR (125 MHz, Chloroform-*d*) δ [ppm] 151.1, 147.1, 136.0, 135.9, 135.3, 131.9, 131.0, 128.7, 123.8, 122.5, 118.8, 118.5.



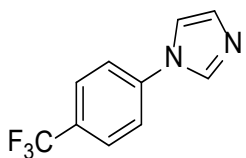
1-(dibenzo[*b,d*]thiophen-4-yl)-1*H*-imidazole (58). The compound was prepared in 74% yield. ^1H NMR (500 MHz, Chloroform-*d*) δ [ppm] 8.25 – 8.16 (m, 2H), 7.98 (s, 1H), 7.90 – 7.80 (m, 1H), 7.57 (t, $J = 7.8$ Hz, 1H), 7.54 – 7.49 (m, 2H), 7.46 (s, 1H), 7.43 (dd, $J = 7.6, 1.0$ Hz, 1H), 7.32 (s, 1H); ^{13}C NMR (125 MHz, Chloroform-*d*) δ [ppm] 139.2, 138.1, 136.9, 135.4, 134.7, 132.8, 130.3, 127.8, 125.7, 125.2, 123.0, 122.24, 122.18, 121.3, 119.4.



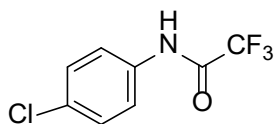
1-(4-chlorophenyl)-4-phenyl-1*H*-imidazole (59). The compound was prepared in 92% yield. ^1H NMR (500 MHz, Chloroform-*d*) δ [ppm] 7.86 (d, $J = 1.4$ Hz, 1H), 7.83 (dd, $J = 8.2, 1.4$ Hz, 2H), 7.51 (s, 1H), 7.46 (dd, $J = 8.5, 1.6$ Hz, 2H), 7.43 – 7.39 (m, 2H), 7.37 (dd, $J = 8.6, 1.9$ Hz, 2H), 7.32 – 7.27 (m, 1H); ^{13}C NMR (125 MHz, Chloroform-*d*) δ [ppm] 143.5, 135.8, 135.7, 133.6, 133.2, 130.1, 128.8, 127.4, 125.0, 122.5, 113.7.



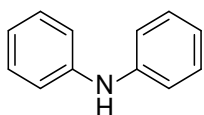
1-(4-chlorophenyl)-4-methyl-1*H*-imidazole (60). The compound was prepared in 90% yield. ^1H NMR (500 MHz, Chloroform-*d*) δ [ppm] 7.71 (d, $J = 1.4$ Hz, 1H), 7.42 (d, $J = 8.9$ Hz, 2H), 7.28 (d, $J = 8.9$ Hz, 2H), 6.96 (t, $J = 1.2$ Hz, 1H), 2.28 (d, $J = 1.0$ Hz, 3H); ^{13}C NMR (125 MHz, Chloroform-*d*) δ [ppm] 139.9, 136.9, 136.1, 135.1, 134.6, 134.4, 132.8, 130.3, 130.0, 129.8, 127.8, 126.9, 122.3, 114.6, 13.8, 9.9.



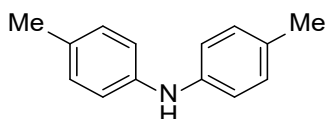
1-(4-(trifluoromethyl)phenyl)-1*H*-imidazole (61). The compound was prepared in 90% yield. ^1H NMR (500 MHz, Chloroform-*d*) δ [ppm] 7.93 (s, 1H), 7.76 (d, $J = 8.3$ Hz, 2H), 7.53 (d, $J = 8.3$ Hz, 2H), 7.35 (s, 1H), 7.26 (s, 1H); ^{13}C NMR (125 MHz, Chloroform-*d*) δ [ppm] 140.16, 135.80, 131.36, 129.7 (q, $J = 33.8$ Hz, 1C), 127.4 (q, $J = 3.8$ Hz, 1C), 124.84, 121.45, 118.13; ^{19}F NMR (471 MHz, Chloroform-*d*) δ -62.52.



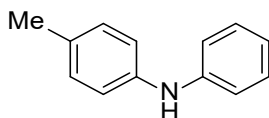
N-(4-chlorophenyl)-2,2,2-trifluoroacetamide (62). The compound was prepared in 73% yield. NaOtBu was used. $^1\text{H NMR}$ (500 MHz, Chloroform-*d*) δ [ppm] 7.93 (br, 1H), 7.53 (d, $J = 8.9$ Hz, 2H), 7.37 (d, $J = 8.9$ Hz, 2H); $^{13}\text{C NMR}$ (125 MHz, Chloroform-*d*) δ [ppm] 154.8 (d, $J = 37.5$ Hz), 133.6, 131.7, 129.5, 121.8, 115.6 (q, $J = 288.6$ Hz); $^{19}\text{F NMR}$ (471 MHz, Chloroform-*d*) δ [ppm] -75.68.



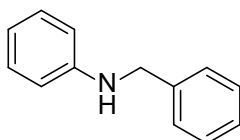
diphenylamine (63). The compound was prepared in 63% yield. $^1\text{H NMR}$ (500 MHz, Chloroform-*d*) δ [ppm] 7.29-7.26 (m, 4H), 7.10-7.08 (m, 4H), 6.95-6.92 (m, 2H).



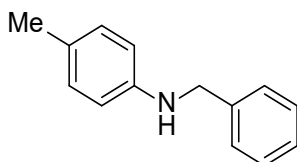
di-*p*-tolylamine (64). The compound was prepared in 68% yield. $^1\text{H NMR}$ (500 MHz, Chloroform-*d*) δ [ppm] 7.42 (d, $J = 8.1$ Hz, 4H), 7.30 (d, $J = 8.1$ Hz, 4H), 2.64 (s, 6H).



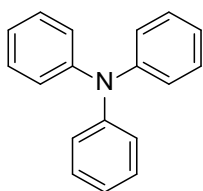
4-methyl-N-phenylaniline (65). The compound was prepared in 72% yield. $^1\text{H NMR}$ (500 MHz, Chloroform-*d*) δ [ppm] 7.25 (t, $J = 7.4$ Hz, 2H), 7.10 (d, $J = 8.0$ Hz, 2H), 7.03 (m, 4H), 6.89 (t, $J = 7.4$ Hz, 1H), 2.31 (s, 1H).



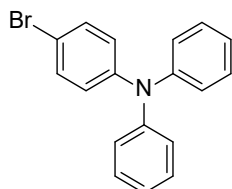
N-benzylaniline (66). The compound was prepared in 81% yield. $^1\text{H NMR}$ (500 MHz, Chloroform-*d*) δ [ppm] 7.38-7.33 (m, 4H), 7.29 (d, $J = 7.1$ Hz, 1H), 7.20 (m, 2H), 6.74 (t, $J = 8.0$ Hz, 1H), 6.68 (d, $J = 8.0$ Hz, 2H), 2.34 (s, 2H).



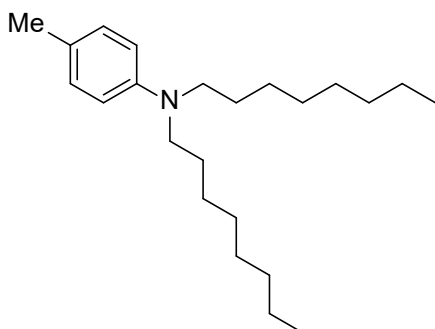
N-benzyl-4-methylaniline (67). The compound was prepared in 79% yield. $^1\text{H NMR}$ (500 MHz, Chloroform-*d*) δ [ppm] 7.38-7.32 (m, 4H), 7.29 (d, $J = 7.1$ Hz, 1H), 7.00 (d, $J = 8.1$ Hz, 2H), 6.59 (d, $J = 8.1$ Hz, 2H), 4.32 (s, 2H), 2.24 (s, 3H).



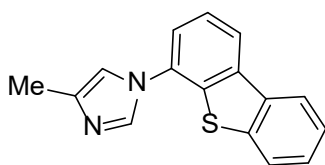
triphenylamine (68). The compound was prepared in 76% yield. $^1\text{H NMR}$ (500 MHz, Chloroform-*d*) δ [ppm] 7.26-7.23 (m, 6H), 7.10-7.08 (m, 6H), 7.02-6.99 (m, 3H).



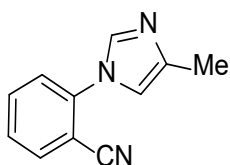
4-bromo-*N,N*-diphenylaniline (69). The compound was prepared in 71% yield. $^1\text{H NMR}$ (500 MHz, Chloroform-*d*) δ [ppm] 7.33 (m, 2H), 7.27-7.24 (m, 4H), 7.08 (m, 4H), 7.05-7.02 (m, 2H).



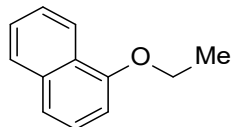
4-methyl-*N,N*-dioctylaniline (70). The compound was prepared in 72% yield. $^1\text{H NMR}$ (300 MHz, Chloroform-*d*) δ [ppm] 7.02 (d, $J = 8.2$ Hz, 2H), 6.58 (d, $J = 8.2$ Hz, 2H), 3.20 (t, $J = 7.6$ Hz, 4H), 2.23 (s, 1H), 1.29 (br, 24H), 0.88 (br, 6H).



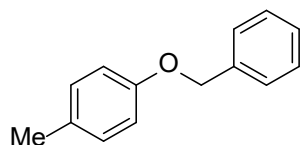
1-(dibenzo[*b,d*]thiophen-4-yl)-4-methyl-1*H*-imidazole (71). The compound was prepared in 78% yield. $^1\text{H NMR}$ (500 MHz, Chloroform-*d*) δ [ppm] 8.22 – 8.13 (m, 2H), 7.90 – 7.81 (m, 2H), 7.58 – 7.48 (m, 3H), 7.40 (dd, $J = 7.6, 1.0$ Hz, 1H), 7.18 (s, 1H), 2.37 (s, 3H); $^{13}\text{C NMR}$ (125 MHz, Chloroform-*d*) δ [ppm] 139.5, 139.2, 138.1, 135.9, 135.4, 134.4, 132.9, 127.7, 125.6, 125.1, 122.9, 122.1, 121.9, 120.9, 115.7, 13.9.



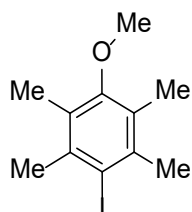
2-(4-methyl-1H-imidazol-1-yl)benzonitrile (72). The compound was prepared in 90% yield. $^1\text{H NMR}$ (500 MHz, Chloroform-*d*) δ [ppm] 7.78 (d, $J = 7.8$ Hz, 1H), 7.73 (s, 1H), 7.70 (t, $J = 7.9$ Hz, 1H), 7.47 (t, $J = 7.7$ Hz, 1H), 7.41 (d, $J = 8.2$ Hz, 1H), 7.05 (s, 1H), 2.28 (s, 3H); $^{13}\text{C NMR}$ (125 MHz, Chloroform-*d*) δ [ppm] 140.9, 139.5, 135.9, 134.6, 134.4, 128.1, 125.4, 116.1, 116.0, 107.6, 13.7.



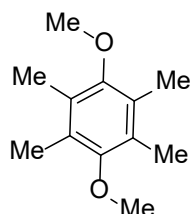
1-ethoxynaphthalene (73). The compound was prepared in 93% yield. $^1\text{H NMR}$ (500 MHz, Chloroform-*d*) δ [ppm] 8.34–8.32 (m, 1H), 7.82–7.80 (m, 1H), 7.52–7.46 (m, 2H), 7.45–7.43 (m, 1H), 7.40–7.37 (m, 1H), 6.82 (d, $J = 7.4$ Hz, 1H), 4.23 (q, $J = 7.0$ Hz, 2H), 1.57 (t, $J = 7.0$ Hz, 3H); $^{13}\text{C NMR}$ (125 MHz, Chloroform-*d*) δ [ppm] 154.9, 134.6, 127.5, 126.4, 126.0, 125.9, 125.2, 122.2, 120.1, 104.7, 63.8, 15.0.



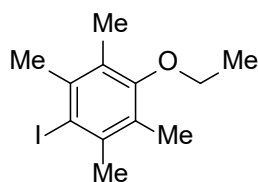
1-(benzyloxy)-4-methylbenzene (74). The compound was prepared in 87% yield. $^1\text{H NMR}$ (500 MHz, Chloroform-*d*) δ [ppm] 7.45 (d, $J = 7.2$ Hz, 2H), 7.42–7.38 (m, 2H), 7.36–7.31 (m, 1H), 7.11 (d, $J = 8.2$ Hz, 2H), 6.94–6.86 (m, 2H), 5.06 (s, 2H), 2.31 (s, 3H); $^{13}\text{C NMR}$ (125 MHz, Chloroform-*d*) δ [ppm] 156.8, 137.4, 130.3, 130.0, 128.7, 128.0, 127.6, 114.8, 70.2, 20.6.



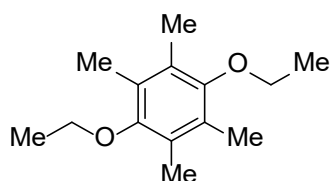
1-iodo-4-methoxy-2,3,5,6-tetramethylbenzene (75). The compound was prepared in 62% yield. $^1\text{H NMR}$ (300 MHz, Chloroform-*d*) δ [ppm] 3.64 (s, 3H), 2.48 (s, 6H), 2.29 (s, 6H).



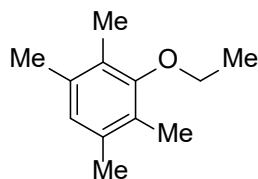
1,4-dimethoxy-2,3,5,6-tetramethylbenzene (76). The compound was prepared in 71% yield. $^1\text{H NMR}$ (300 MHz, Chloroform-*d*) δ [ppm] 3.64 (s, 6H), 2.18 (s, 12H).



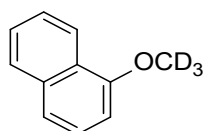
1-ethoxy-4-iodo-2,3,5,6-tetramethylbenzene (77). The compound was prepared in 70% yield. $^1\text{H NMR}$ (500 MHz, Chloroform-*d*) δ [ppm] 3.73 (q, $J = 7.0$ Hz, 2H), 2.48 (m, 6H), 2.29 (s, 6H), 1.41 (t, $J = 7.0$ Hz, 3H); $^{13}\text{C NMR}$ (125 MHz, Chloroform-*d*) δ [ppm] 155.9, 138.5, 127.9, 105.4, 68.6, 27.3, 15.7, 14.8.



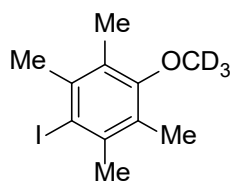
1,4-diethoxy-2,3,5,6-tetramethylbenzene (78). The compound was prepared in 82% yield. 5-equiv alcohol and 4-equiv KO*t*Bu were used. $^1\text{H NMR}$ (500 MHz, Chloroform-*d*) δ [ppm] 3.73 (q, $J = 7.0$ Hz, 4H), 2.16 (s, 12H), 1.40 (t, $J = 7.0$ Hz, 6H); $^{13}\text{C NMR}$ (125 MHz, Chloroform-*d*) δ [ppm] 151.9, 127.8, 68.4, 15.8, 13.0.



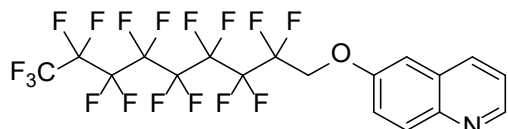
3-ethoxy-1,2,4,5-tetramethylbenzene (79). The compound was prepared in 88% yield. $^1\text{H NMR}$ (500 MHz, Chloroform-*d*) δ [ppm] 6.76 (s, 1H), 3.77 (q, $J = 7.0$ Hz, 2H), 2.22 (s, 6H), 2.18 (s, 6H), 1.43 (t, $J = 7.0$ Hz, 3H); $^{13}\text{C NMR}$ (125 MHz, Chloroform-*d*) δ [ppm] 155.8, 134.8, 126.9, 126.8, 68.3, 19.9, 15.8, 12.5.



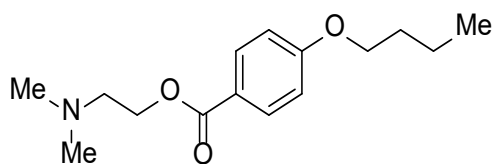
1-[α,α,α -2H3]-methoxynaphthalene (80). The compound was prepared in 90% yield. $^1\text{H NMR}$ (500 MHz, Chloroform-*d*) δ [ppm] 8.34 – 8.27 (m, 1H), 7.85 – 7.79 (m, 1H), 7.55 – 7.48 (m, 2H), 7.47 – 7.45 (m, 1H), 7.43 – 7.39 (m, 1H), 6.83 (dd, $J = 7.5, 1.1$ Hz, 1H); $^{13}\text{C NMR}$ 155.6, 134.6, 127.6, 126.5, 125.9, 125.7, 125.3, 122.1, 120.3, 103.9, 55.2 – 54.6 (m, 1C).



1-iodo-4-[α,α,α - $2H_3$]-methoxy-2,3,5,6-tetramethylbenzene (81). The compound was prepared in 60% yield. 1H NMR (500 MHz, Chloroform-*d*) δ [ppm] 2.49 (s, 6H), 2.30 (s, 6H); ^{13}C NMR 138.6, 127.7, 123.2, 105.7, 54.1 – 53.8 (m, 1C), 27.3, 14.5.

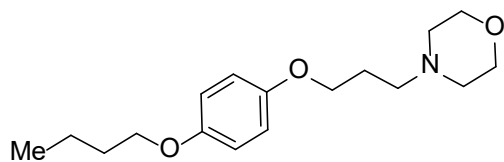


6-[(2,2,3,3,4,4,5,5,6,6,7,7,8,8,9,9,9)-heptafluorononyloxy]quinoline (82). The compound was prepared in 72% yield. 1H NMR (500 MHz, Chloroform-*d*) δ [ppm] 8.83 (dd, $J = 4.2, 1.7$ Hz, 1H), 8.06 (d, $J = 9.5$ Hz, 2H), 7.43 (dd, $J = 9.2, 2.8$ Hz, 1H), 7.39 (dd, $J = 8.2, 4.2$ Hz, 1H), 7.12 (d, $J = 2.9$ Hz, 1H), 4.59 (t, $J = 12.7$ Hz, 2H); ^{13}C NMR (125 MHz, Chloroform-*d*) δ [ppm] 155.5, 132.0, 130.3, 114.8, 111.4–106.9 (m, 1C), 65.8 (t, $J = 30$ Hz, 1C), 20.6; ^{19}F NMR (471 MHz, Chloroform-*d*) δ [ppm] ^{19}F NMR (471 MHz, Chloroform-*d*) δ -80.83 (t, $J = 10.2$ Hz), -119.27, -121.82, -121.84, -121.92, -122.73, -123.04, -126.15.

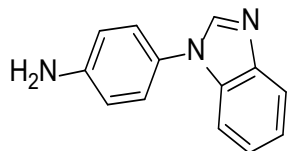


2-(dimethylamino)ethyl 4-butoxybenzoate (91). In a nitrogen-filled glovebox, an oven-dried screw-top reaction tube was equipped with a stir bar. 4-iodobenzoic acid (1.0 mmol, 248.0 mg), 2-(dimethylamino)-ethanol (1.1 mmol, 202.4 mg), DMAP (0.05 mmol, 6.1 mg), EDCI (1.1 mmol, 210.9 mg), and dichloromethane (10.0 mL) were sequentially added. The reaction tube was sealed with a Teflon-lined screw cap and stirred at room temperature overnight. After that, the reaction mixture was filtered by celite, concentrated in vacuo with the aid of a rotary evaporator and dried under vacuum. The resulting residue was used in the next step without further purification. In a nitrogen-filled glovebox, an oven-dried screw-top reaction tube was equipped with a stir bar. *N*-Butanol (2.0 mmol, 148.2 mg), Cu_g/PCN (1.0 mg), $KOtBu$ (1.5 mmol, 168.3 mg) and anhydrous dioxane (5.0 mL) were sequentially added. The aforementioned residue was added the anhydrous dioxane (5.0 mL), then transferred to the screw-top reaction tube. The reaction tube was sealed with a Teflon-lined screw cap, removed from the glovebox, placed in an oil bath preheated to 80 °C and stirred for 18 h. After cooling to rt, the reaction cap was removed, and the reaction mixture was concentrated in vacuo with the aid of a rotary evaporator. The resulting residue was then purified by silica gel column chromatography to give the pure product **91** in 73% yield over two steps. 1H NMR (500 MHz, Chloroform-*d*) δ [ppm] 7.98 (d, $J = 8.8$ Hz, 2H),

6.93 (d, $J = 8.8$ Hz, 2H), 4.29 (t, $J = 6.6$ Hz, 2H), 4.13 (t, $J = 5.6$ Hz, 2H), 2.78 (t, $J = 5.6$ Hz, 2H), 2.37 (s, 6H), 1.72 (dt, $J = 8.3, 6.7$ Hz, 2H), 1.53 – 1.40 (m, 2H), 0.97 (t, $J = 7.3$ Hz, 3H); $^{13}\text{C NMR}$ (125 MHz, Chloroform- d) δ [ppm] 166.6, 162.6, 131.7, 123.2, 114.3, 66.2, 64.7, 58.2, 45.9, 31.0, 19.4, 13.9.

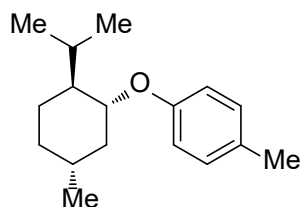


4-(3-(4-butoxyphenoxy)propyl)morpholine (92). In a nitrogen-filled glovebox, an oven-dried screw-top reaction tube was equipped with a stir bar. 4-iodophenol (1.0 mmol, 220.0 mg), $n\text{BuI}$ (1.1 mmol, 202.4 mg), $\text{KO}t\text{Bu}$ (1.1 mmol, 123.4 mg) and anhydrous dioxane (10.0 mL) were sequentially added. The reaction tube was sealed with a Teflon-lined screw cap, removed from the glovebox, placed in an oil bath preheated to 60 °C and stirred for 6 h. After cooling to rt, the reaction tube was transferred to the glovebox, the reaction cap was removed, and Cu_g/PCN (1.0 mg), 3-morpholinopropan-1-ol (1.2 mmol, 174.2 mg), $\text{KO}t\text{Bu}$ (1.5 mmol, 168.3 mg) were sequentially added. The reaction tube was sealed with a Teflon-lined screw cap, removed from the glovebox, placed in an oil bath preheated to 80 °C and stirred for 18 h. After cooling to rt, the reaction cap was removed, and the reaction mixture was concentrated in vacuo with the aid of a rotary evaporator. The resulting residue was then purified by silica gel column chromatography to give the pure product **92** in 80% yield over two steps. $^1\text{H NMR}$ (500 MHz, Chloroform- d) δ [ppm] 6.82 – 6.81 (comp, 4H), 3.96 (t, $J = 6.3$ Hz, 2H), 3.90 (t, $J = 6.5$ Hz, 2H), 3.72 (t, $J = 4.7$ Hz, 4H), 2.54 – 2.49 (m, 2H), 2.46 (t, $J = 4.6$ Hz, 4H), 1.98 – 1.89 (m, 2H), 1.80 – 1.68 (m, 2H), 1.54 – 1.41 (m, 2H), 0.96 (t, $J = 7.4$ Hz, 3H); $^{13}\text{C NMR}$ (125 MHz, Chloroform- d) δ [ppm] 153.5, 153.1, 115.54, 115.53, 68.5, 67.1, 66.9, 55.77, 53.9, 31.6, 26.7, 19.4, 14.0.

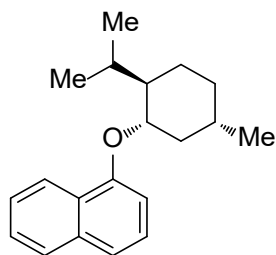


4-(1H-benzo[d]imidazol-1-yl)aniline (93). In a nitrogen-filled glovebox, an oven-dried screw-top reaction tube was equipped with a stir bar. 1H-benzo[d]imidazole (3.0 mmol, 354.3 mg), 1,4-diodobenzene (3.3 mmol, 1.09 g), Cu_g/PCN (10.0 mg), K_3PO_4 (6.0 mmol, 1.27 g) and anhydrous DMSO (10.0 mL) were sequentially added. The reaction tube was sealed with a Teflon-lined screw cap, placed in an oil bath preheated to 110 °C and stirred for 28 h. After cooling to rt, the reaction cap was removed. Then trifluoroacetamide (4.5 mmol, 508.7 mg) was added to the aforementioned screw-top reaction tube. The reaction tube was sealed with a Teflon-lined screw cap, placed in an oil bath preheated to 110 °C and stirred for further 28 h. After cooling to rt, the reaction tube was removed from the glovebox, the most DMSO was removed in vacuo, and the residue was filtered by celite, and washed with ethyl acetate. Then the organic phase was collected and concentrated in vacuo. After that, the methanol (10 mL) and H_2O (10 mL) were added to the residue and the mixture was heated to 75 °C for 10 h. After the reaction completed, the reaction mixture was quenched with saturated NH_4Cl solution

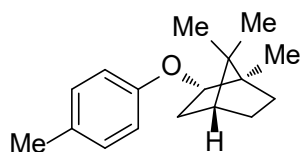
and extracted with ethyl acetate (30 mL X 3). The combined organic extract was washed with brine, dried over anhydrous MgSO₄, and concentrated under reduced pressure to give crude product. The residue was purified by chromatography on silica gel to afford the desired product **93** in 64% yield. ¹H NMR (500 MHz, Chloroform-*d*) δ [ppm] 8.04 (s, 1H), 7.90 – 7.83 (m, 1H), 7.45 (dd, *J* = 7.5, 1.9 Hz, 1H), 7.36 – 7.29 (comp, 2H), 7.25 (d, *J* = 8.6 Hz, 2H), 6.82 (d, *J* = 8.6 Hz, 2H), 3.58 (br, 2H); ¹³C NMR (125 MHz, Chloroform-*d*) δ [ppm] 146.7, 143.7, 142.8, 134.5, 127.0, 125.9, 123.5, 122.5, 120.4, 115.8, 110.6.



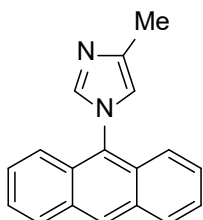
1-((1R,2S,5R)-2-isopropyl-5-methylcyclohexyl)oxy-4-methylbenzene (94). The compound was prepared in 92% yield. 100°C was used. ¹H NMR (500 MHz, Chloroform-*d*) δ [ppm] 7.08 (d, *J* = 8.5 Hz, 2H), 6.82 (d, *J* = 8.5 Hz, 2H), 3.98 (td, *J* = 10.5, 4.1 Hz, 1H), 2.29 (s, 3H), 2.24 (qd, *J* = 7.0, 2.8 Hz, 1H), 2.20–2.13 (m, 1H), 1.77–1.68 (m, 2H), 1.55–1.41 (m, 2H), 1.18–1.06 (m, 1H), 1.05–0.95 (m, 2H), 0.95–0.91 (comp, 6H), 0.79 (d, *J* = 7.0 Hz, 3H); ¹³C NMR (125 MHz, Chloroform-*d*) δ [ppm] 156.3, 130.1, 129.8, 116.1, 77.9, 48.3, 40.5, 34.7, 31.6, 26.2, 23.8, 22.3, 20.9, 20.6, 16.7.



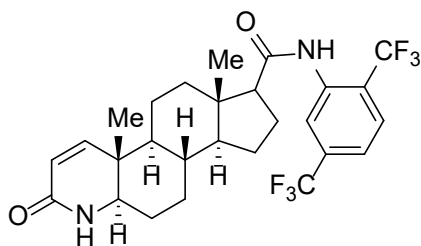
1-((1S,2R,5S)-2-isopropyl-5-methylcyclohexyl)oxy-naphthalene (95). The compound was prepared in 86% yield. 100°C was used. ¹H NMR (500 MHz, Chloroform-*d*) δ [ppm] 8.32 – 8.26 (m, 1H), 7.79 (dd, *J* = 8.2, 1.4 Hz, 1H), 7.46 (pd, *J* = 6.9, 1.6 Hz, 2H), 7.41 – 7.34 (m, 2H), 6.85 (dd, *J* = 6.9, 1.7 Hz, 1H), 4.29 (td, *J* = 10.5, 4.1 Hz, 1H), 2.37 – 2.24 (m, 2H), 1.86 – 1.65 (comp, 3H), 1.57 – 1.49 (m, 1H), 1.23 – 1.15 (m, 1H), 1.11 (td, *J* = 12.4, 10.8 Hz, 1H), 1.02 (ddd, *J* = 13.7, 11.7, 4.2 Hz, 1H), 0.97 (d, *J* = 7.1 Hz, 3H), 0.93 (d, *J* = 6.6 Hz, 3H), 0.79 (d, *J* = 6.9, 3H); ¹³C NMR (125 MHz, Chloroform-*d*) δ [ppm] 154.0, 134.9, 127.6, 126.7, 126.4, 126.1, 125.0, 122.6, 119.7, 105.5, 77.5, 48.3, 40.1, 34.8, 31.6, 26.6, 24.1, 22.3, 21.0, 17.0.



(1*R*,2*R*,4*R*)-1,7,7-trimethyl-2-(*p*-tolxyloxy)bicyclo[2.2.1]heptane (96). The compound was prepared in 79% yield. 100°C was used. ¹H NMR (500 MHz, Chloroform-*d*) δ [ppm] 7.06 (d, *J* = 8.5 Hz, 2H), 6.76 (d, *J* = 8.5 Hz, 2H), 4.01 (dd, *J* = 7.2, 3.7 Hz, 1H), 2.28 (s, 3H), 1.90 – 1.78 (m, 2H), 1.77 – 1.71 (m, 2H), 1.64 – 1.57 (m, 1H), 1.18 – 1.09 (comp, 2H), 1.07 (s, 3H), 0.99 (s, 3H), 0.88 (s, 3H); ¹³C NMR (125 MHz, Chloroform-*d*) δ [ppm] 156.0, 129.9, 129.3, 115.4, 84.6, 49.3, 47.1, 45.5, 39.6, 34.4, 27.6, 20.6, 20.5, 20.3, 12.0.

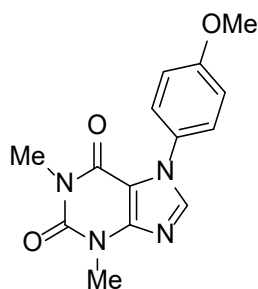


1-(anthracen-9-yl)-4-methyl-1*H*-imidazole (97). The compound was prepared in 67% yield. ¹H NMR (500 MHz, Chloroform-*d*) δ [ppm] 8.57 (s, 1H), 8.11 – 8.02 (m, 2H), 7.66 (s, 1H), 7.57 – 7.44 (comp, 6H), 6.98 (s, 1H), 2.45 (s, 3H); ¹³C NMR (125 MHz, Chloroform-*d*) δ [ppm] 138.9, 138.8, 131.4, 129.3, 128.9, 128.5, 128.4, 127.6, 126.0, 122.8, 119.4, 13.9.

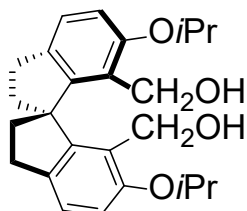


17β-*N*-[2,5-Bis(trifluoromethyl)phenyl]carbamoyl-4-aza-5α-androst-1-ene-3-one (Dutasteride, 98): In a nitrogen-filled glovebox, an oven-dried screw-top reaction tube was equipped with a stir bar. 3-Oxo-4-aza-5*r*-androst-1-ene-17-β-carboxamide (0.5 mmol, 158 mg), 2-Bromo-1,4-bis(trifluoromethyl)benzene (0.75 mmol, 219 mg), Cu_g/PCN (2.5 mg), K₃PO₄ (1.0 mmol, 213 mg) and anhydrous DMSO (2.5 mL) were sequentially added. The reaction tube was sealed with a Teflon-lined screw cap, placed in an oil bath preheated to 120 °C and stirred for 24 h. After cooling to rt, the reaction cap was removed. The most DMSO was removed in vacuo, and the residue was washed with H₂O, and extracted with ethyl acetate (30 mL X 3). The combined organic extract was washed with brine, dried over anhydrous NaSO₄, and concentrated under reduced pressure. Then the residue purified by chromatography on silica gel (Hexane: EA= 8:1 to EA) to afford the desired product **98** in 62% yield. ¹H NMR (500 MHz, Chloroform-*d*) δ [ppm] 1H NMR (500 MHz, Chloroform-*d*) δ 8.76 (s, 1H), 7.73 (d, *J* = 8.2 Hz, 1H), 7.50 (s, 1H), 7.44 (d, *J* = 8.3 Hz, 1H), 6.79 (d, *J* = 9.8 Hz, 1H), 5.81 (d, *J* = 9.8 Hz, 1H), 5.70 (s, br, 1H), 3.35 (t, *J* = 8.7 Hz, 1H), 2.36 (td, *J* = 9.2, 2.5 Hz, 1H), 2.33 – 2.22 (m, 1H), 2.09-2.14 (m, 1H), 1.95 – 1.81 (m, 2H), 1.79 – 1.74 (m, 3H), 1.56-1.67 (m, 2H), 1.31- 1.44 (m, 2H), 1.27 – 1.22 (m, 1H), 1.11 – 1.04 (m, 2H), 0.98 (s, 3H), 0.78 (s, 3H); ¹³C NMR (125 MHz, Chloroform-*d*) δ

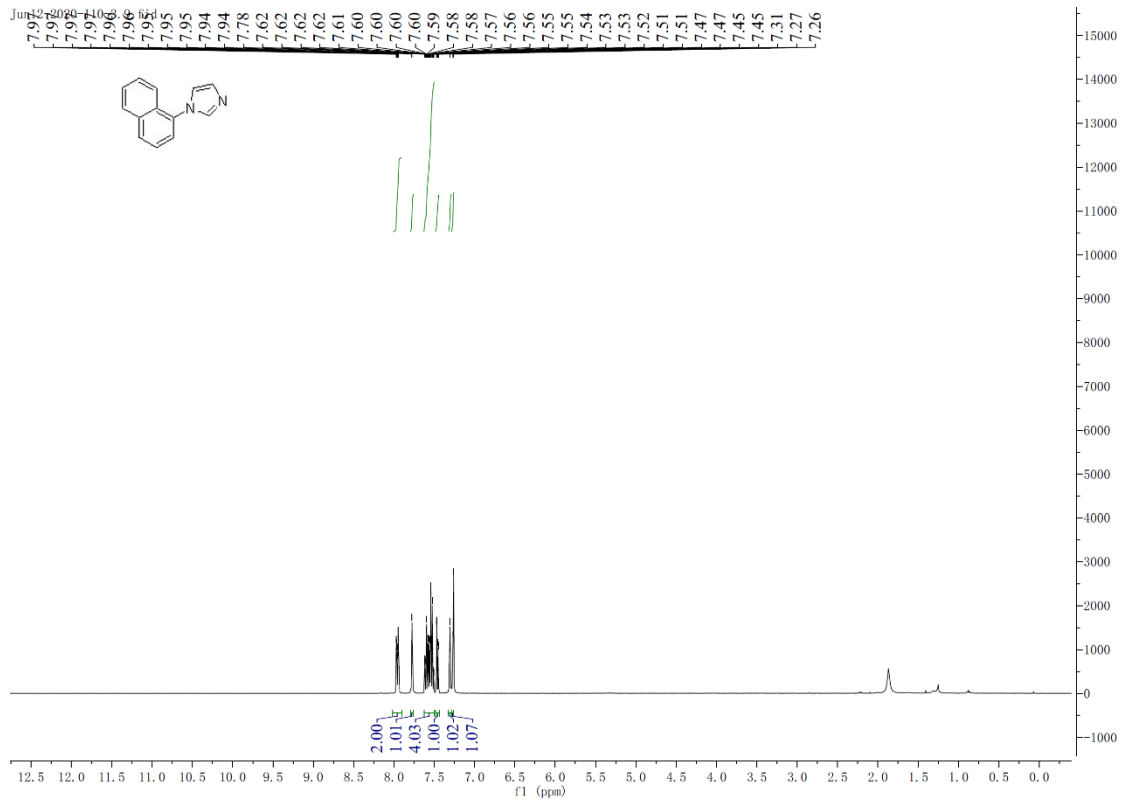
[ppm] δ 171.3, 150.8, 136.4, 135.2, 126.8 (q, $J=5.5\text{Hz}$), 124.5, 123.1, 122.4, 121.6, 120.4 (q, $J=3.8\text{Hz}$), 120.3 (q, $J=3.8\text{Hz}$), 120.2, 59.6, 58.4, 55.7, 47.5, 44.82 39.4, 37.9, 35.3, 29.4, 25.9, 24.2, 23.6, 21.2, 13.4, 12.0. ^{19}F NMR (471 MHz, Chloroform-*d*) δ -61.00, -63.38.



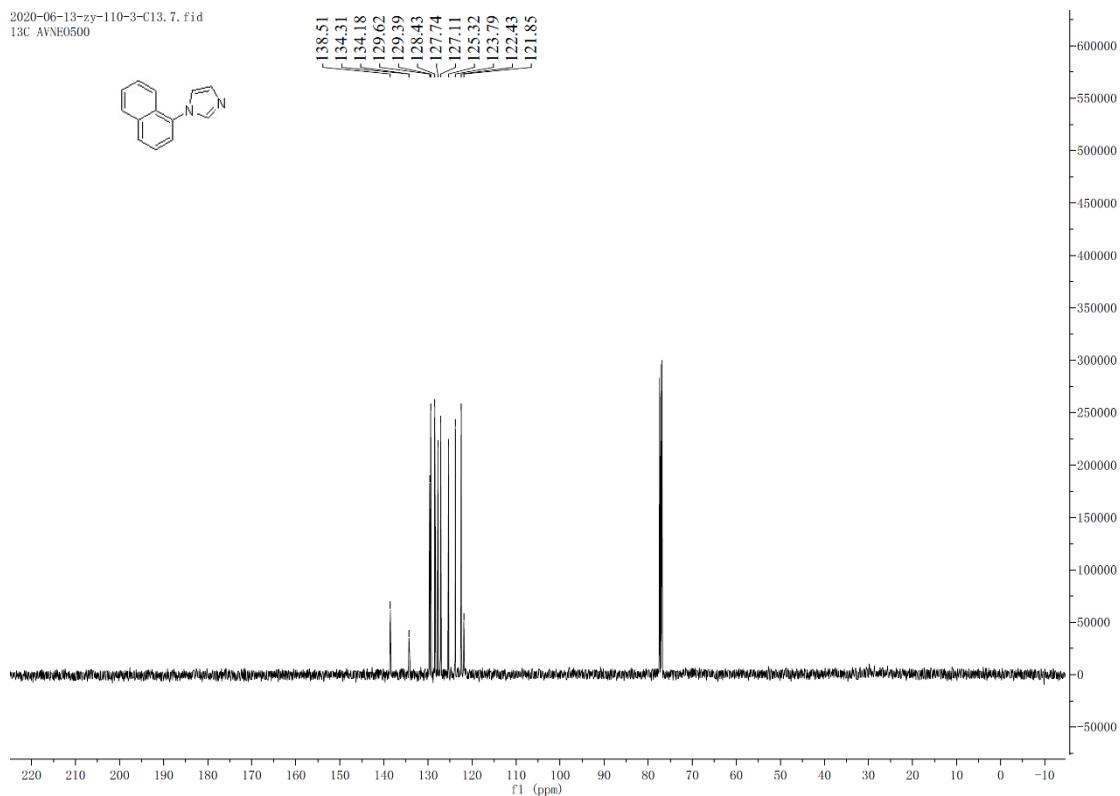
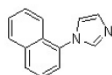
7-(4-methoxyphenyl)-1,3-dimethyl-1H-purine-2,6(3H,7H)-dione (99): In a nitrogen-filled glovebox, an oven-dried screw-top reaction tube was equipped with a stir bar. Theophylline (1 mmol, 354.3 mg), 1-bromo-4-methoxybenzene (1.5 mmol, 1.09 g), Cu_g/PCN (1.4 mg), K_3PO_4 (2.0 mmol, 1.27 g) and anhydrous DMSO (5.0 mL) were sequentially added. The reaction tube was sealed with a Teflon-lined screw cap, placed in an oil bath preheated to 120 °C and stirred for 24 h. After cooling to rt, the reaction cap was removed. The most DMSO was removed in vacuo, and the residue was purified by chromatography on silica gel (CH_2Cl_2 : MeOH=20:1) to afford the desired product **99** in 68% yield. ^1H NMR (500 MHz, Chloroform-*d*) δ [ppm] 7.68 (s, 1H), 7.40 – 7.34 (m, 2H), 7.03 – 6.96 (m, 2H), 3.85 (s, 3H), 3.64 (s, 3H), 3.38 (s, 3H).; ^{13}C NMR (125 MHz, Chloroform-*d*) δ [ppm] δ 160.0, 154.4, 151.6, 149.3, 141.2, 127.7, 126.4, 114.3, 107.4, 55.6, 29.9, 28.1.



(S)-(6,6'-diisopropoxy-2,2',3,3'-tetrahydro-1,1'-spirobi[indene]-7,7'-diyl)dimethanol (100): In a nitrogen-filled glovebox, an oven-dried screw-top reaction tube was equipped with a stir bar. Diiodination compound (532.2 mg, 1.0 mmol), Cu_g/PCN (20 mg, 5.6 mol% Cu), KO^tBu (336.6 mg, 3.0 mmol) and anhydrous isopropanol (5 mL) were sequentially added. The reaction tube was sealed with a Teflon-lined screw cap, removed from the glovebox, placed in an oil bath preheated to 80 °C and stirred for 48 h. After cooling to room temperature (rt), the reaction cap was removed, and the reaction mixture was concentrated in vacuo with the aid of a rotary evaporator. The resulting residue was then purified by silica gel column chromatography to give 206.2 mg (52% yield) of product **100**. ^1H -NMR (400 MHz, CDCl_3) δ 7.12 (d, $J=8.4$ Hz, 2H), 6.80 (d, $J=8.4$ Hz, 2H), 4.58 (sept, $J=6.0$ Hz, 2H), 4.26 (s, 4H), 2.58 (brs, 2H), 2.93-2.89 (m, 4H), 2.32-2.67 (m, 2H), 2.06-1.98 (m, 2H), 1.35 (d, $J=6.4$ Hz, 12H).

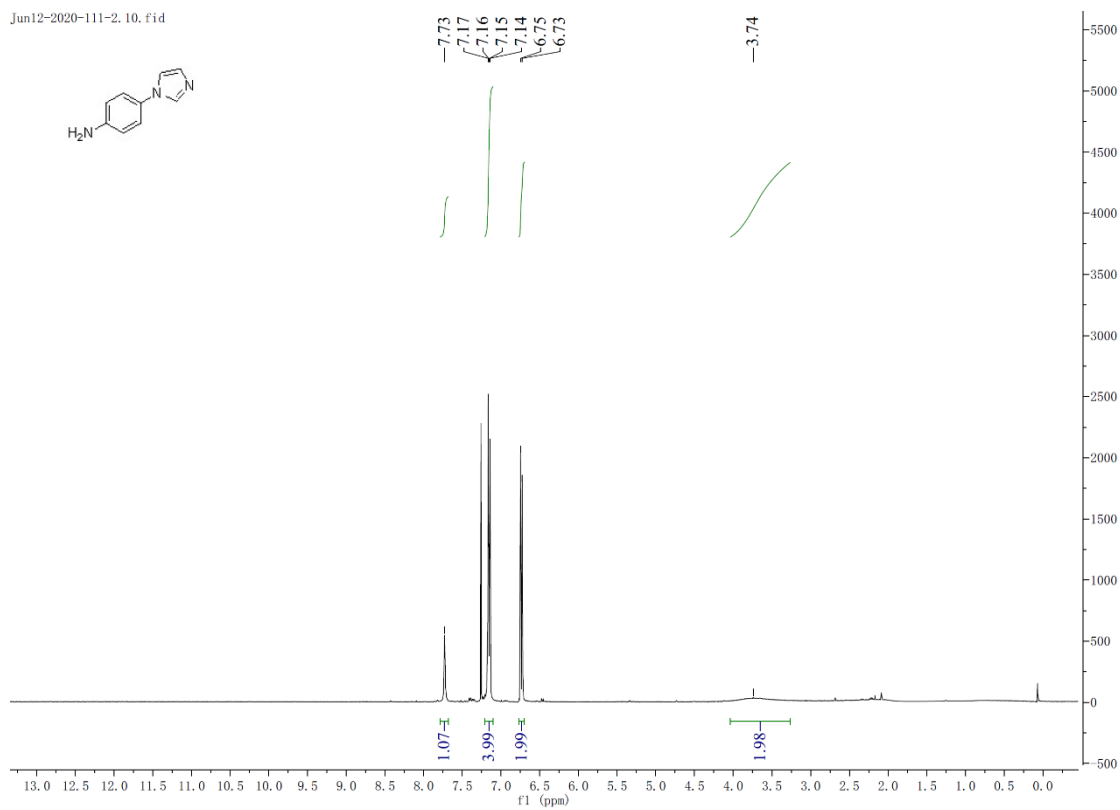
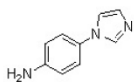


2020-06-13-zy-110-3-C13.7.fid
13C AVNE0500

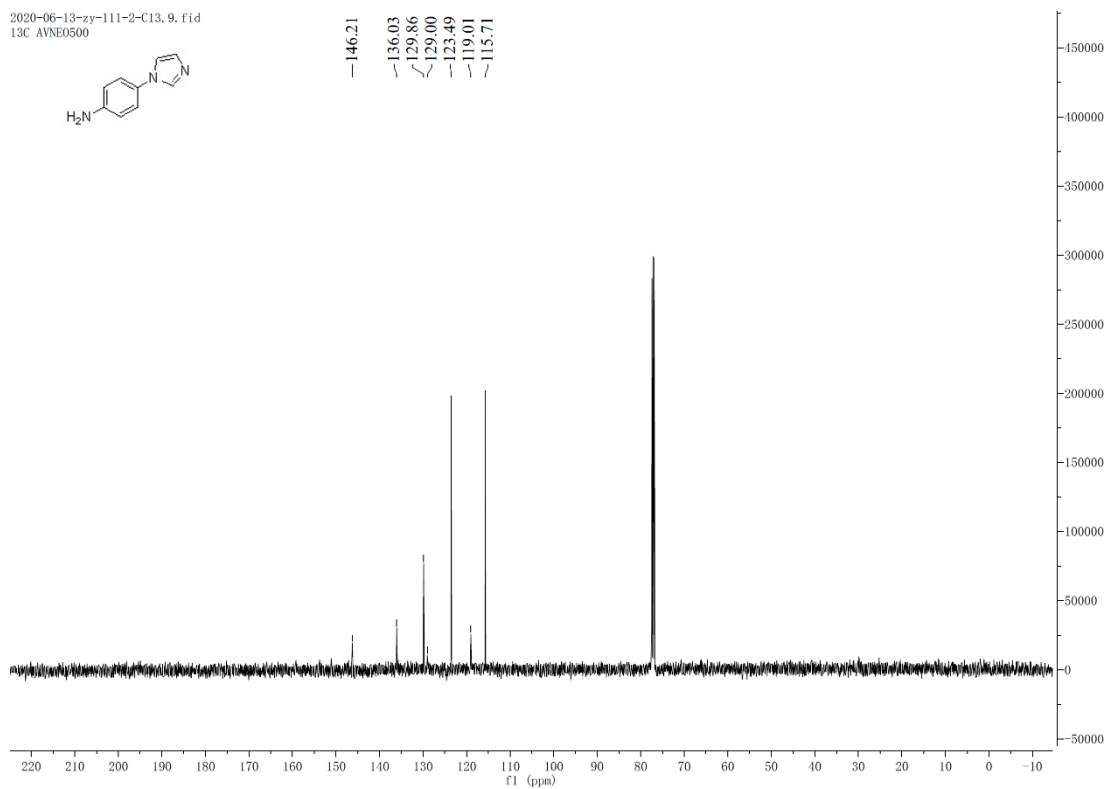


¹H and ¹³C-NMR spectra of product 1

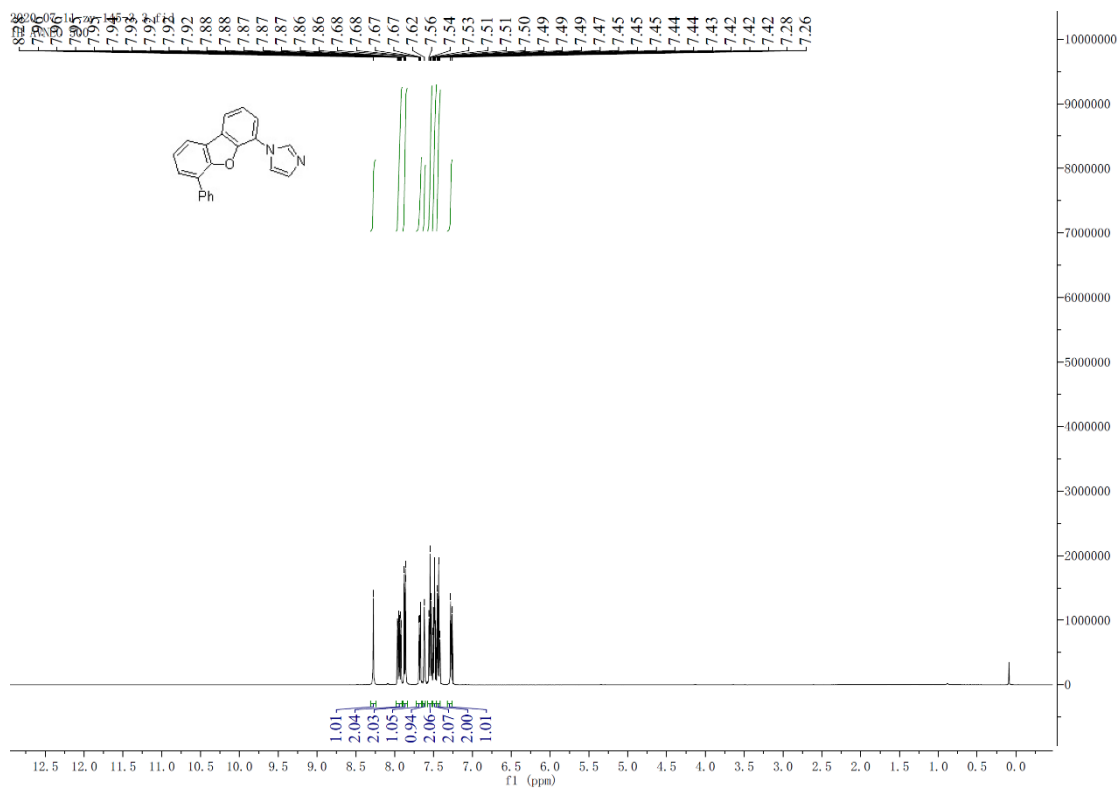
Jun12-2020-111-2.10.fid



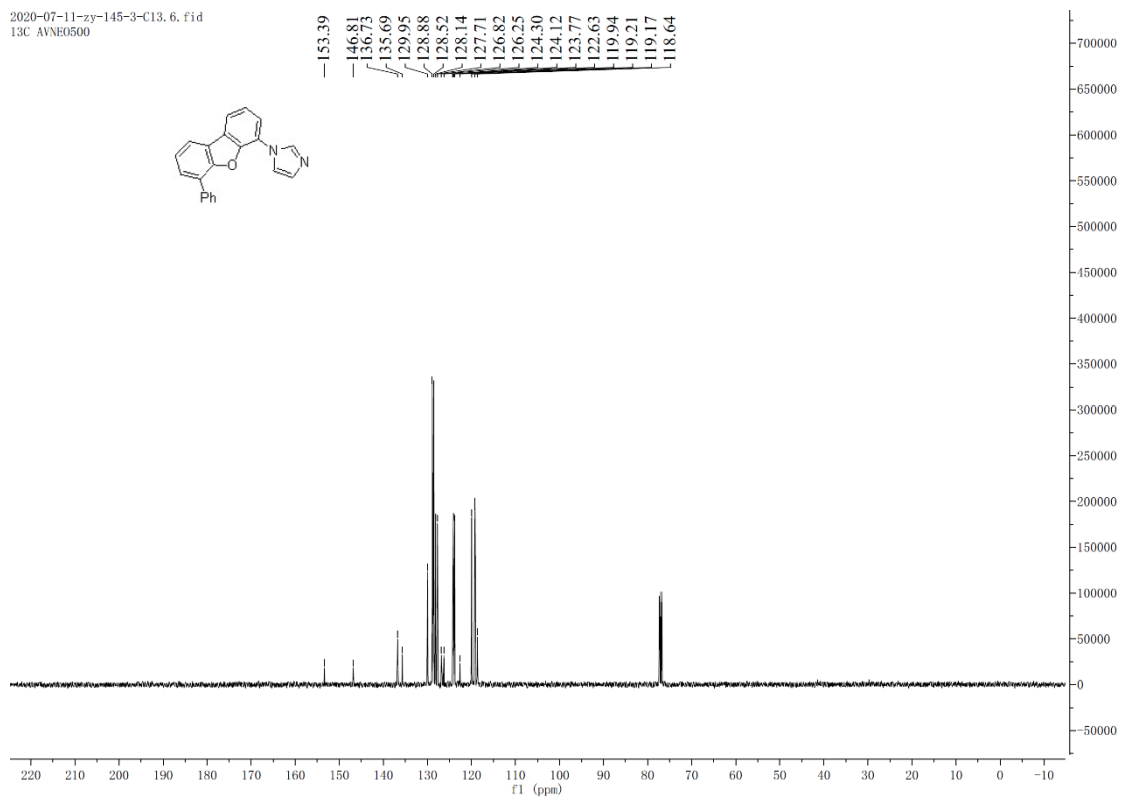
2020-06-13-zy-111-2-C13. 9. fid
13C AVNE0500



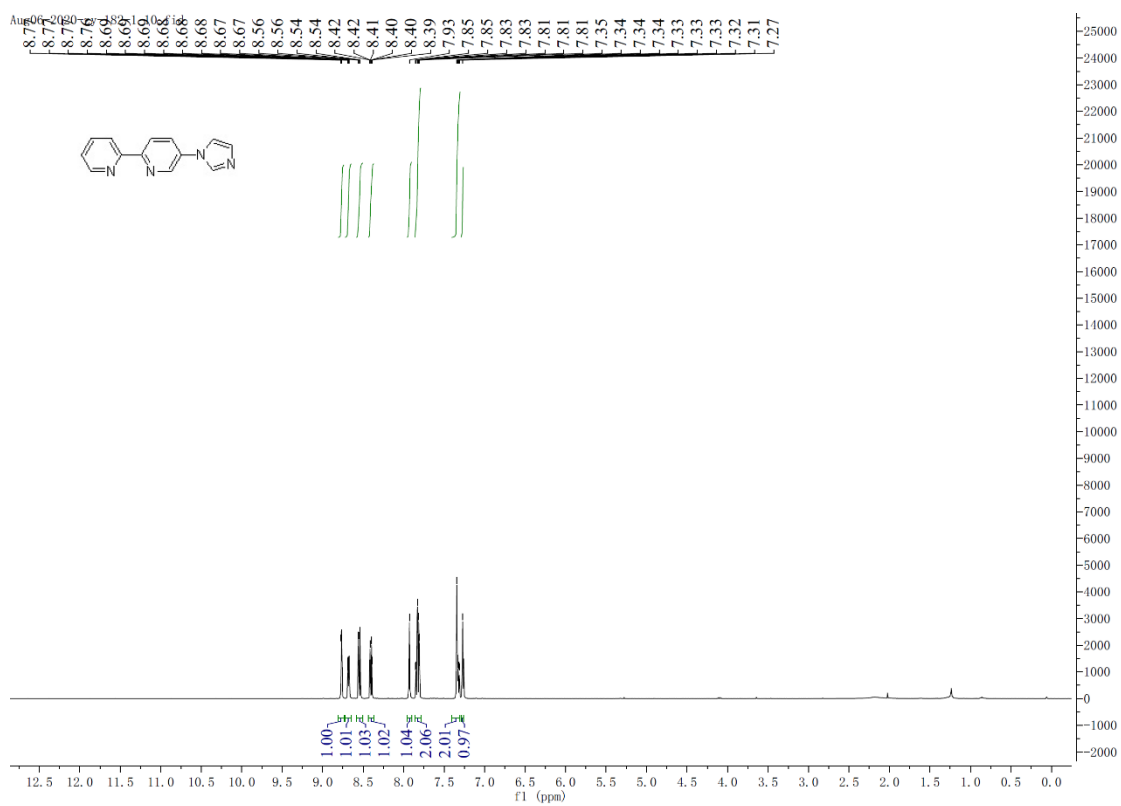
¹H and ¹³C-NMR spectra of product 2.



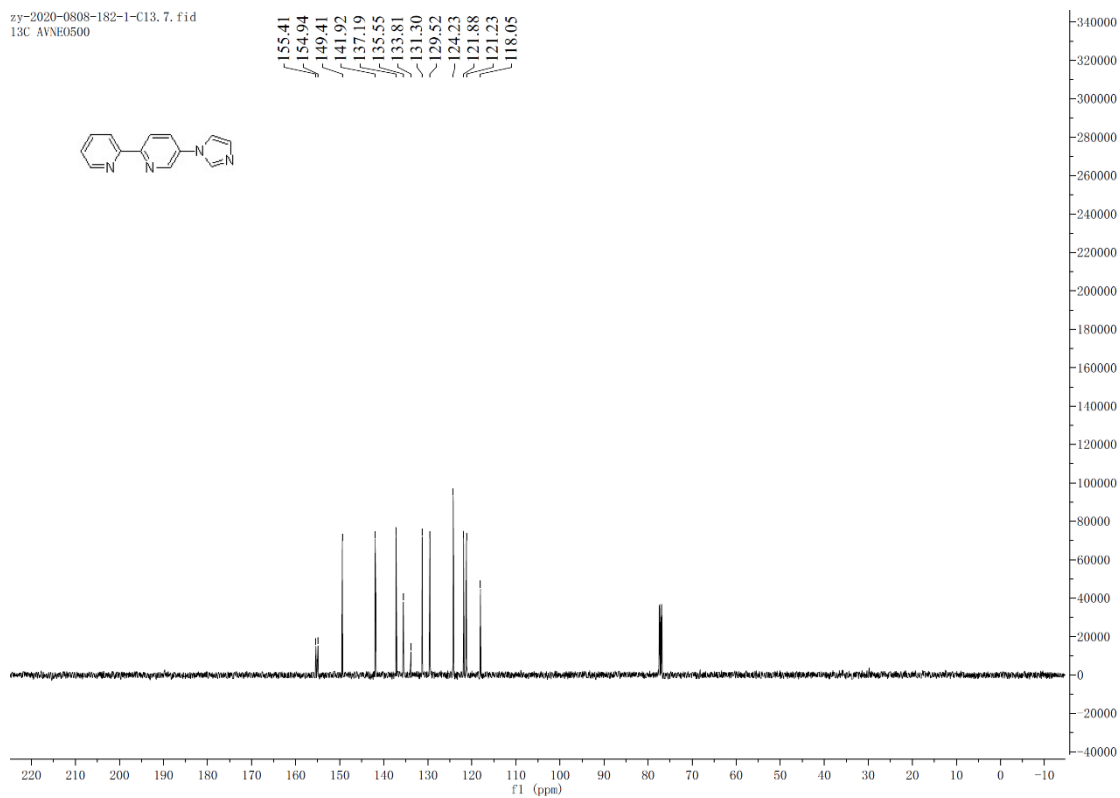
2020-07-11-zy-145-3-C13.6.fid
13C AVNE0500



¹H and ¹³C-NMR spectra of product 3.

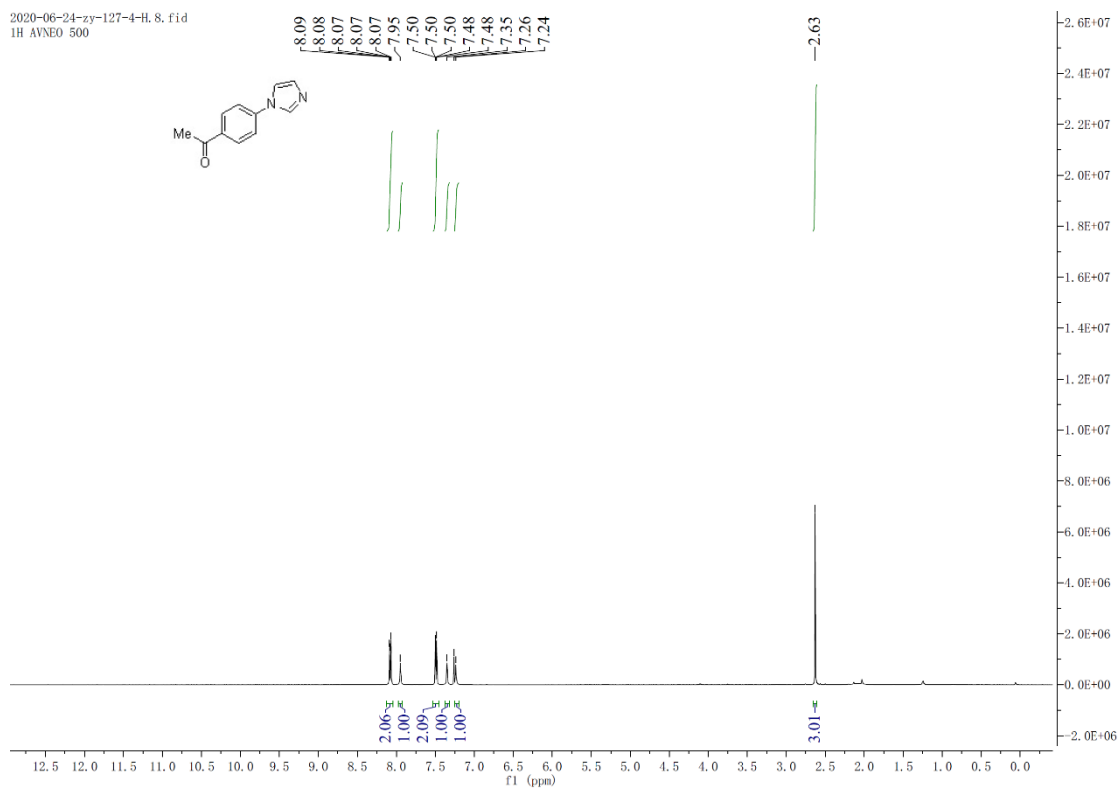


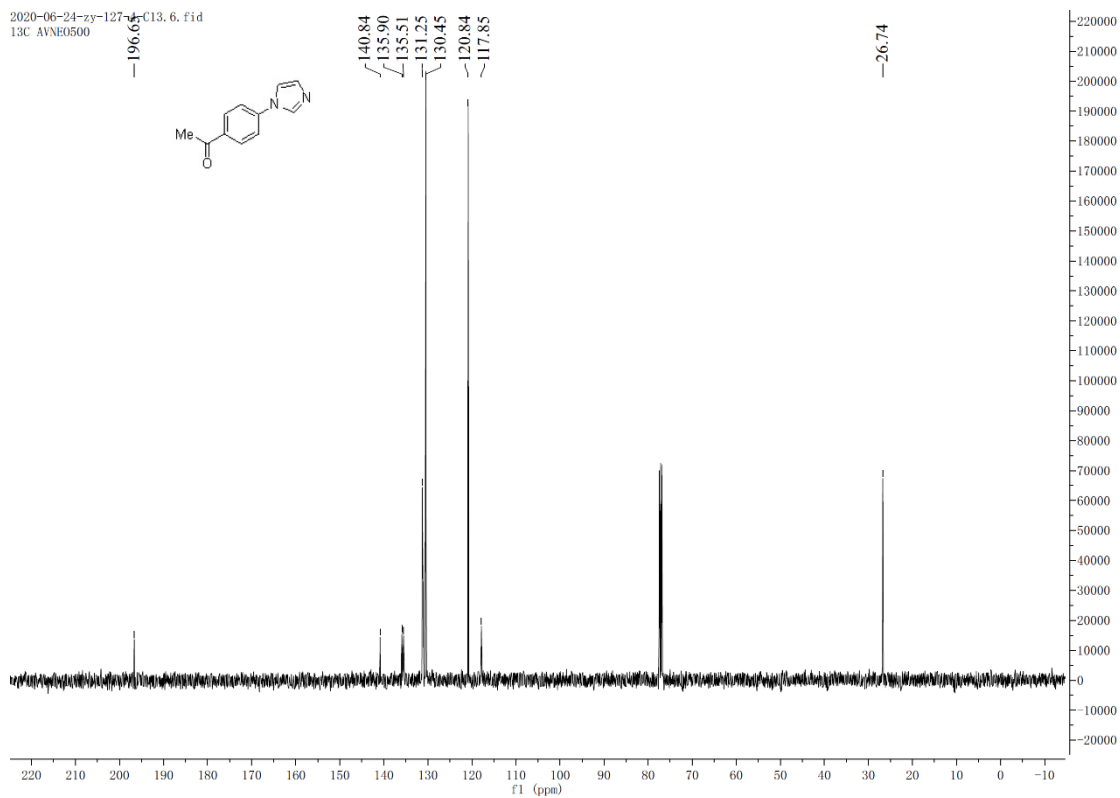
zy-2020-0808-182-1-C13. 7. fid
13C AVNE0500



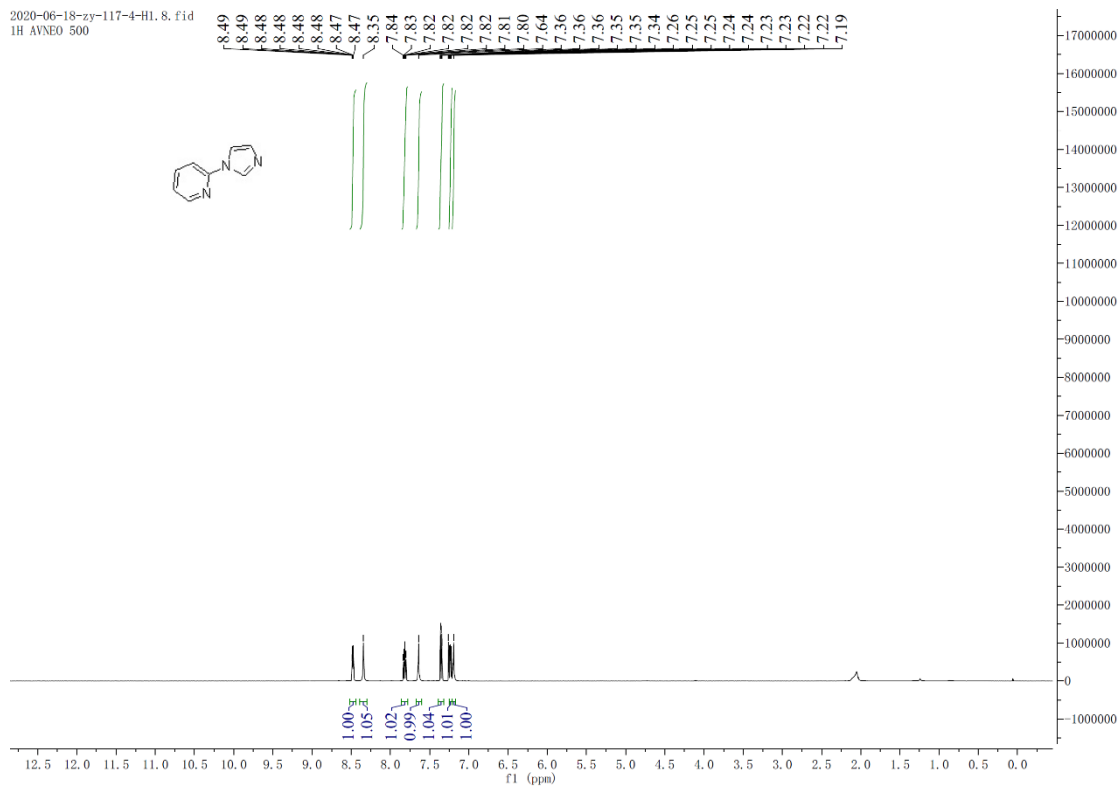
¹H and ¹³C-NMR spectra of product 4.

2020-06-24-zy-127-4-H. 8. fid
1H AVNE0 500

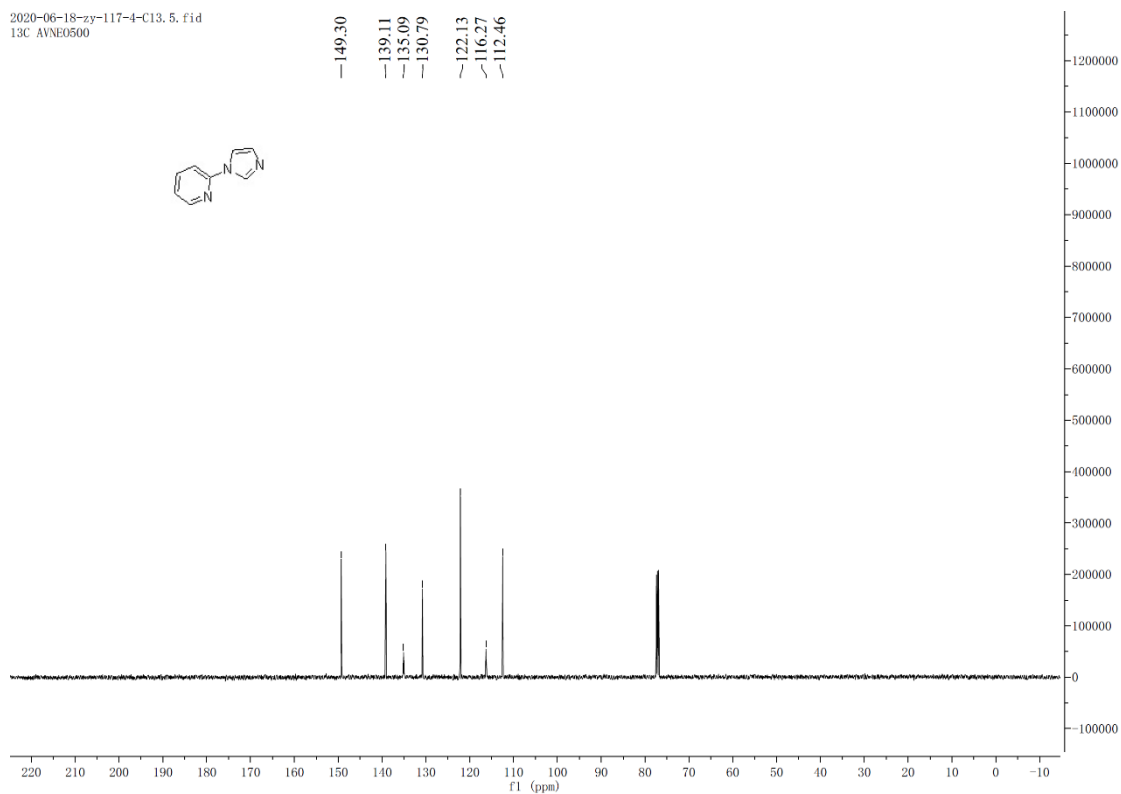




¹H and ¹³C-NMR spectra of product 5.

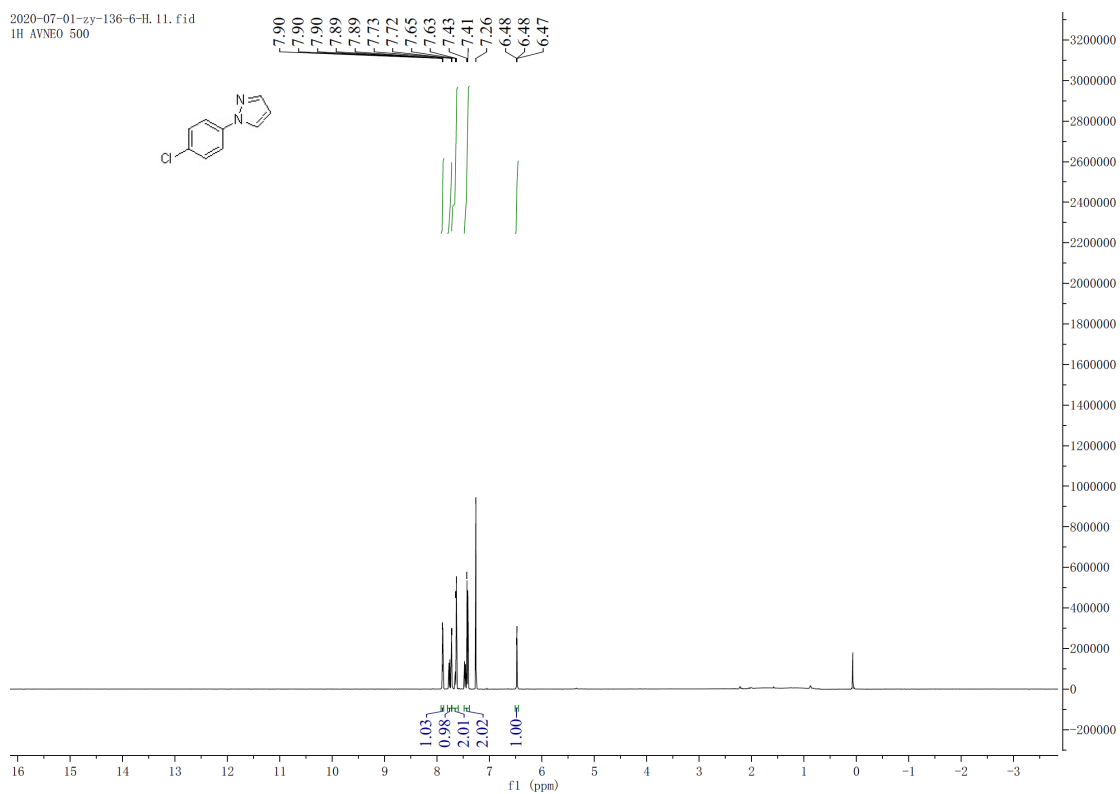


2020-06-18-zy-117-4-C13. 5. fid
13C AVNE0500

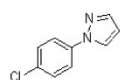


¹H and ¹³C-NMR spectra of product 6.

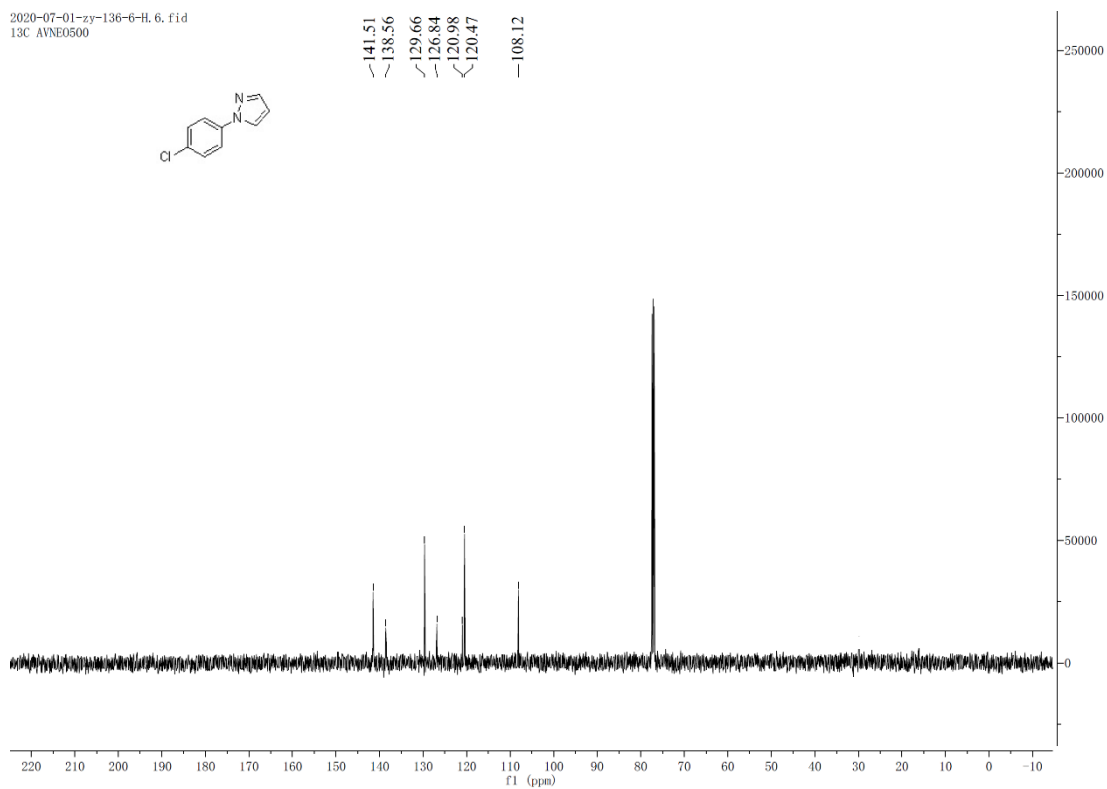
2020-07-01-zy-136-6-H.11. fid
1H AVNE0 500



2020-07-01-zy-136-6-H. 6. fid
13C AVNE0500

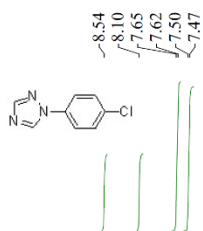


141.51
138.56
129.66
126.84
120.98
120.47
108.12

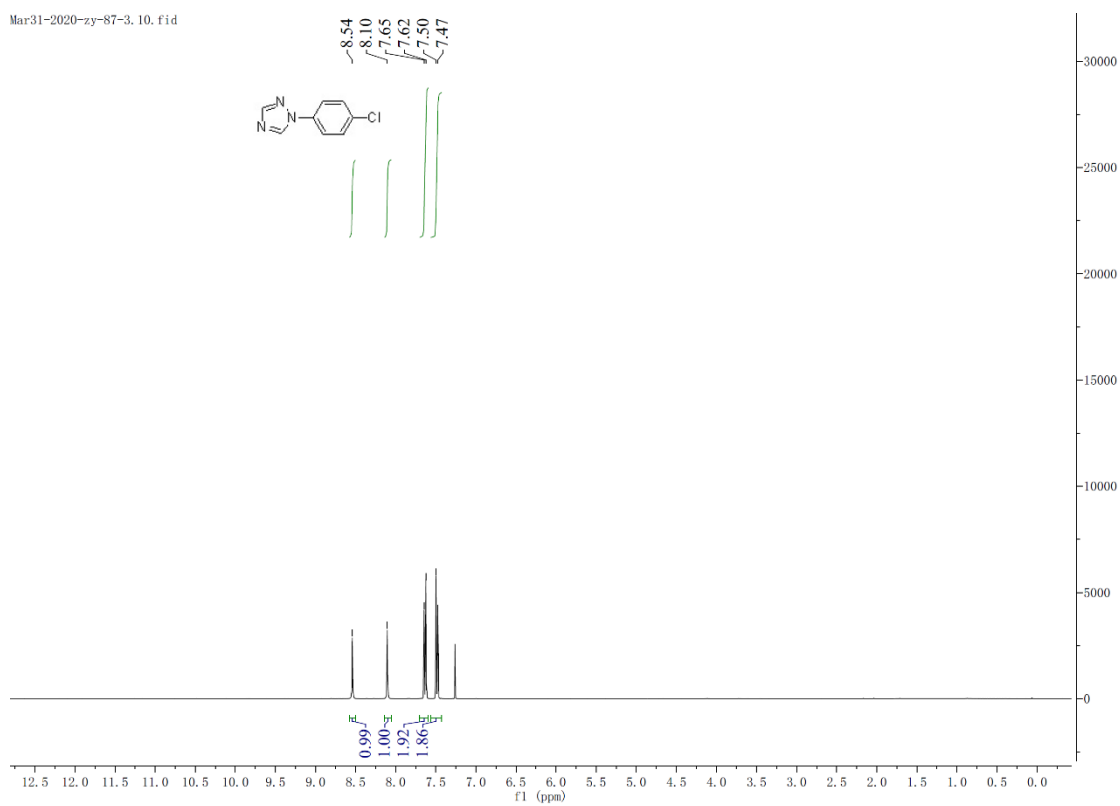


¹H and ¹³C-NMR spectra of product 7.

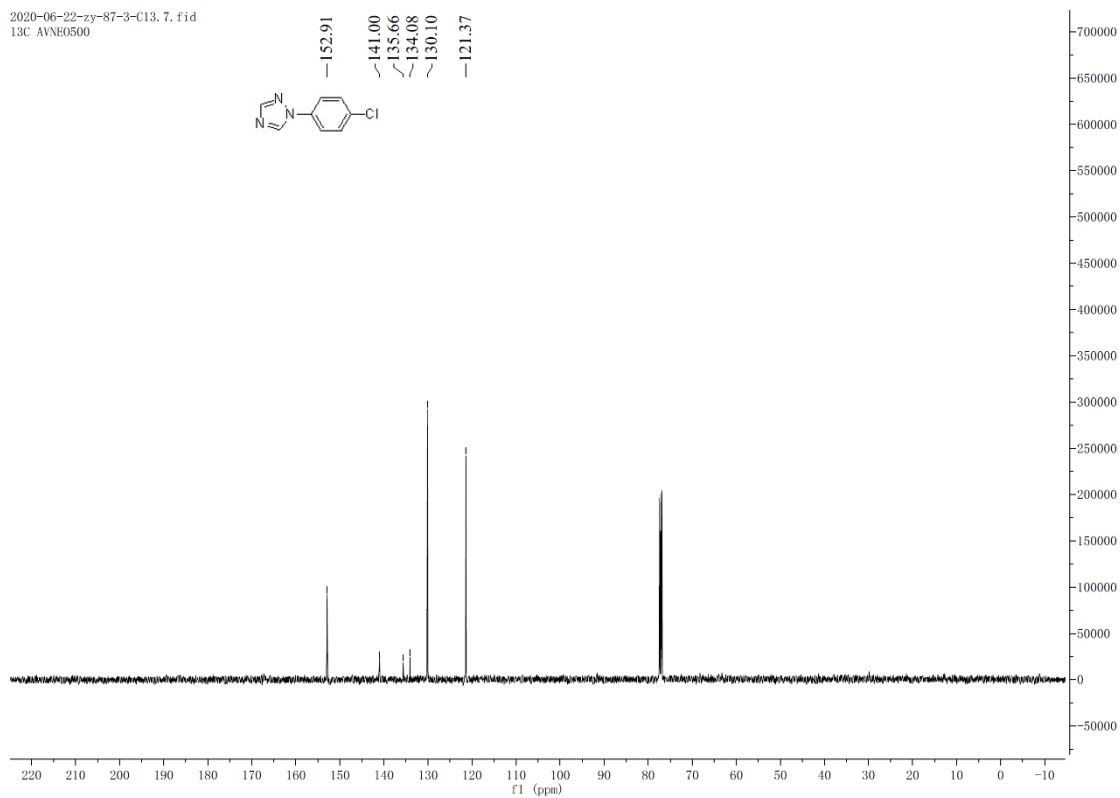
Mar31-2020-zy-87-3. 10. fid



8.54
8.10
7.65
7.62
7.50
7.47

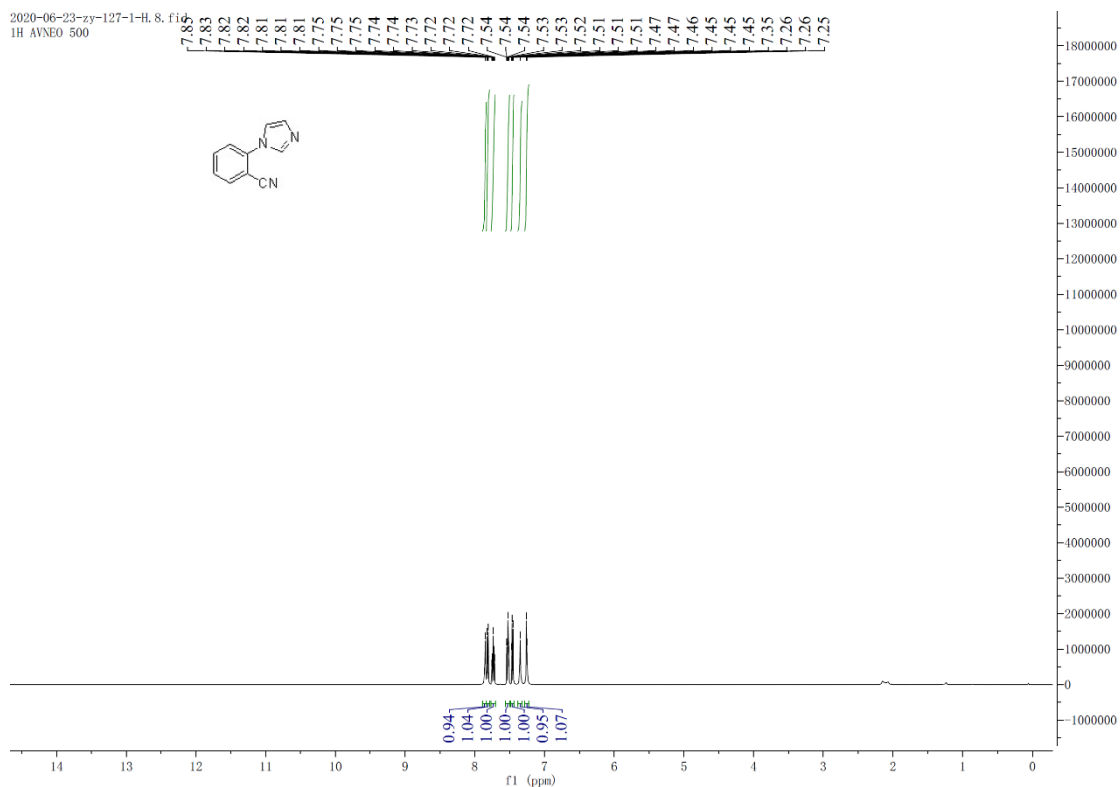


2020-06-22-zy-87-3-C13. 7. fid
13C AVNE0500

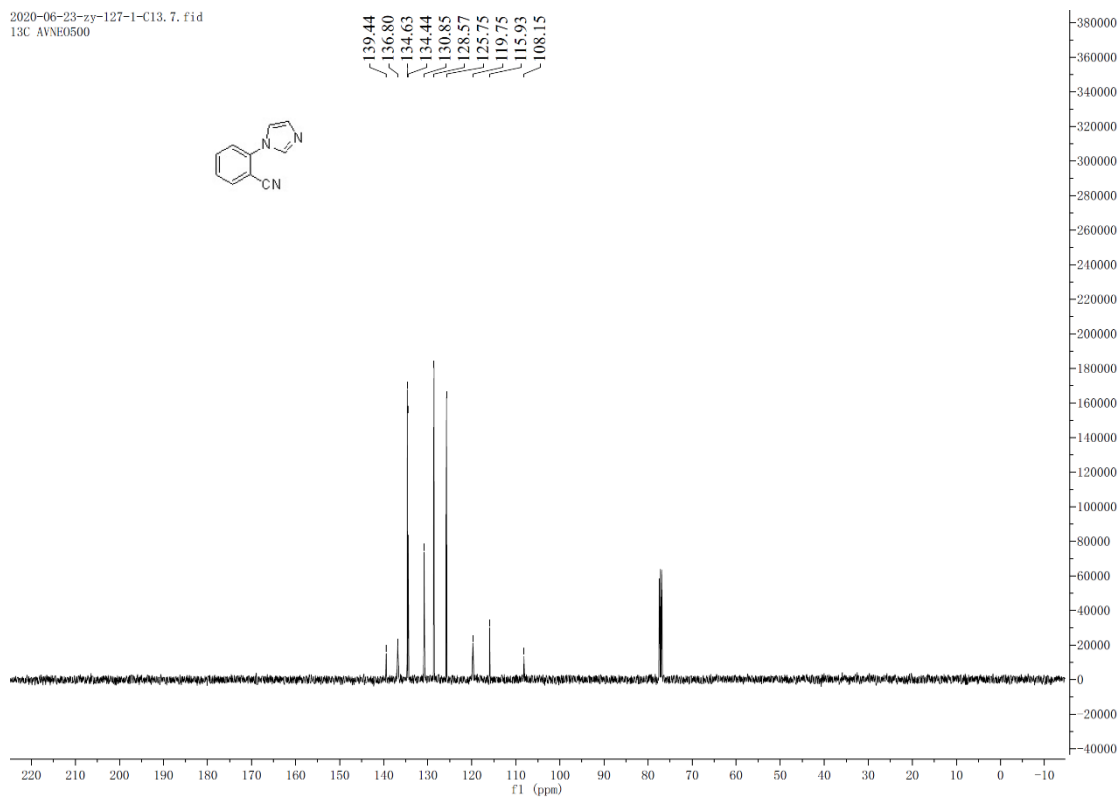


¹H and ¹³C-NMR spectra of product 8.

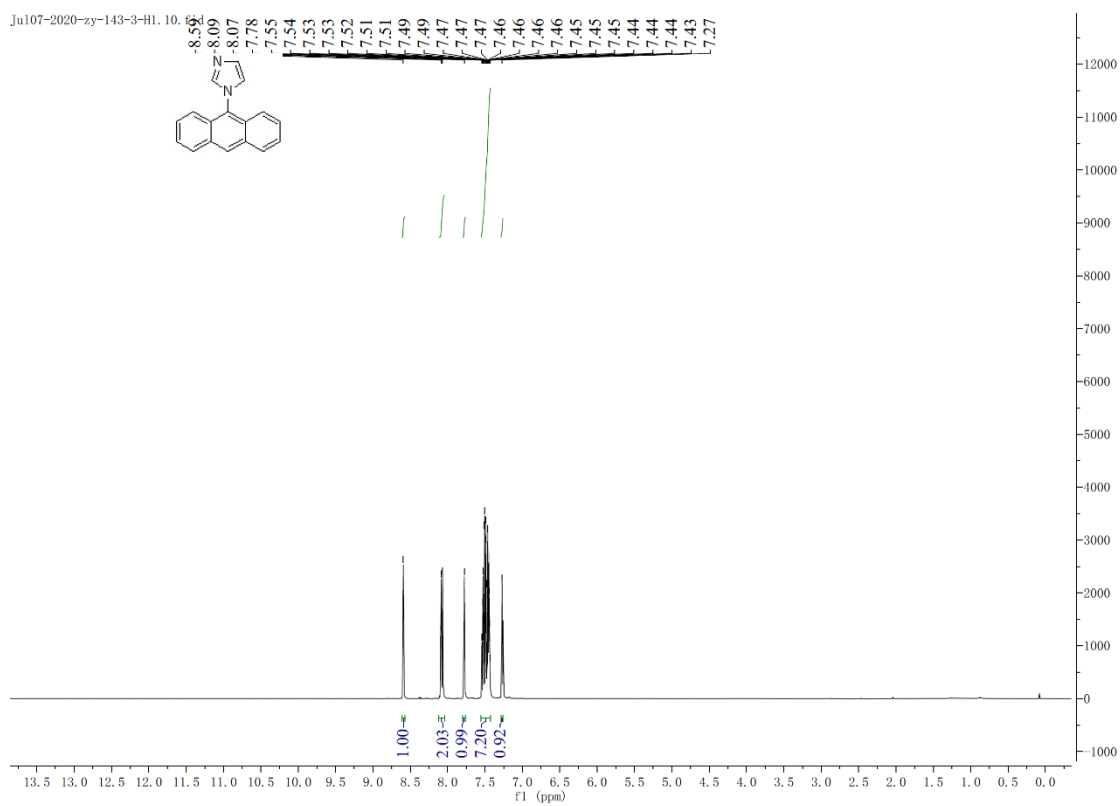
2020-06-23-zy-127-1-H. 8. fid
1H AVNE0 500



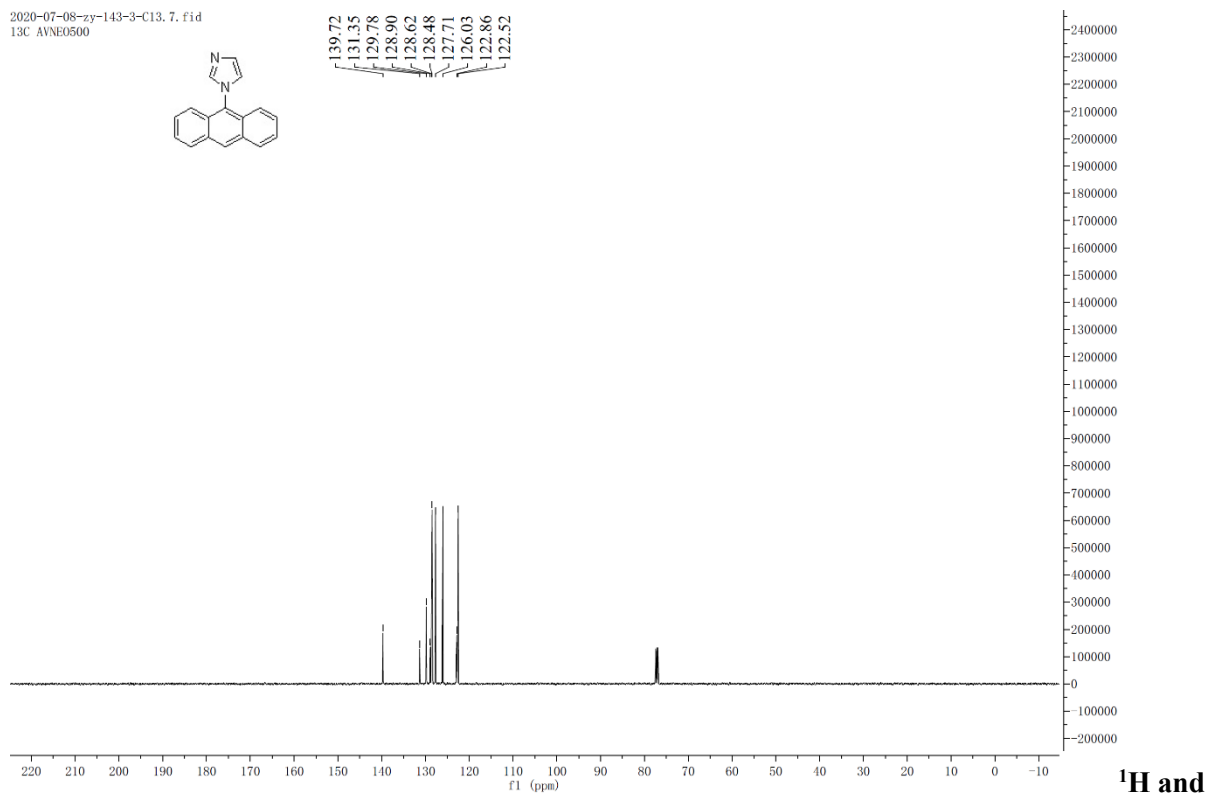
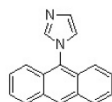
2020-06-23-zy-127-1-C13.7.fid
13C AVNE0500



¹H and ¹³C-NMR spectra of product 9.

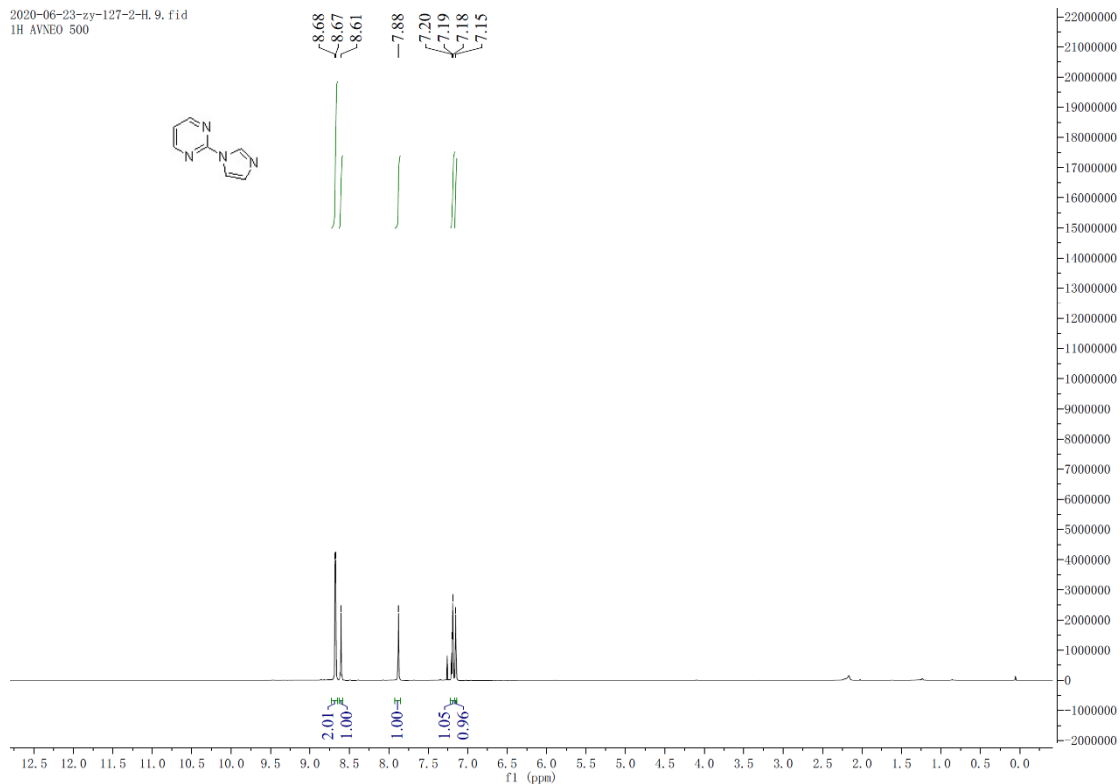


2020-07-08-zy-143-3-C13.7.fid
13C AVNE0500

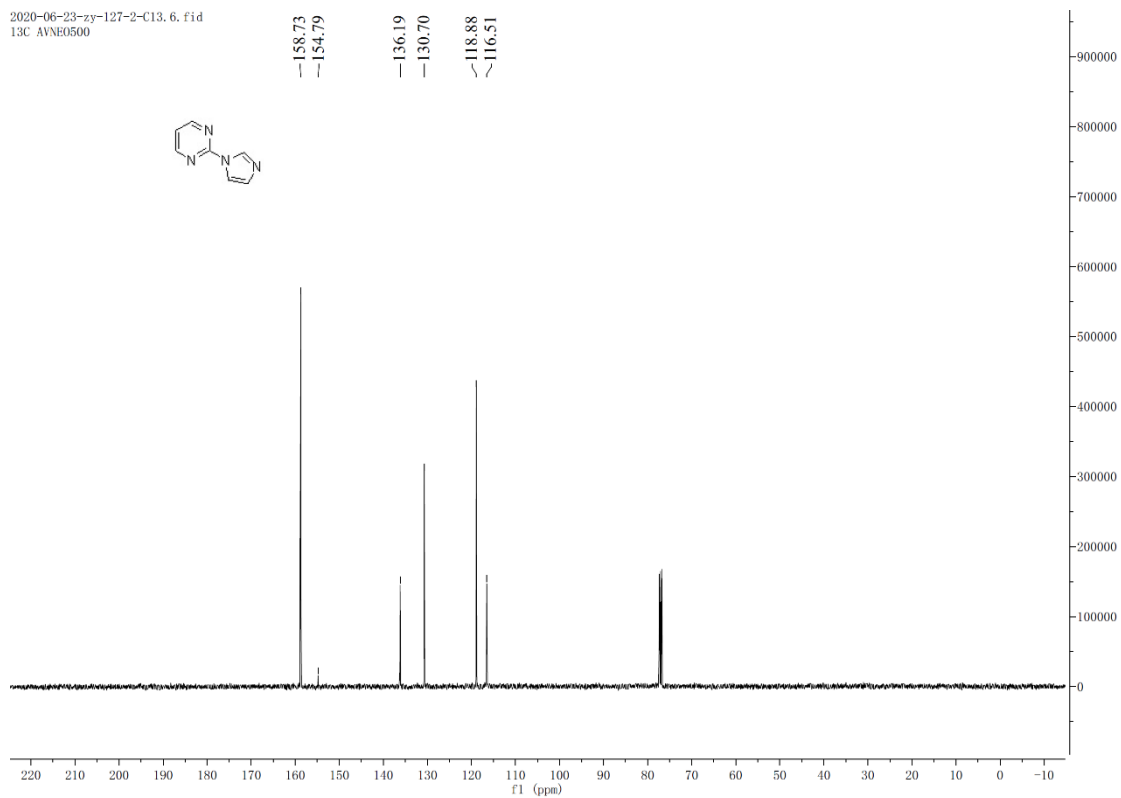


¹³C-NMR spectra of product 10.

2020-06-23-zy-127-2-H.9.fid
1H AVNE0 500

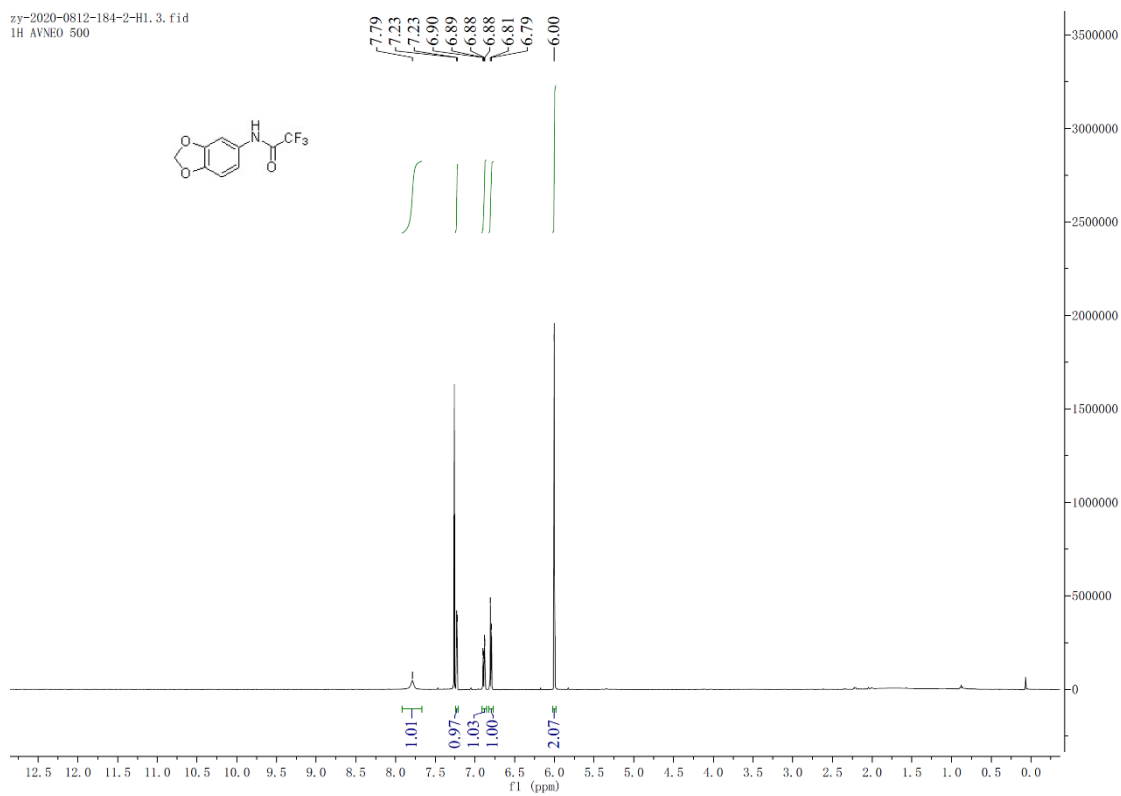


2020-06-23-zy-127-2-C13.6.fid
13C AVNE0500

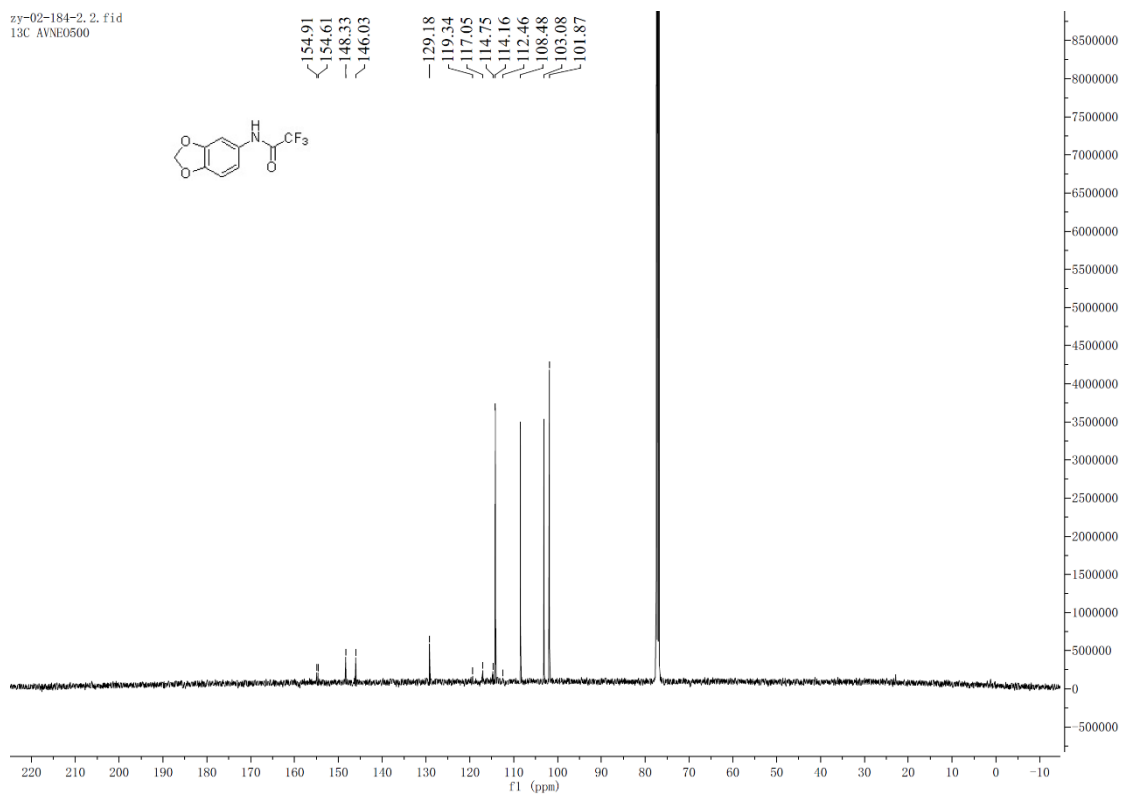


¹H and ¹³C-NMR spectra of product 11.

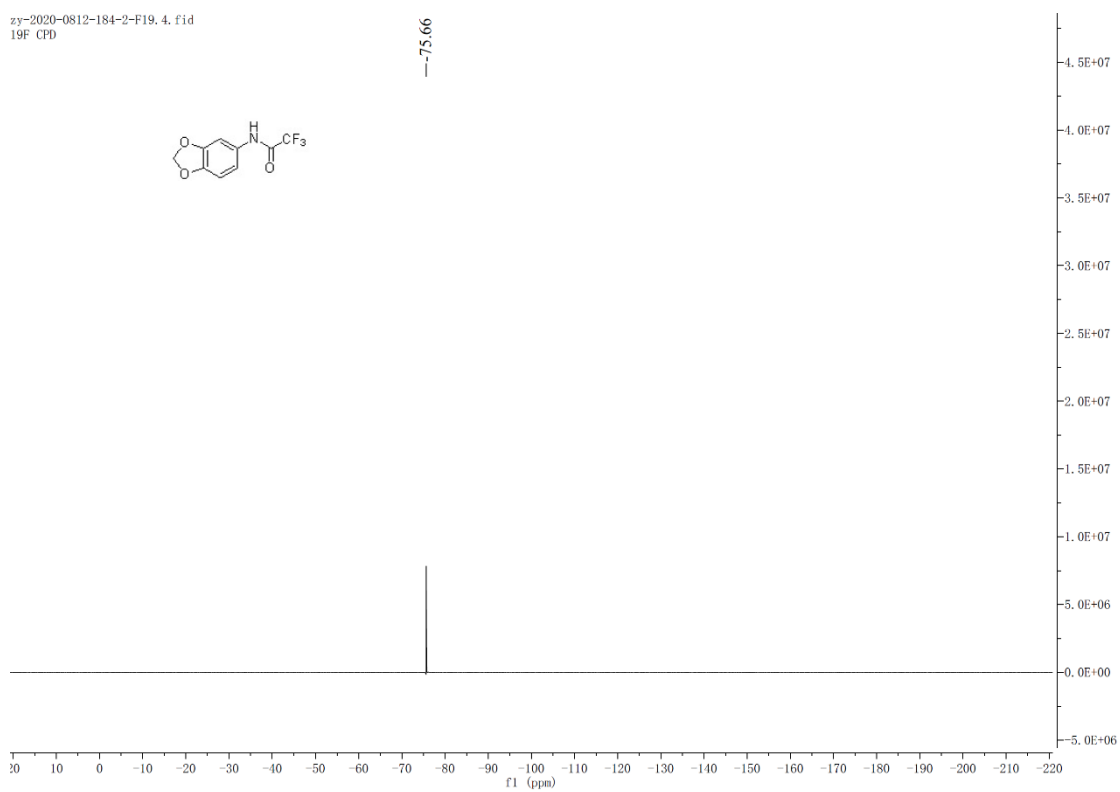
zy-2020-0812-184-2-H1.3.fid
1H AVNE0 500



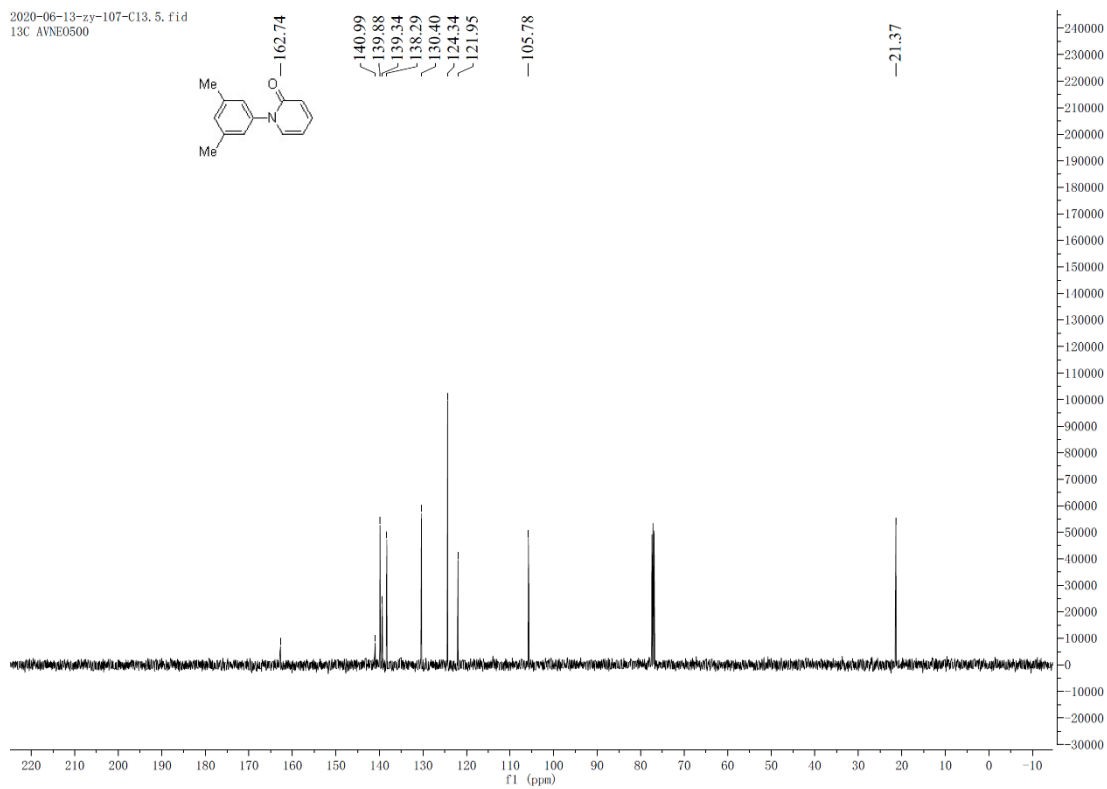
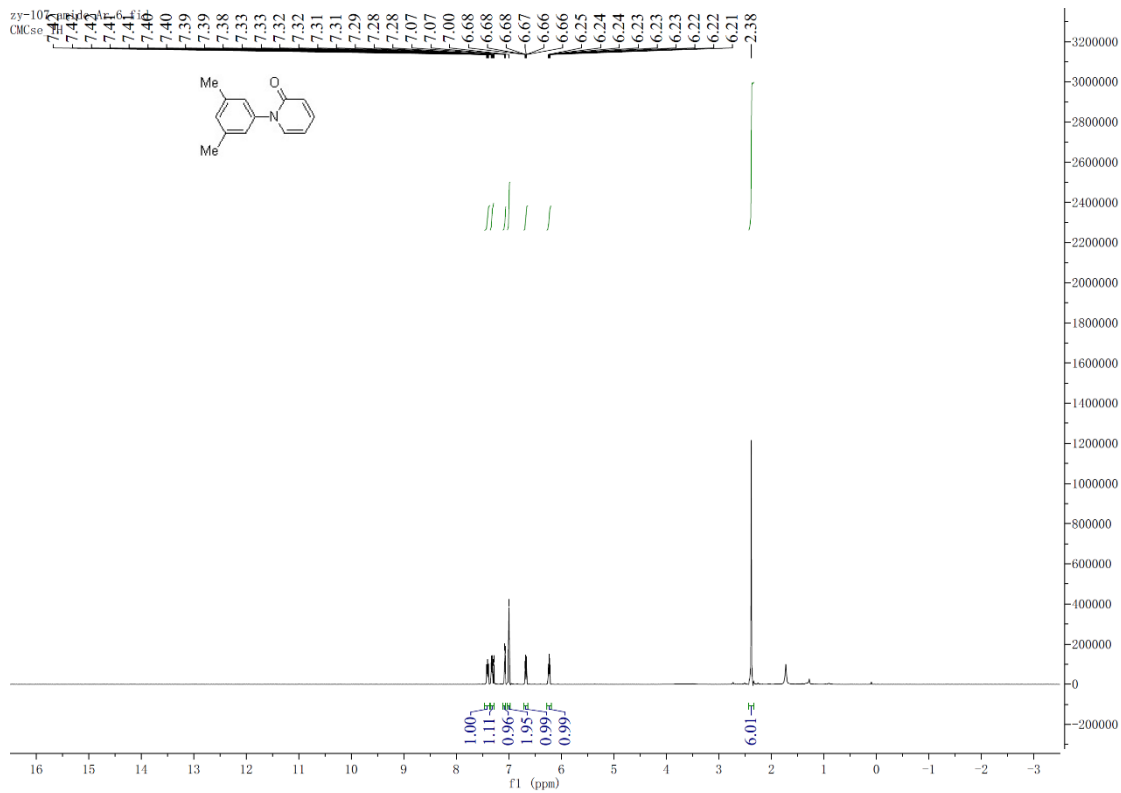
zy-02-184-2.2.fid
13C AVNE0500



zy-2020-0812-184-2-F19.4.fid
19F CPD

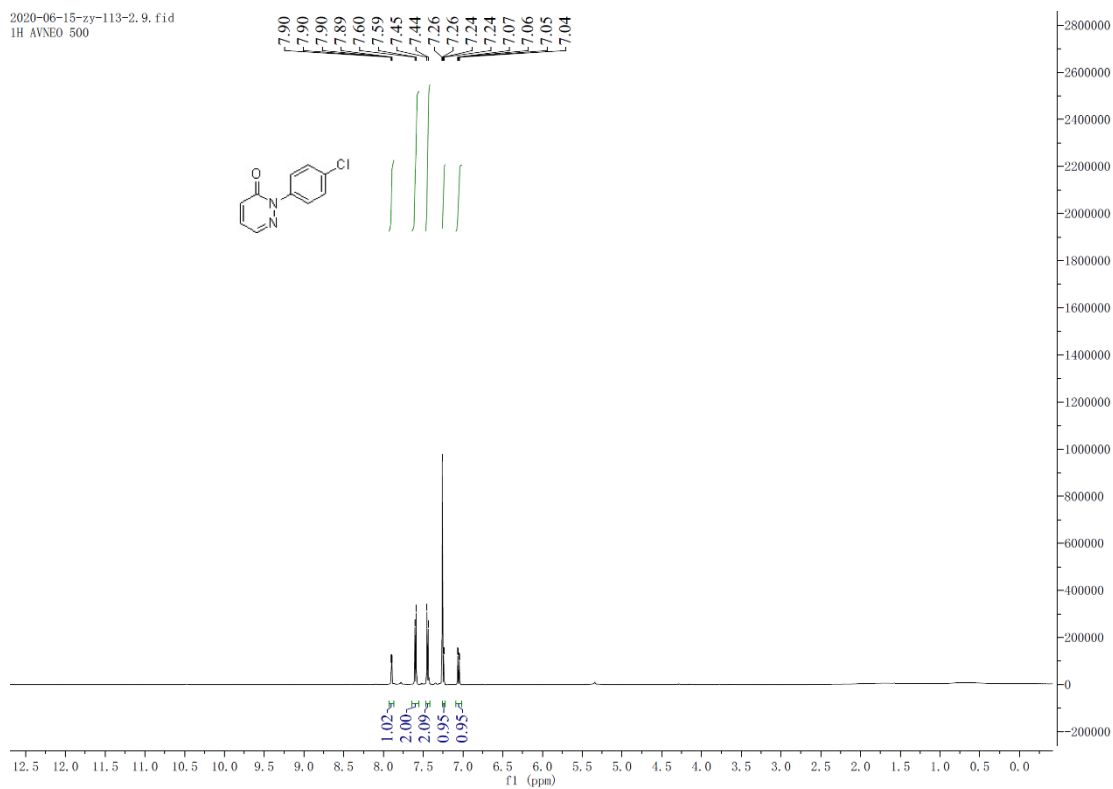


¹H, ¹³C, and ¹⁹F-NMR spectra of product 12.

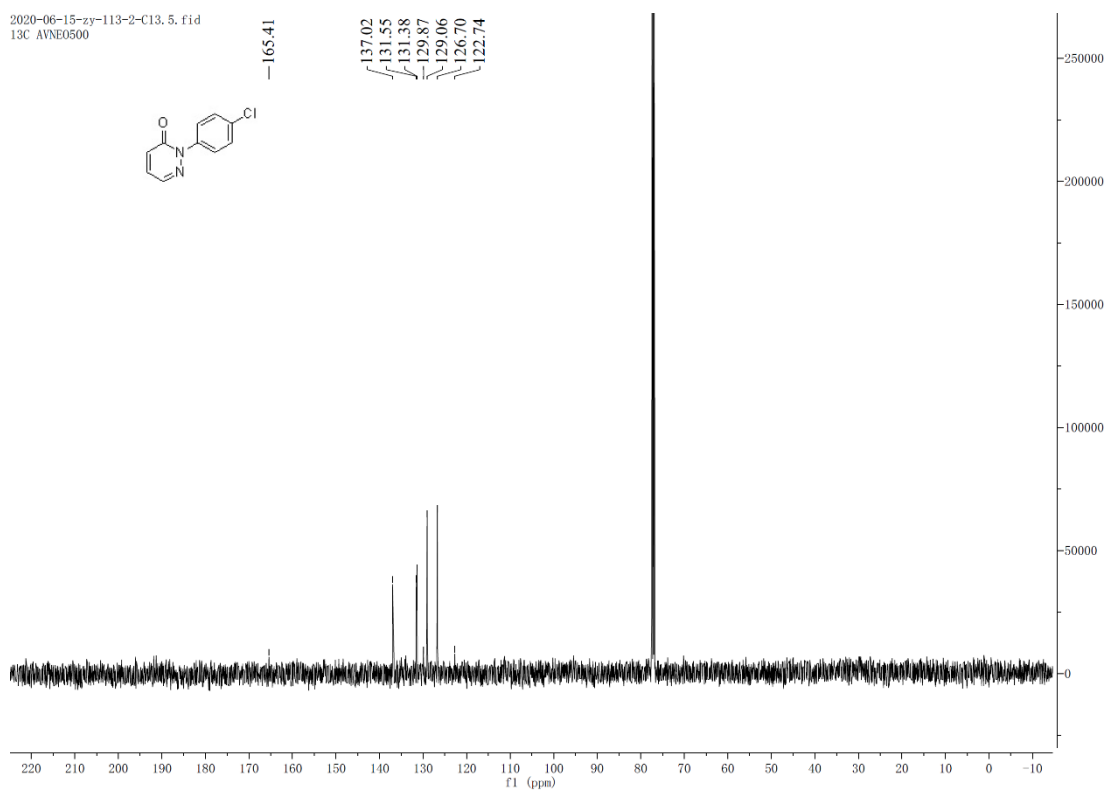


^1H and ^{13}C -NMR spectra of product 13.

2020-06-15-zy-113-2.9.fid
1H AVNEO 500

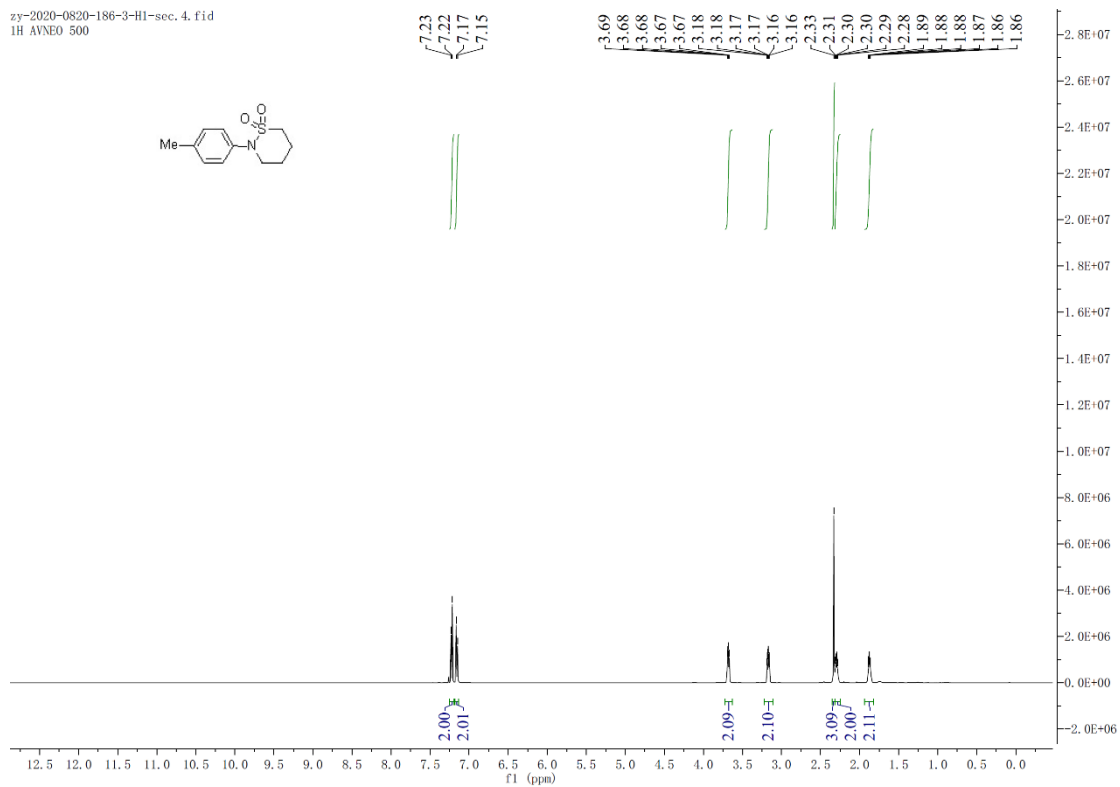


2020-06-15-zy-113-2-C13.5.fid
13C AVNEO500

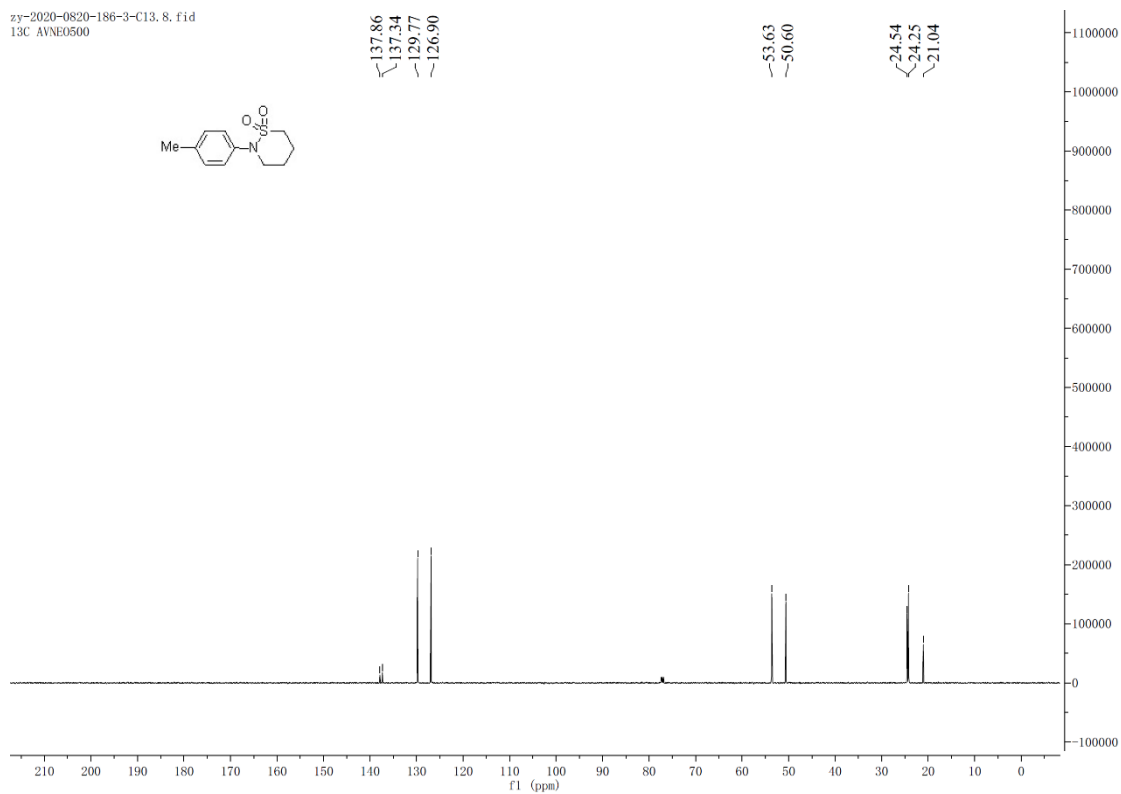


¹H and ¹³C-NMR spectra of product 14.

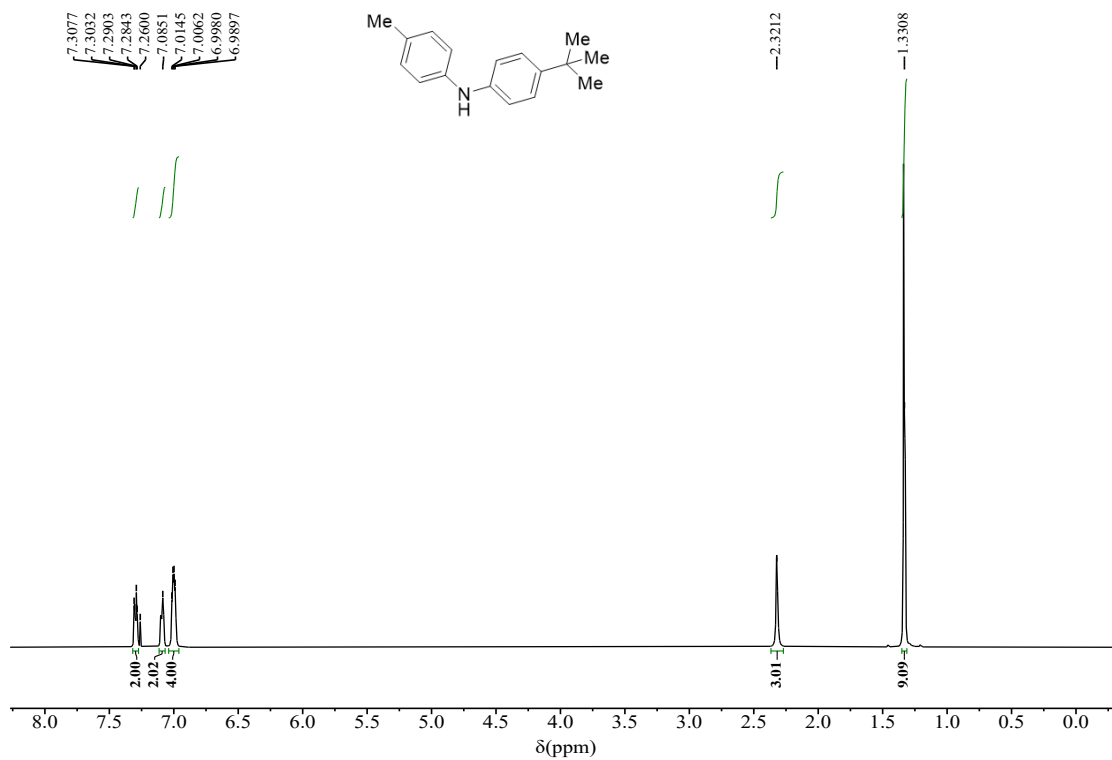
zy-2020-0820-186-3-H1-sec. 4. fid
1H AVNEO 500



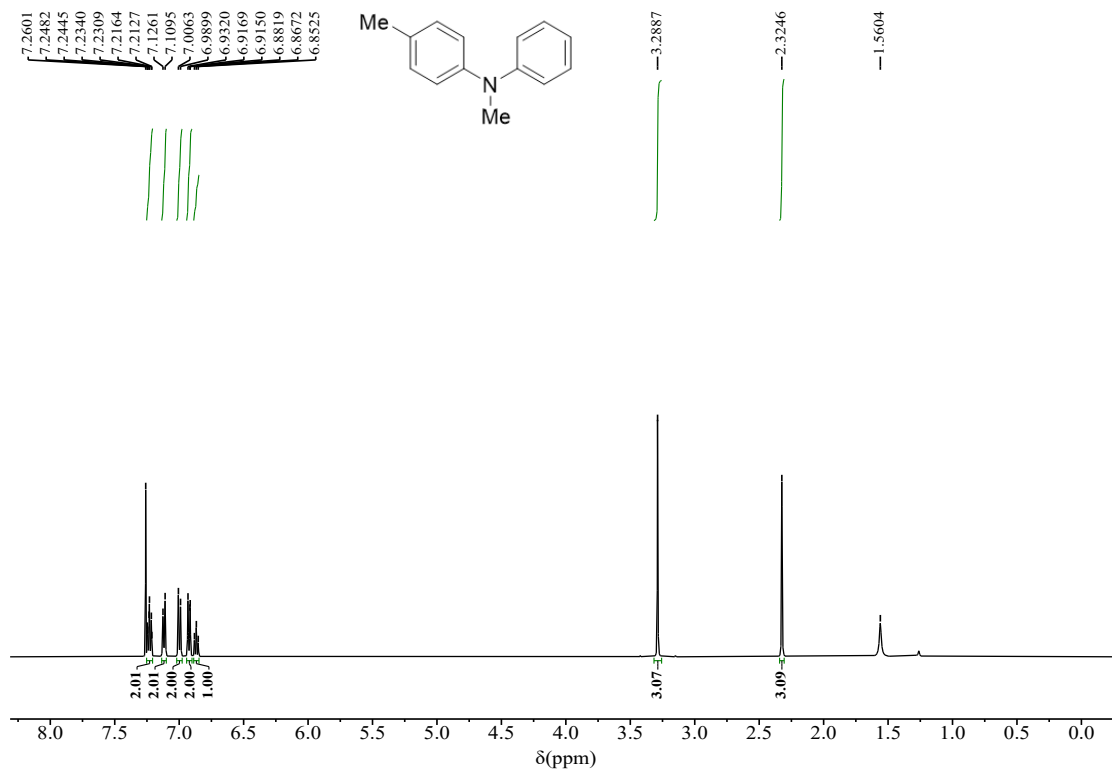
zy-2020-0820-186-3-C13. 8. fid
13C AVNEO500



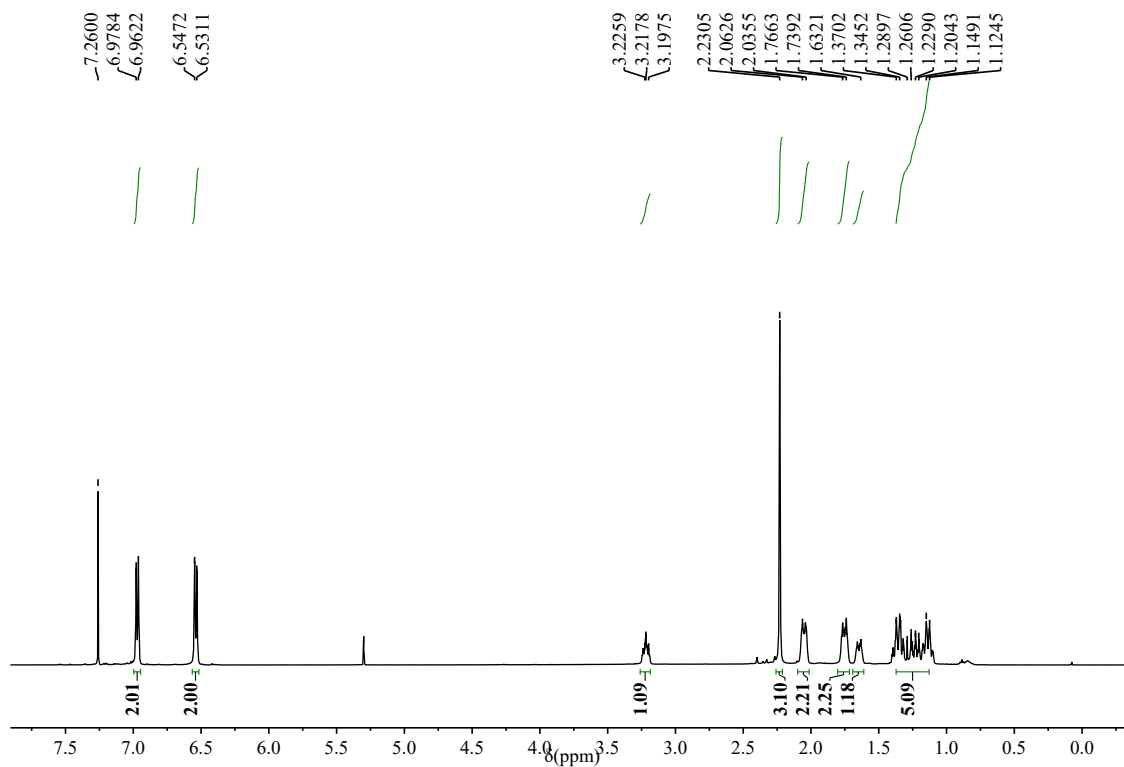
¹H and ¹³C-NMR spectra of product 15.



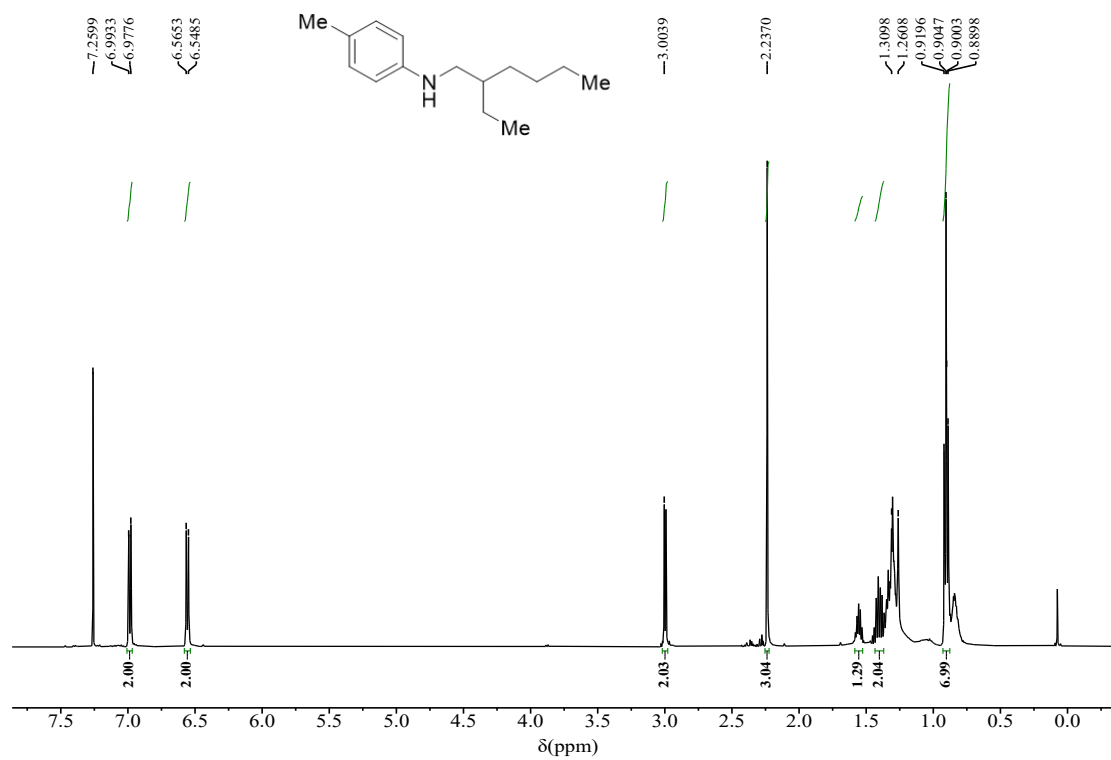
¹H spectra of product 16.



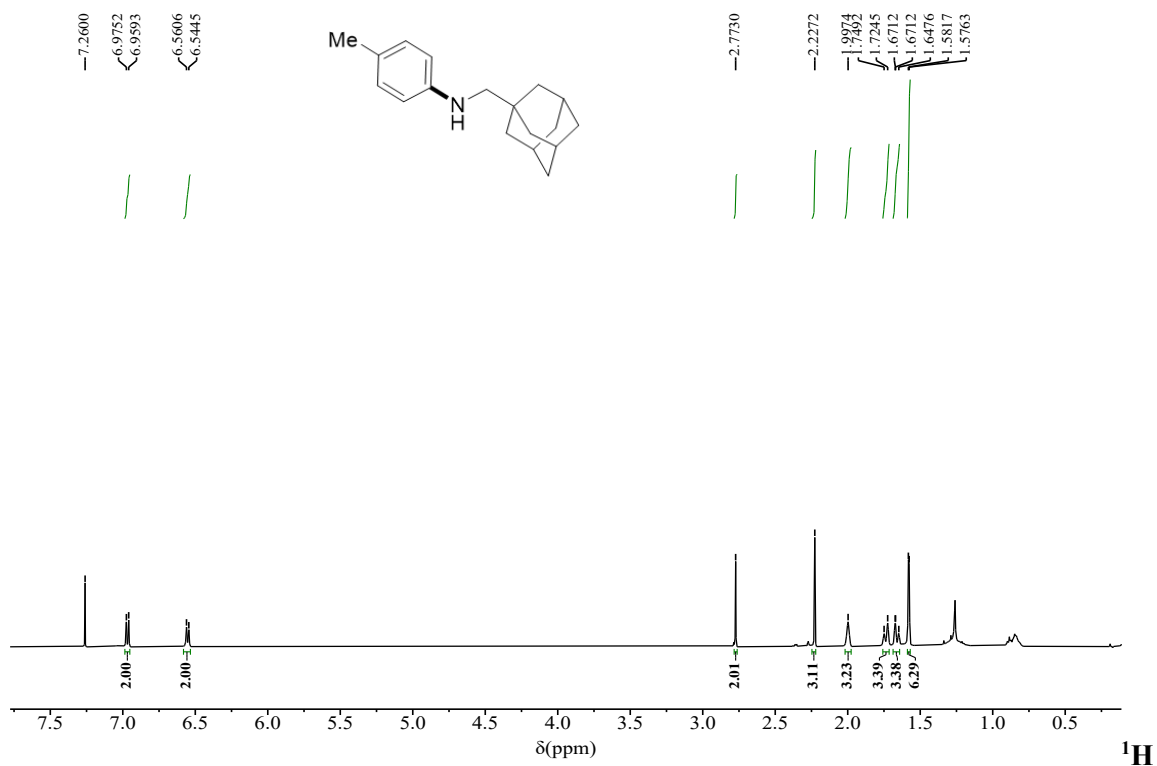
¹H spectra of product 17.



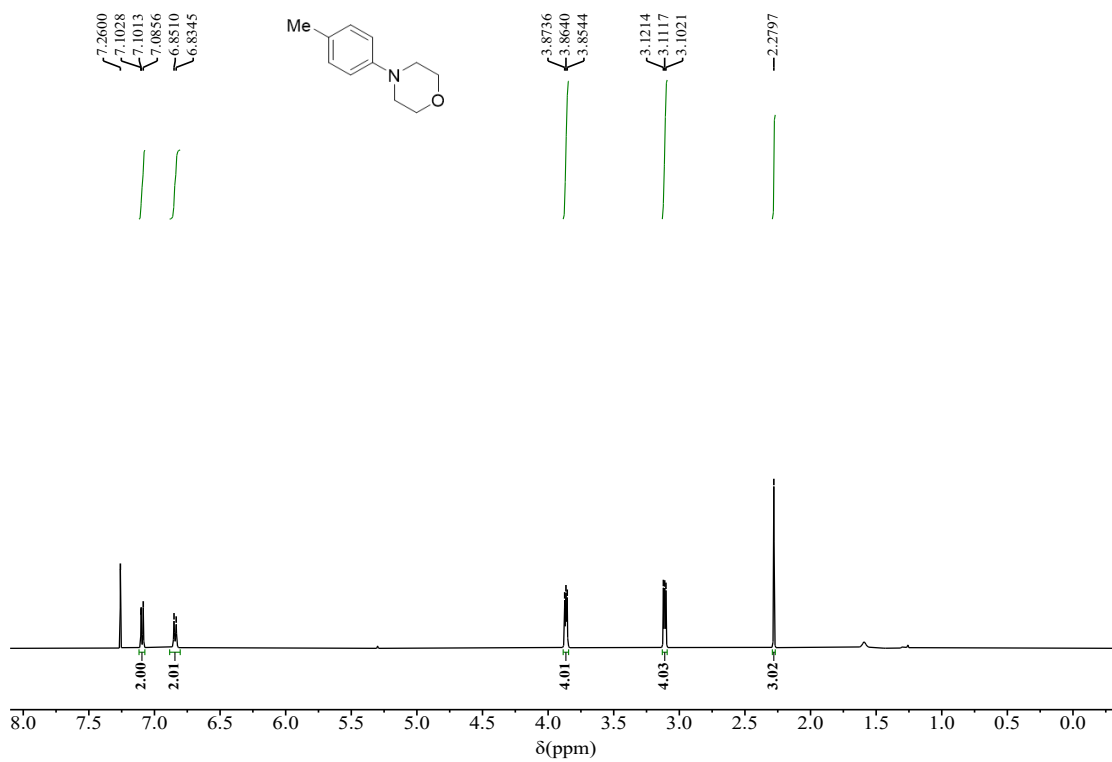
¹H spectra of product 18.



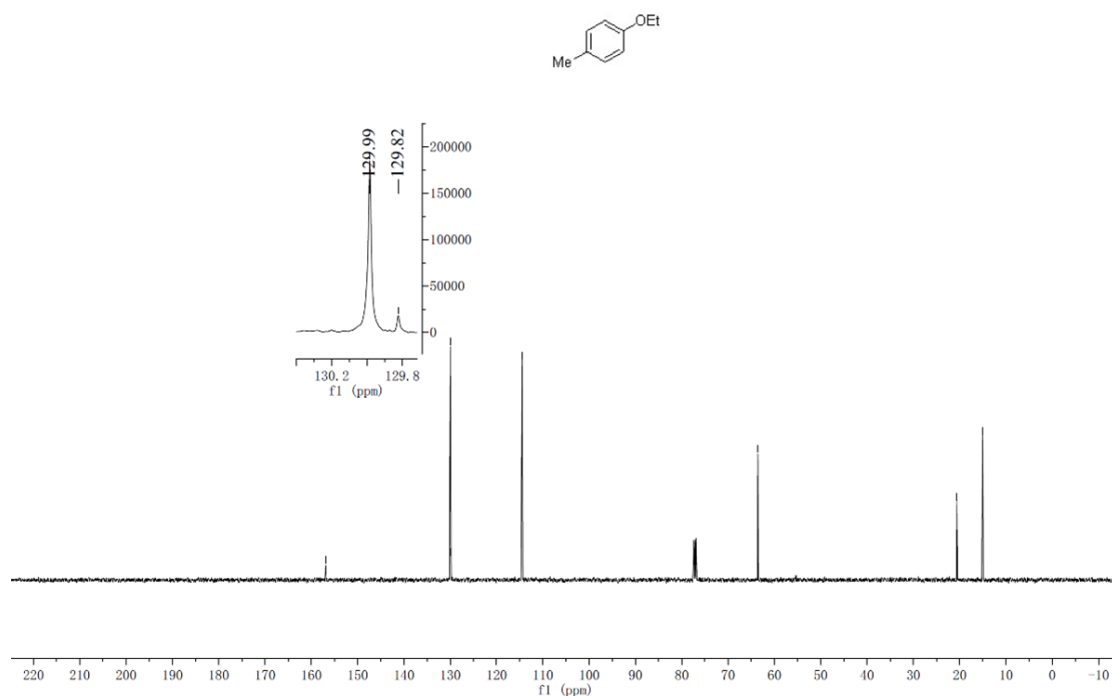
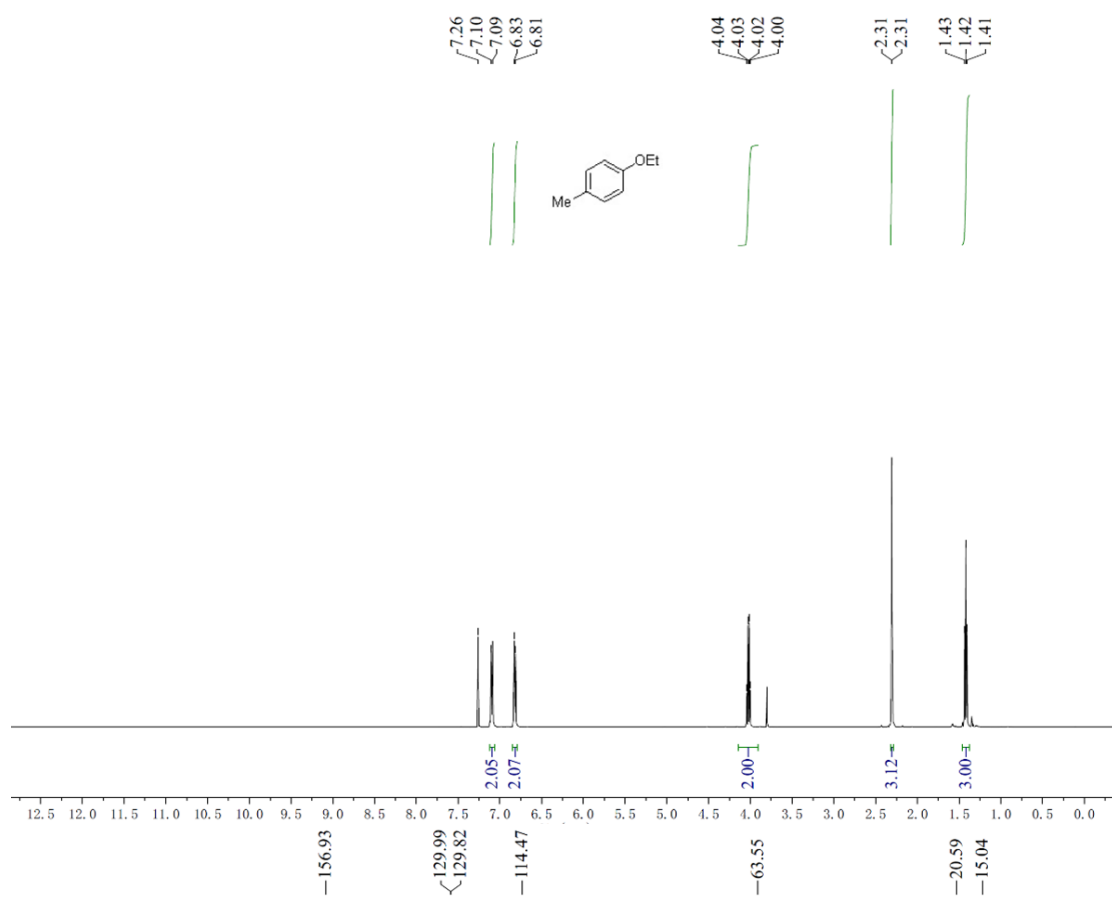
¹H spectra of product 19.



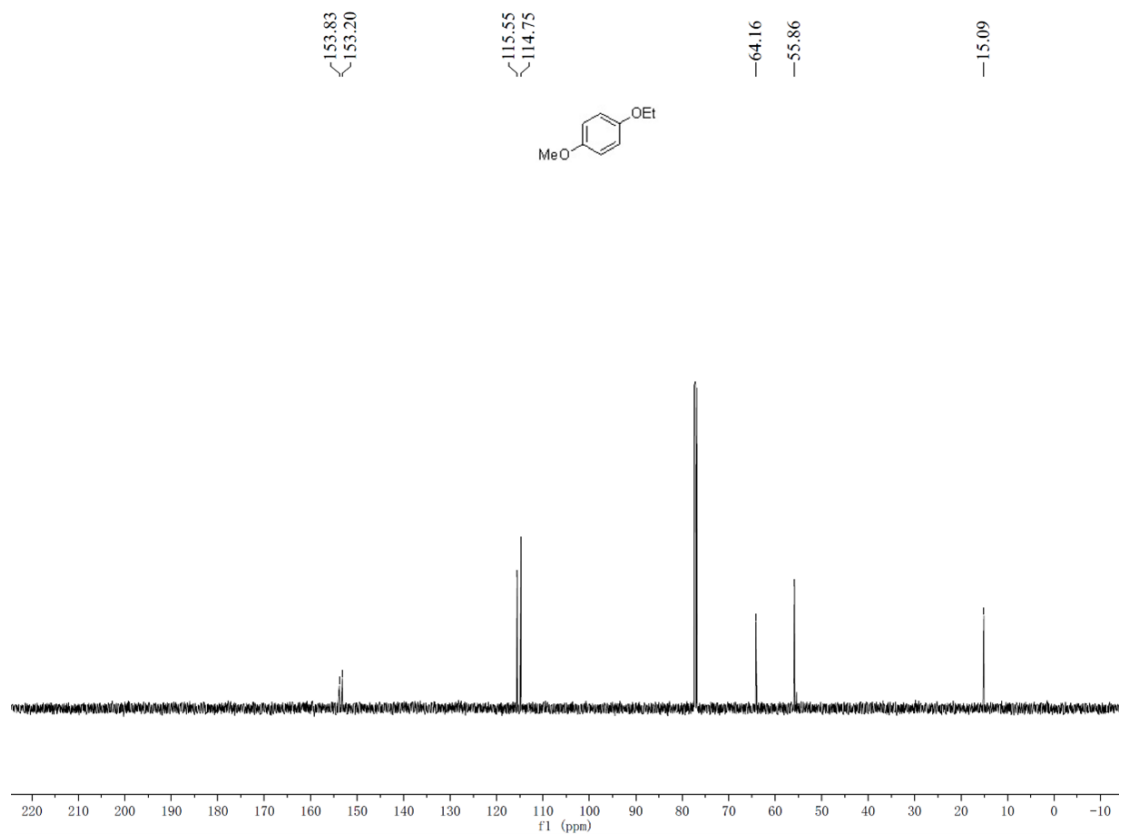
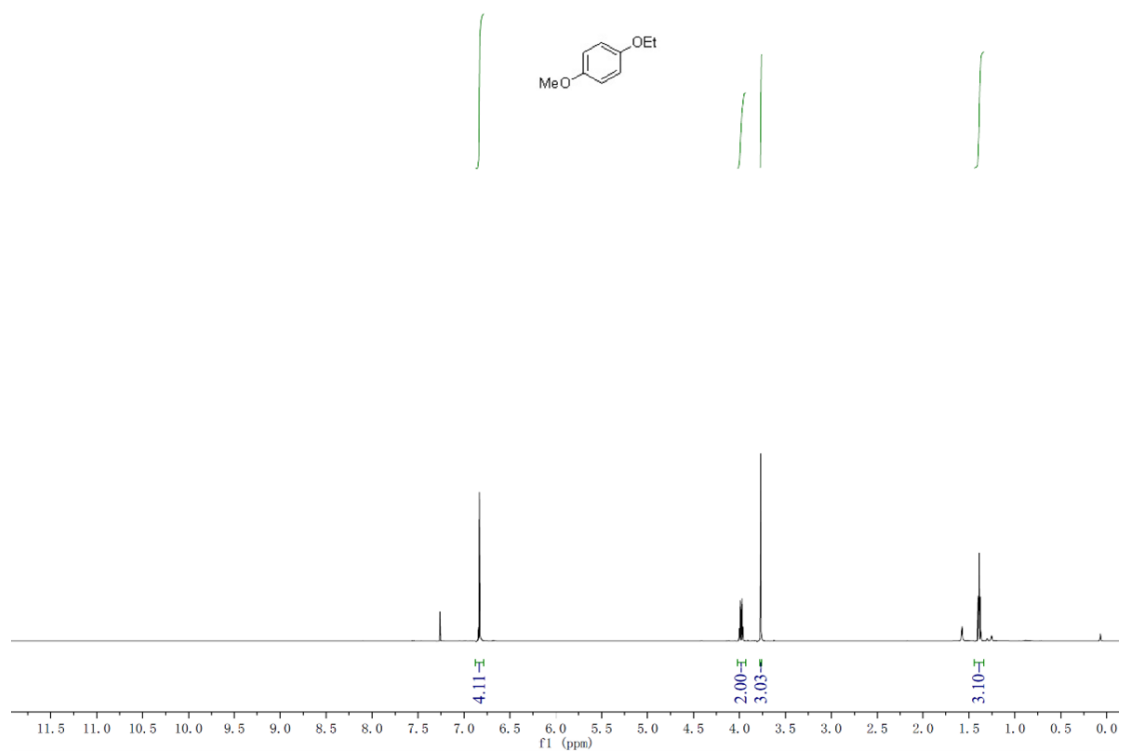
spectra of product 20.



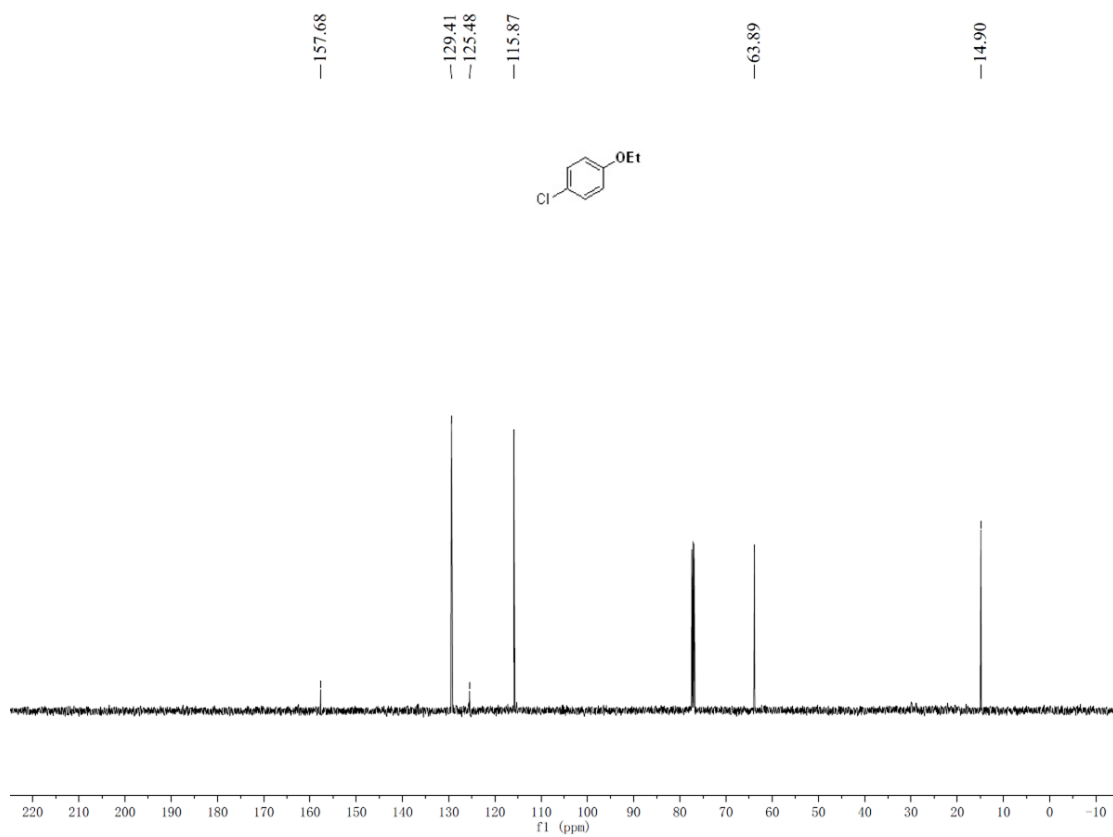
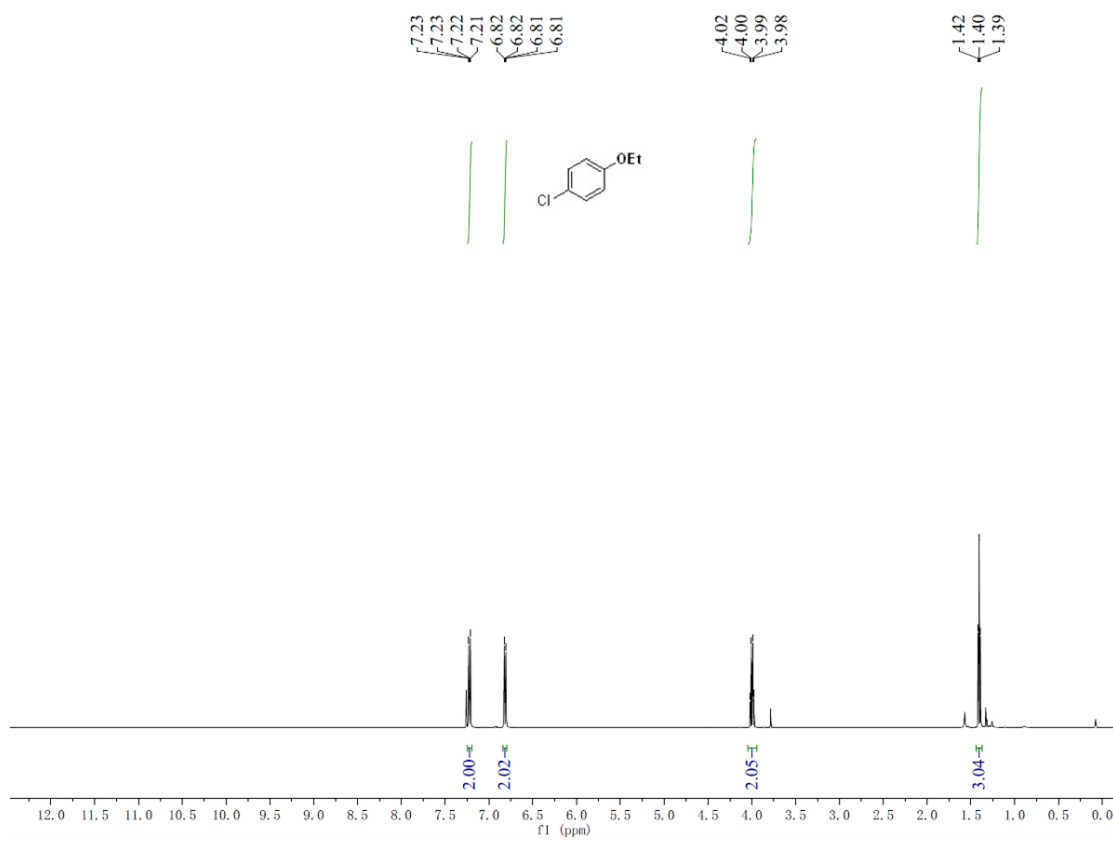
^1H spectra of product 21.



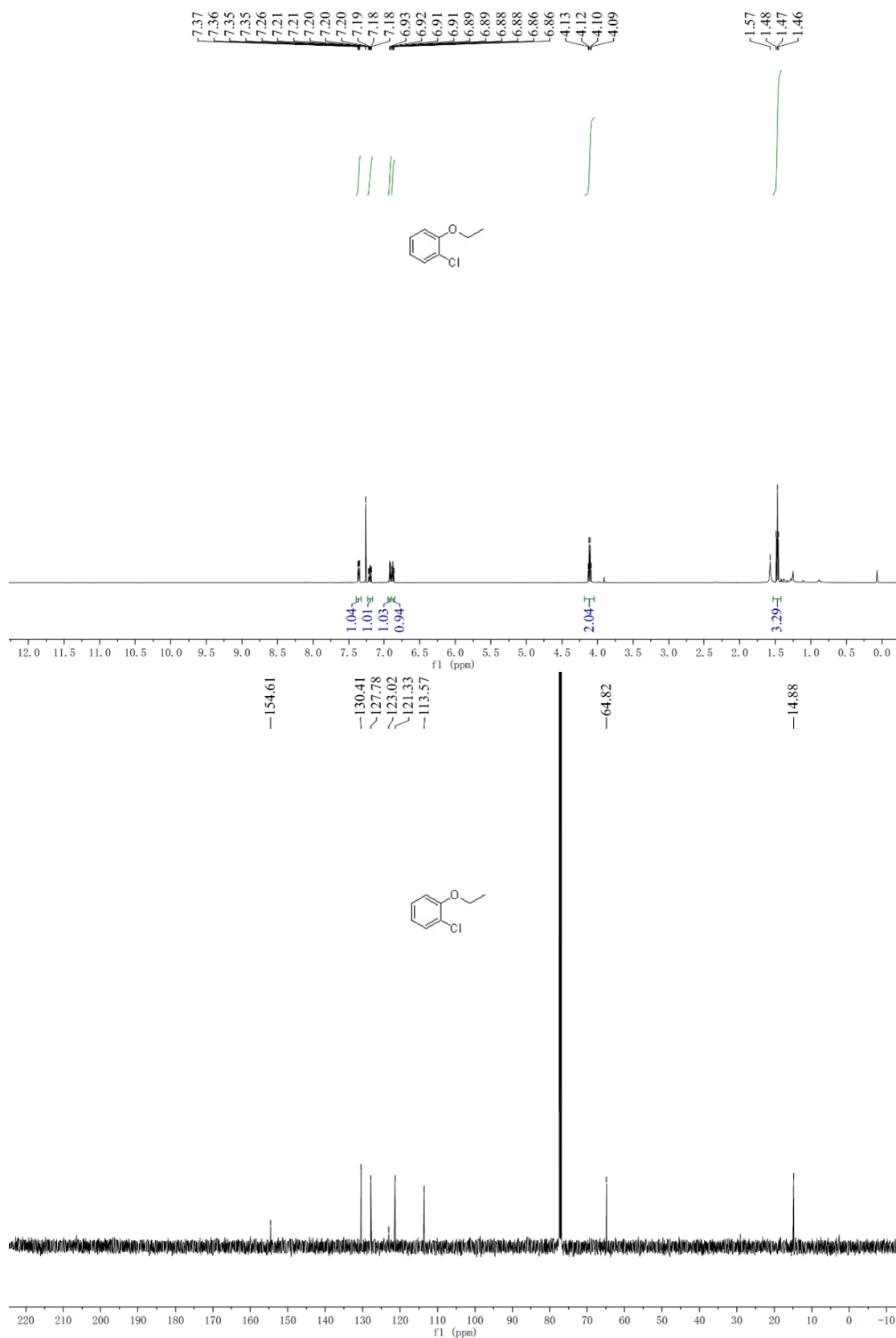
¹H and ¹³C-NMR spectra of product 22.



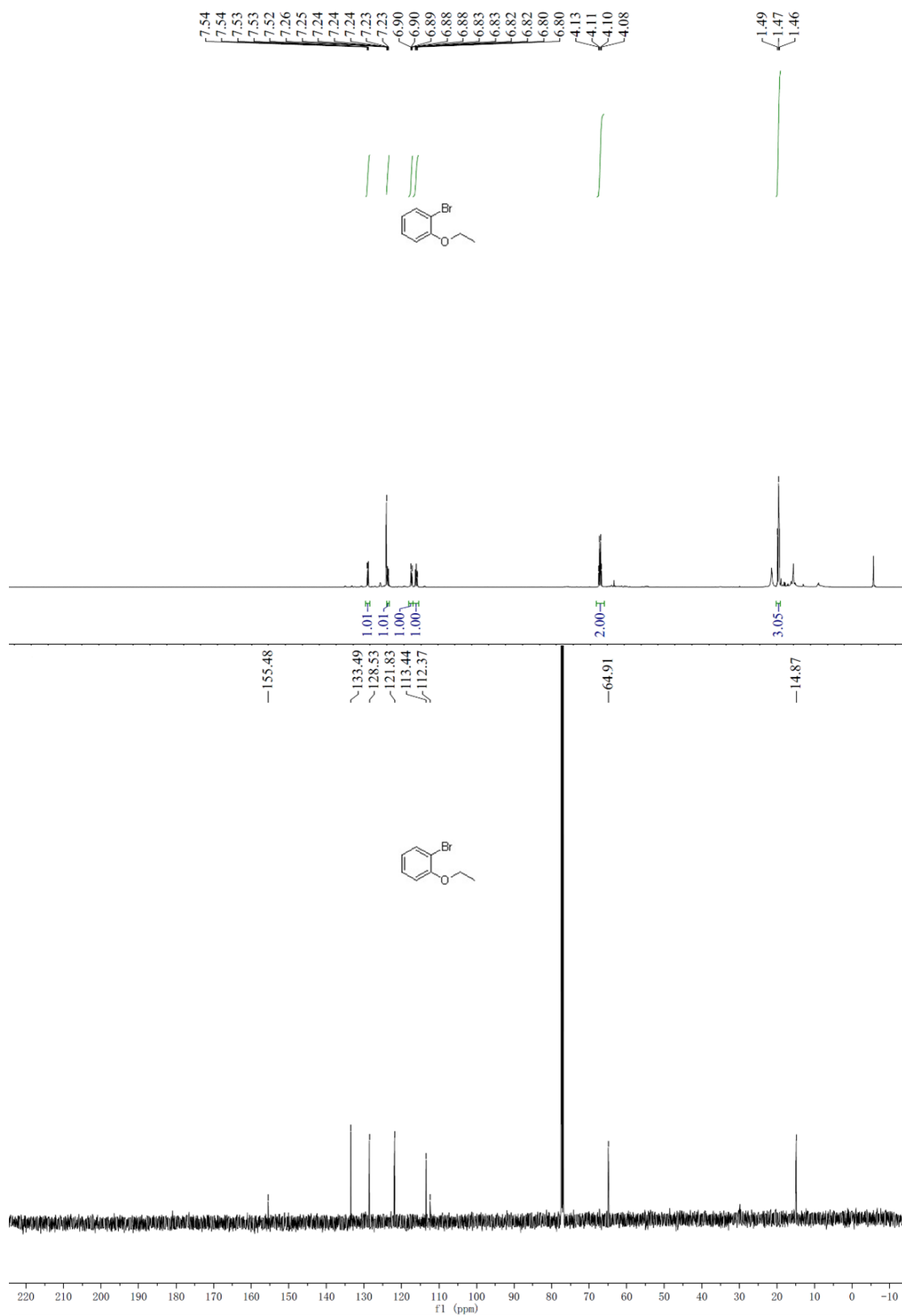
¹H and ¹³C-NMR spectra of product 23.



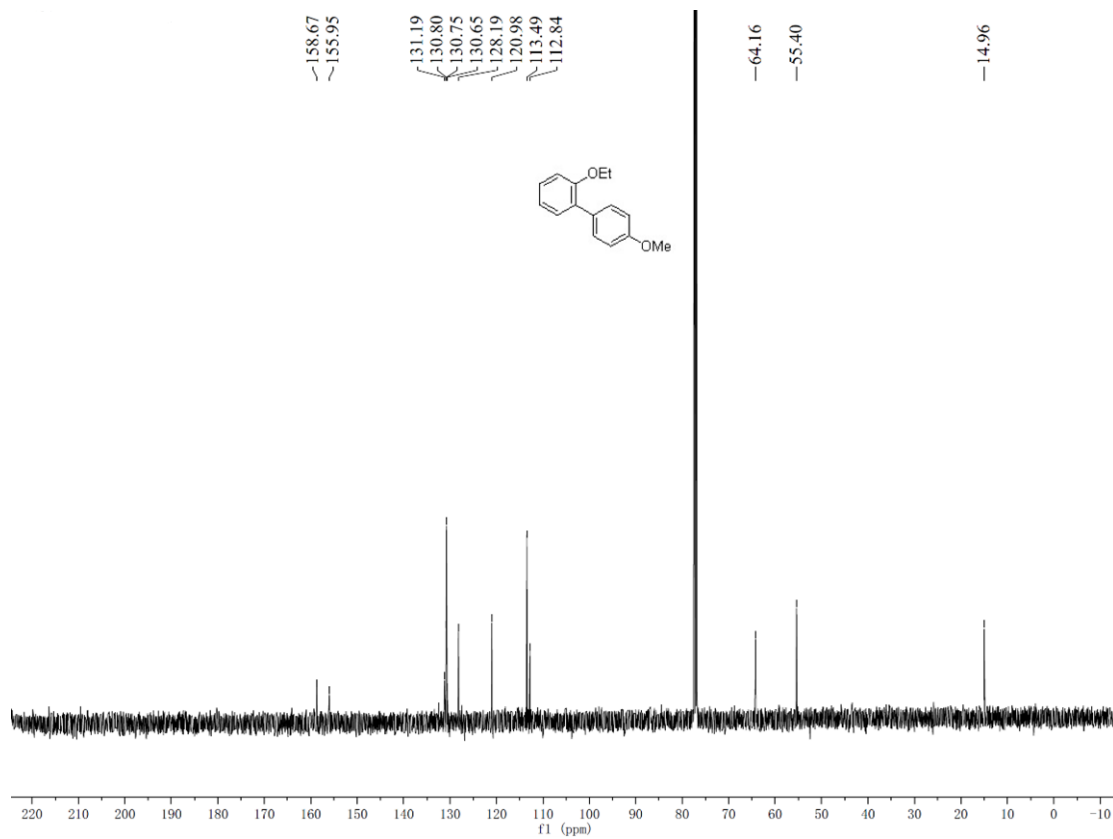
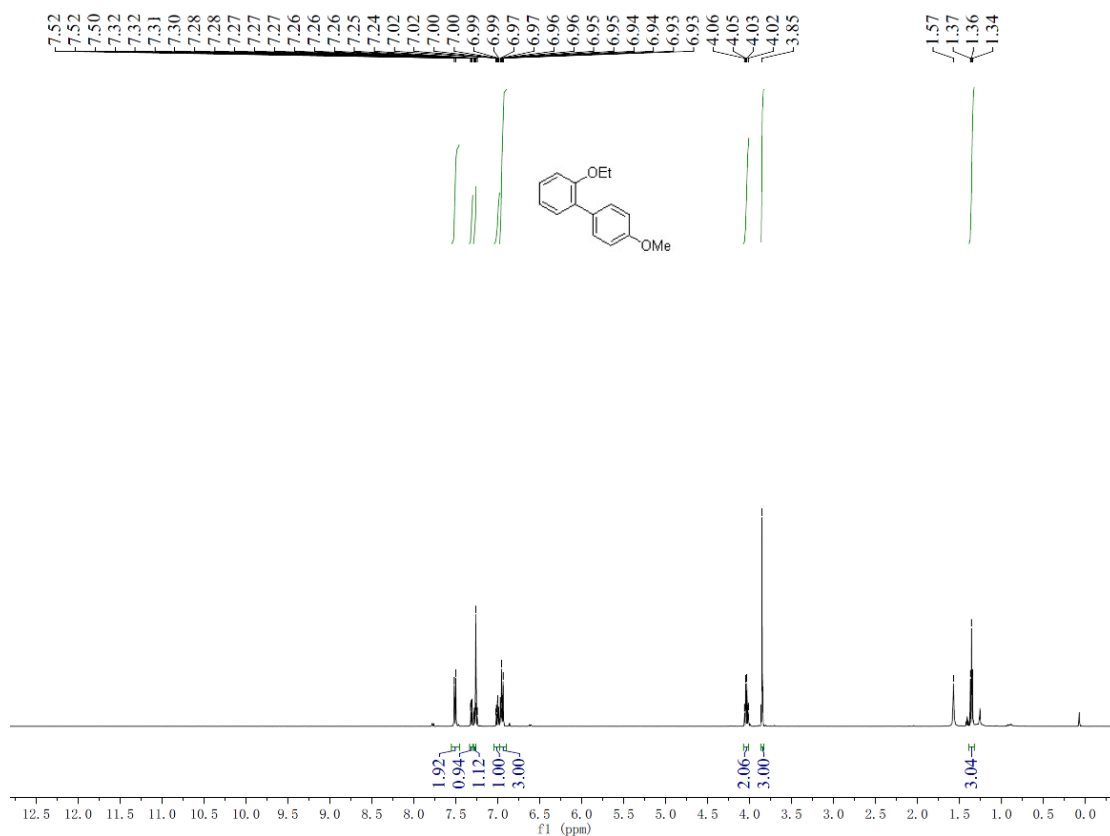
^1H and ^{13}C -NMR spectra of product 24.



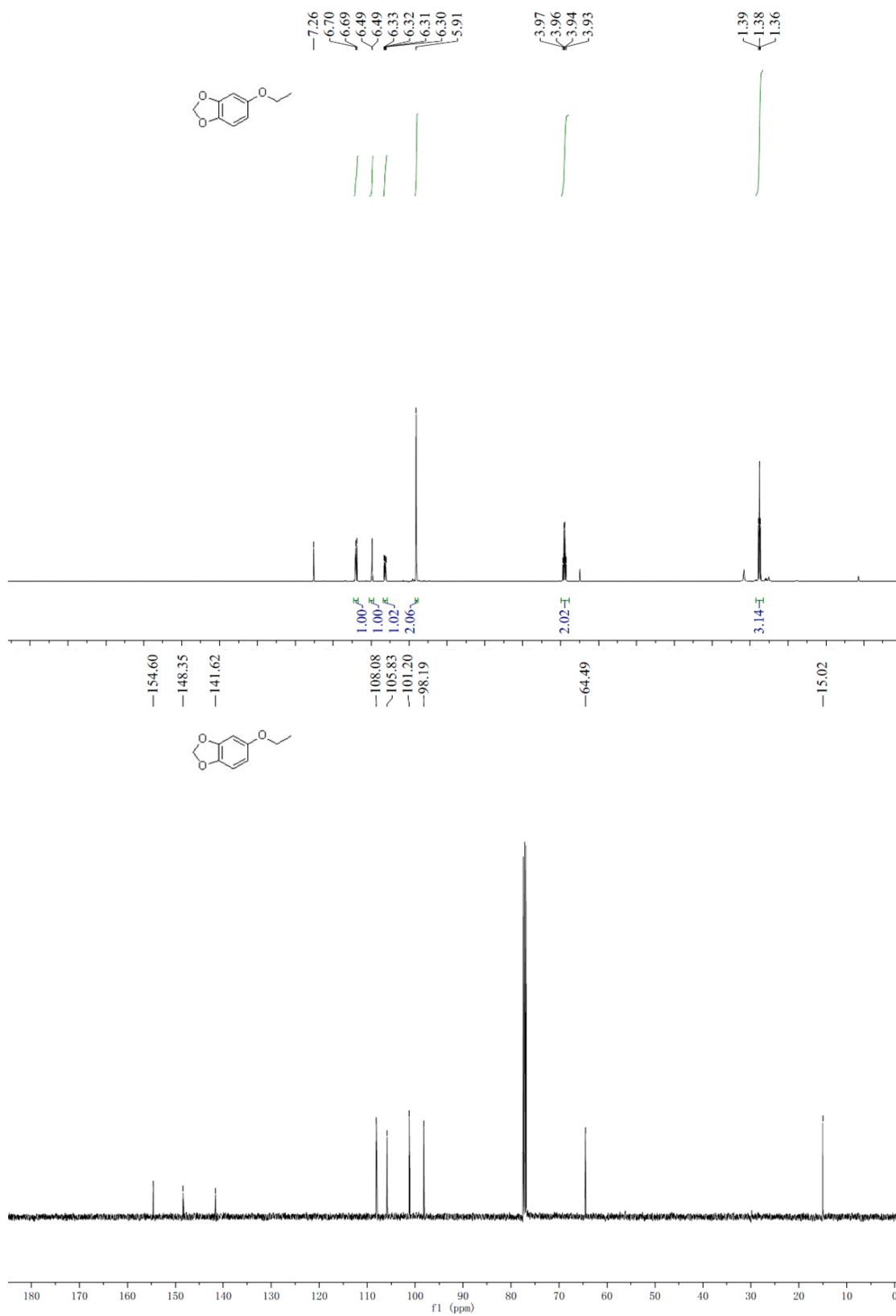
¹H and ¹³C-NMR spectra of product 25.



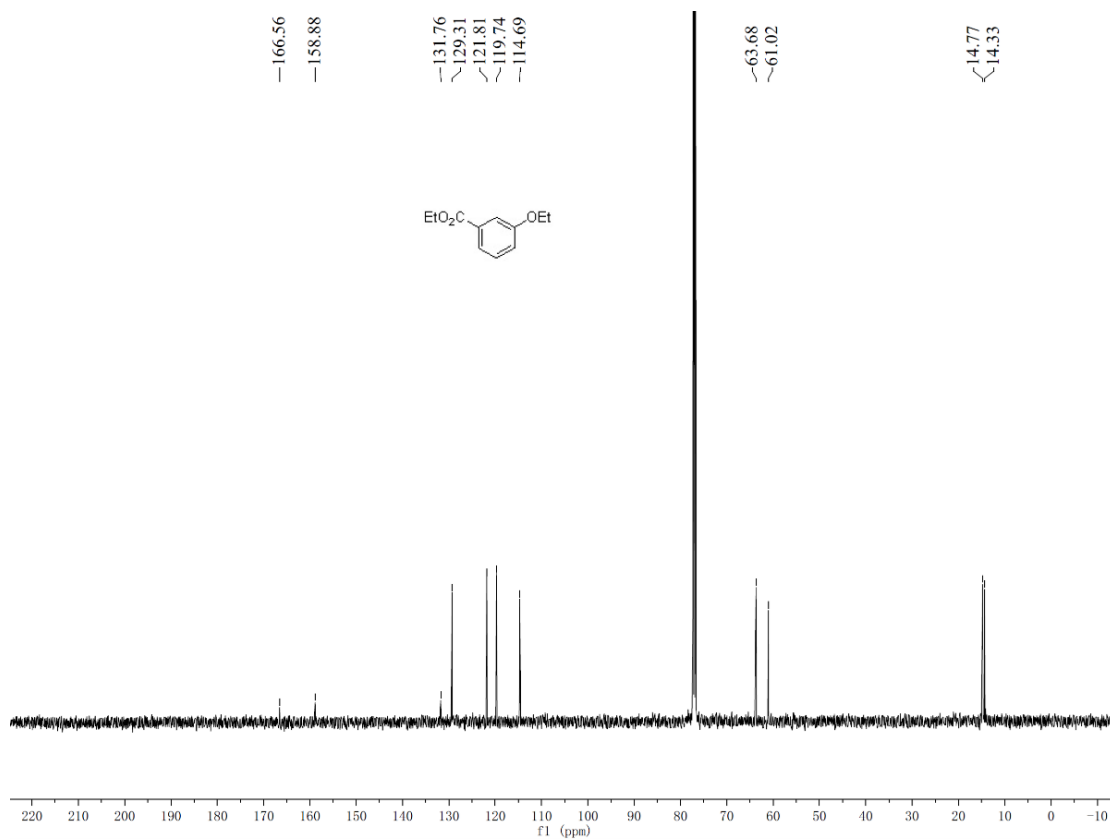
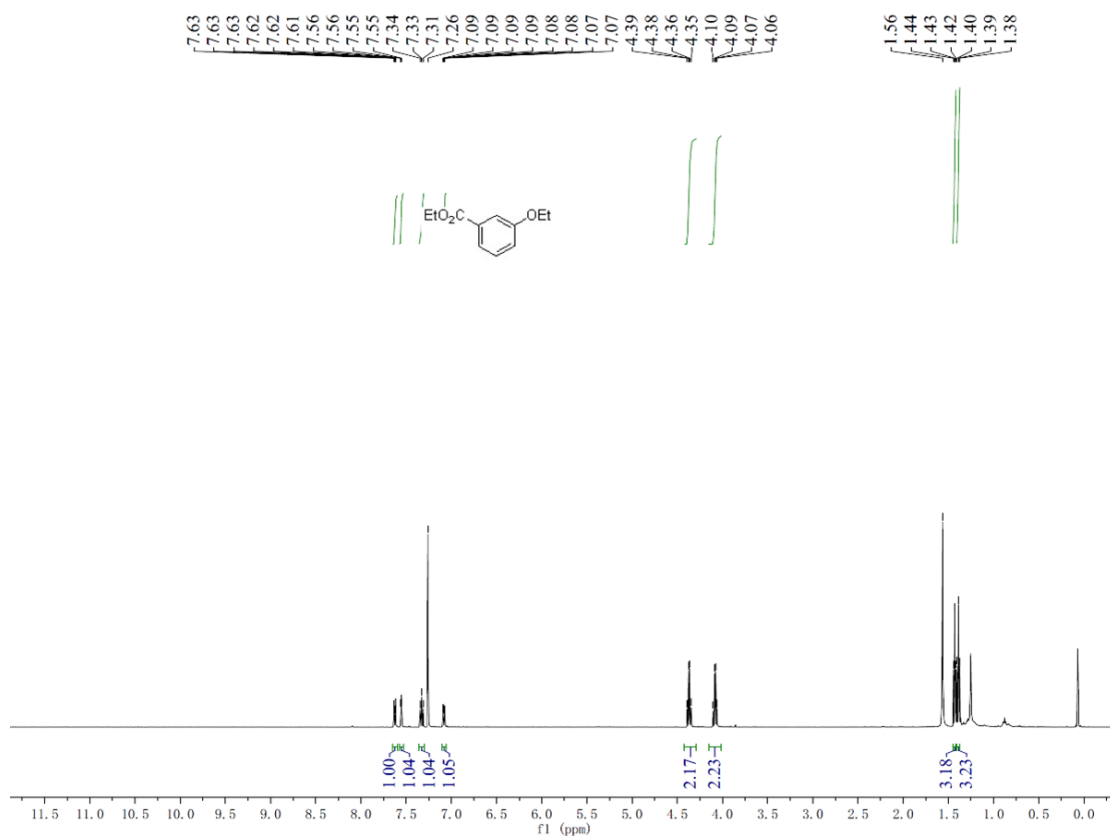
¹H and ¹³C-NMR spectra of product 26.



¹H and ¹³C-NMR spectra of product 27.

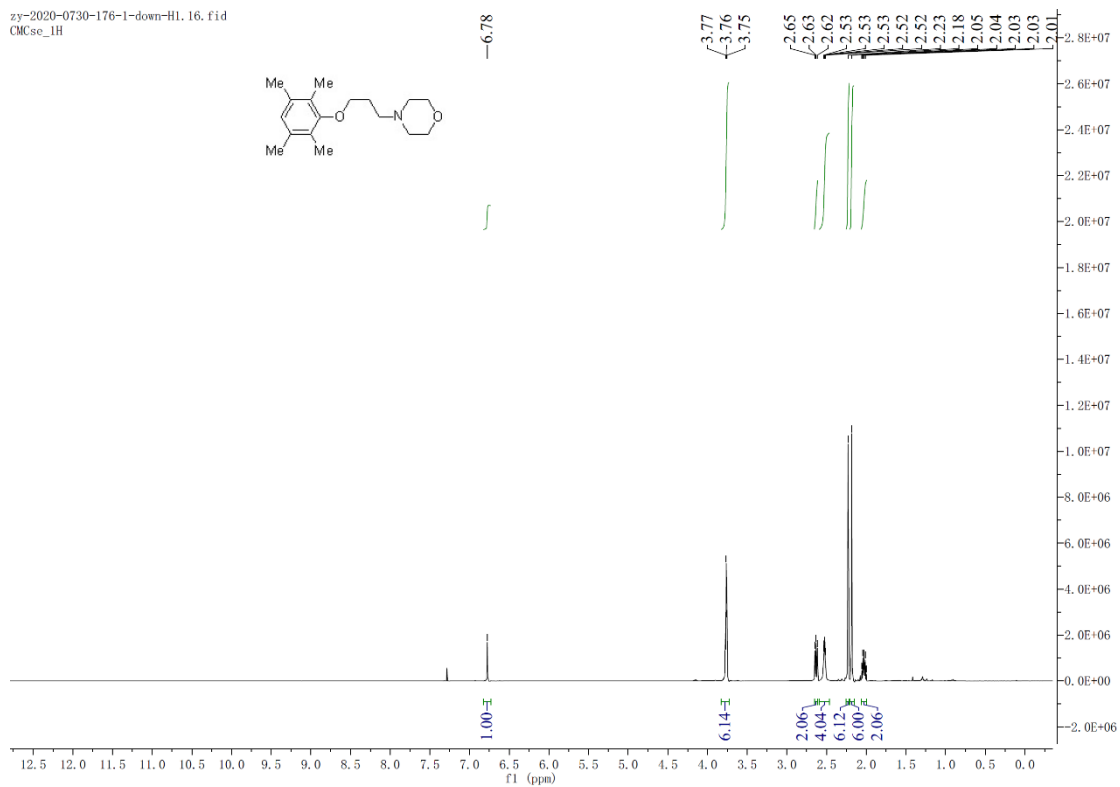


¹H and ¹³C-NMR spectra of product 28.

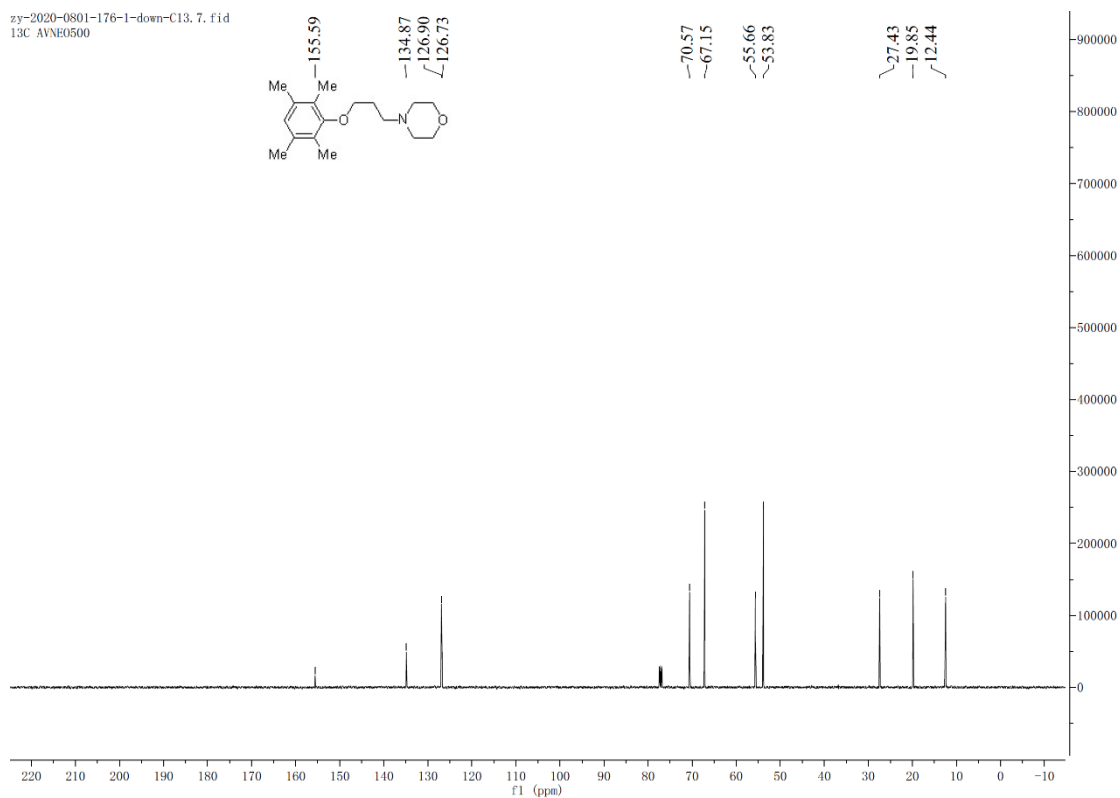


¹H and ¹³C-NMR spectra of product 29.

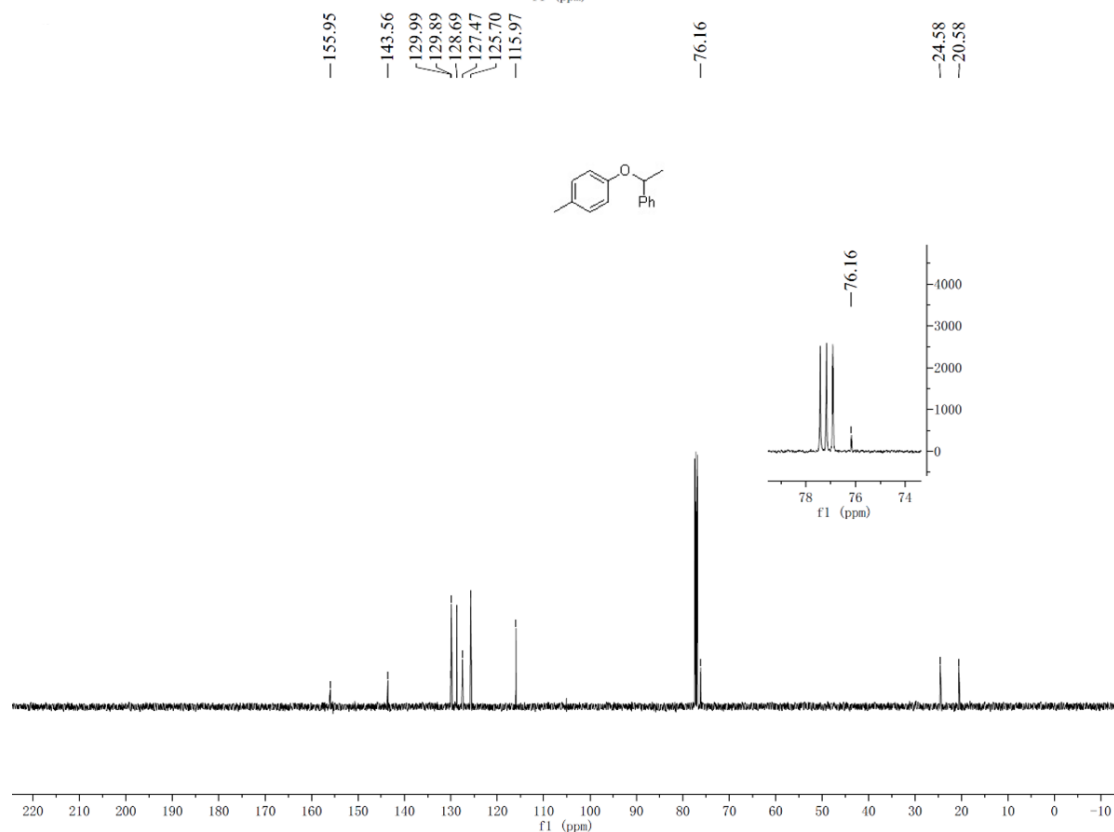
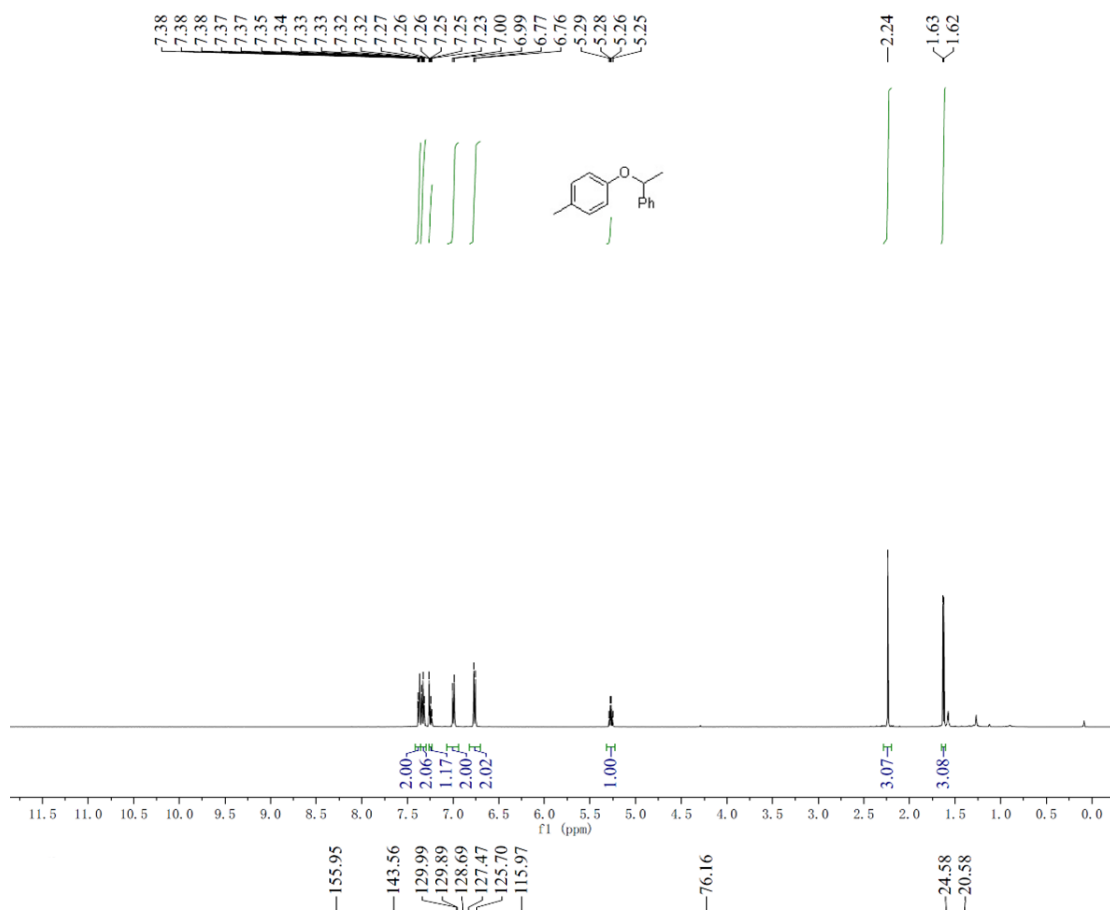
zy-2020-0730-176-1-down-H1.16.fid
CMCse_1H



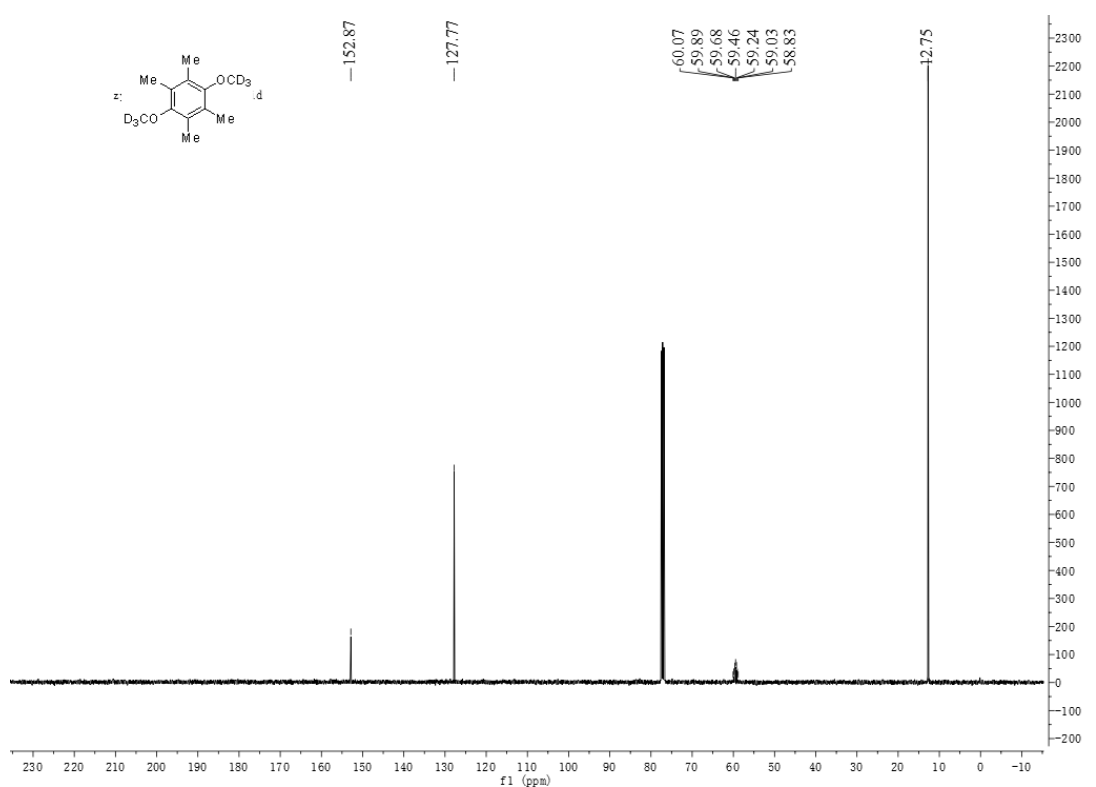
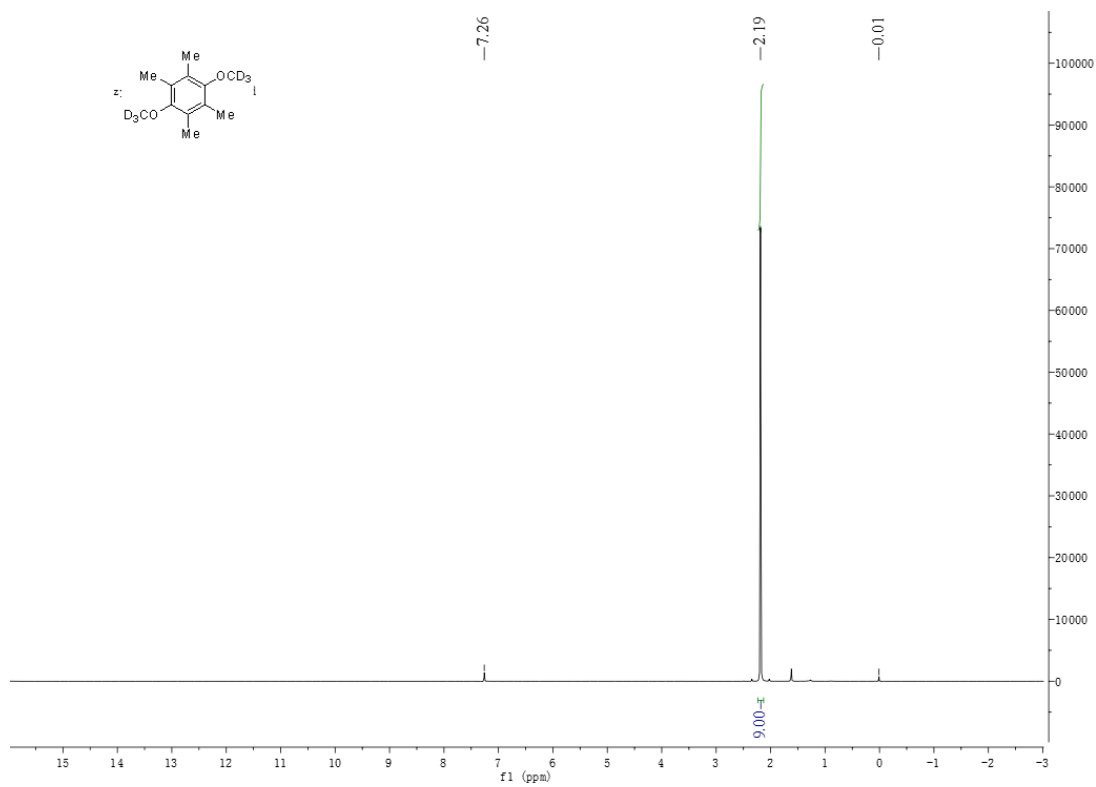
zy-2020-0801-176-1-down-C13.7.fid
13C AVN0500



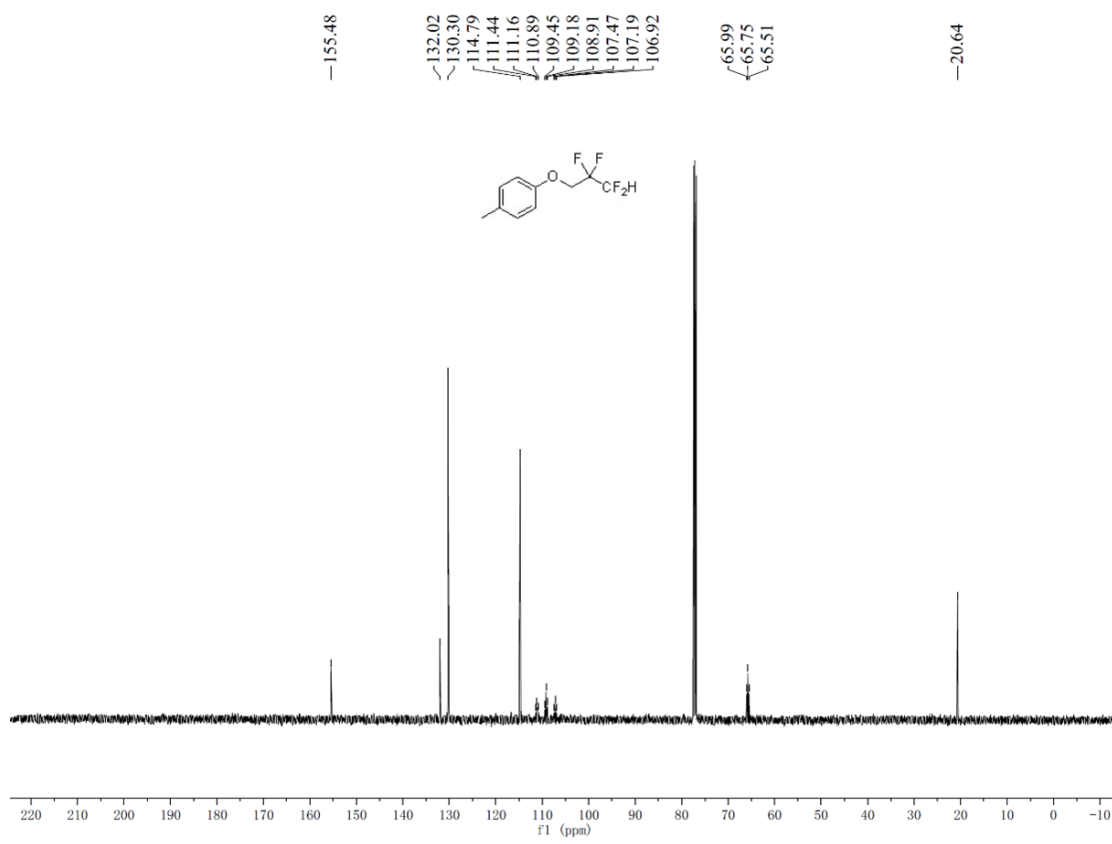
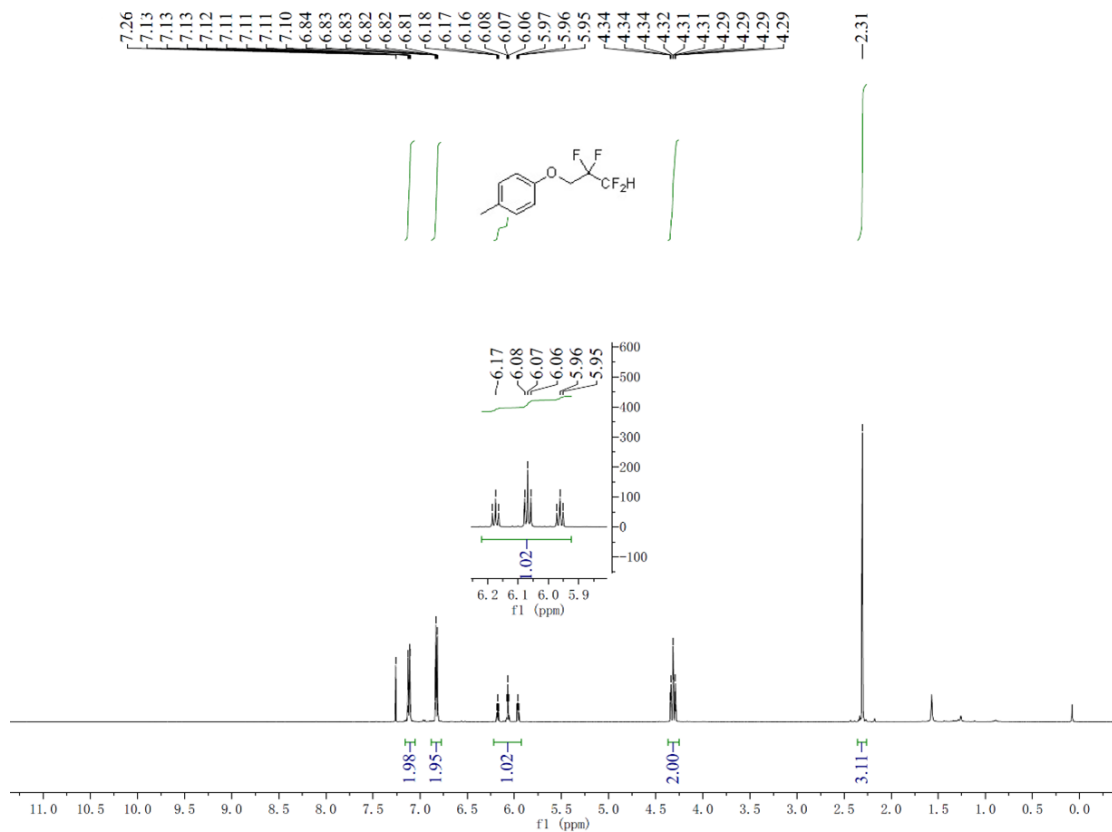
^1H and ^{13}C -NMR spectra of product 30.

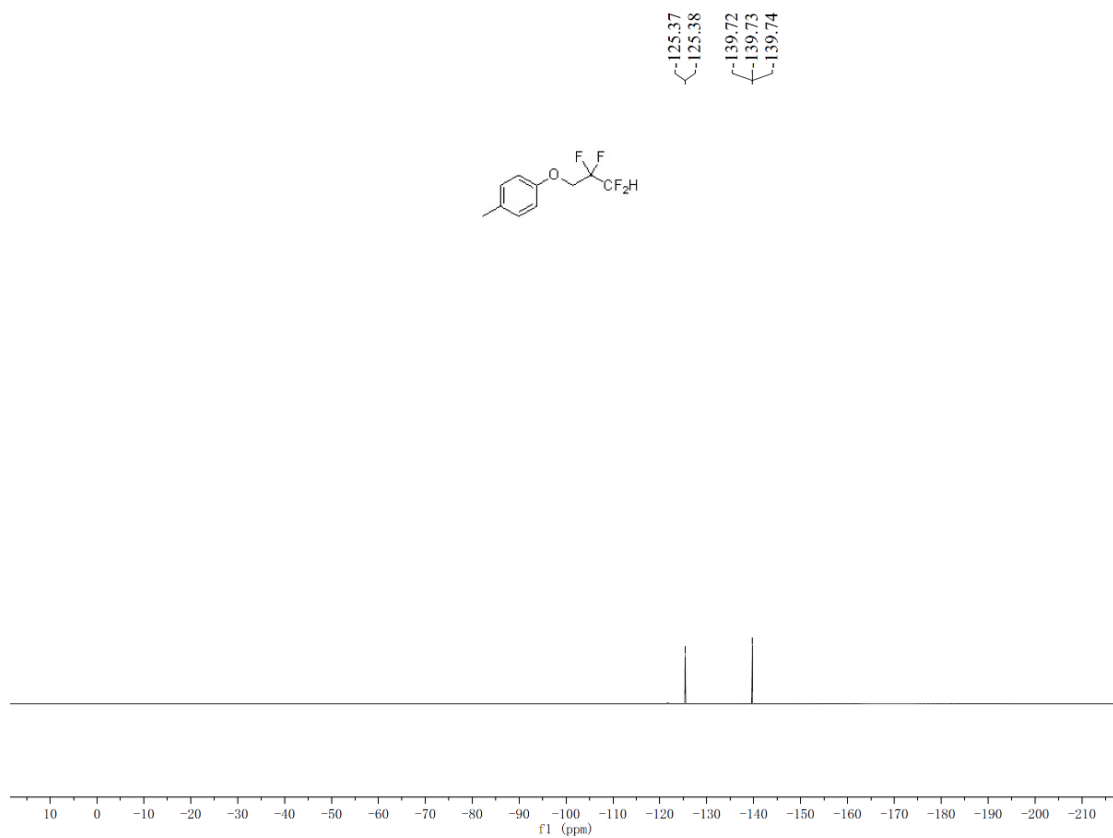


¹H and ¹³C-NMR spectra of product 31.

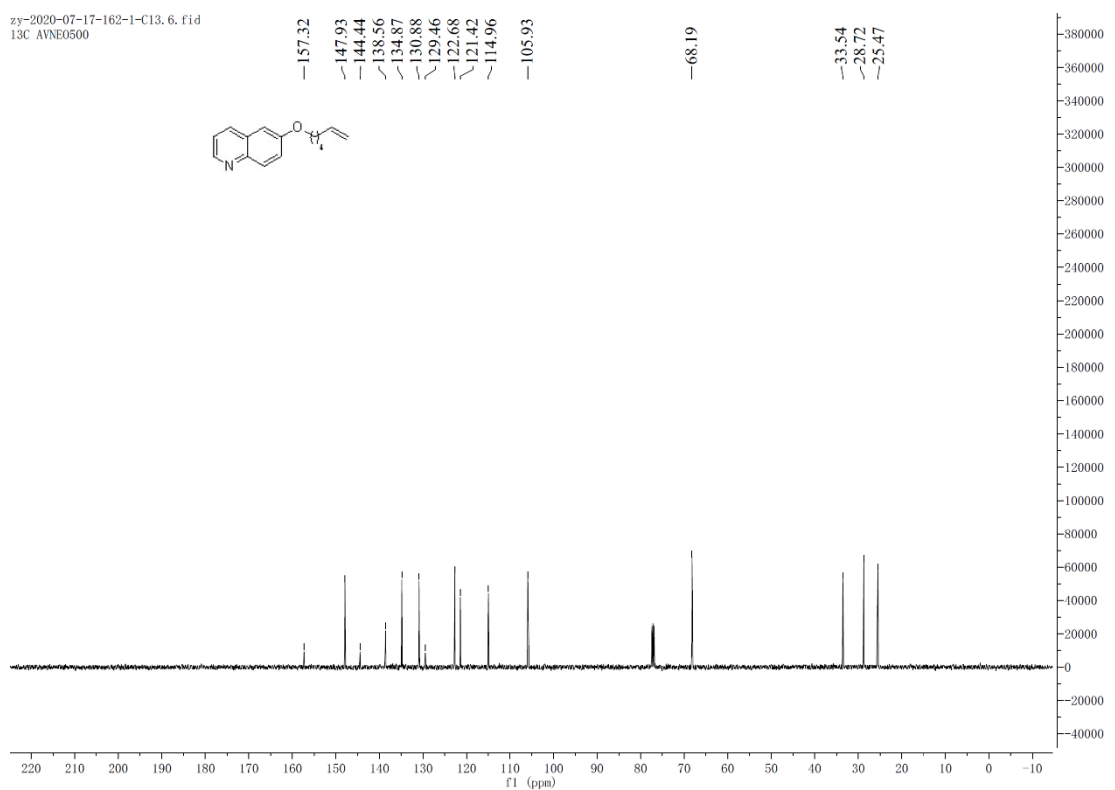
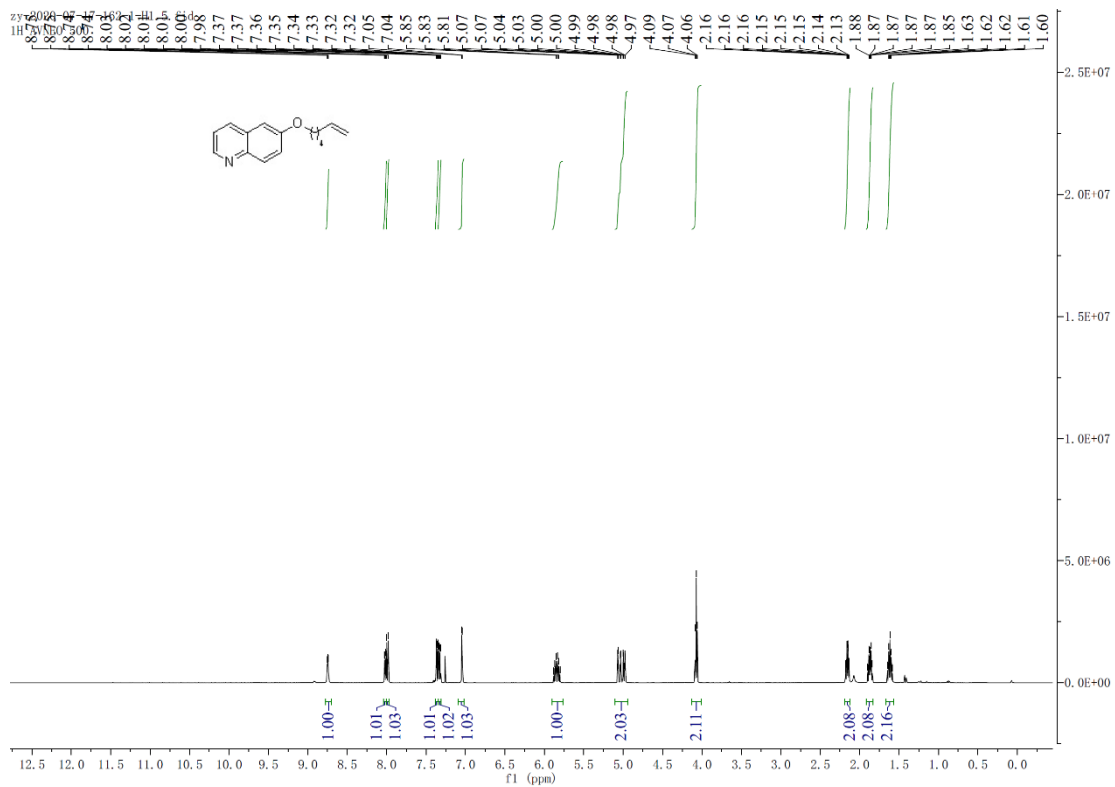


¹H and ¹³C-NMR spectra of product 32.

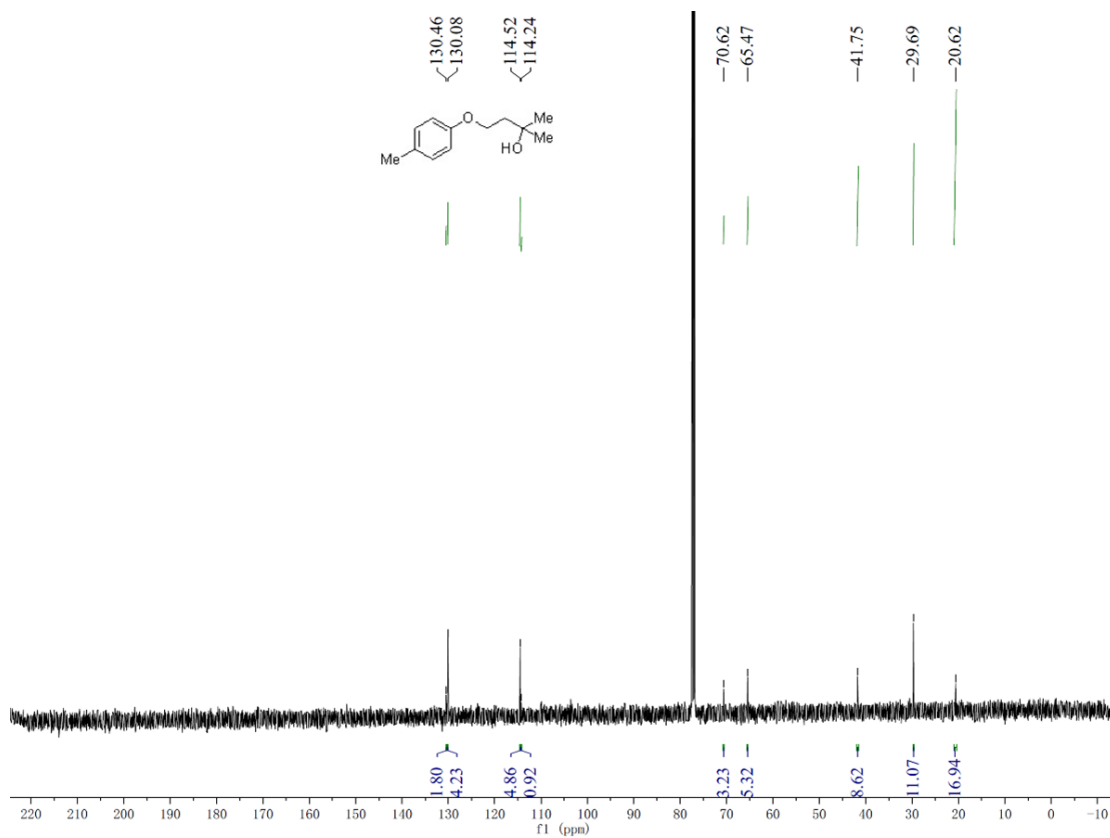
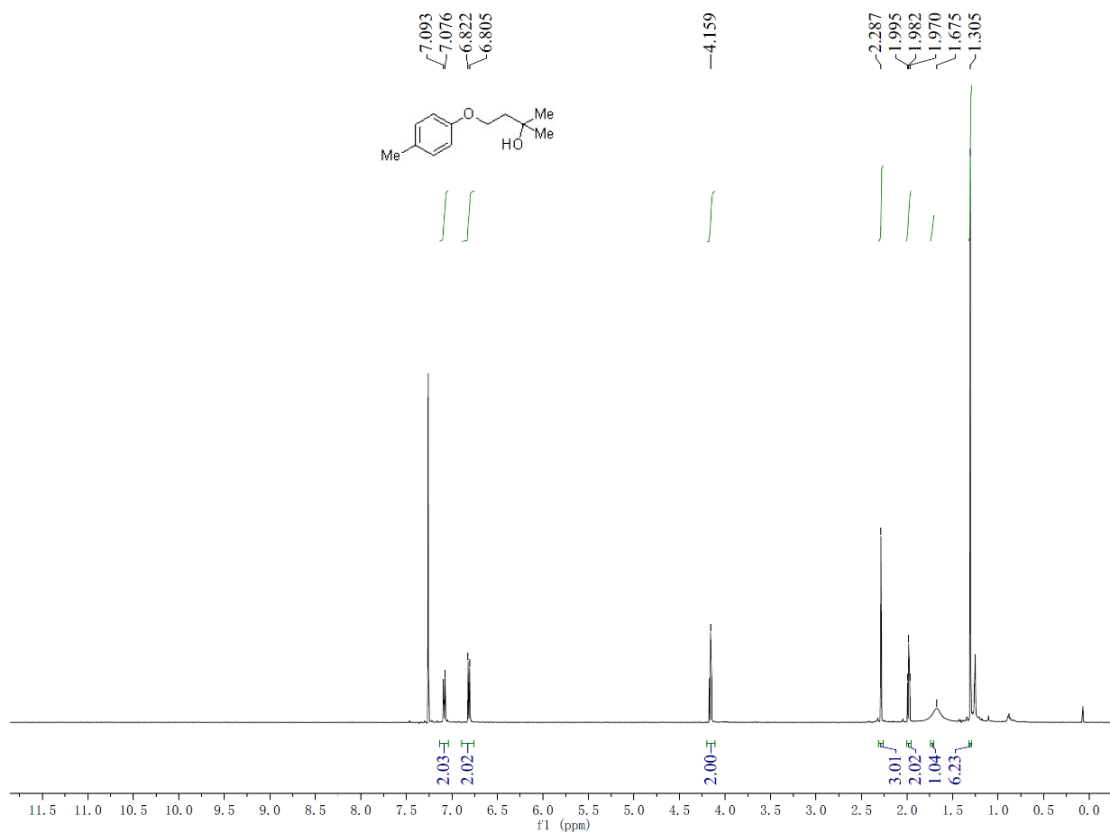




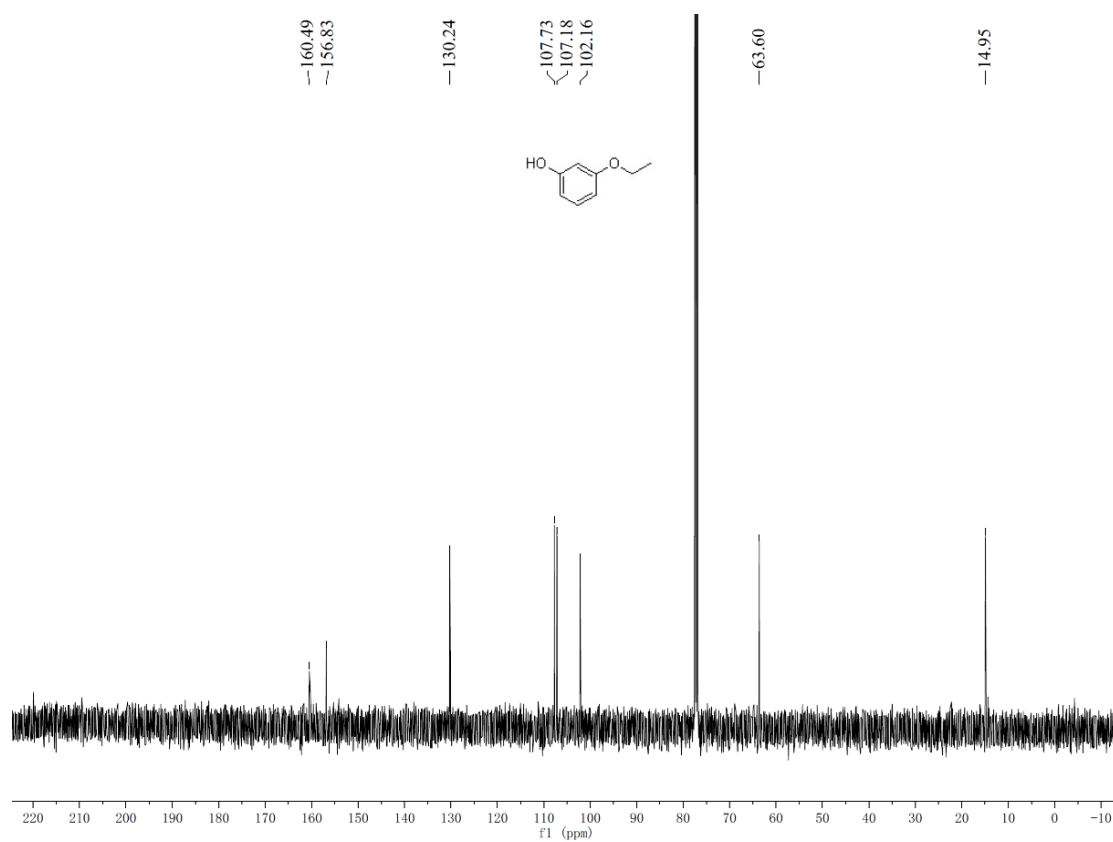
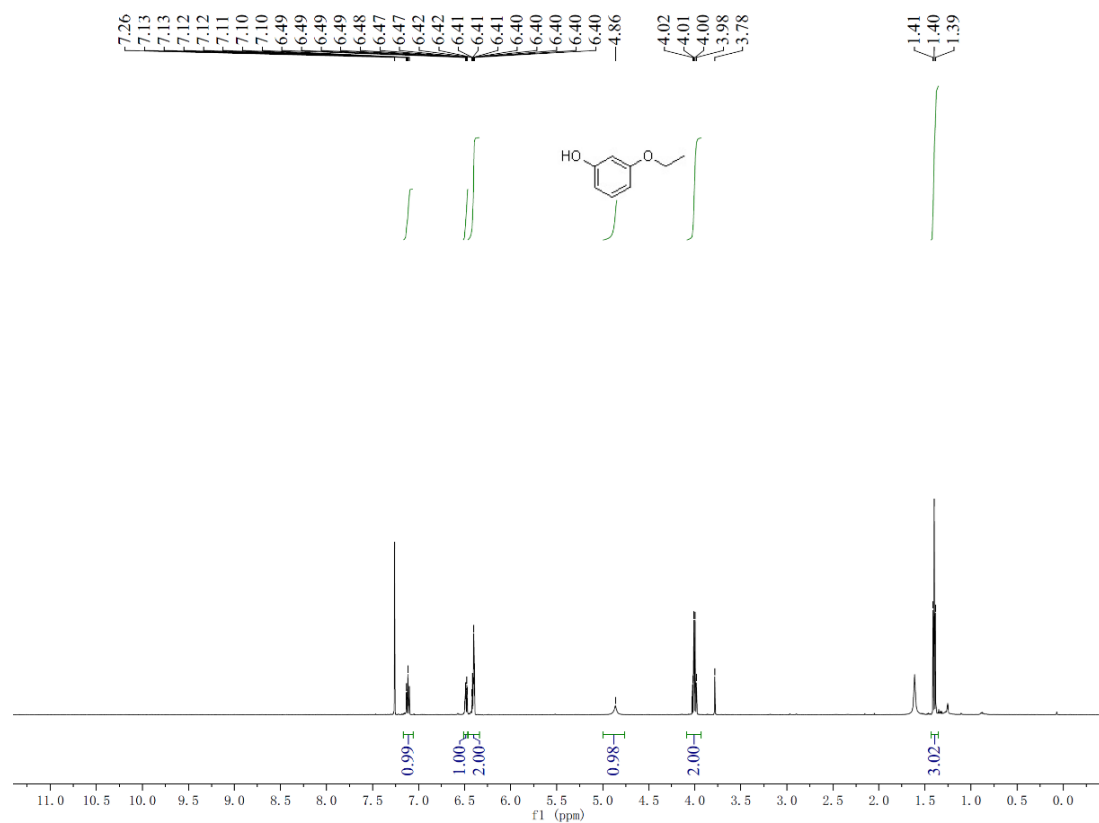
^1H , ^{13}C , and ^{19}F -NMR spectra of product 33.



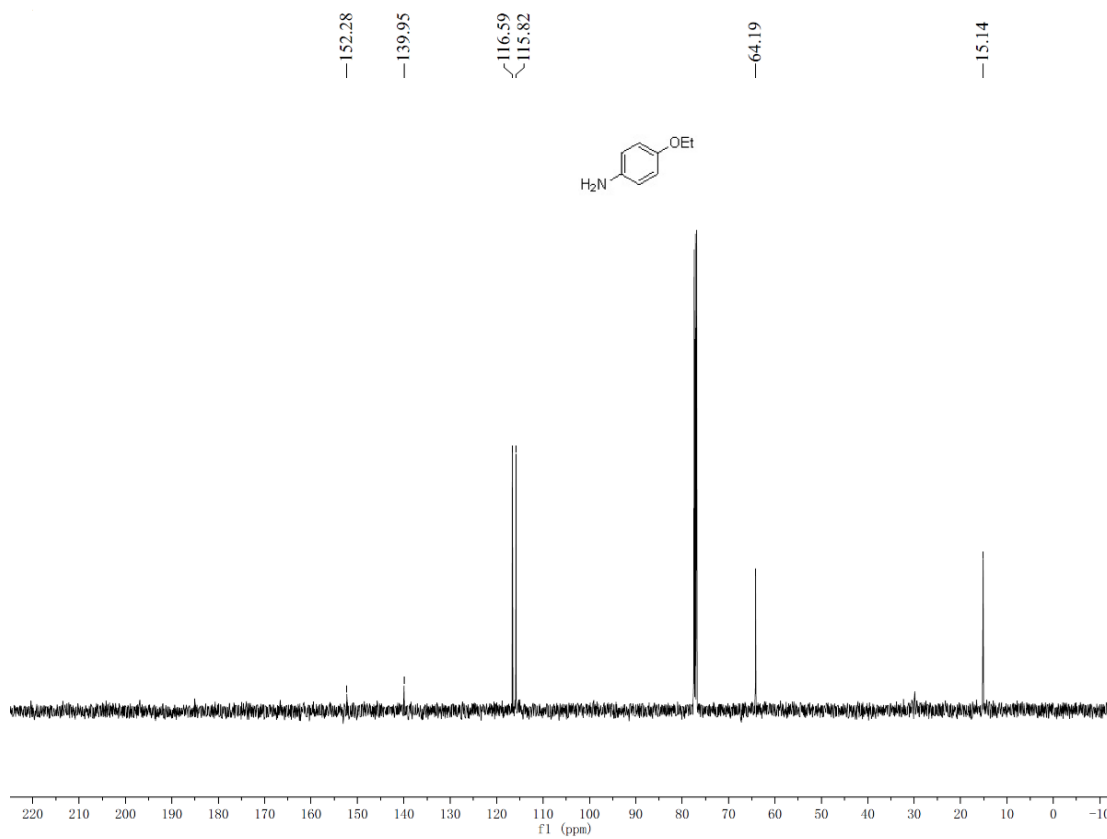
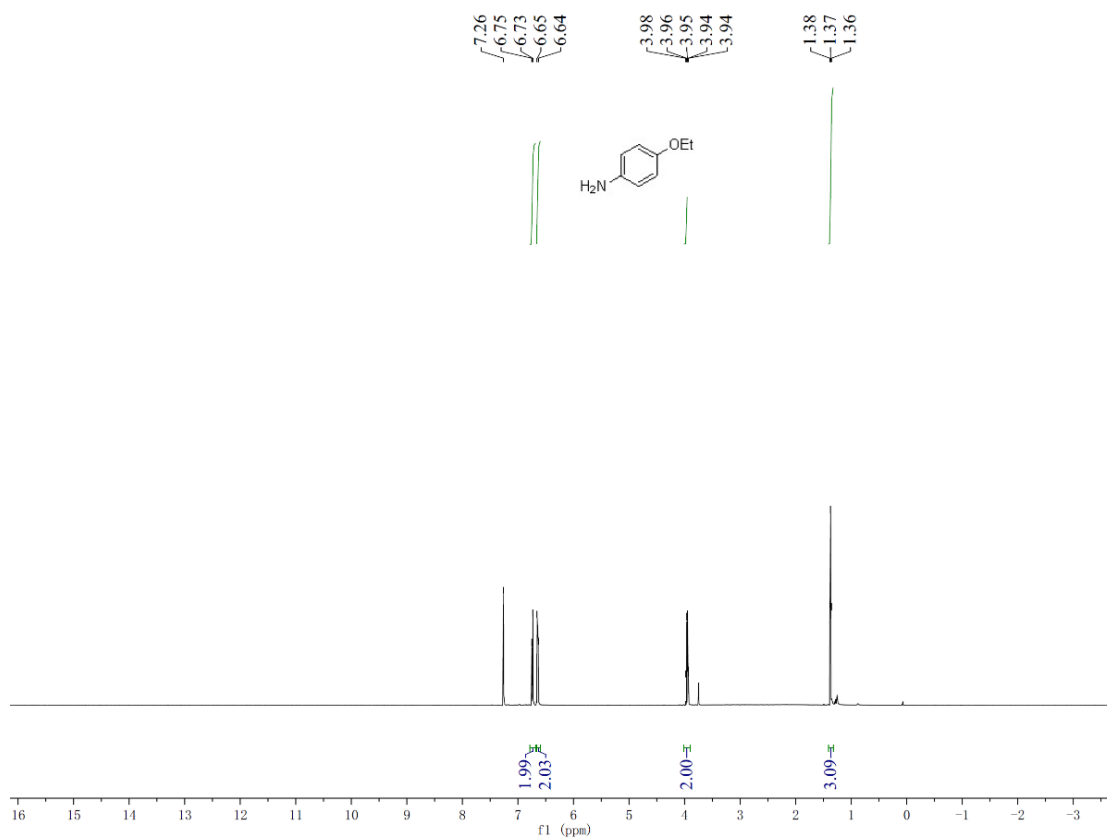
¹H and ¹³C-NMR spectra of product 34.



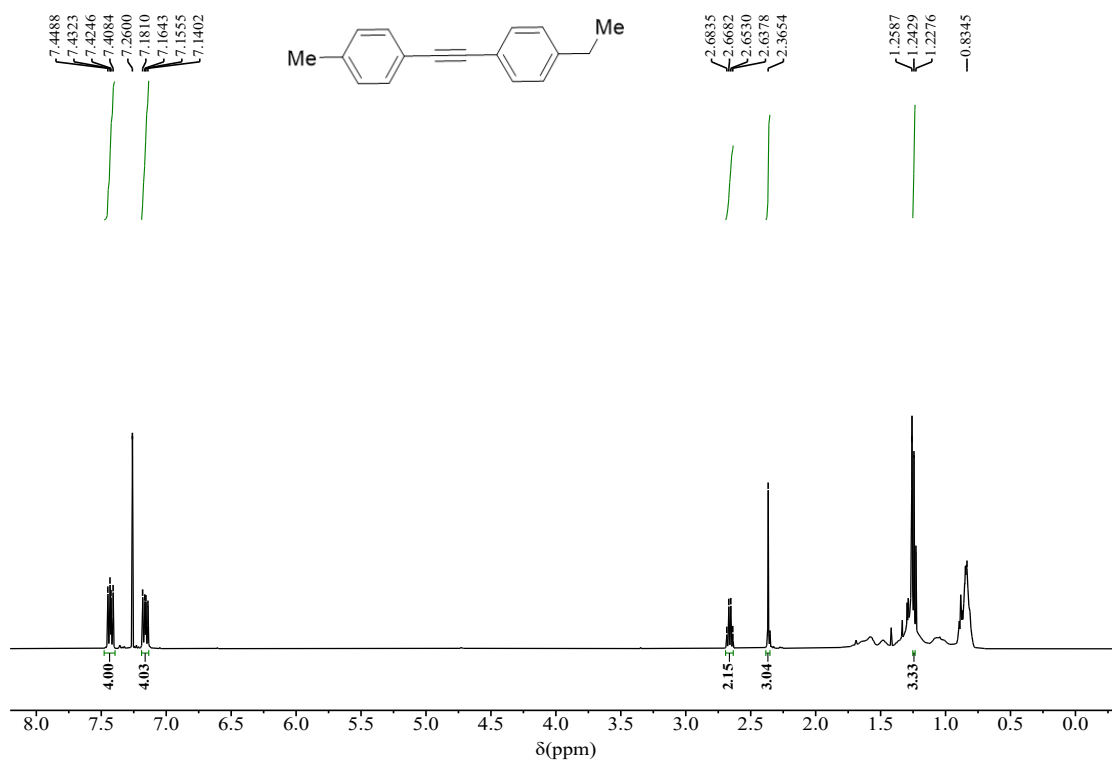
¹H and ¹³C-NMR spectra of product 35.



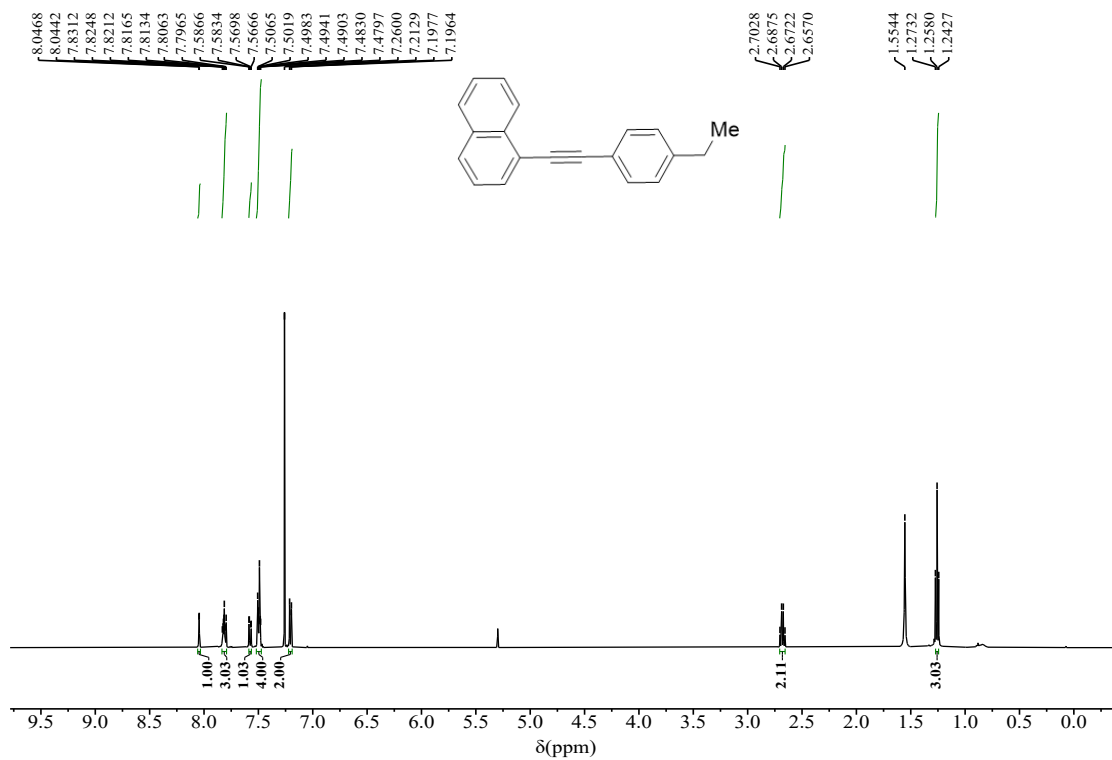
¹H and ¹³C-NMR spectra of product 36.



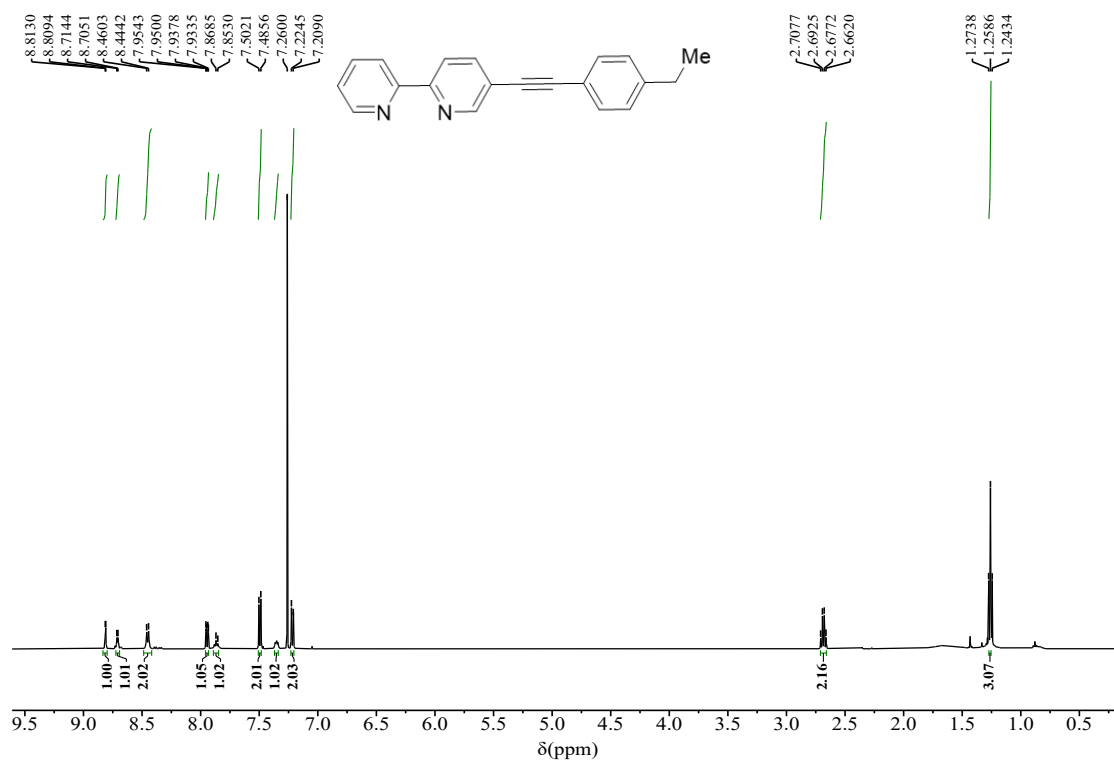
¹H and ¹³C-NMR spectra of product 37.



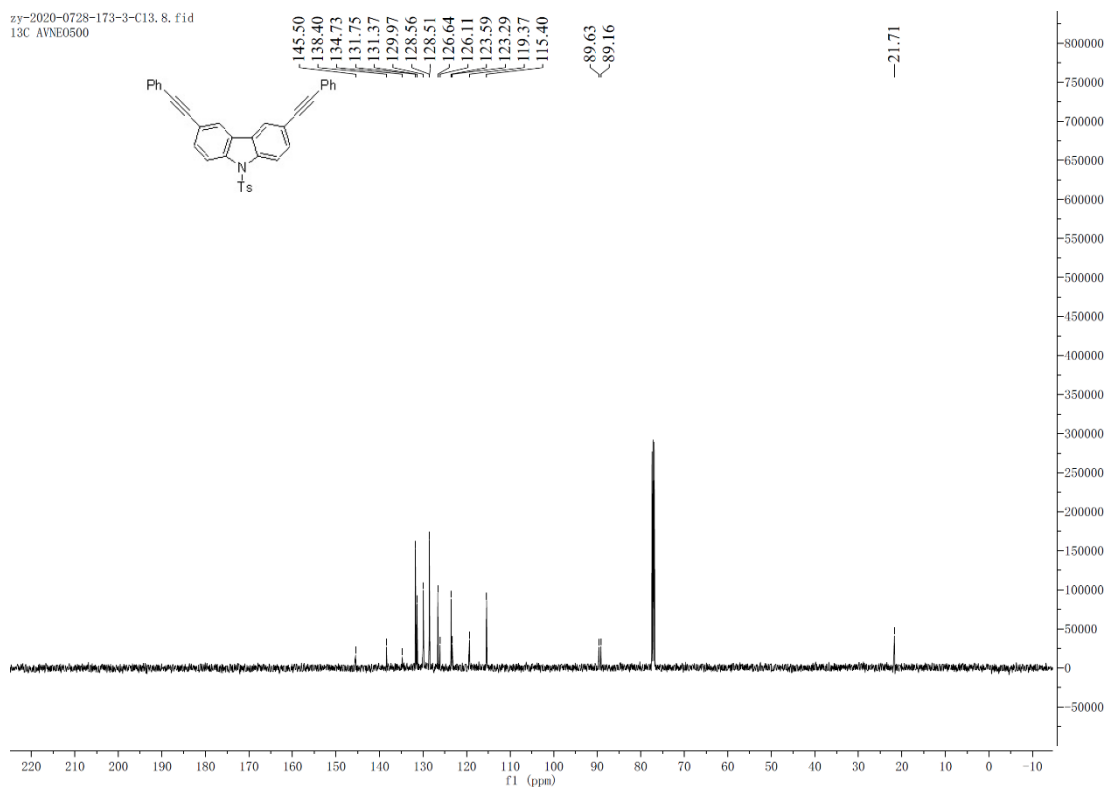
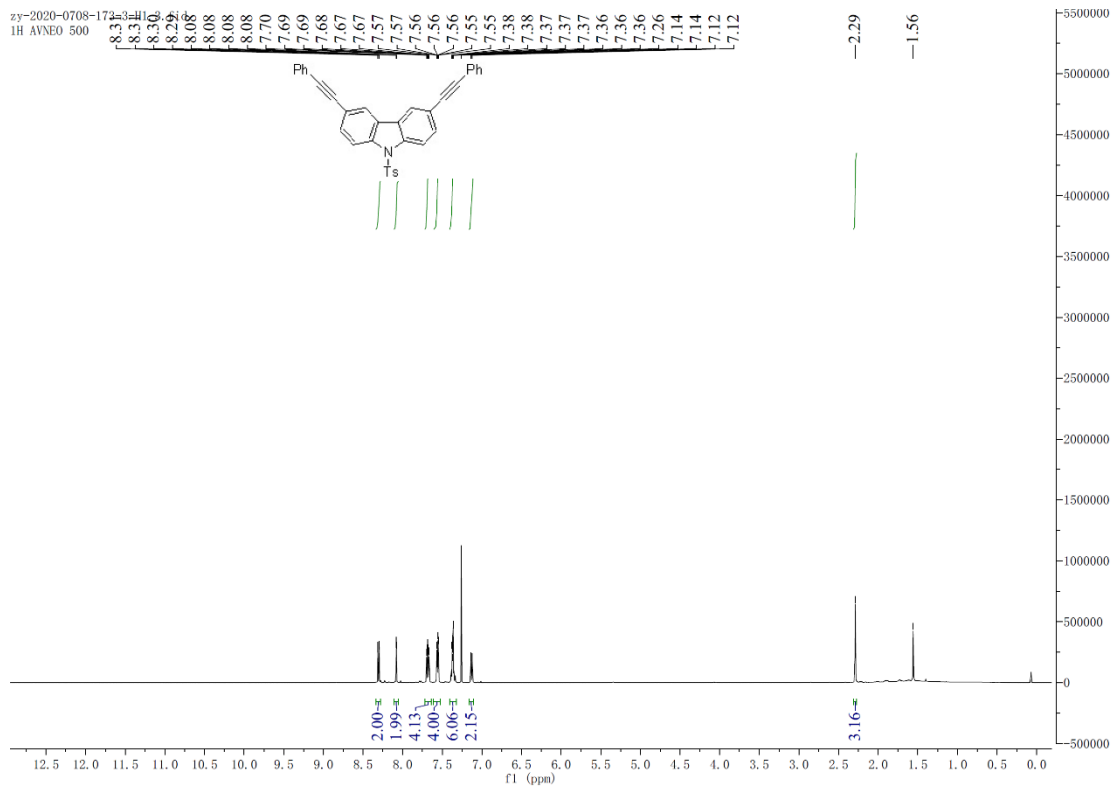
¹H spectra of product 38.



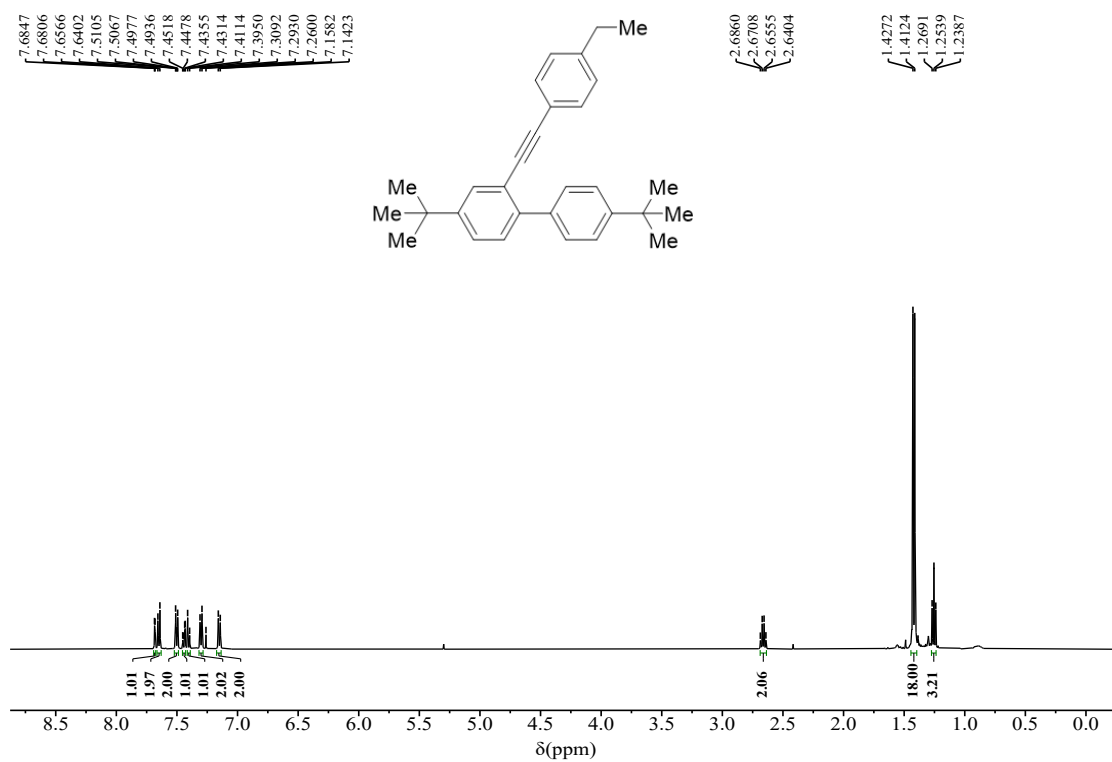
¹H spectra of product 39.



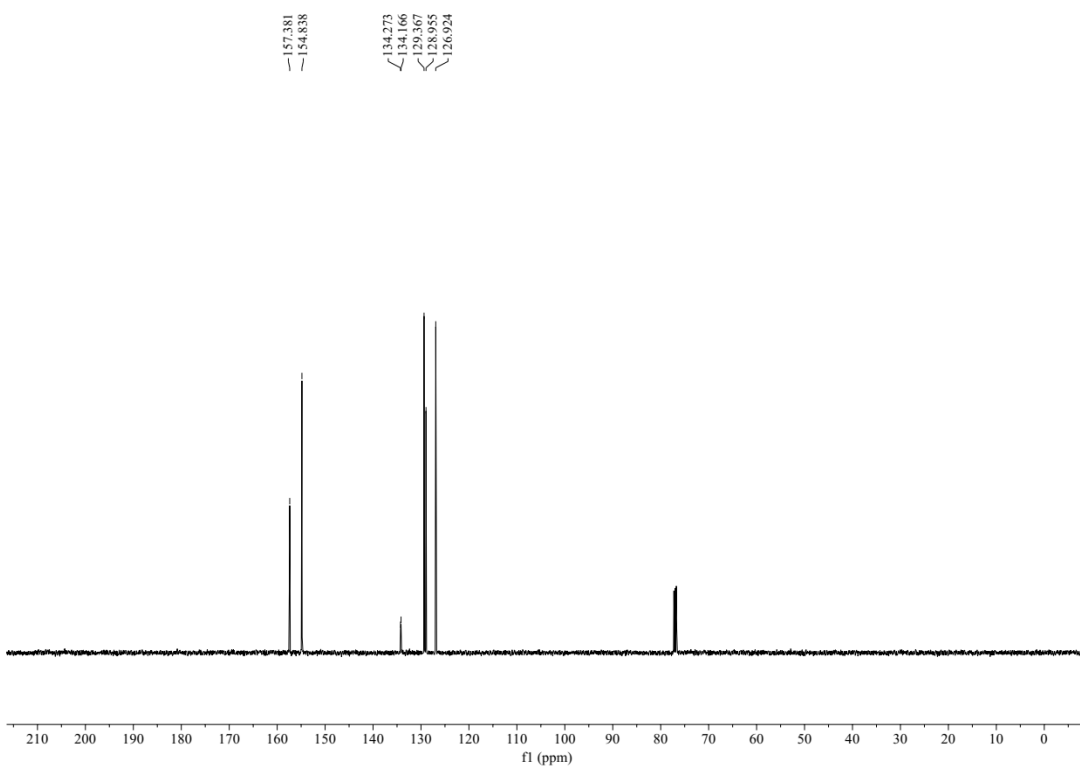
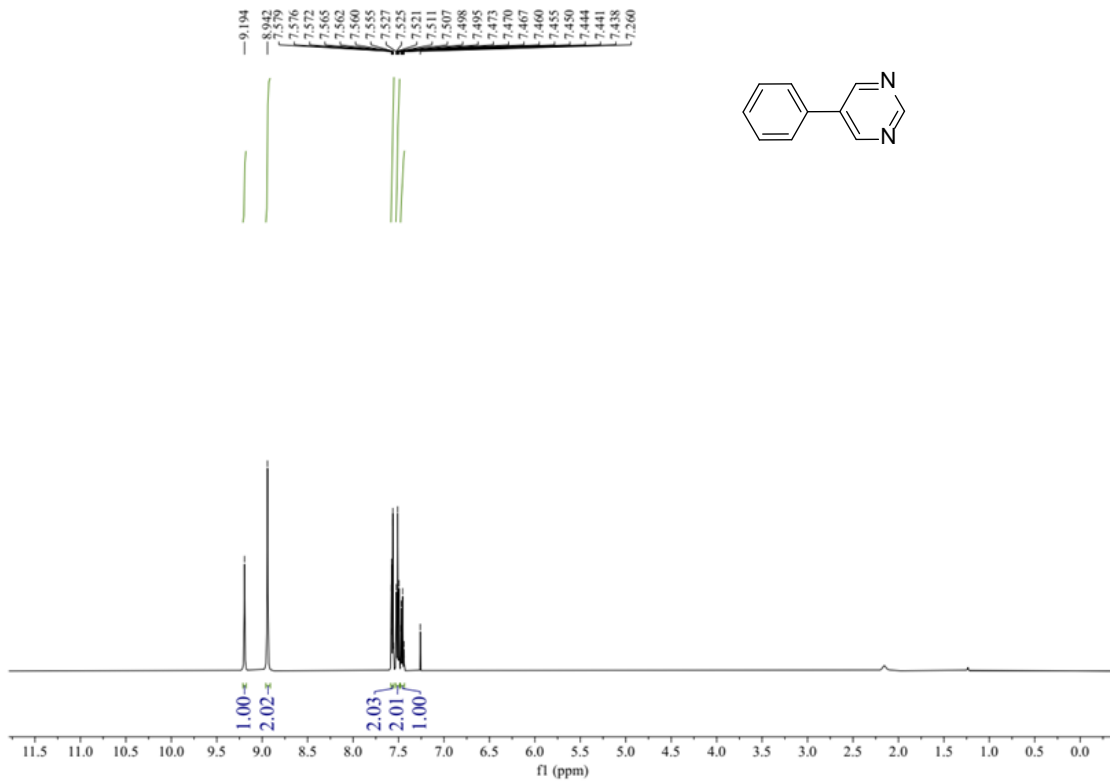
¹H spectra of product 40.



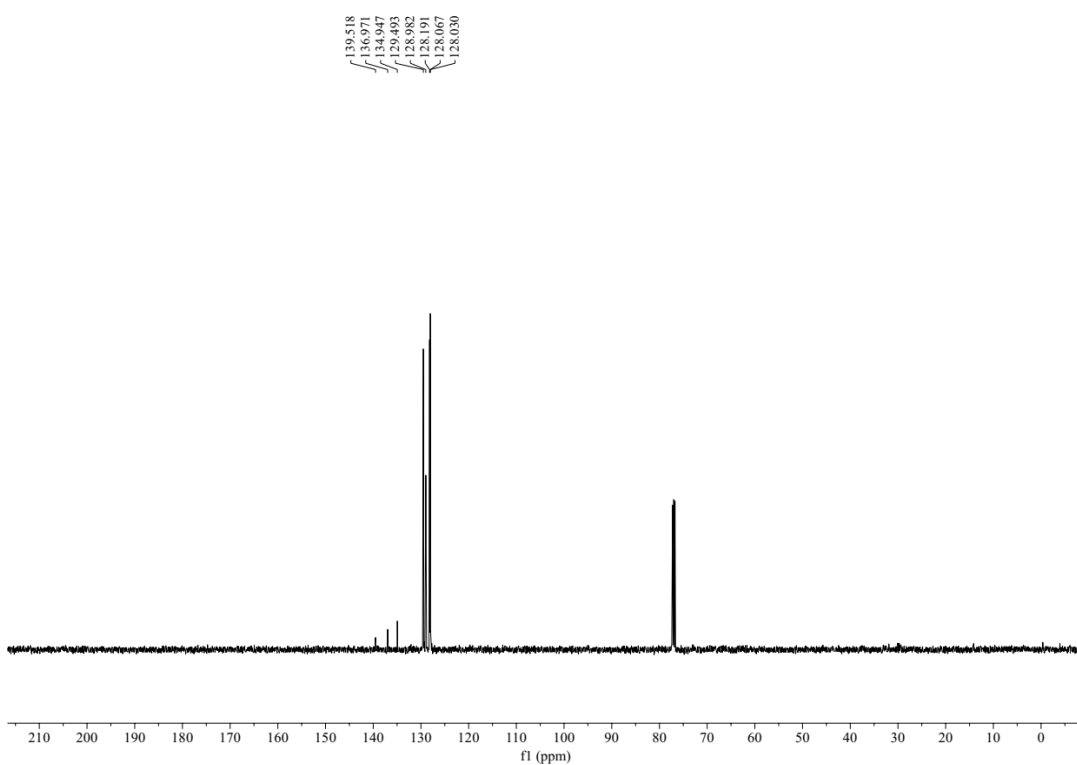
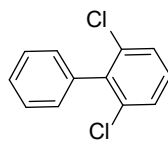
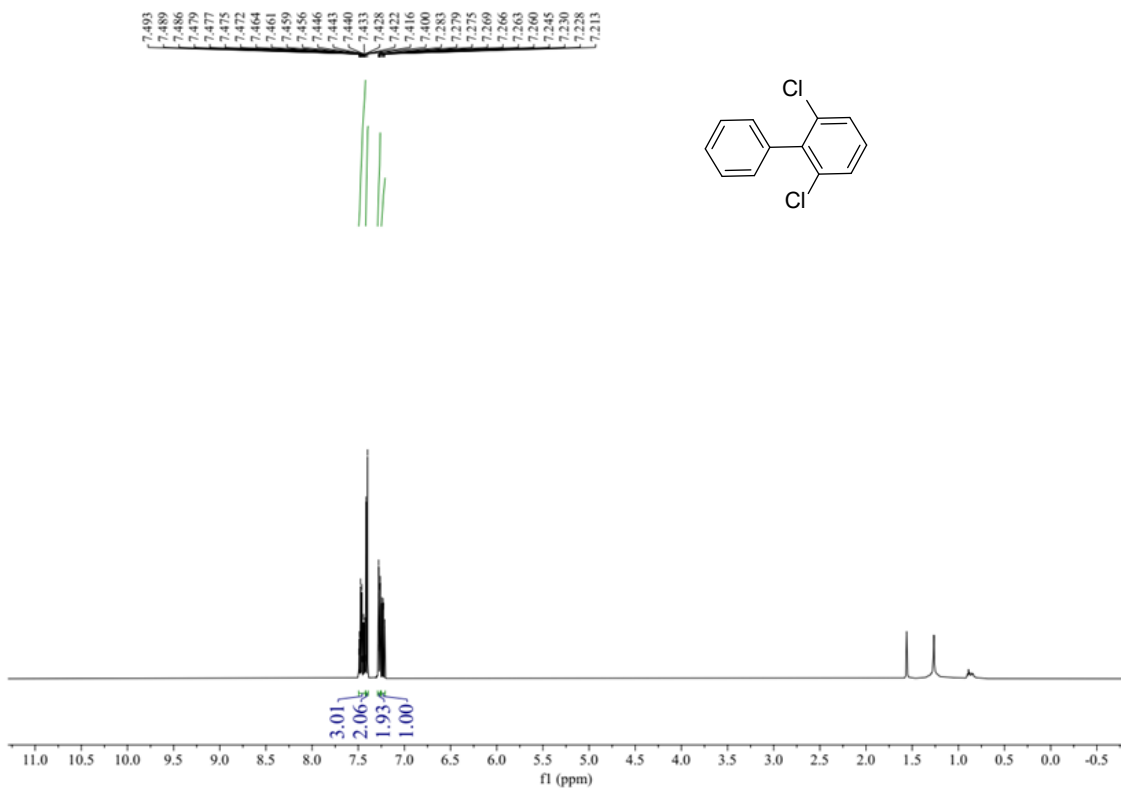
¹H and ¹³C-NMR spectra of product 41.



¹H spectra of product 42.

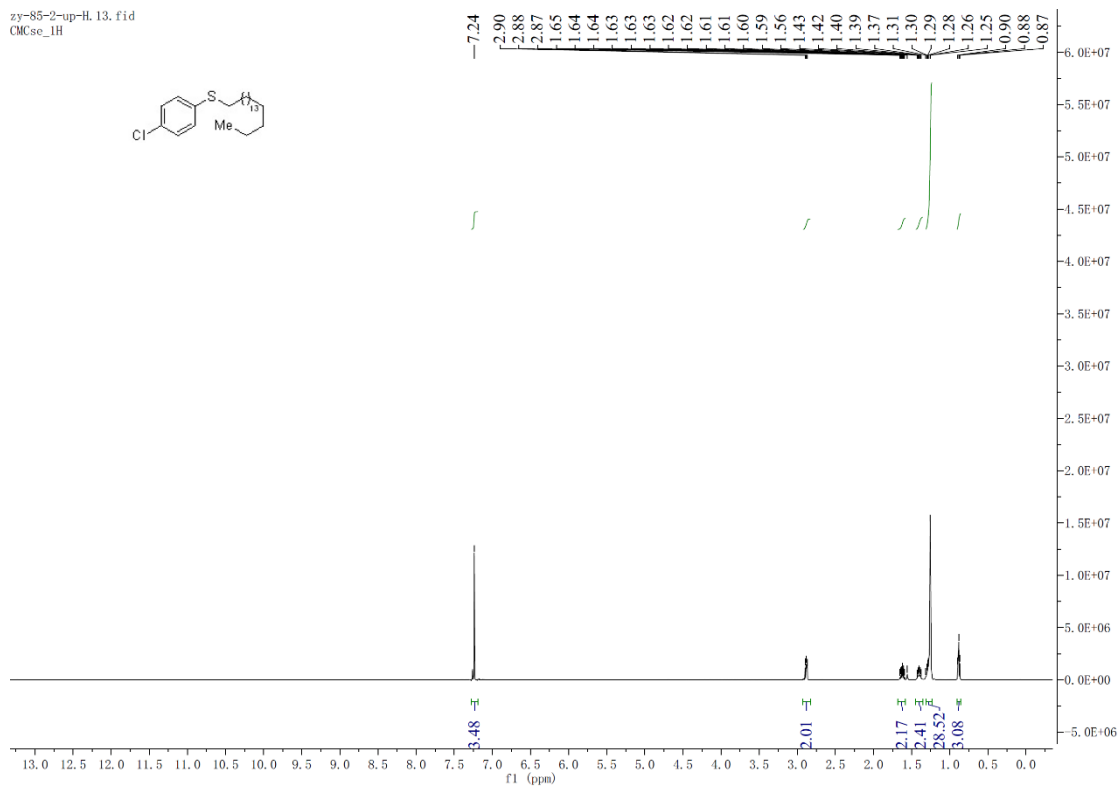
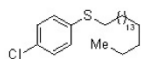


¹H and ¹³C-NMR spectra of product 43.

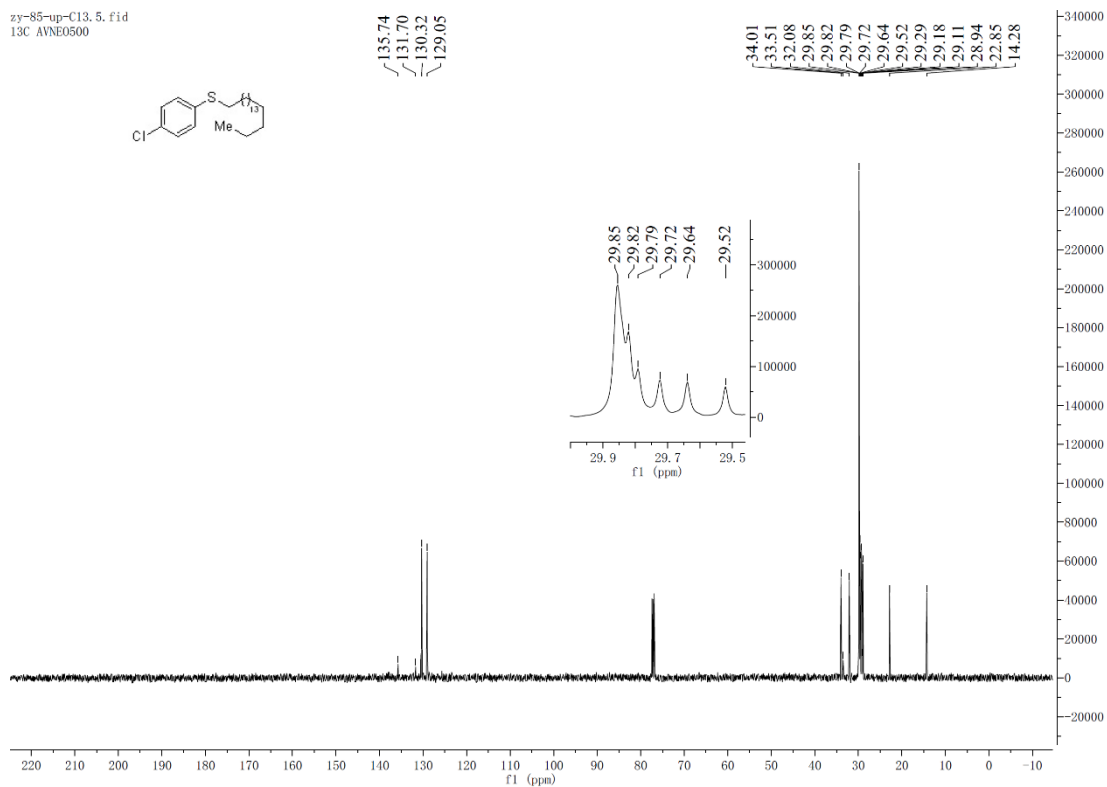
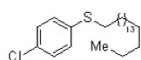


¹H and ¹³C-NMR spectra of product 44.

zy-85-2-up-H. 13. fid
CMCse_1H

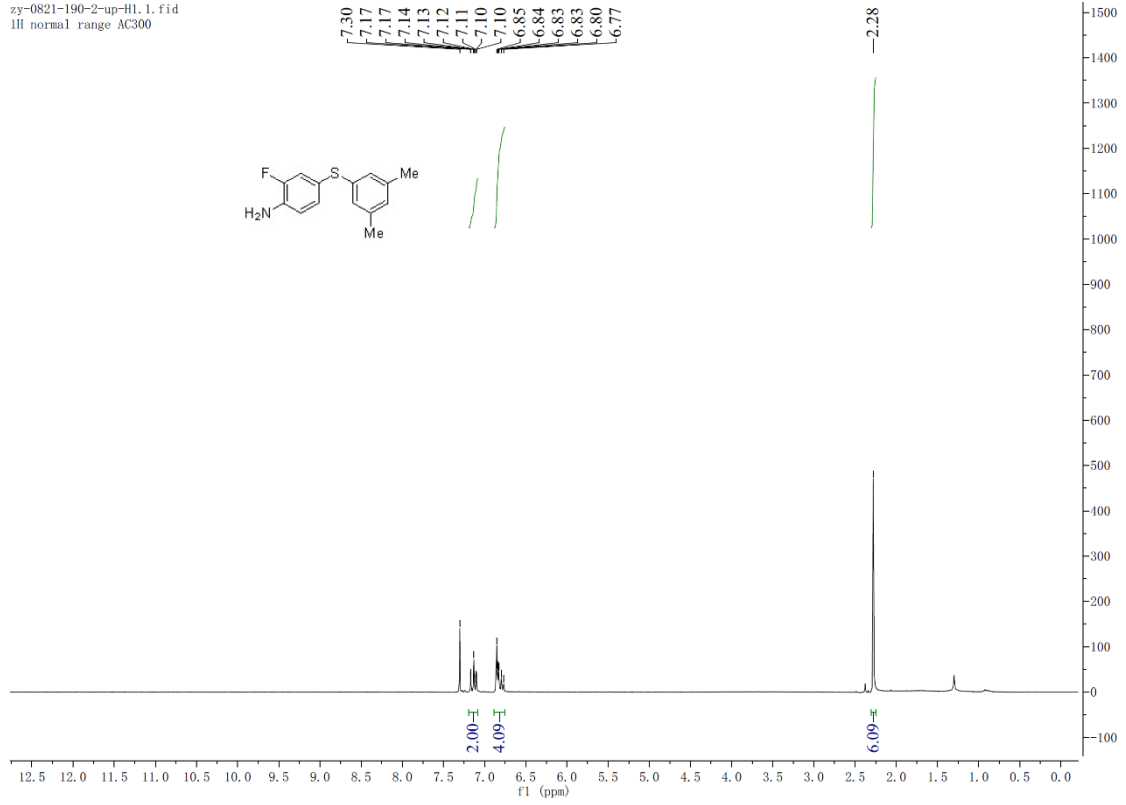


zy-85-up-C13. 5. fid
13C AVNE0500

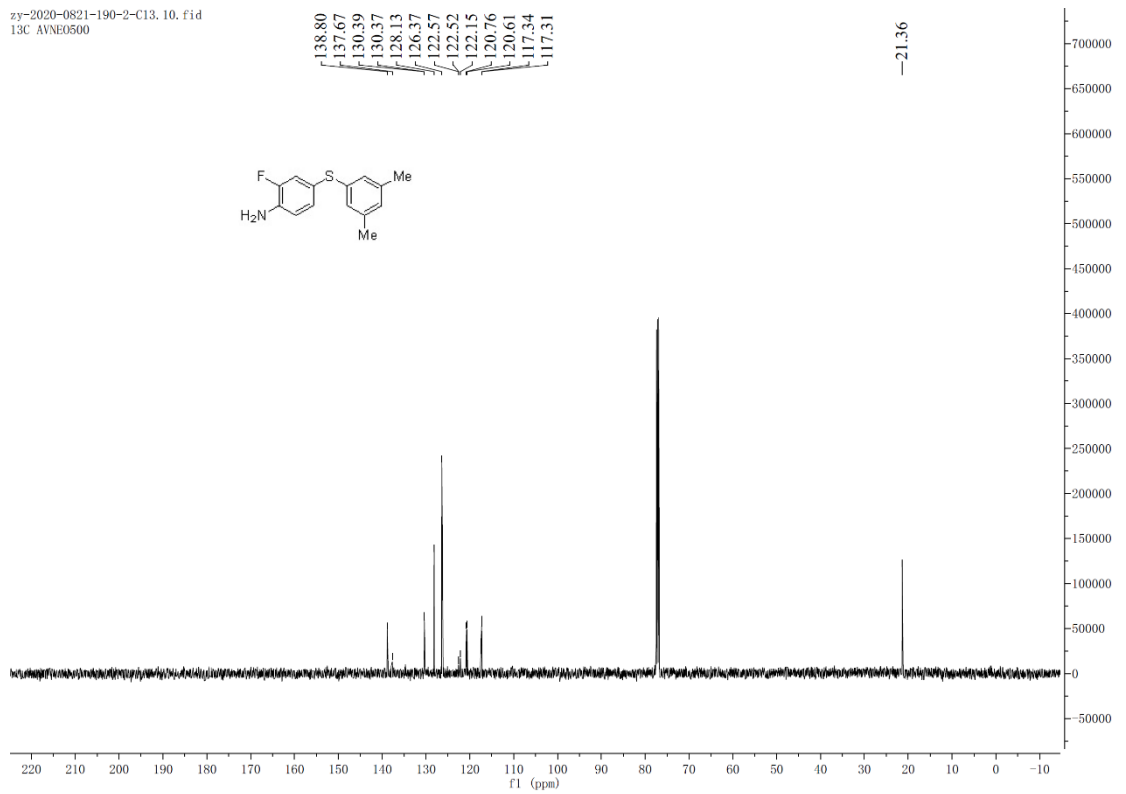


¹H and ¹³C-NMR spectra of product 45.

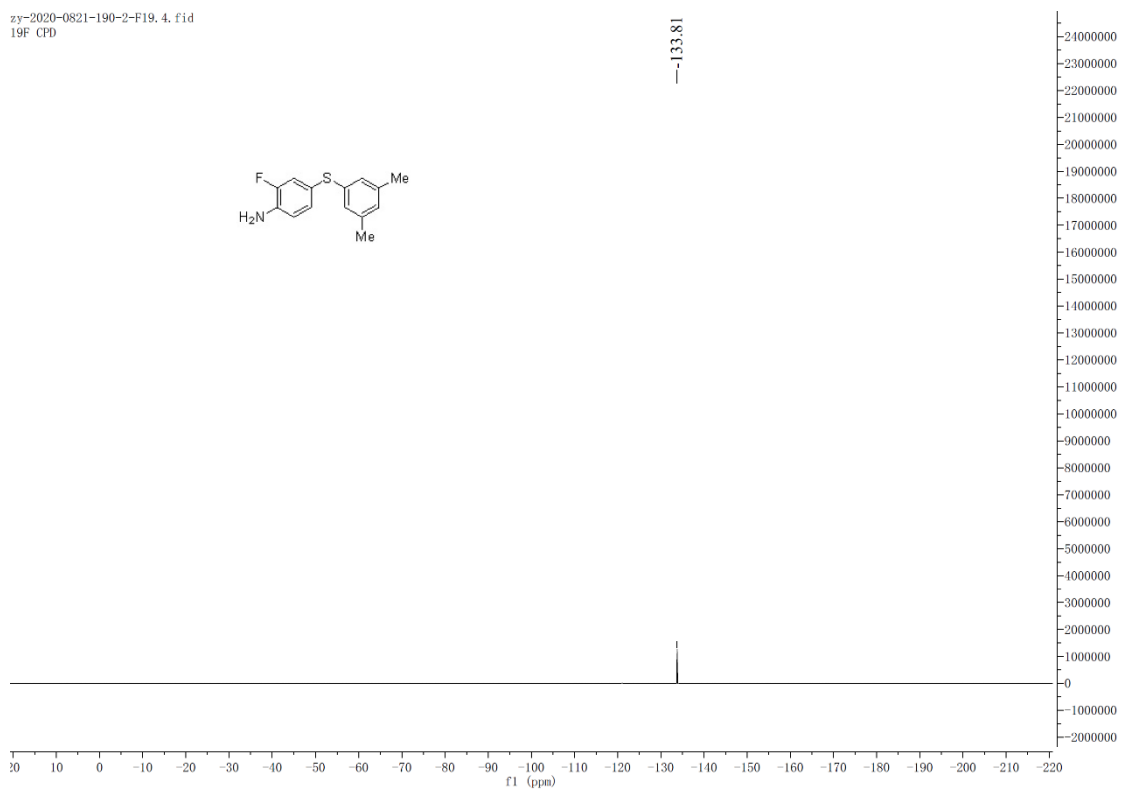
zy-0821-190-2-up-H1.1.fid
1H normal range AC300



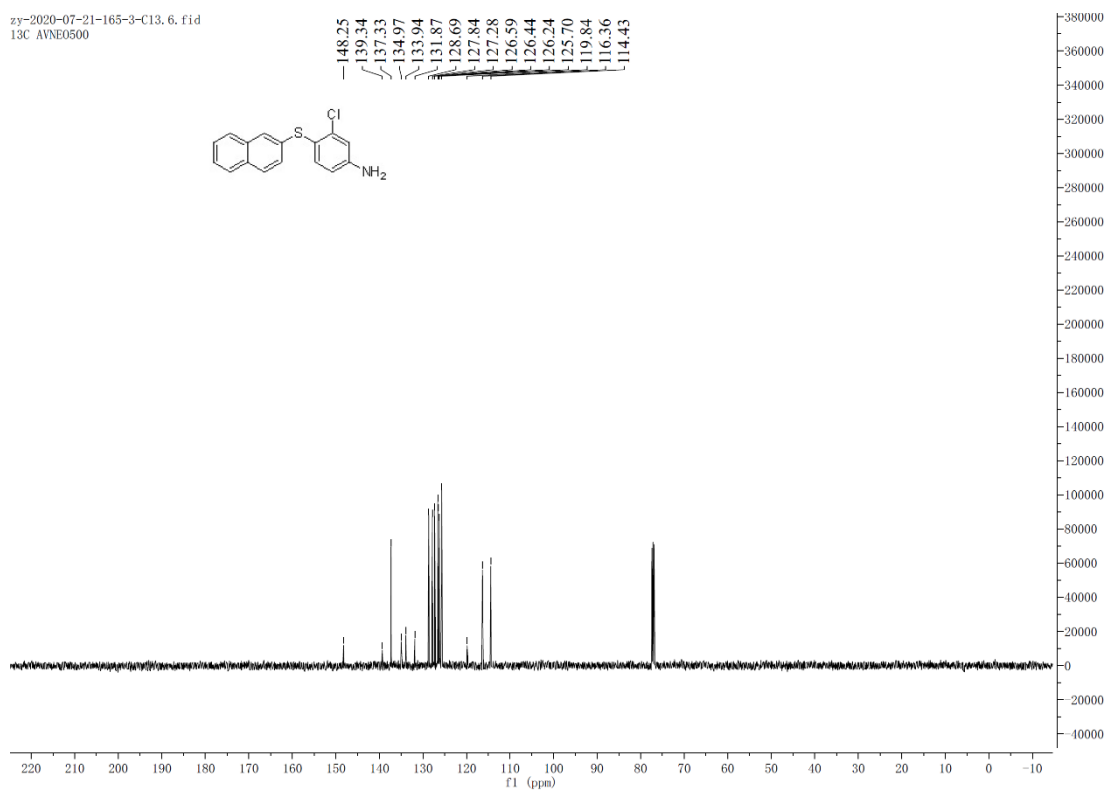
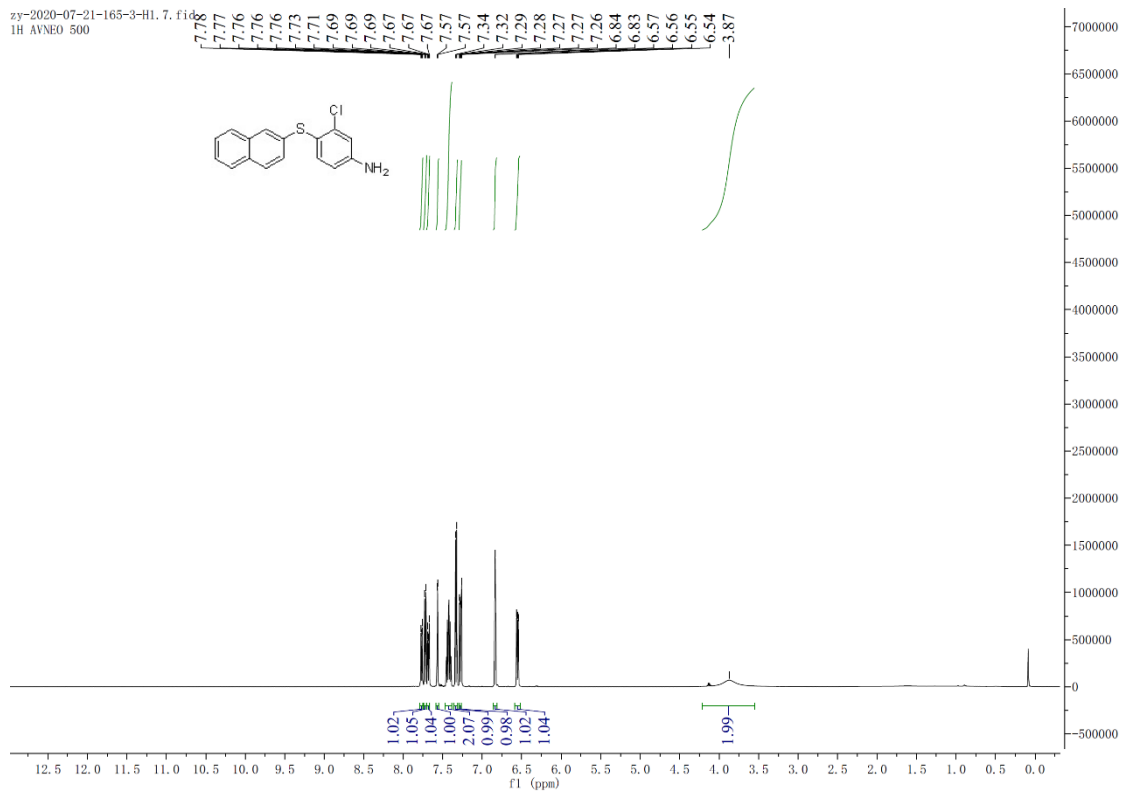
zy-2020-0821-190-2-C13.10.fid
13C ANNE0500



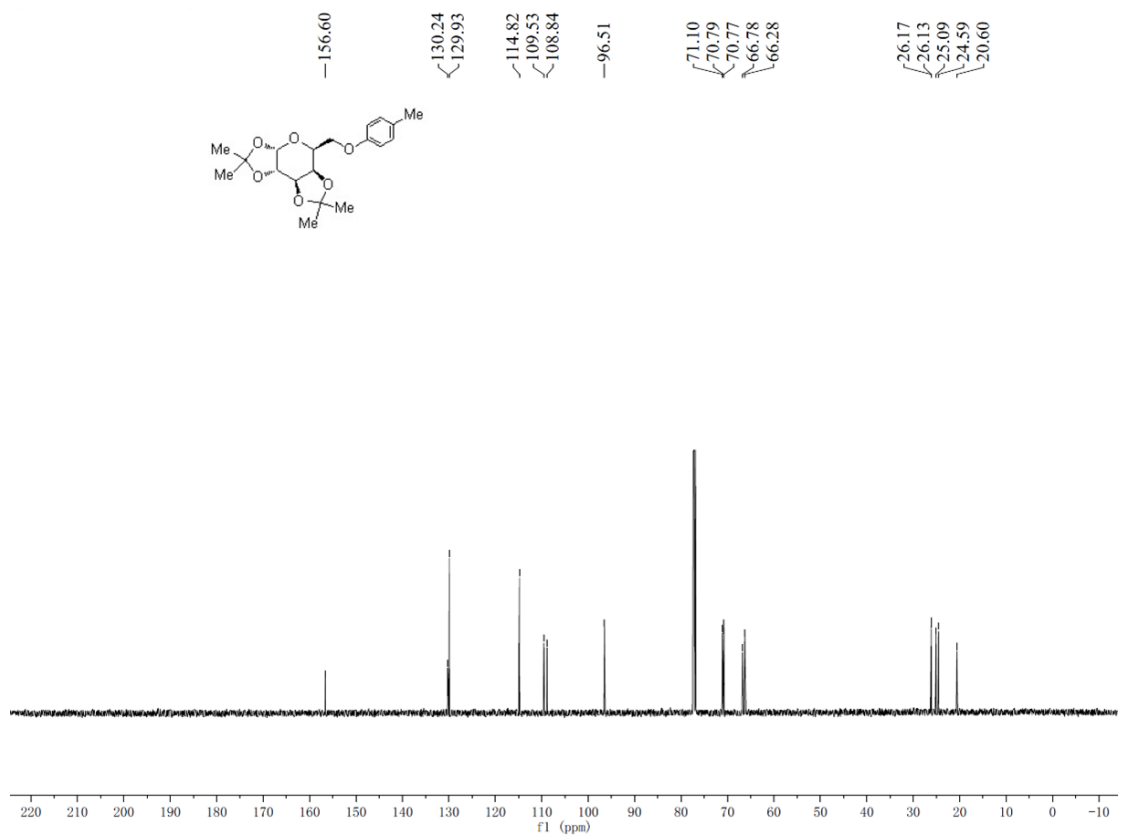
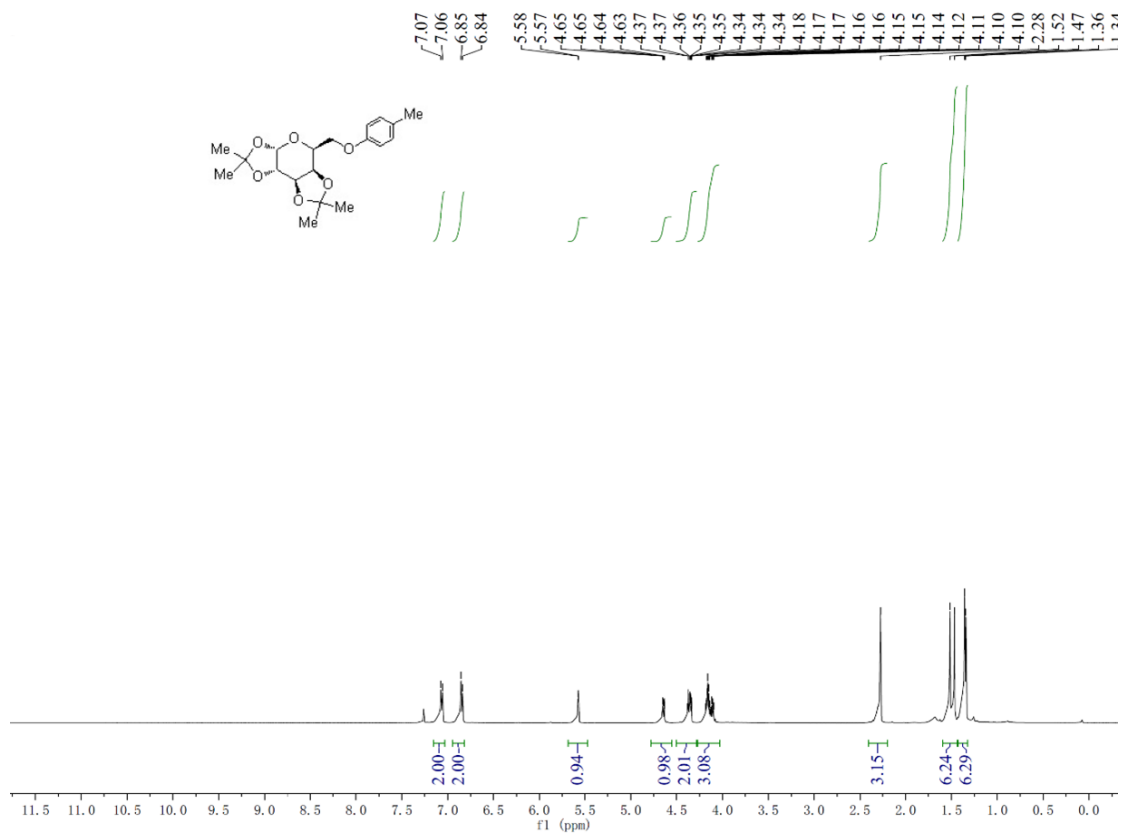
z3-2020-0821-190-2-F19. 4. fid
19F CPD



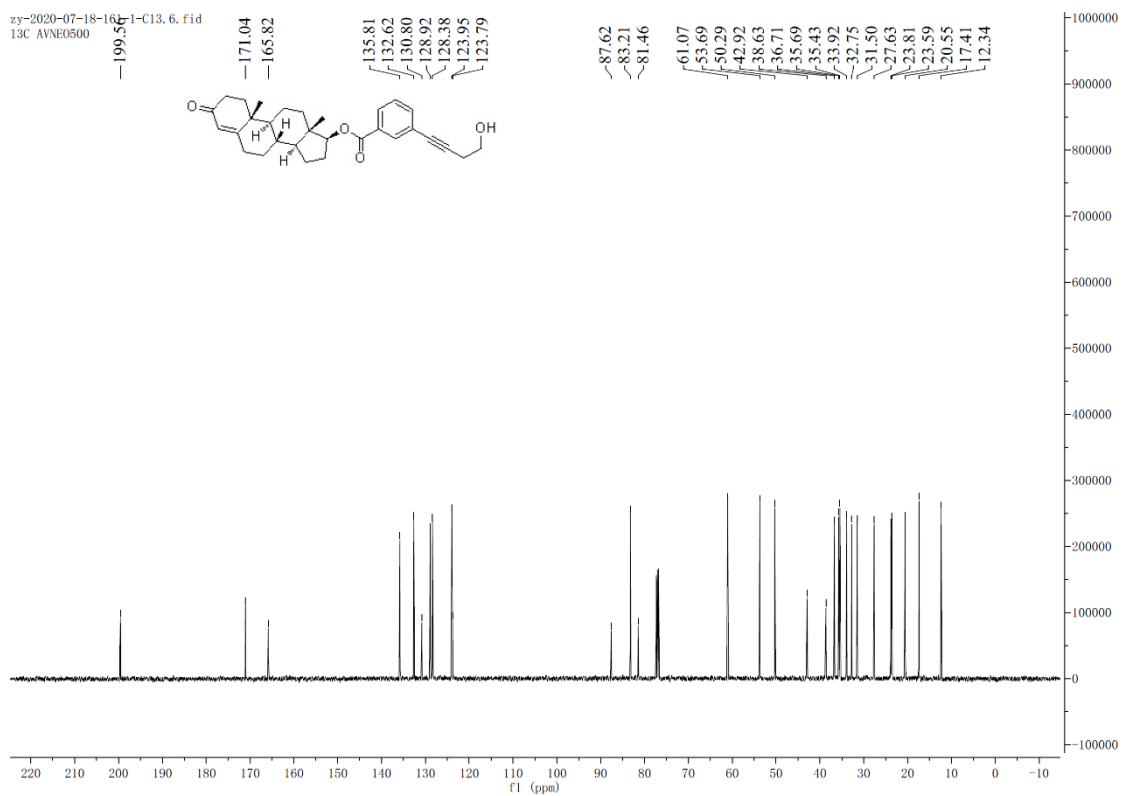
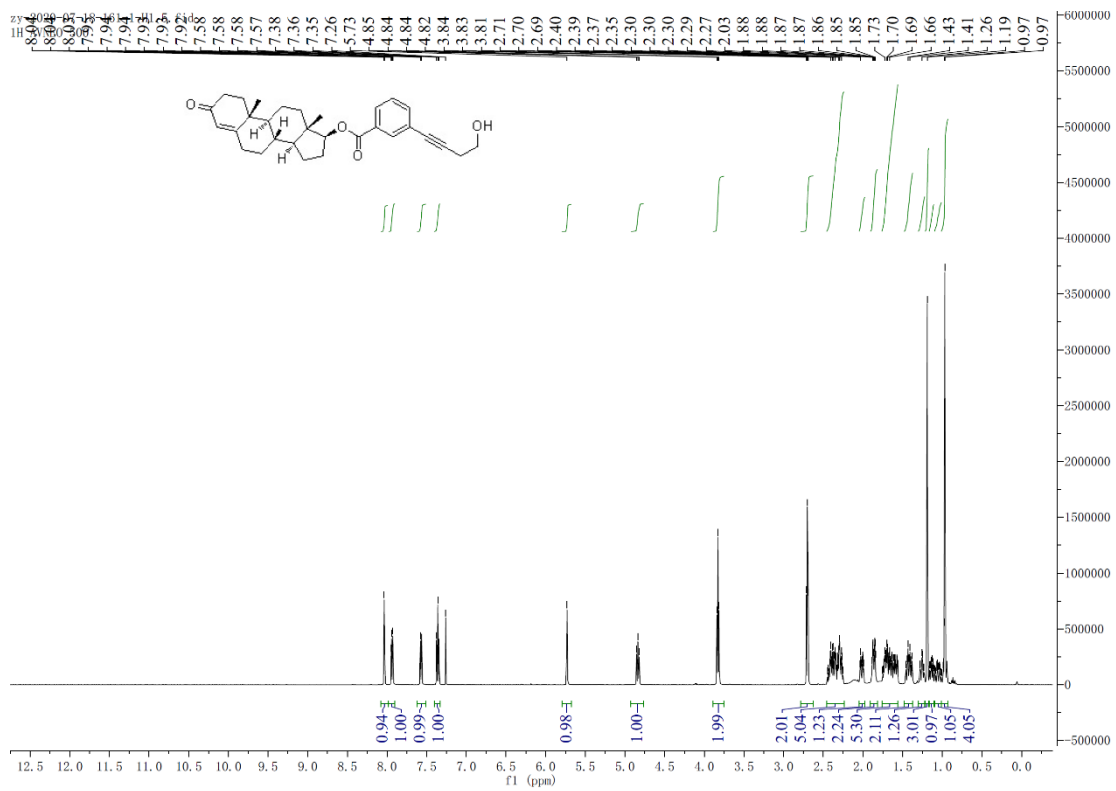
¹H, ¹³C, and ¹⁹F-NMR spectra of product 46.



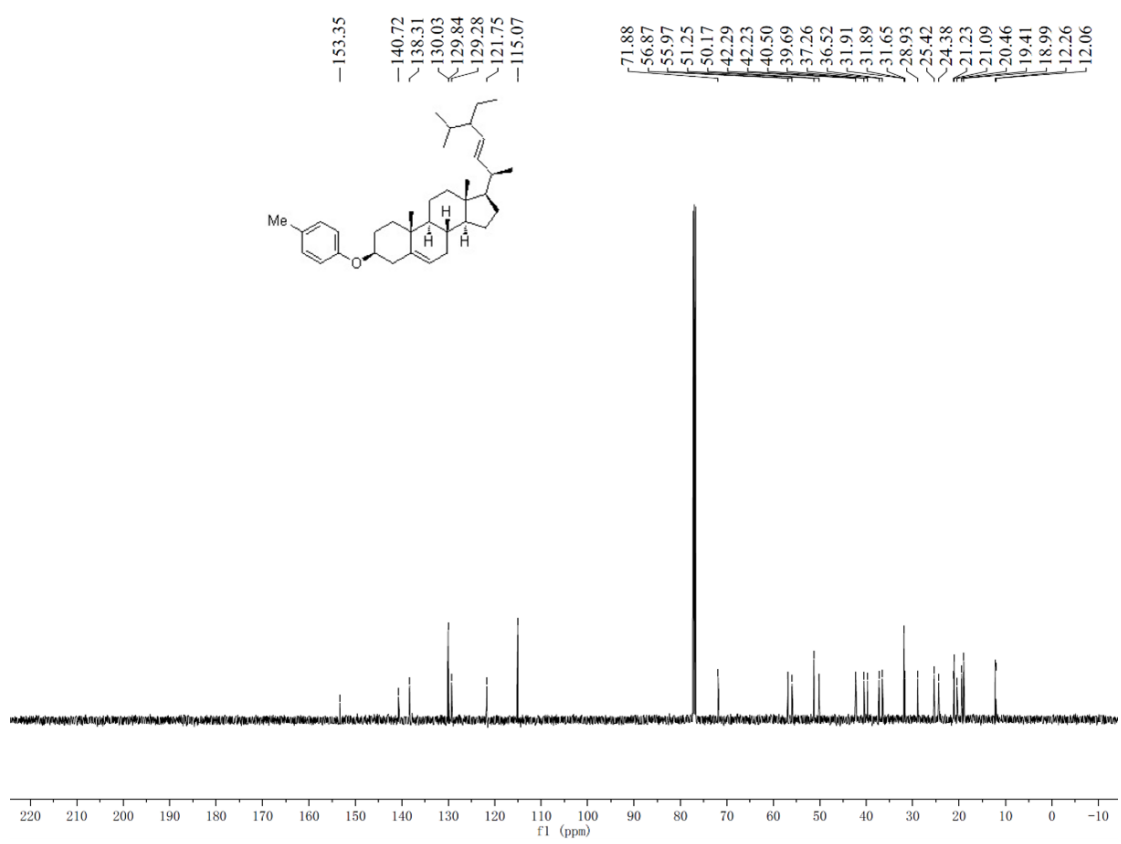
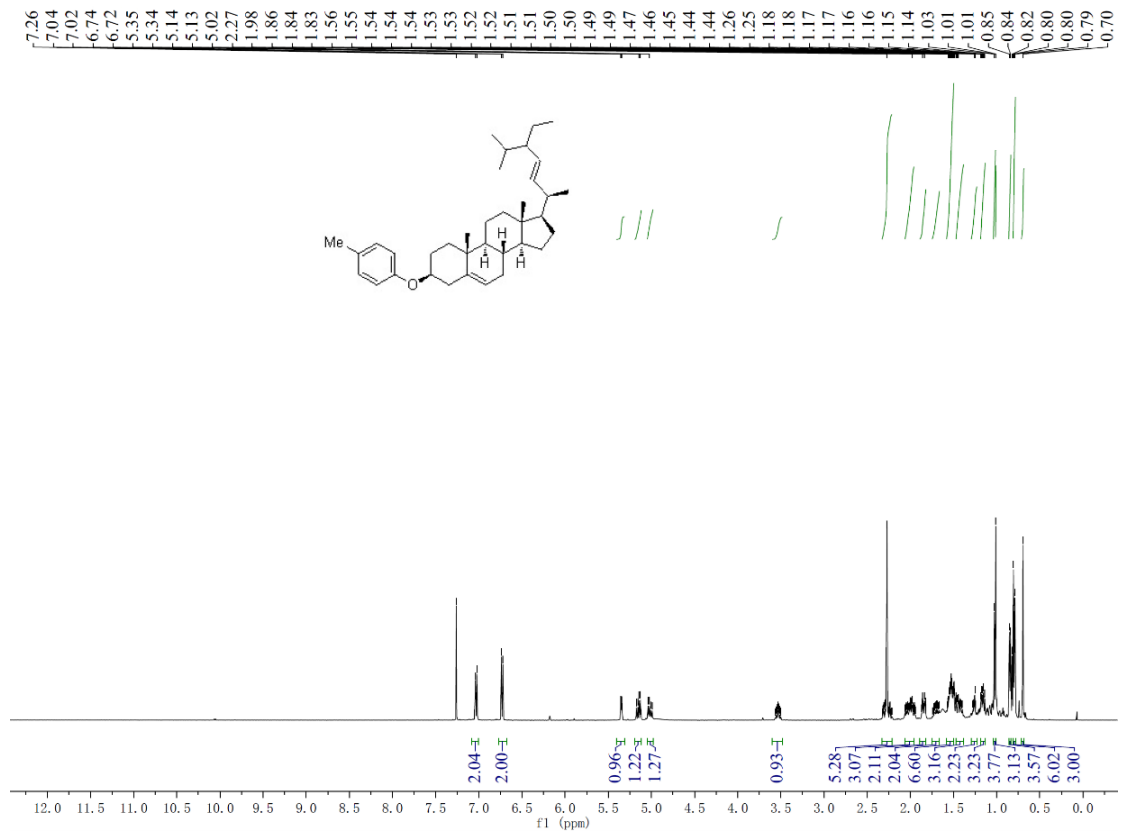
^1H and ^{13}C -NMR spectra of product 47.



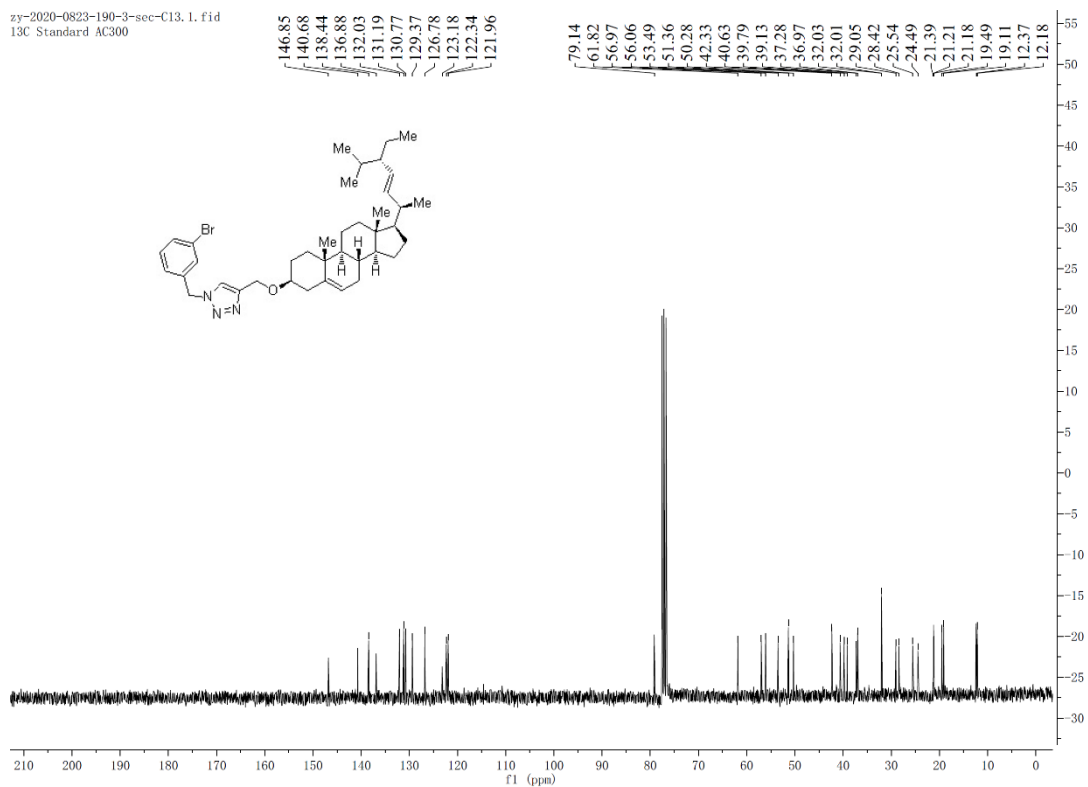
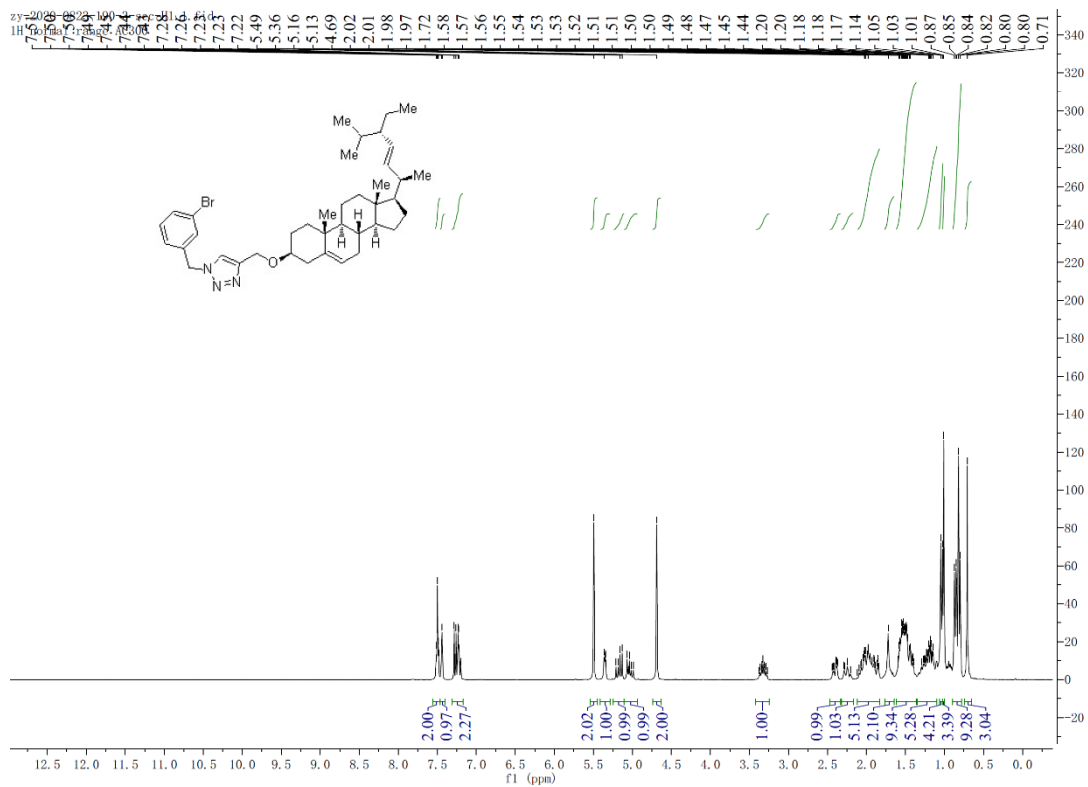
¹H and ¹³C-NMR spectra of product 48.



¹H and ¹³C-NMR spectra of product 49.

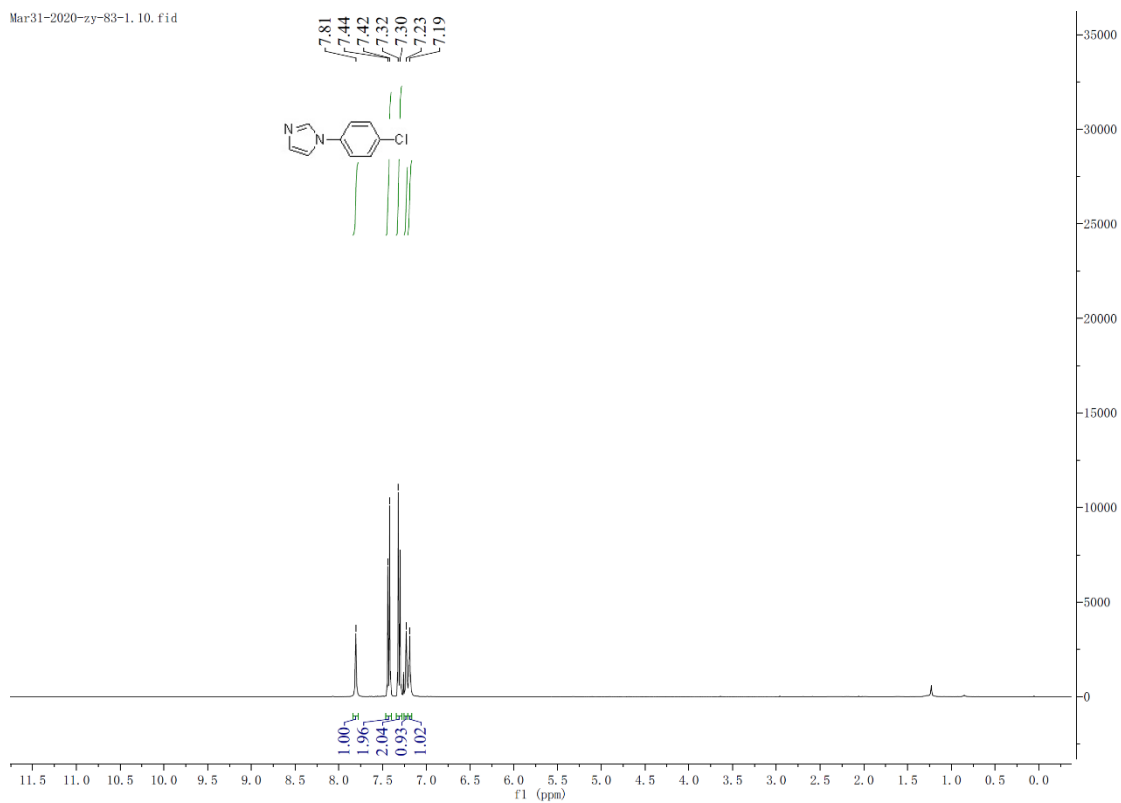


¹H and ¹³C-NMR spectra of product 50.

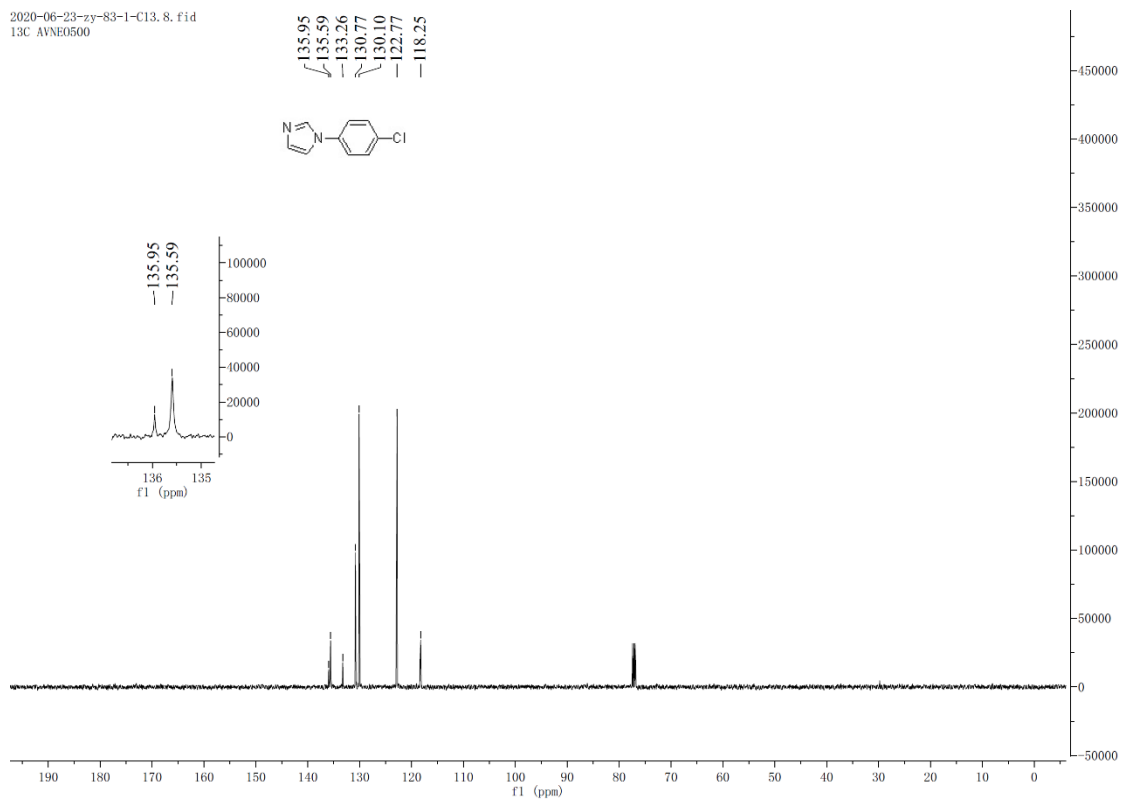


^1H and ^{13}C -NMR spectra of product 51.

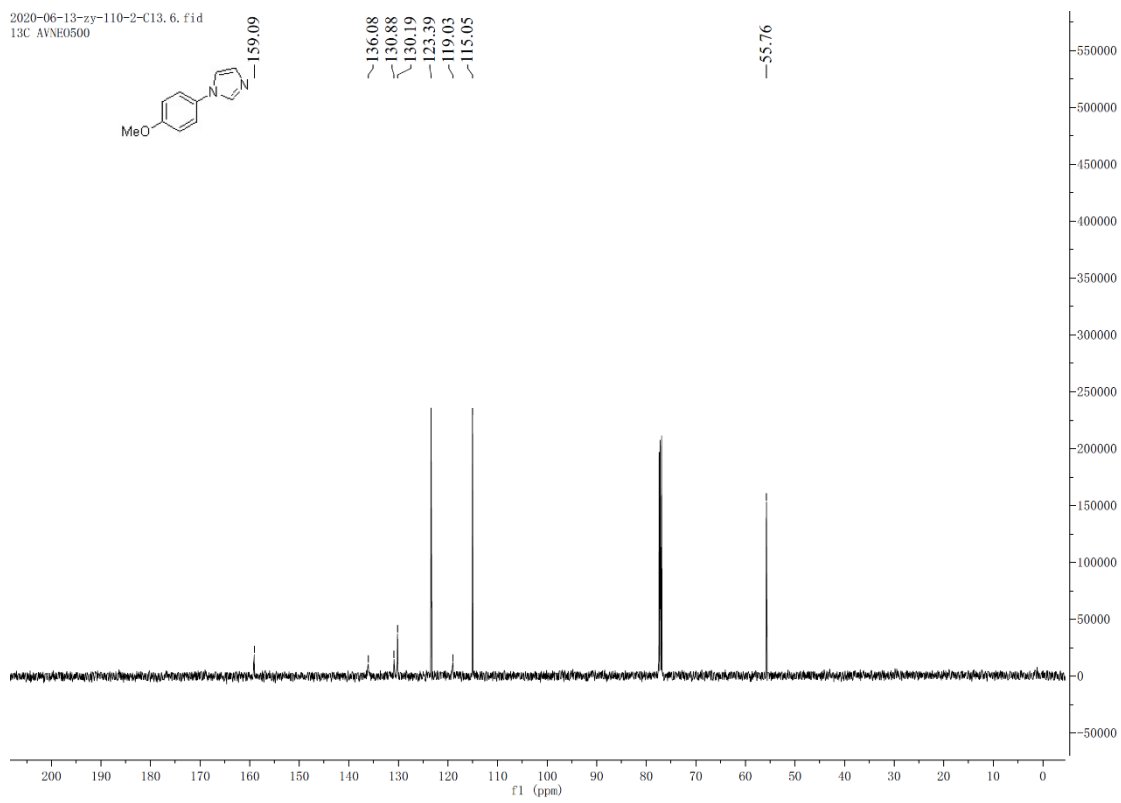
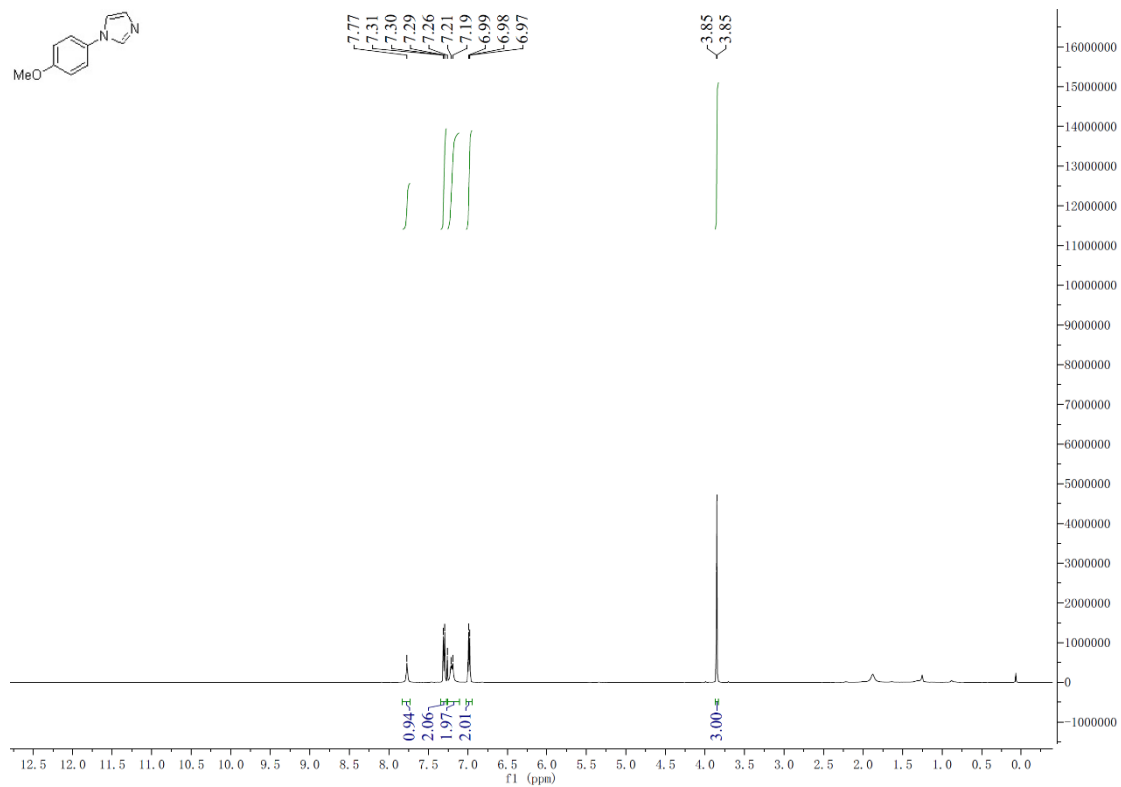
Mar31-2020-zy-83-1. 10. fid



2020-06-23-zy-83-1-C13. 8. fid
13C AVNE0500

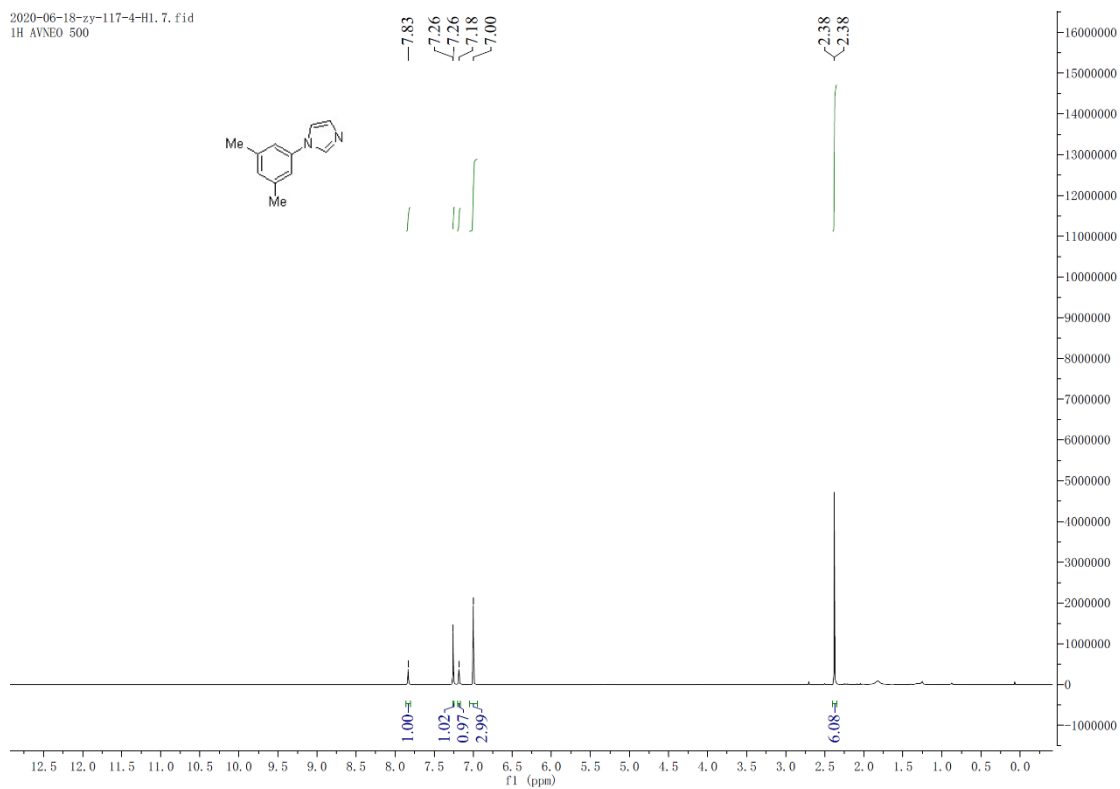


^1H and ^{13}C -NMR spectra of product 52.

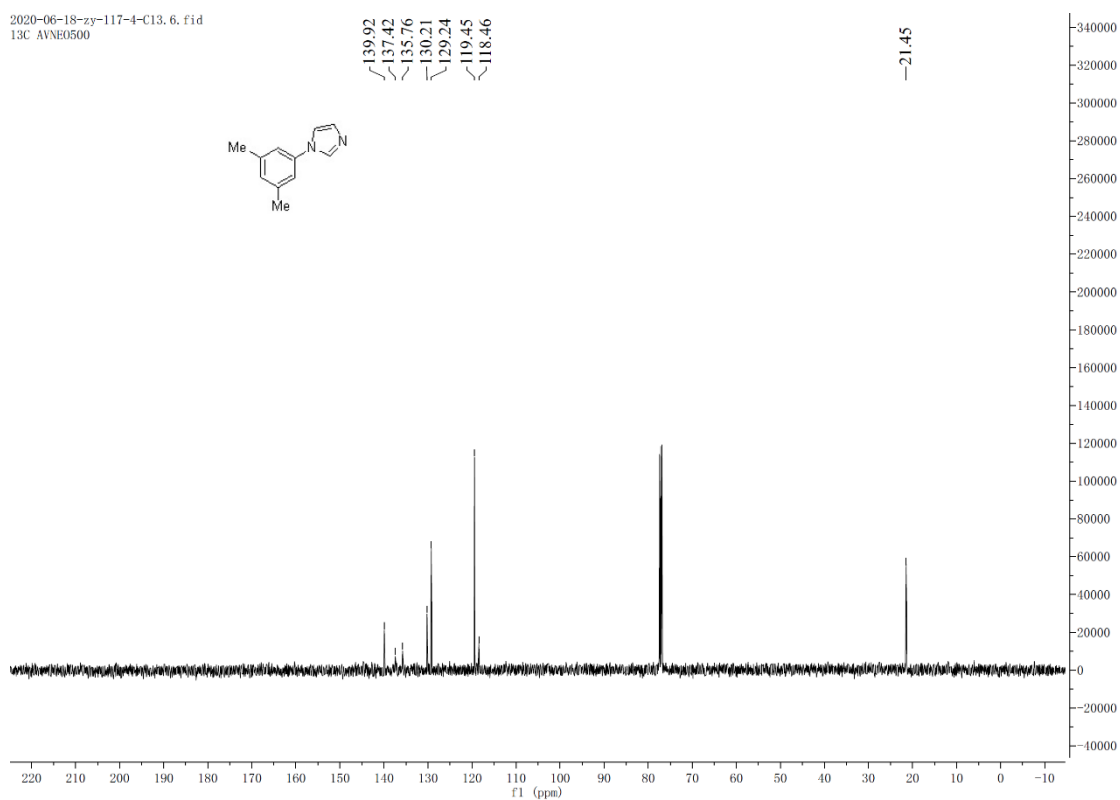


¹H and ¹³C-NMR spectra of product 53.

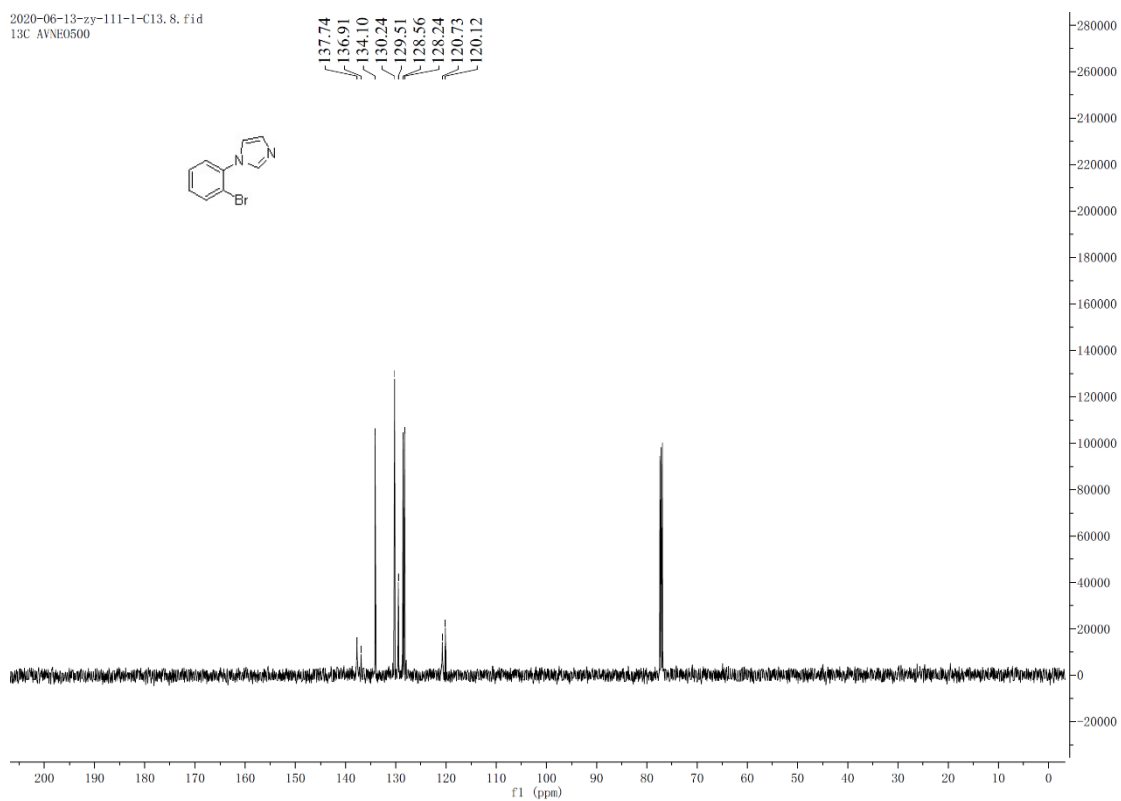
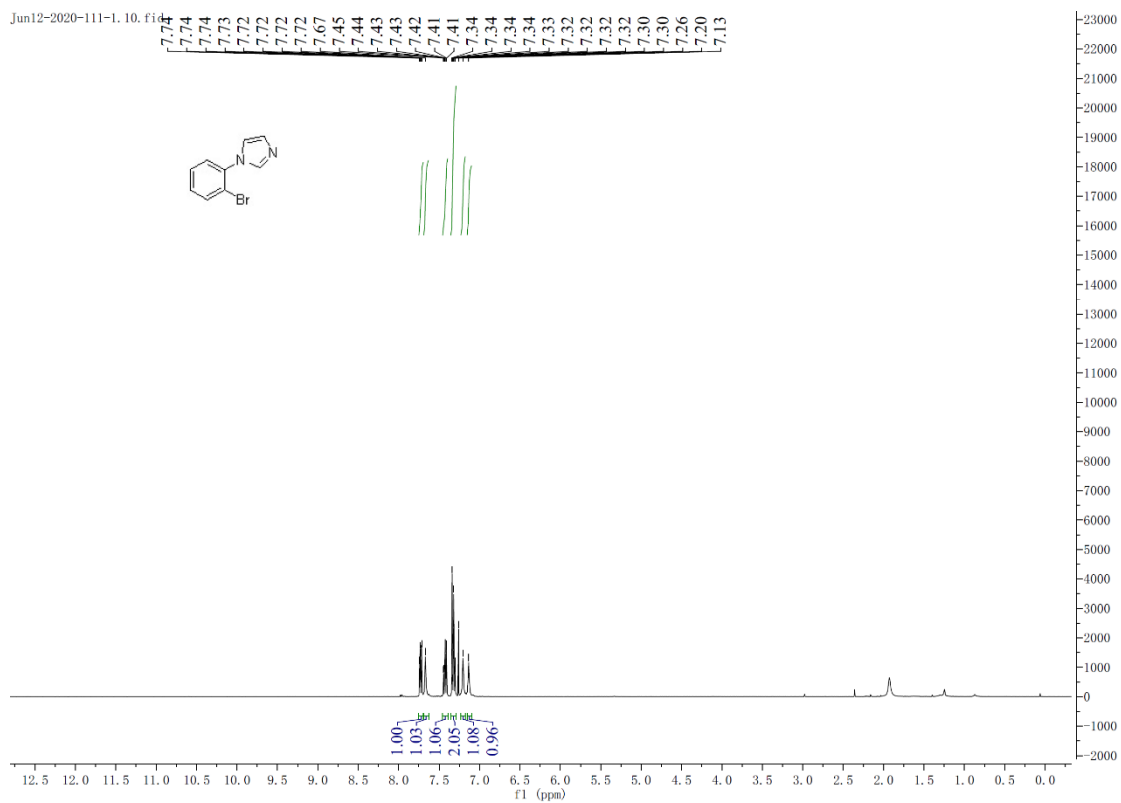
2020-06-18-zy-117-4-H1. 7. fid
1H AVNEO 500



2020-06-18-zy-117-4-C13. 6. fid
13C AVNEO500

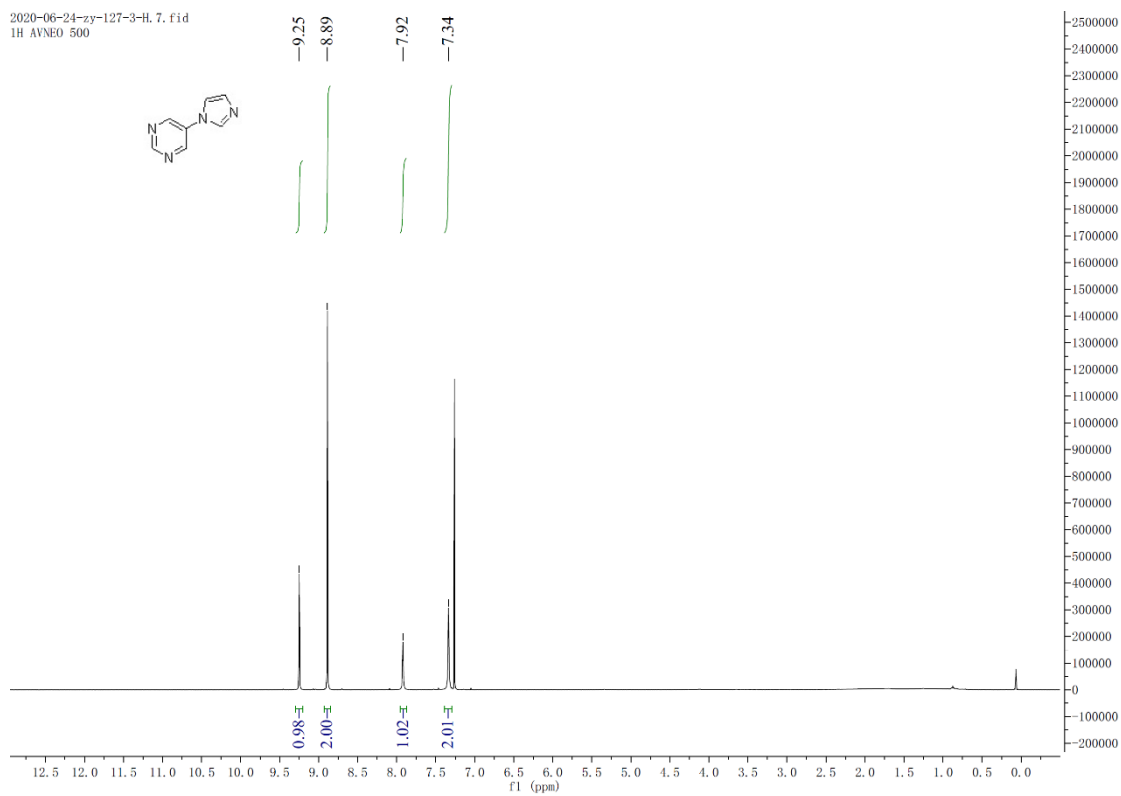


¹H and ¹³C-NMR spectra of product 54.

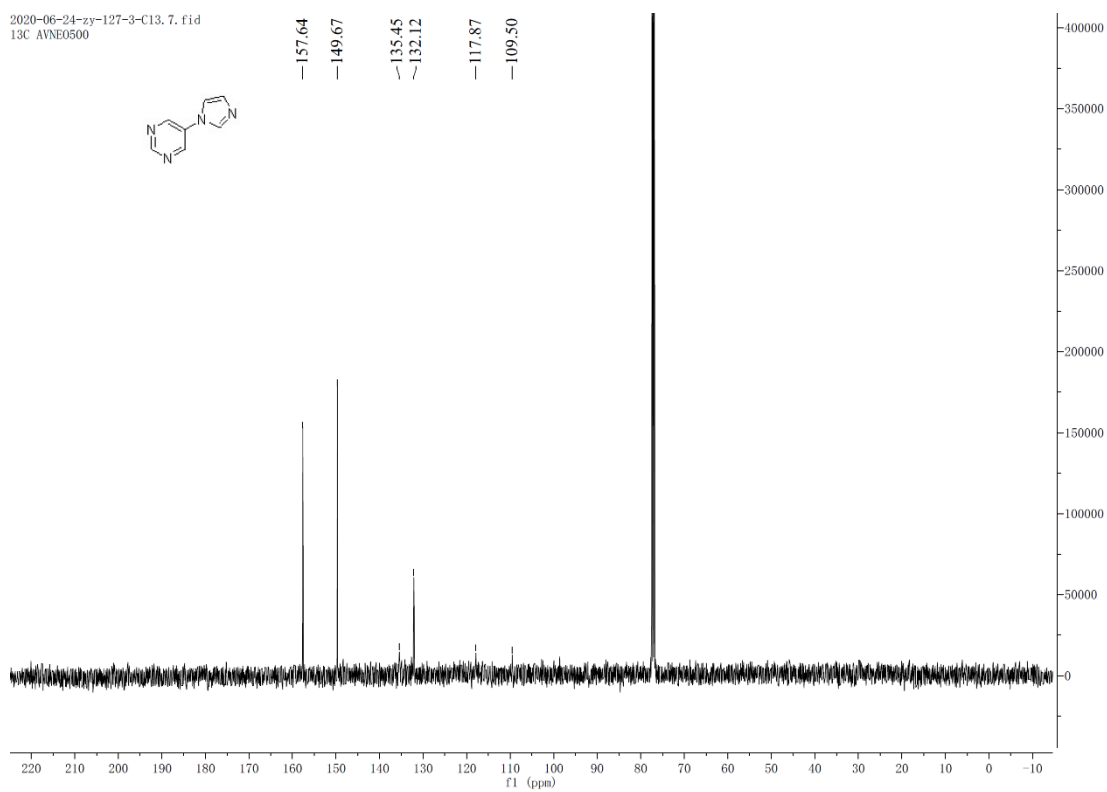


^1H and ^{13}C -NMR spectra of product 55.

2020-06-24-zy-127-3-H. 7. fid
1H AVNEO 500

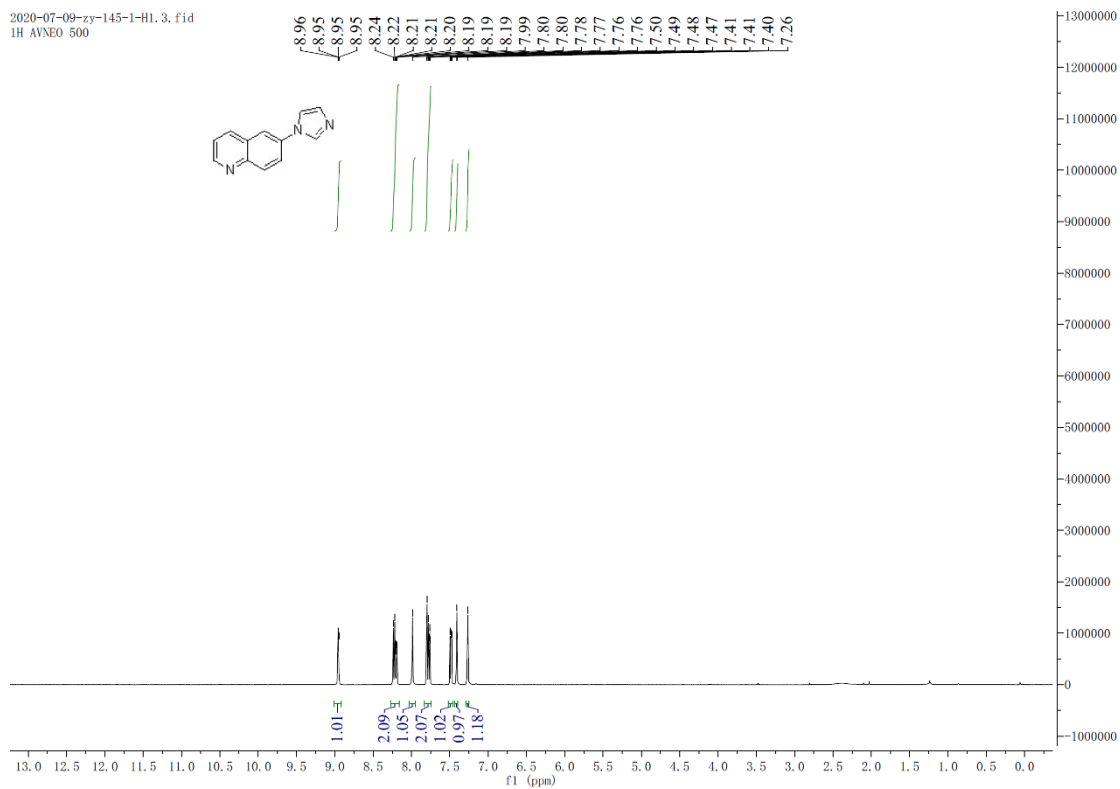


2020-06-24-zy-127-3-C13. 7. fid
13C AVNEO500

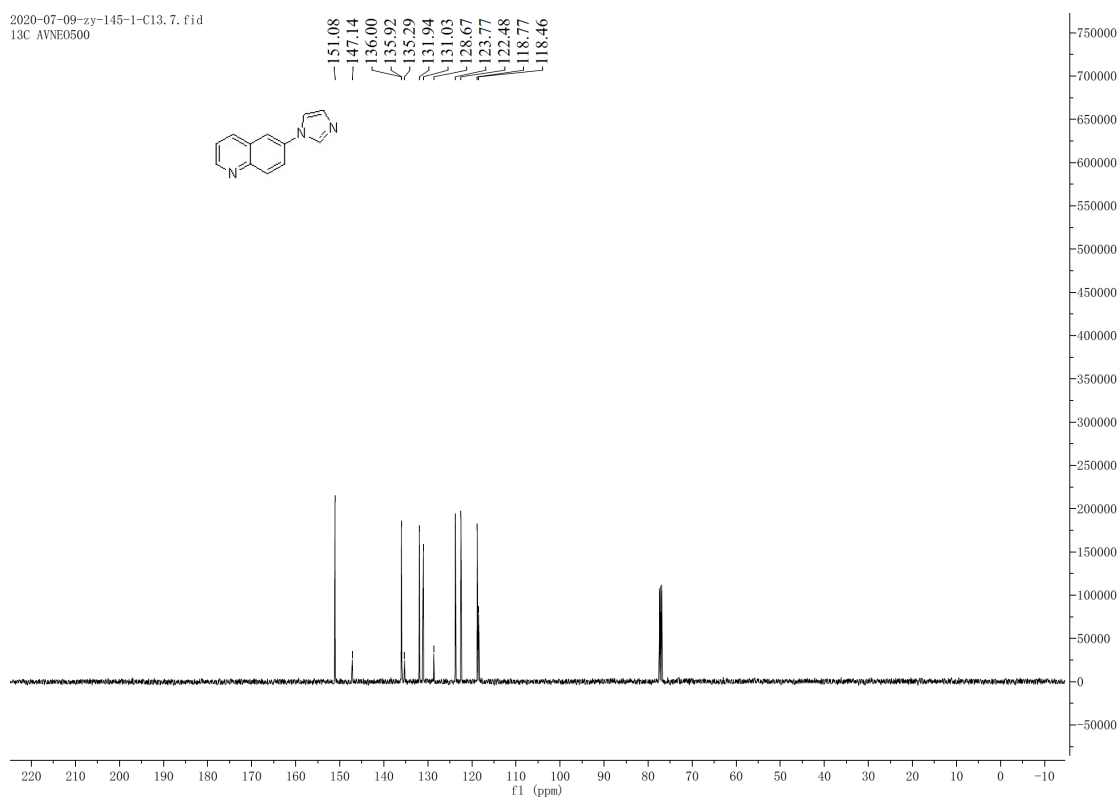


¹H and ¹³C-NMR spectra of product 56.

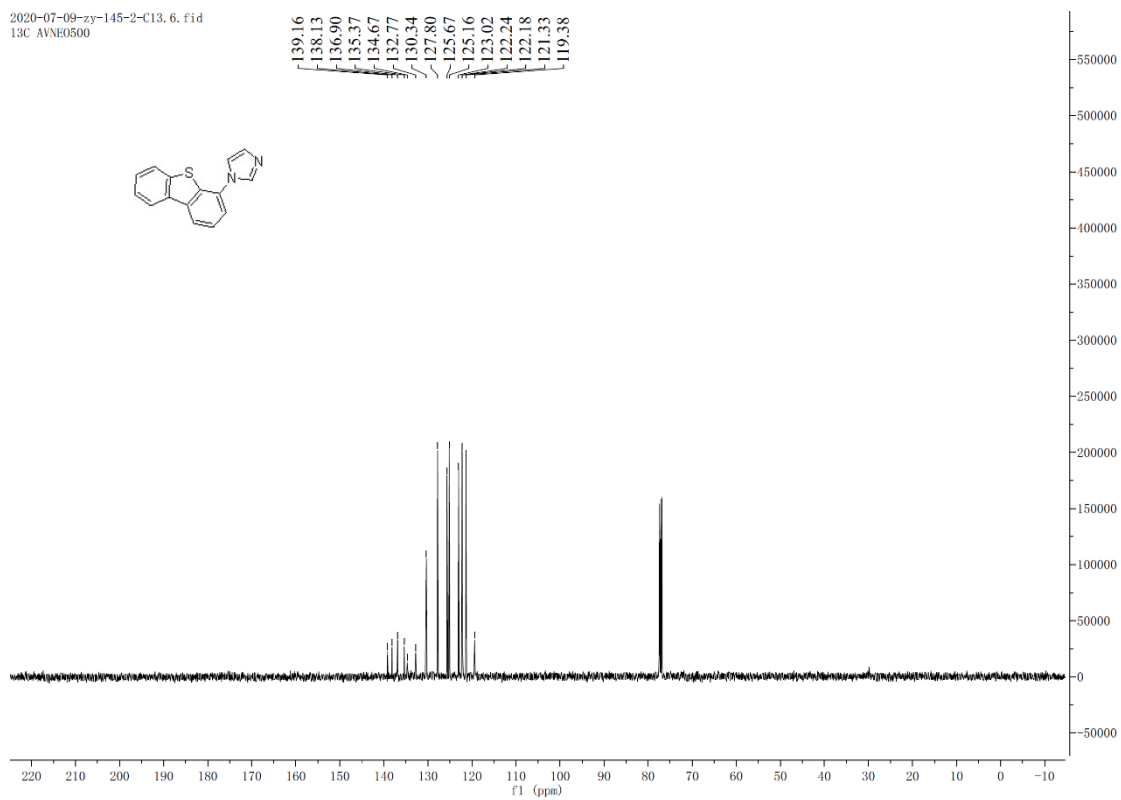
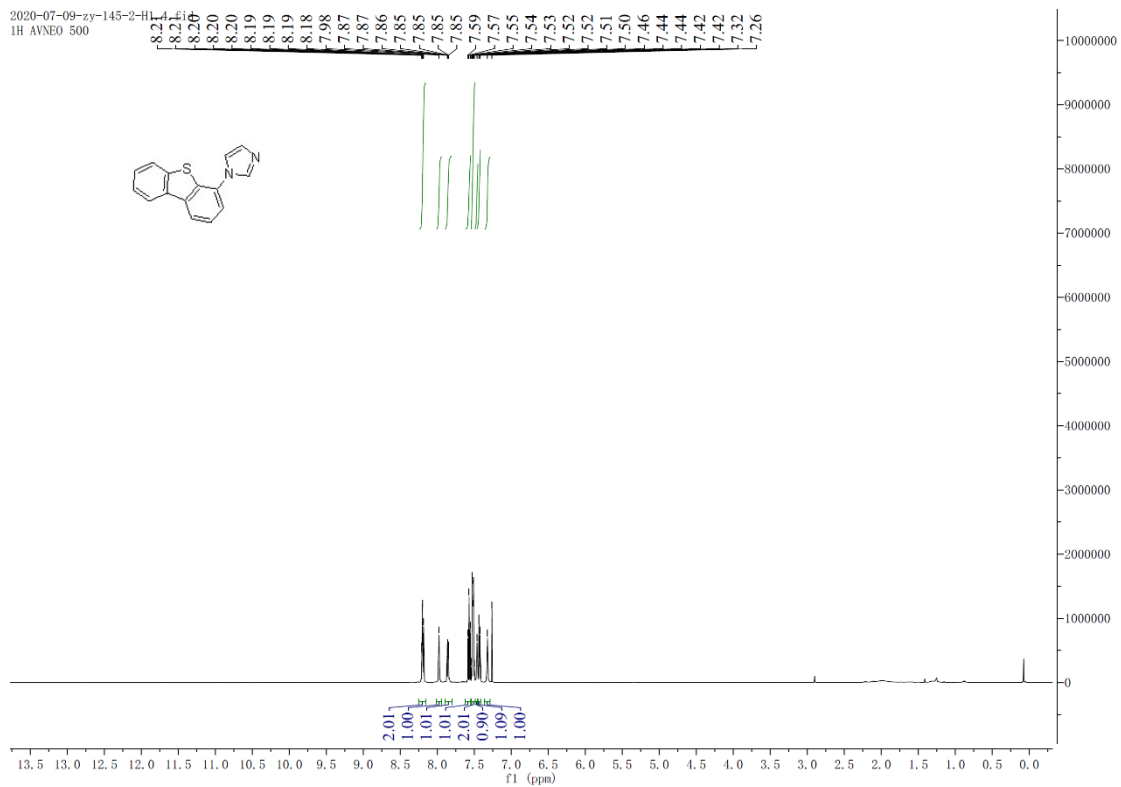
2020-07-09-zy-145-1-H1.3.fid
1H AVNEO 500



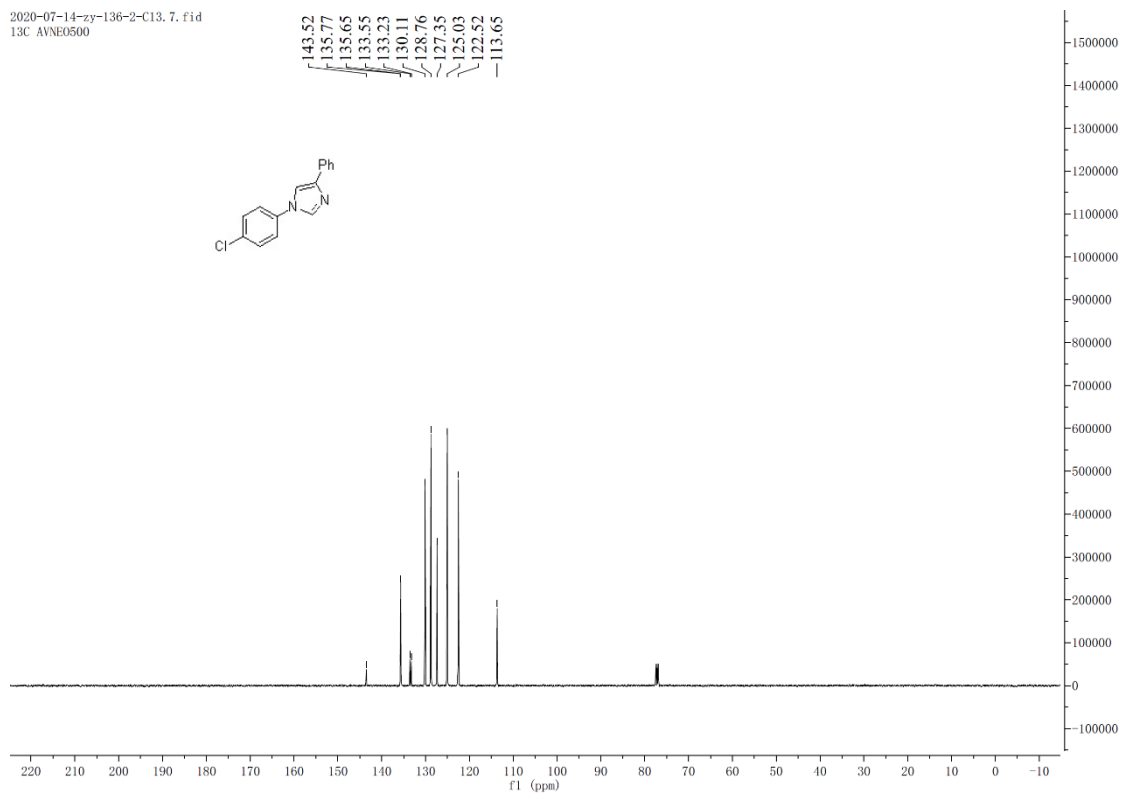
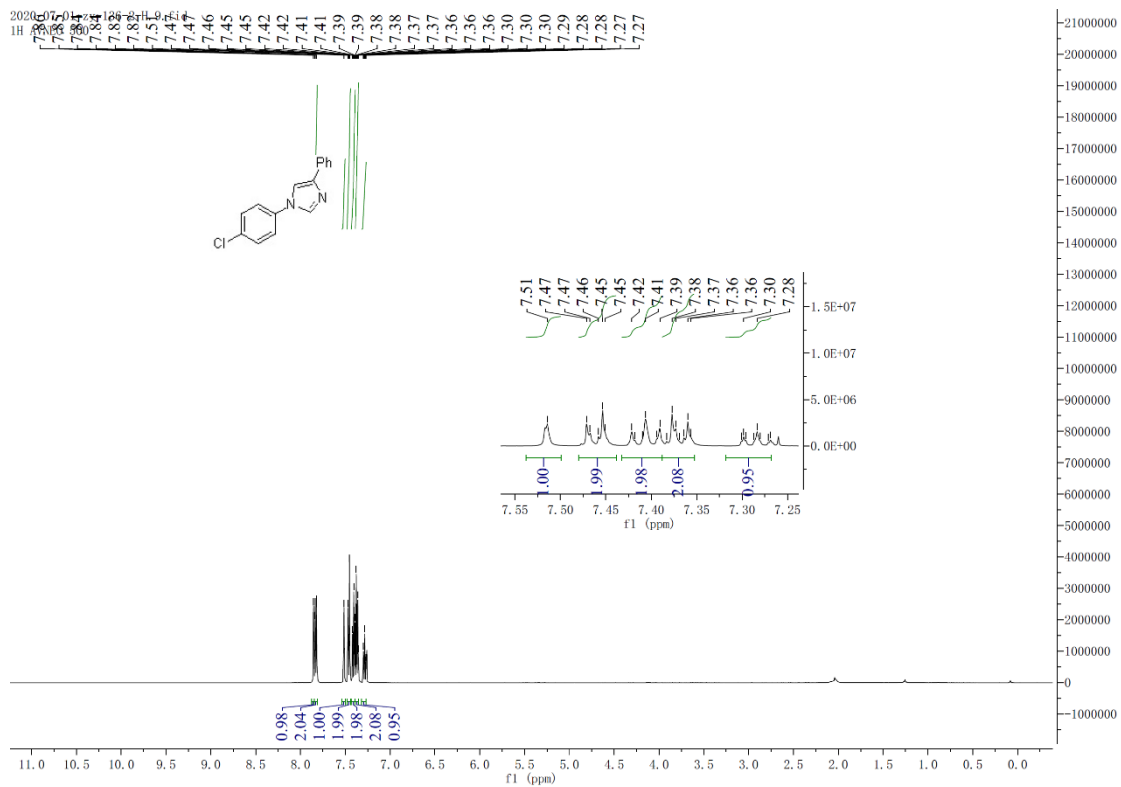
2020-07-09-zy-145-1-C13.7.fid
13C AVNEO500



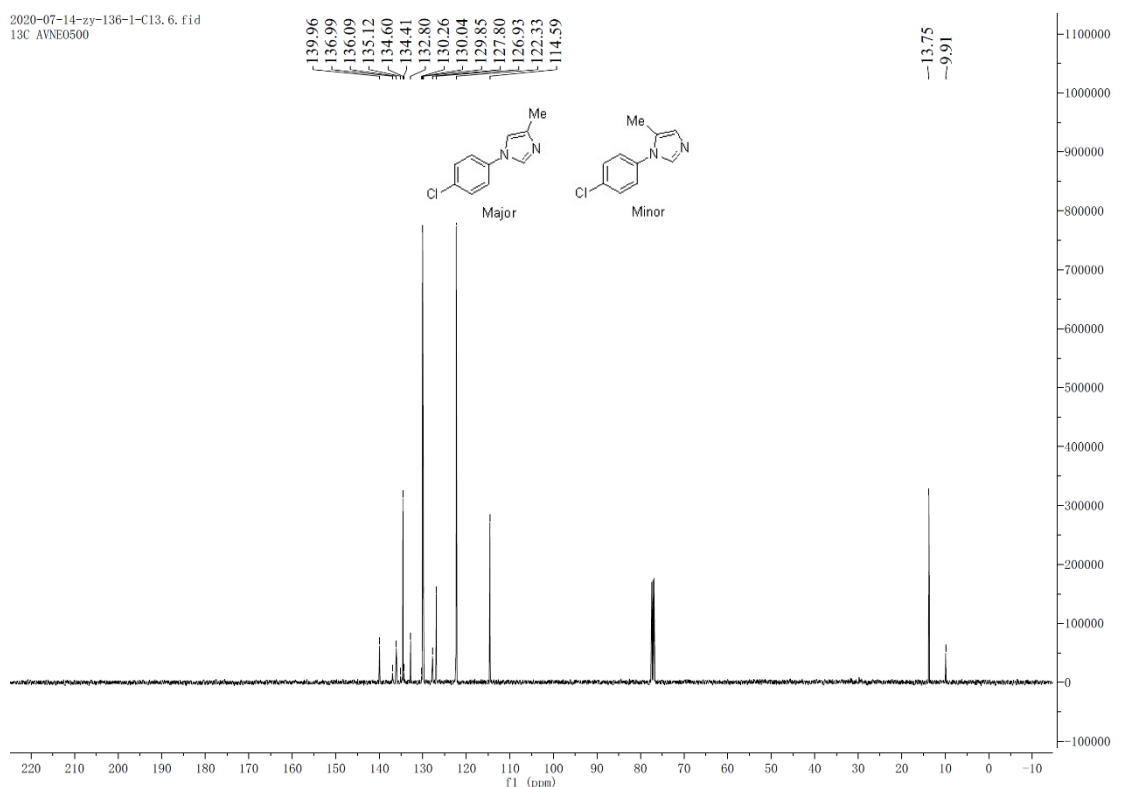
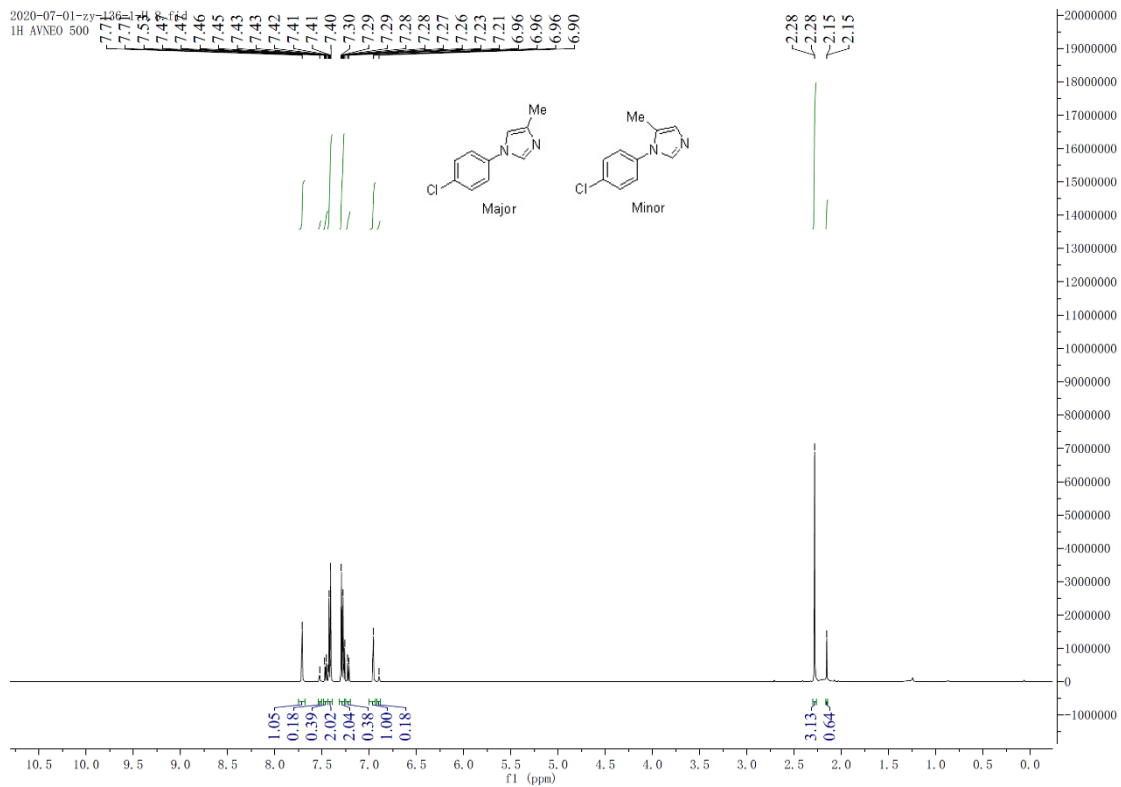
¹H and ¹³C-NMR spectra of product 57.



^1H and ^{13}C -NMR spectra of product 58.

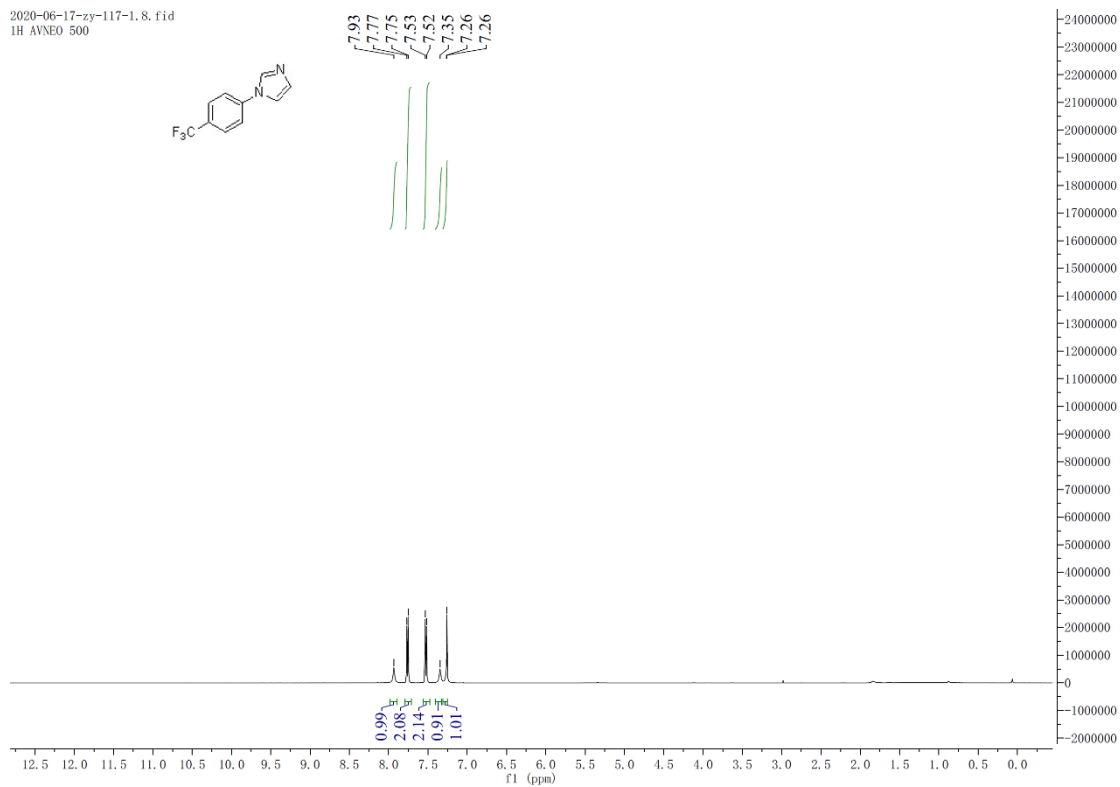
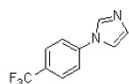


¹H and ¹³C-NMR spectra of product 59.

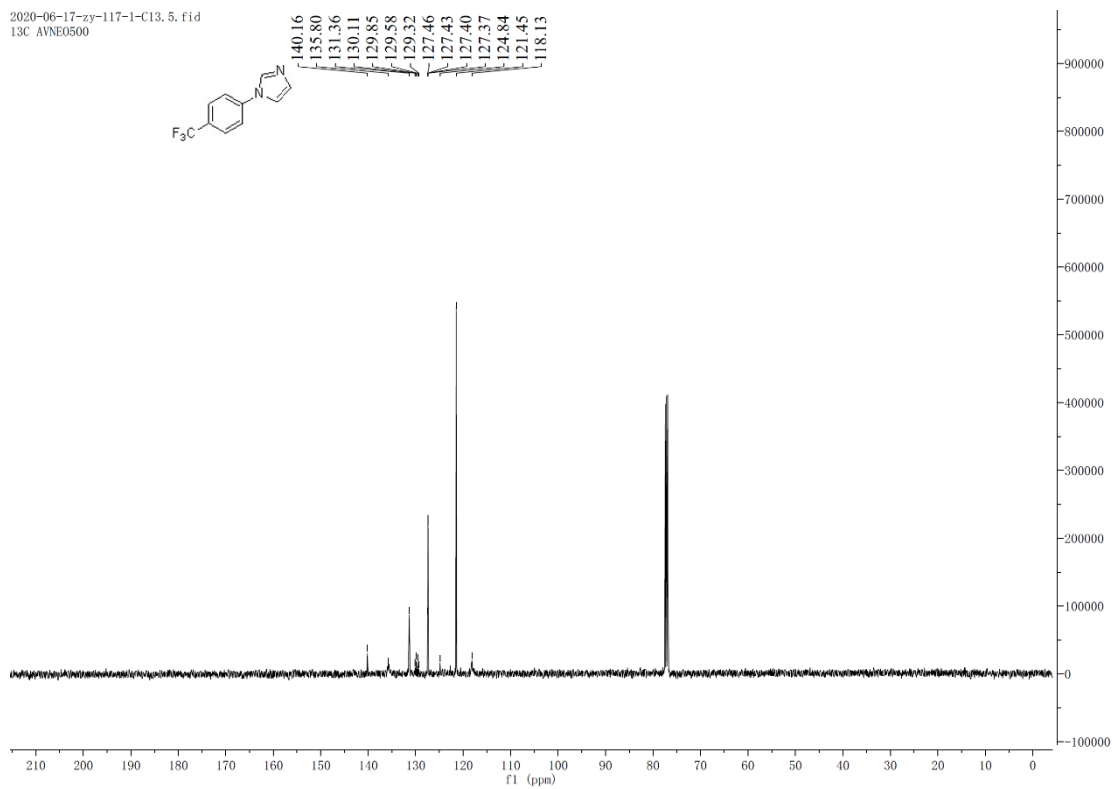
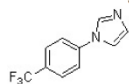


¹H and ¹³C-NMR spectra of product 60.

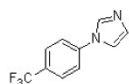
2020-06-17-zy-117-1.8.fid
1H AVNEO 500



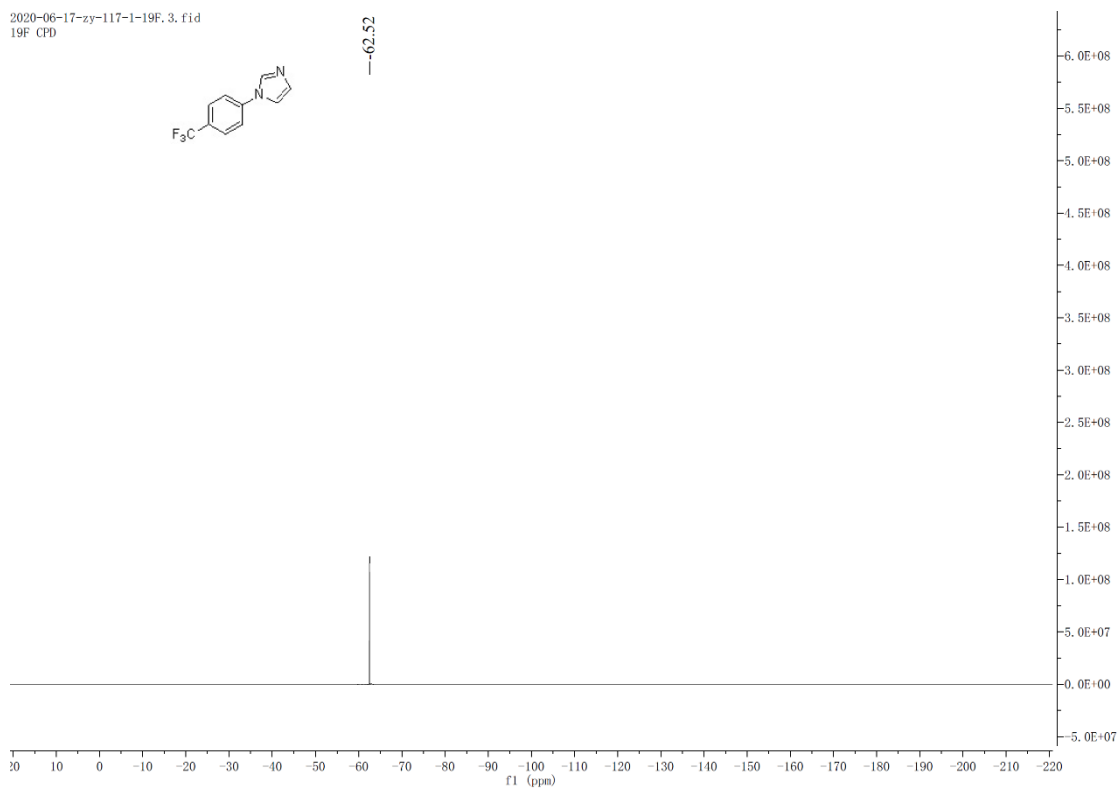
2020-06-17-zy-117-1-C13.5.fid
13C AVNEO500



2020-06-17-zy-117-1-19F. 3. fid
19F CPD

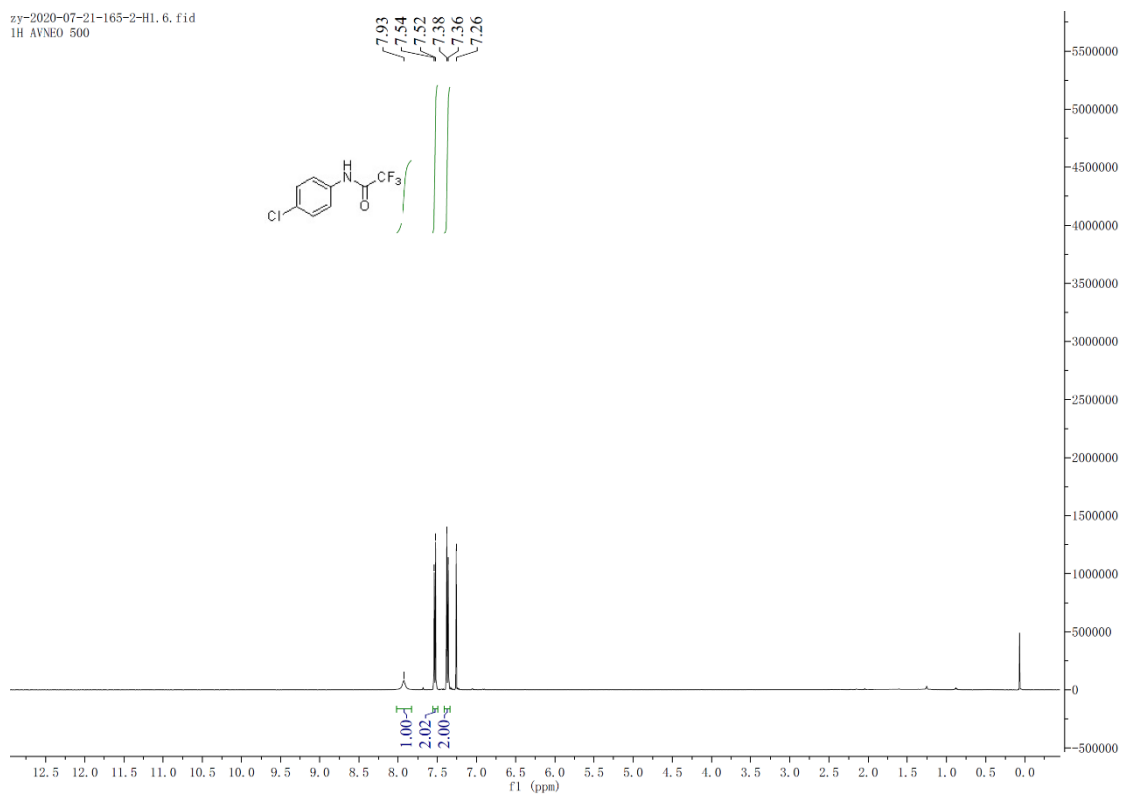


---62.52

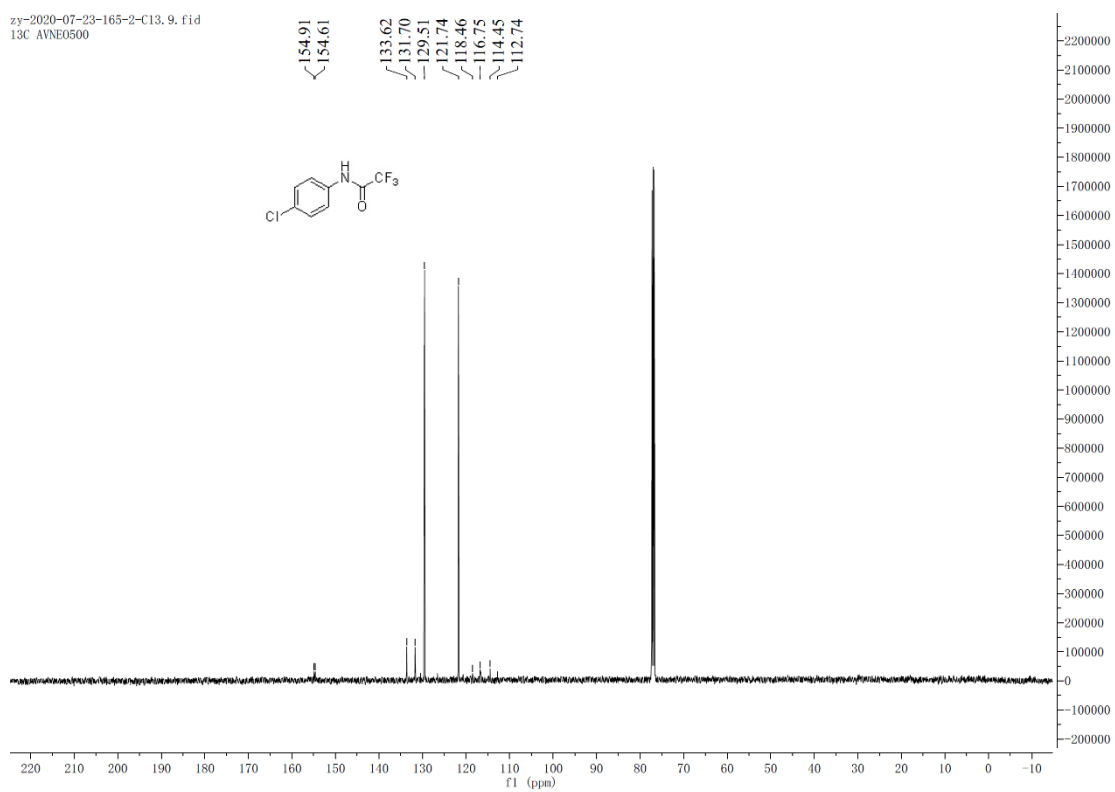


¹H, ¹³C, and ¹⁹F-NMR spectra of product 61.

zy-2020-07-21-165-2-H1. 6. fid
1H AVNEO 500

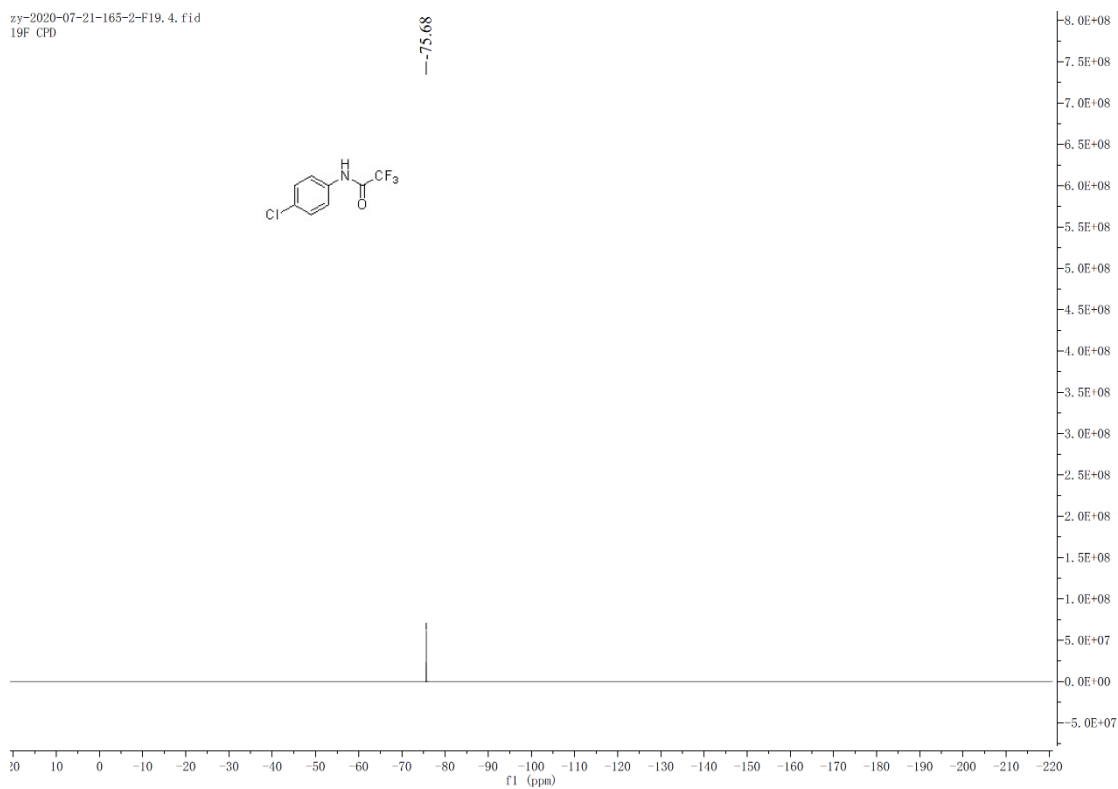
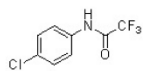


zy-2020-07-23-165-2-C13. 9. fid
13C AVNEO500

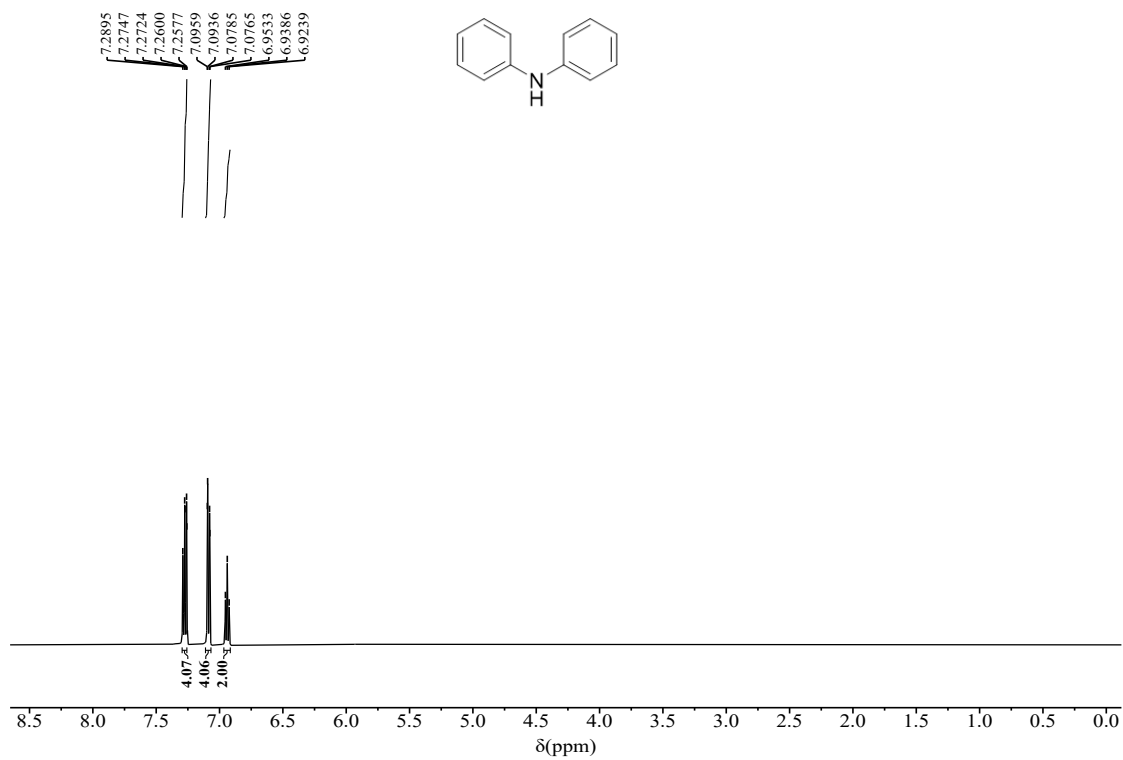


zy-2020-07-21-165-2-F19.4.fid
19F CPD

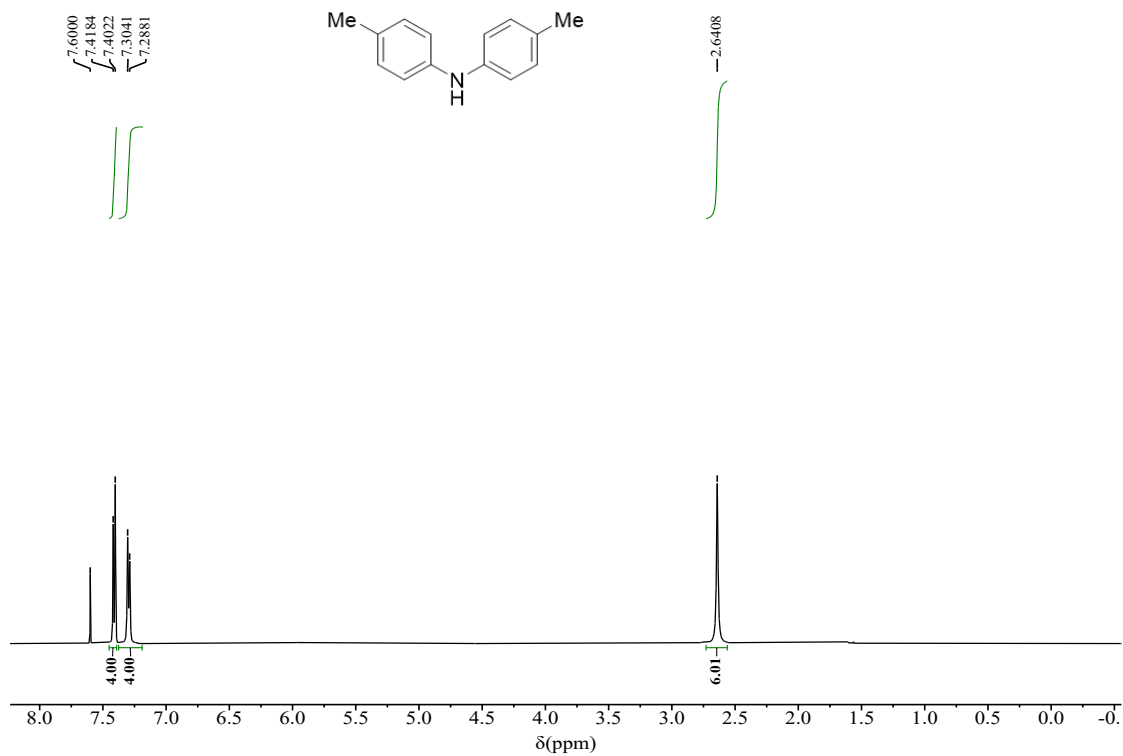
-75.68



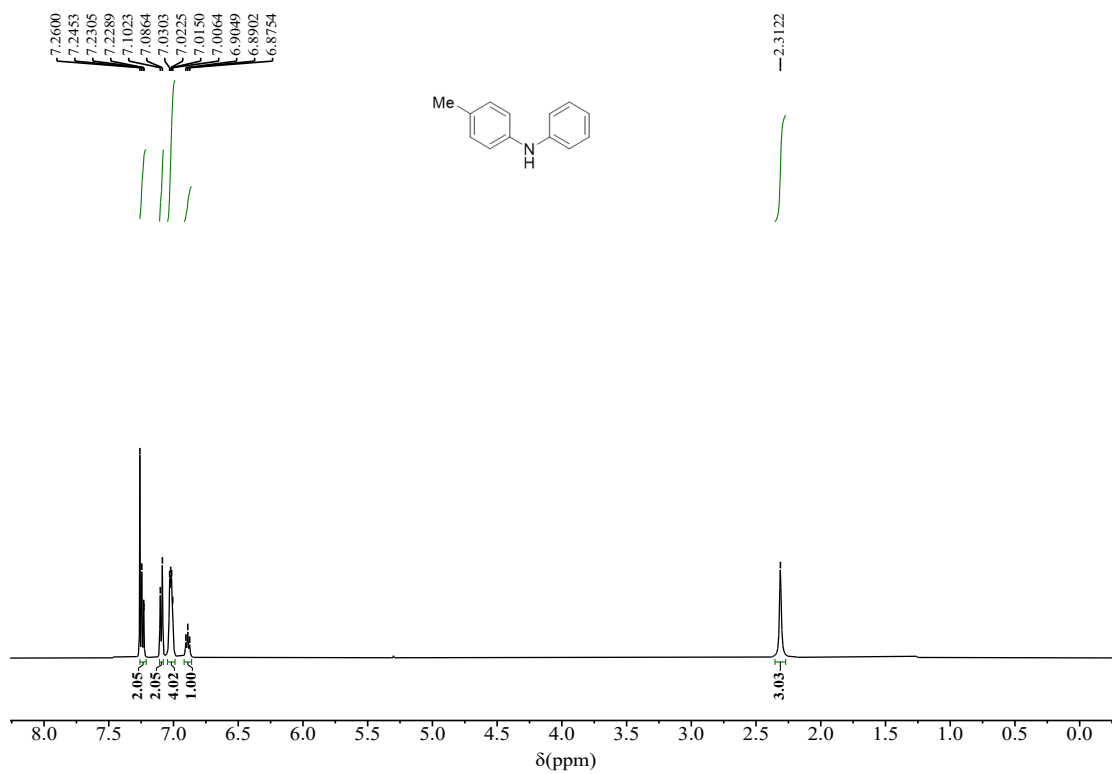
^1H , ^{13}C , and ^{19}F -NMR spectra of product 62.



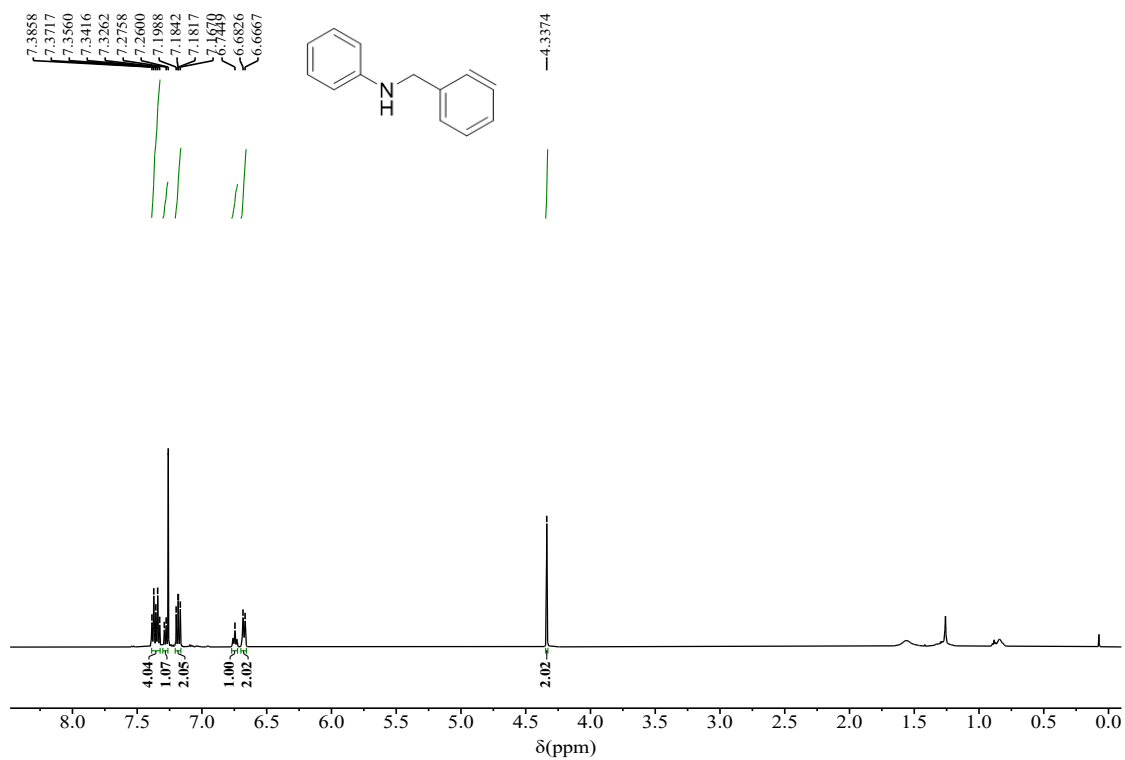
¹H spectra of product 63.



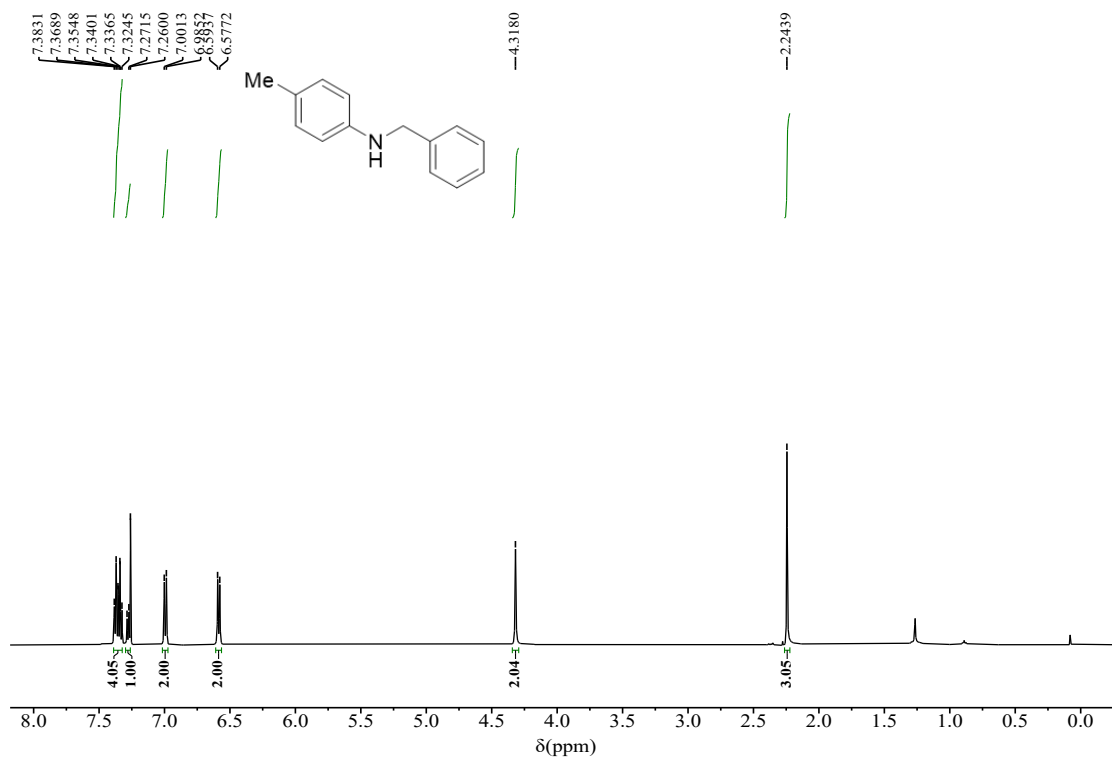
¹H spectra of product 64.



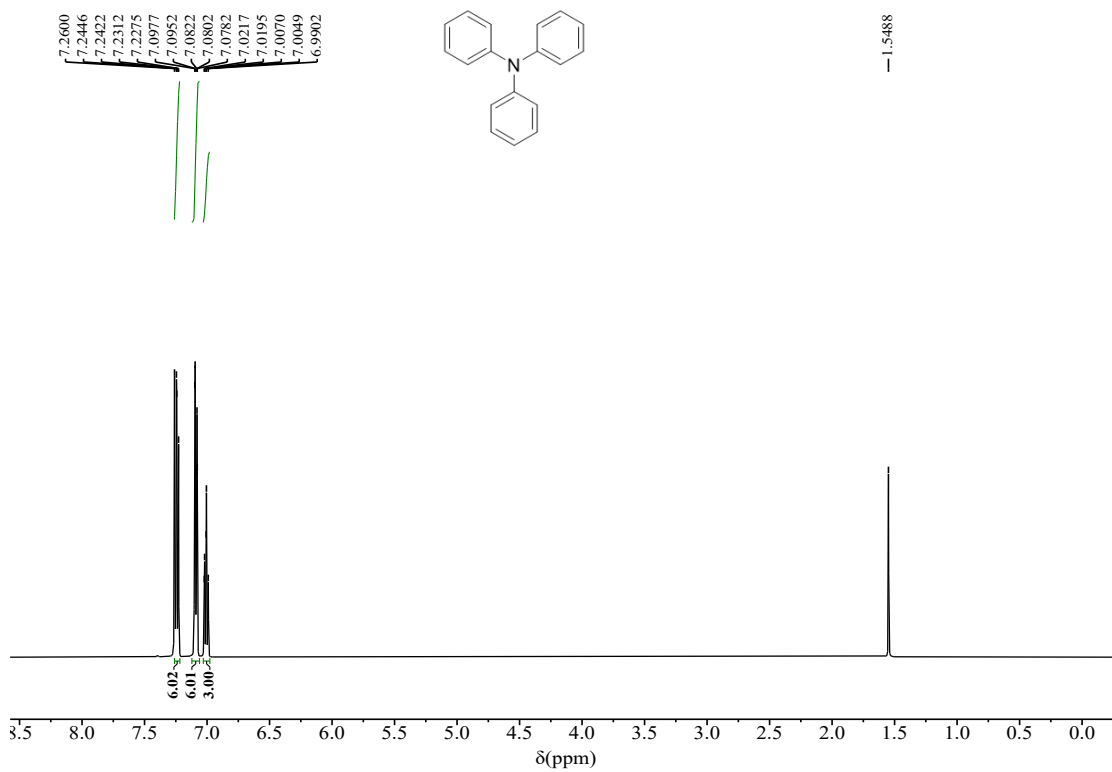
¹H spectra of product 65.



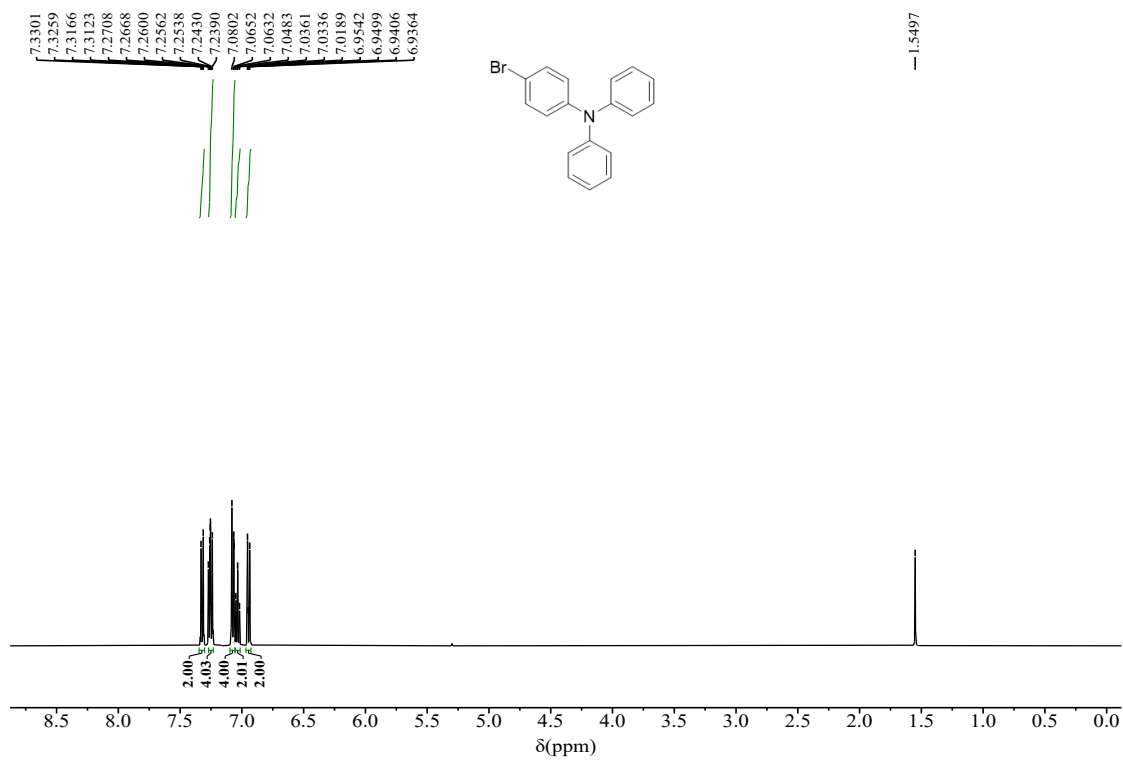
¹H spectra of product 66.



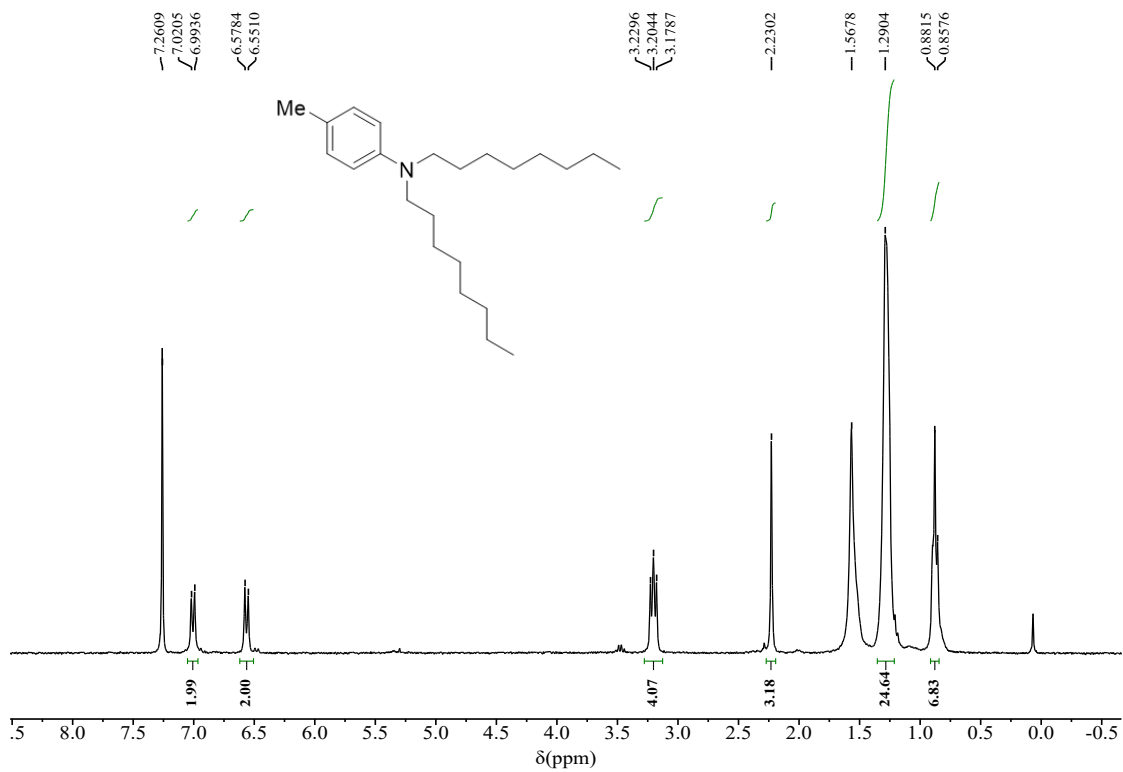
¹H spectra of product 67.



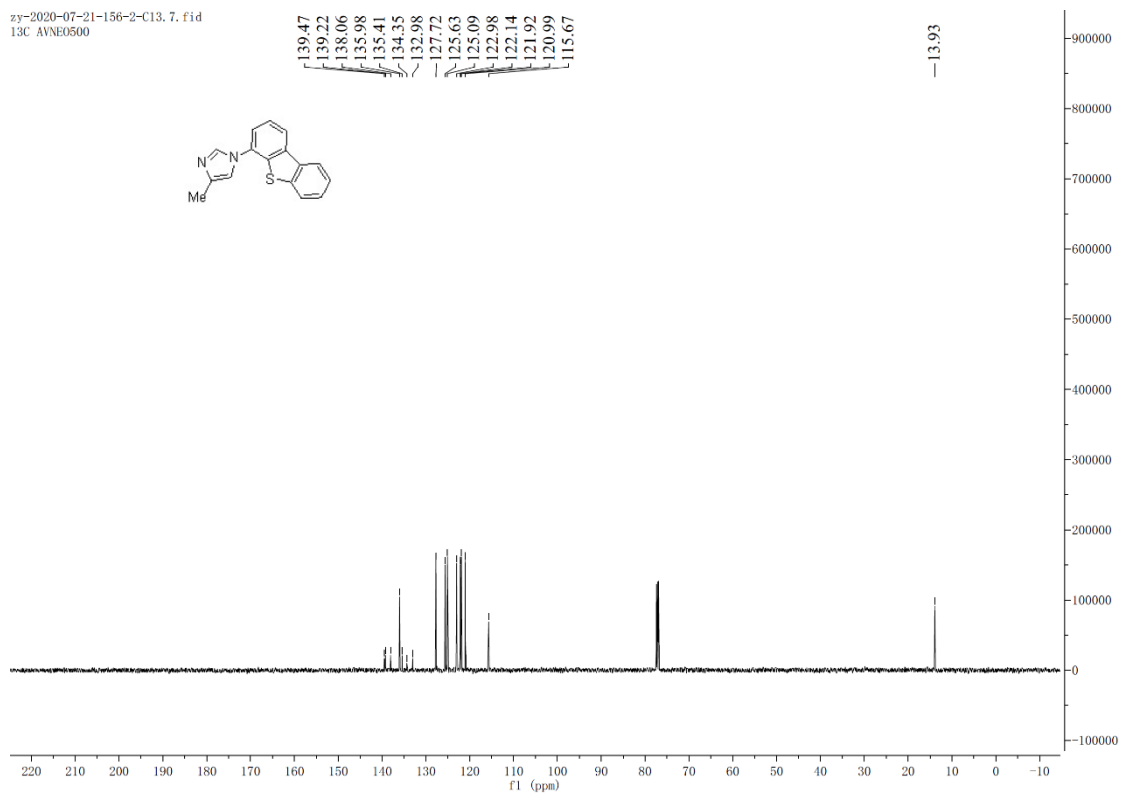
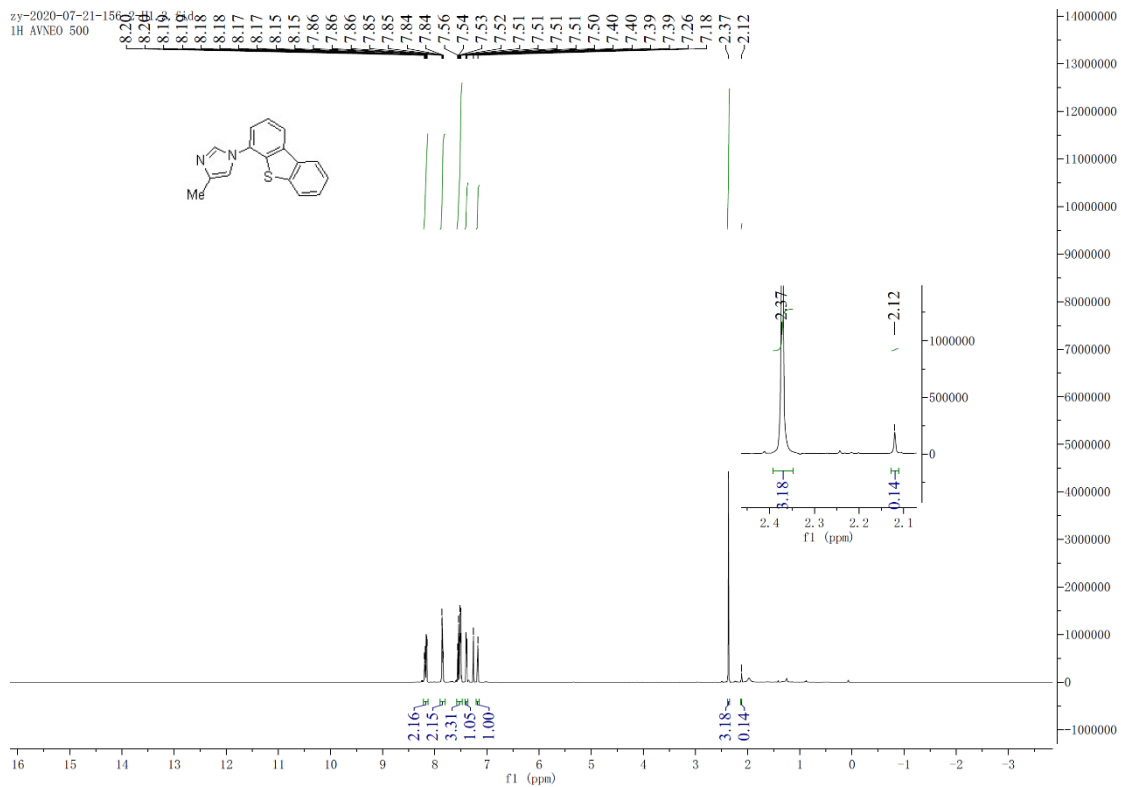
¹H spectra of product 68.



¹H spectra of product 69.

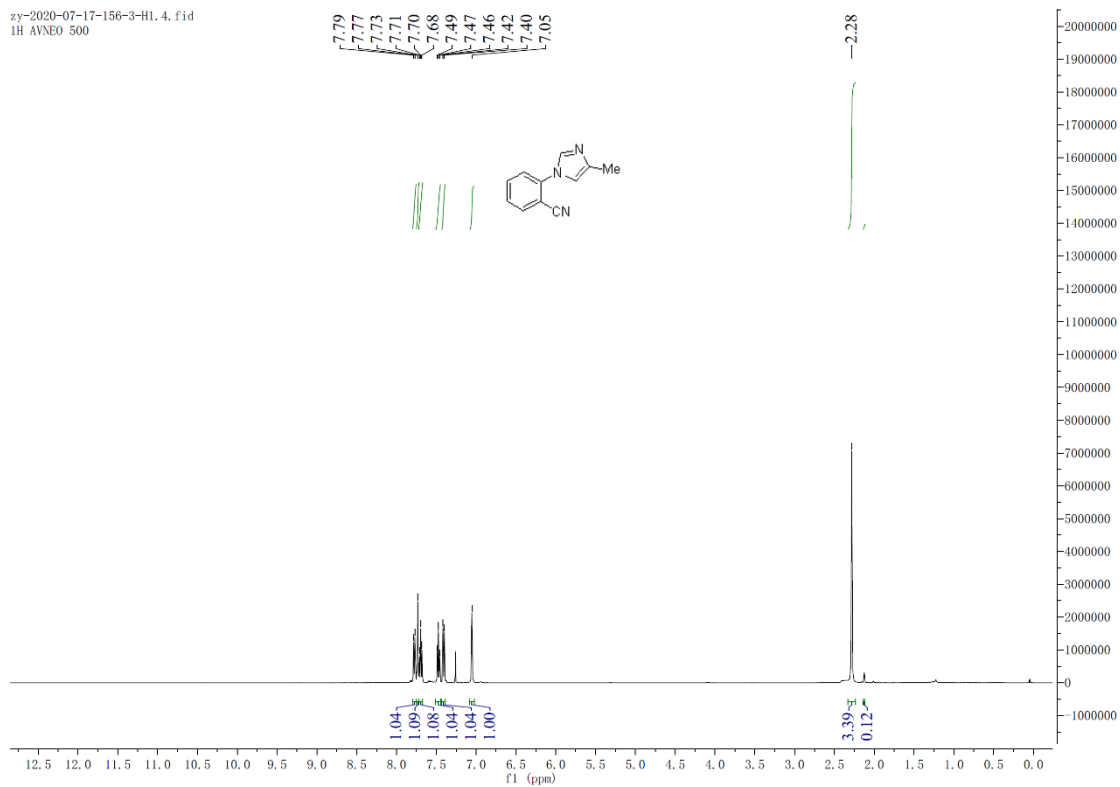


¹H spectra of product 70.

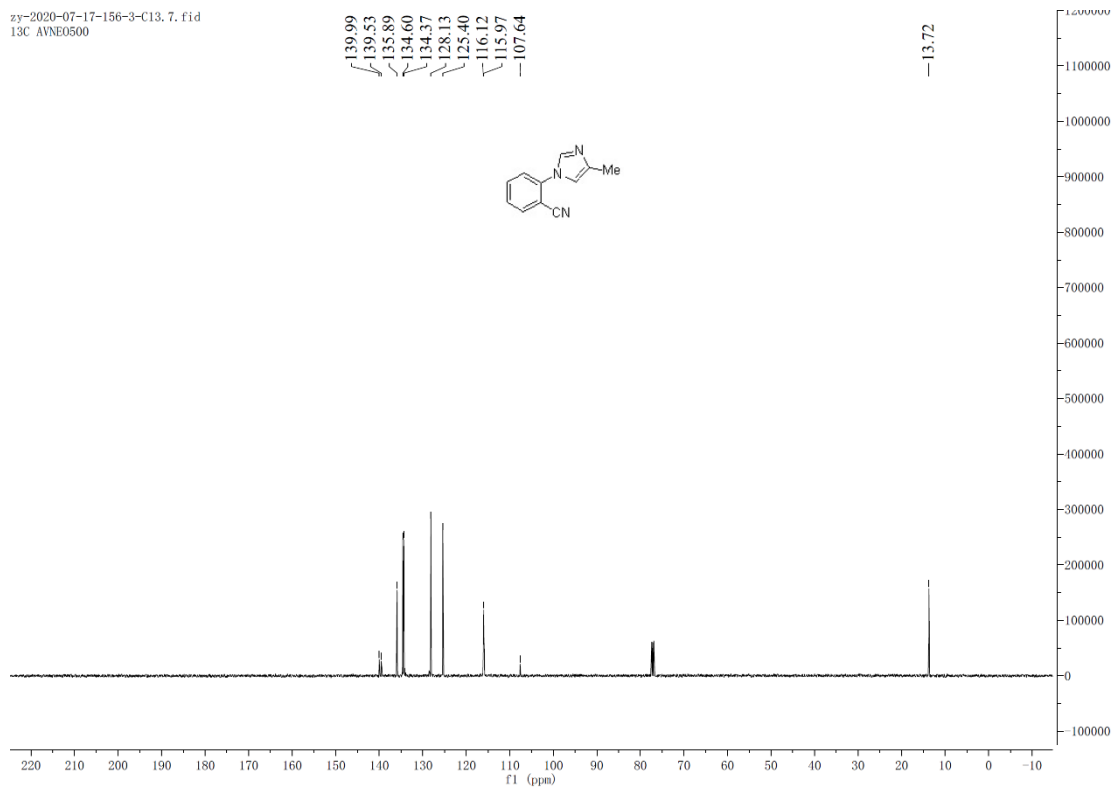


¹H and ¹³C-NMR spectra of product 71.

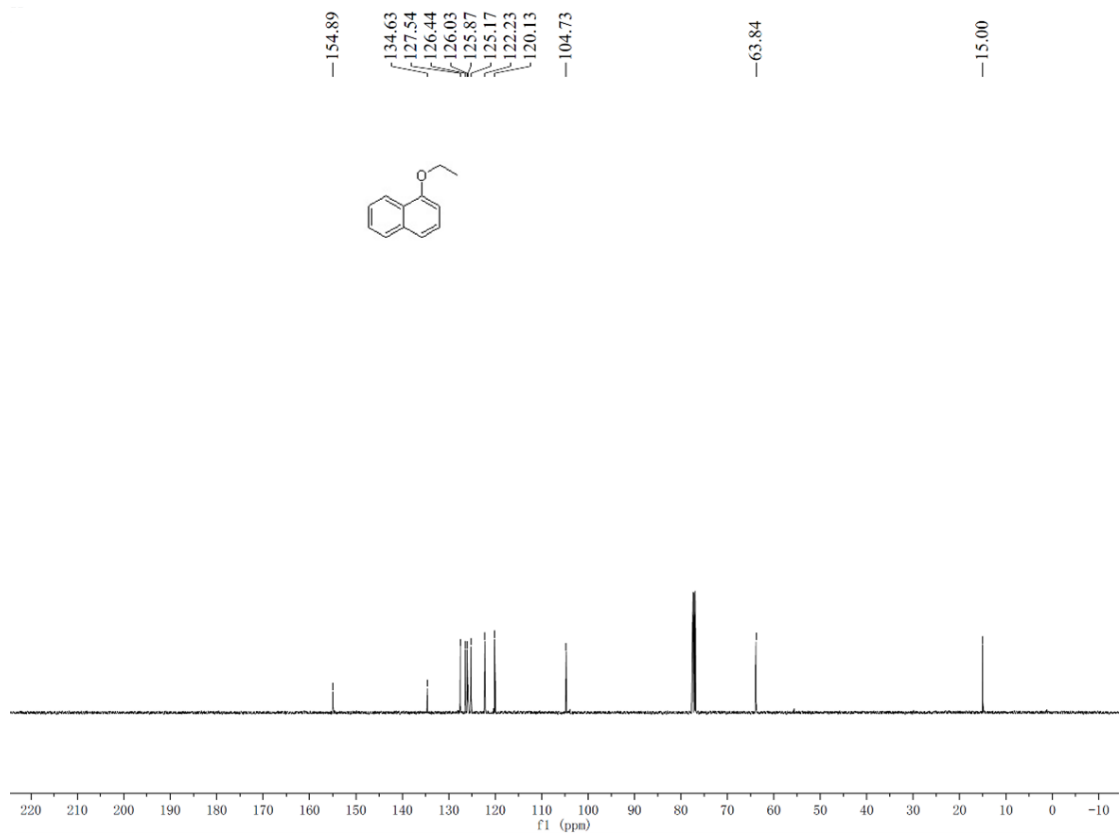
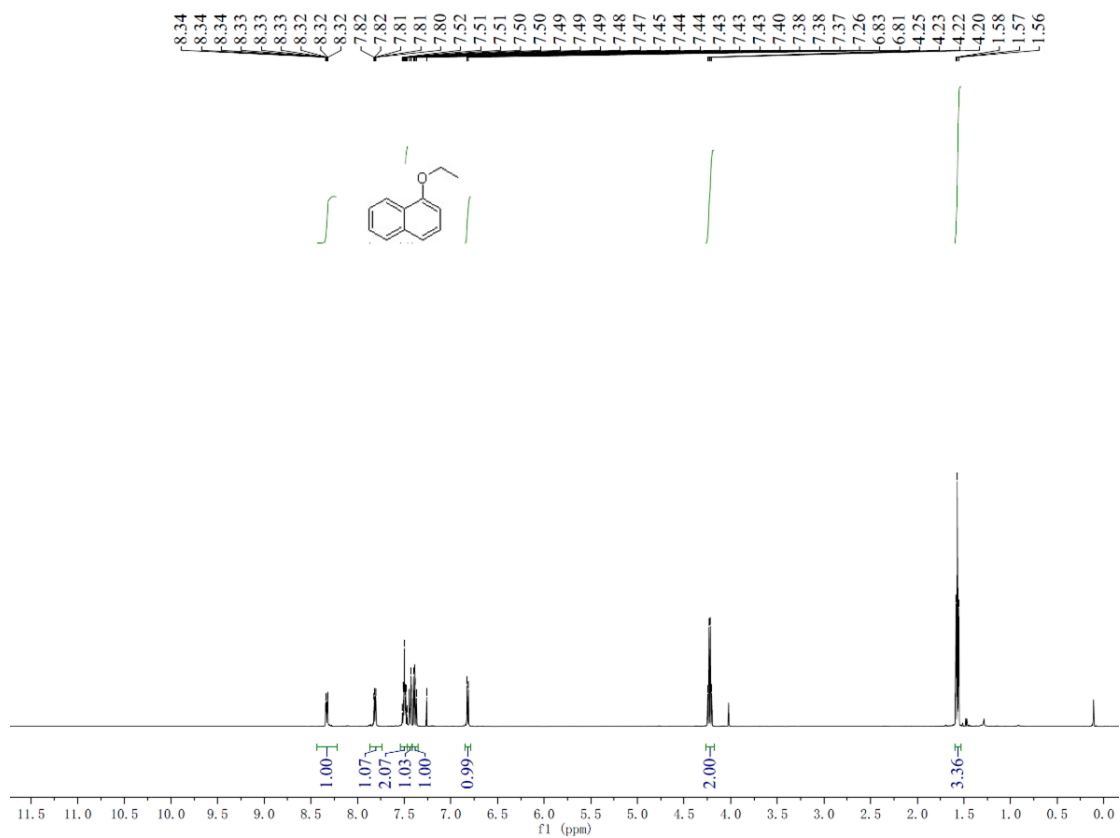
zy-2020-07-17-156-3-H1. 4. fid
1H AVNEO 500



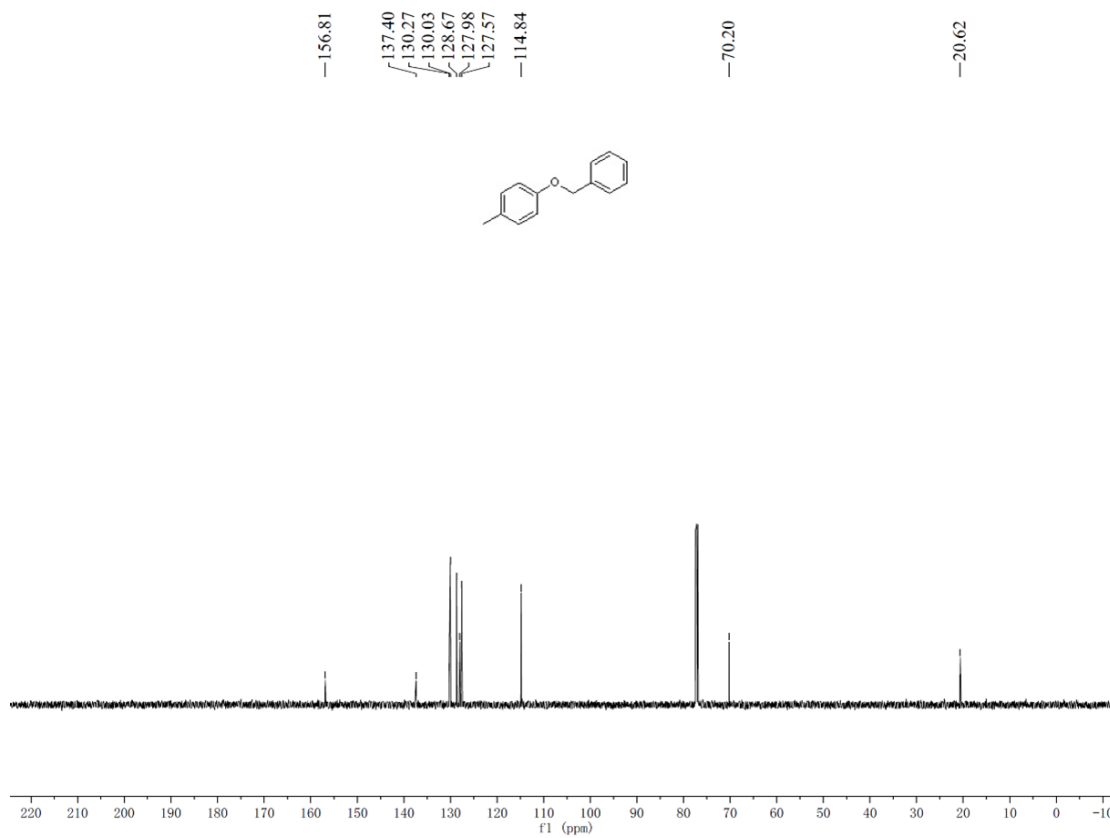
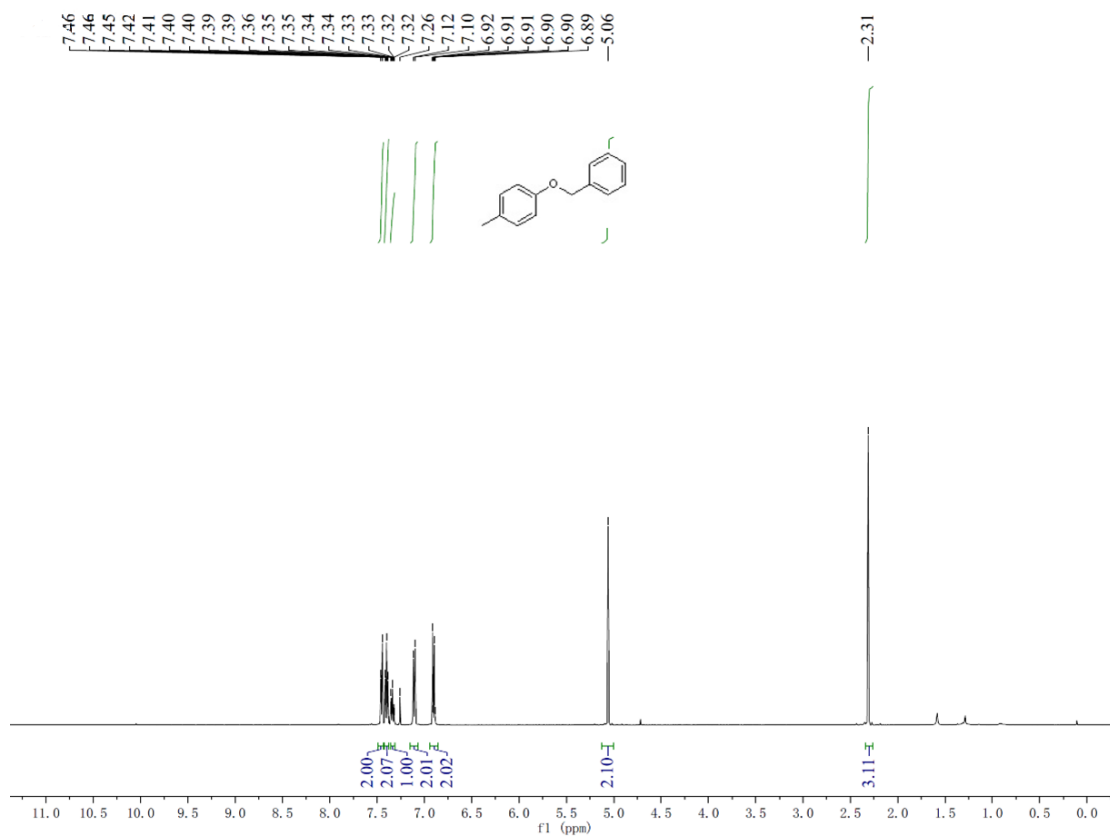
zy-2020-07-17-156-3-C13. 7. fid
13C AVNEO500



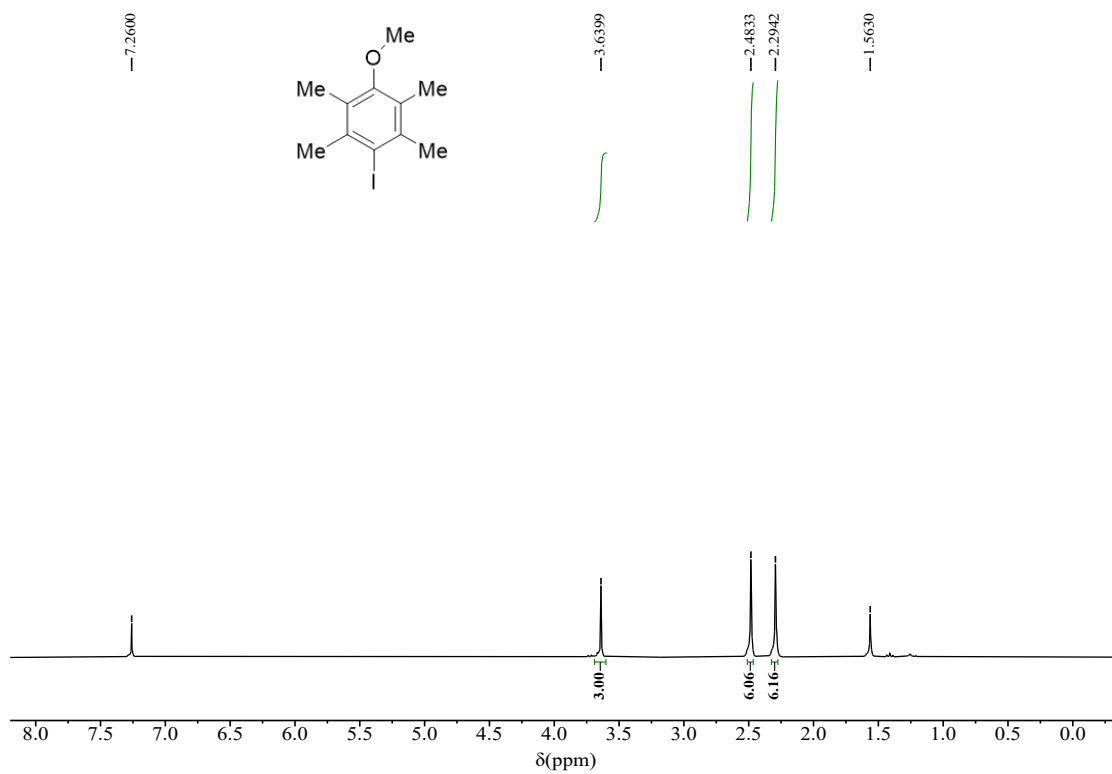
¹H and ¹³C-NMR spectra of product 72.



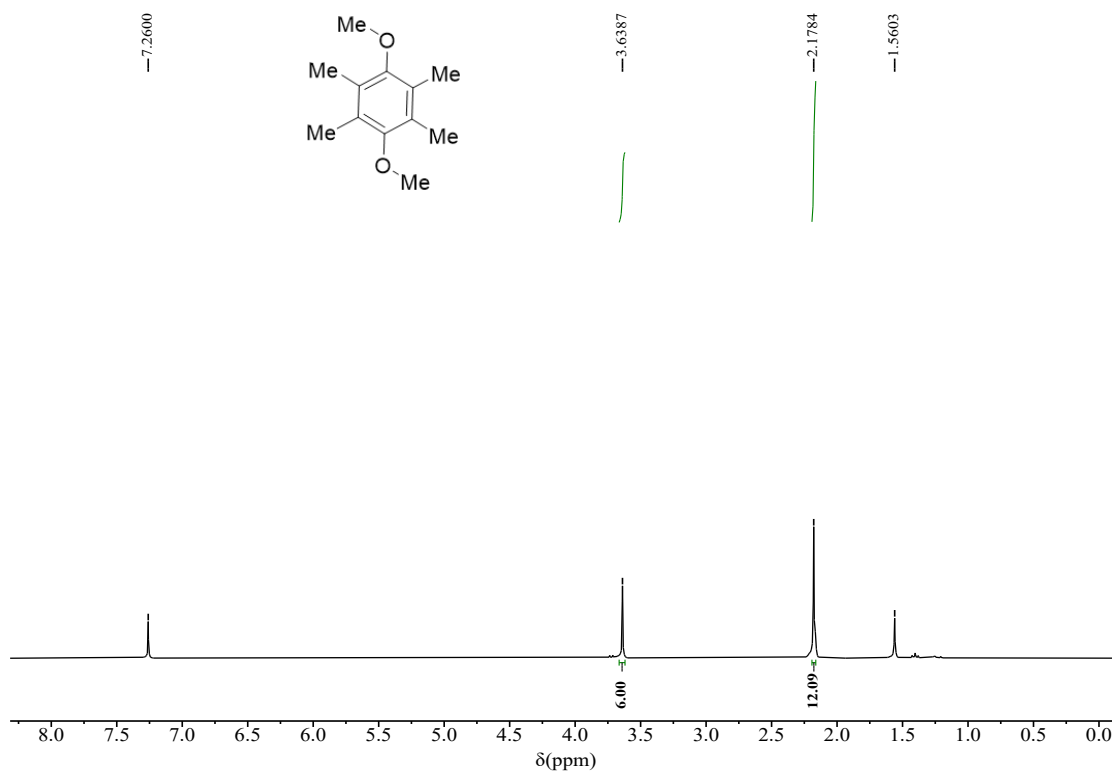
^1H and ^{13}C -NMR spectra of product 73.



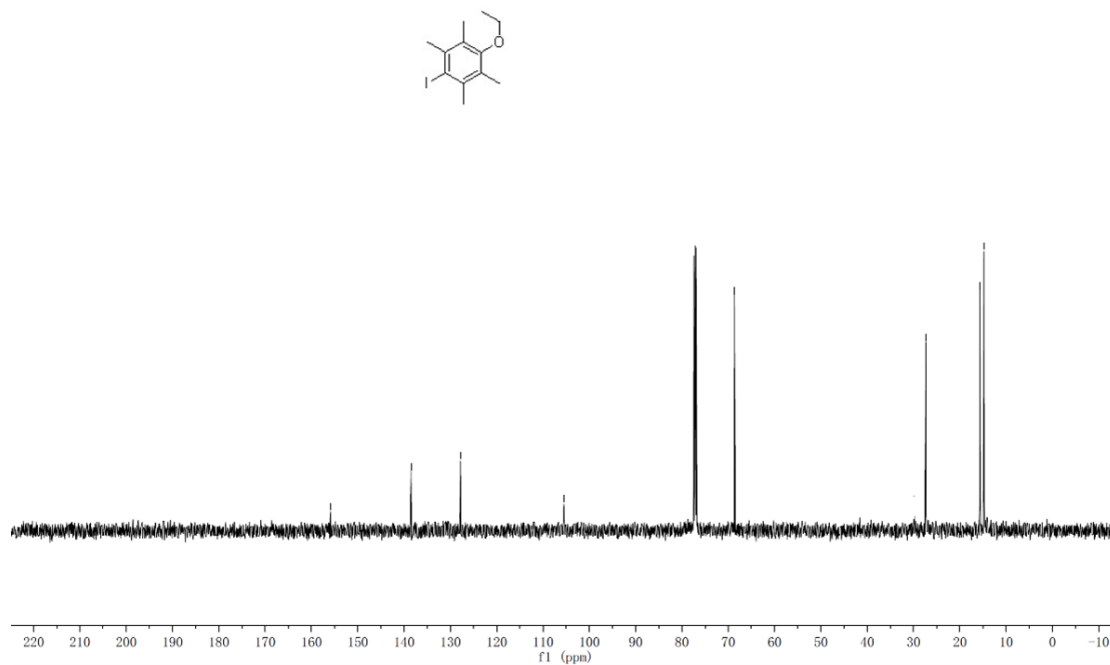
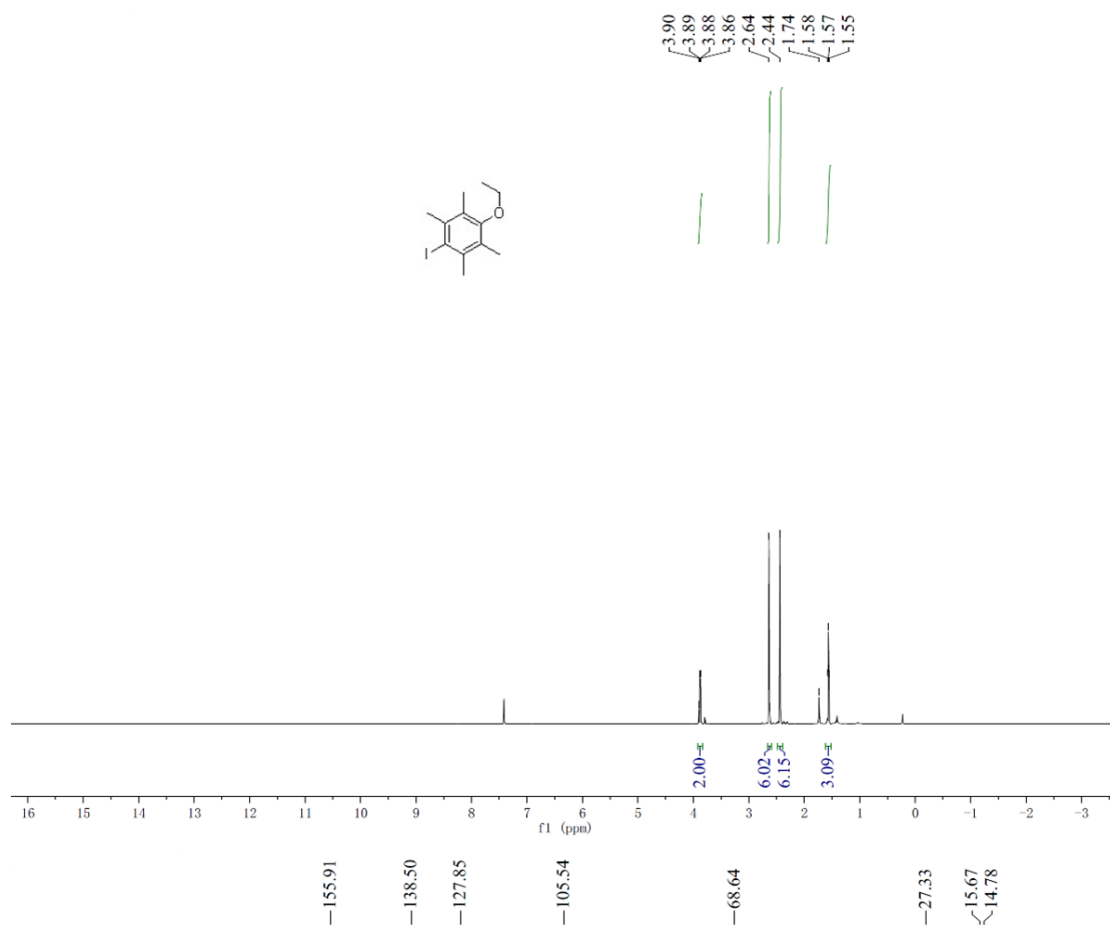
¹H and ¹³C-NMR spectra of product 74.



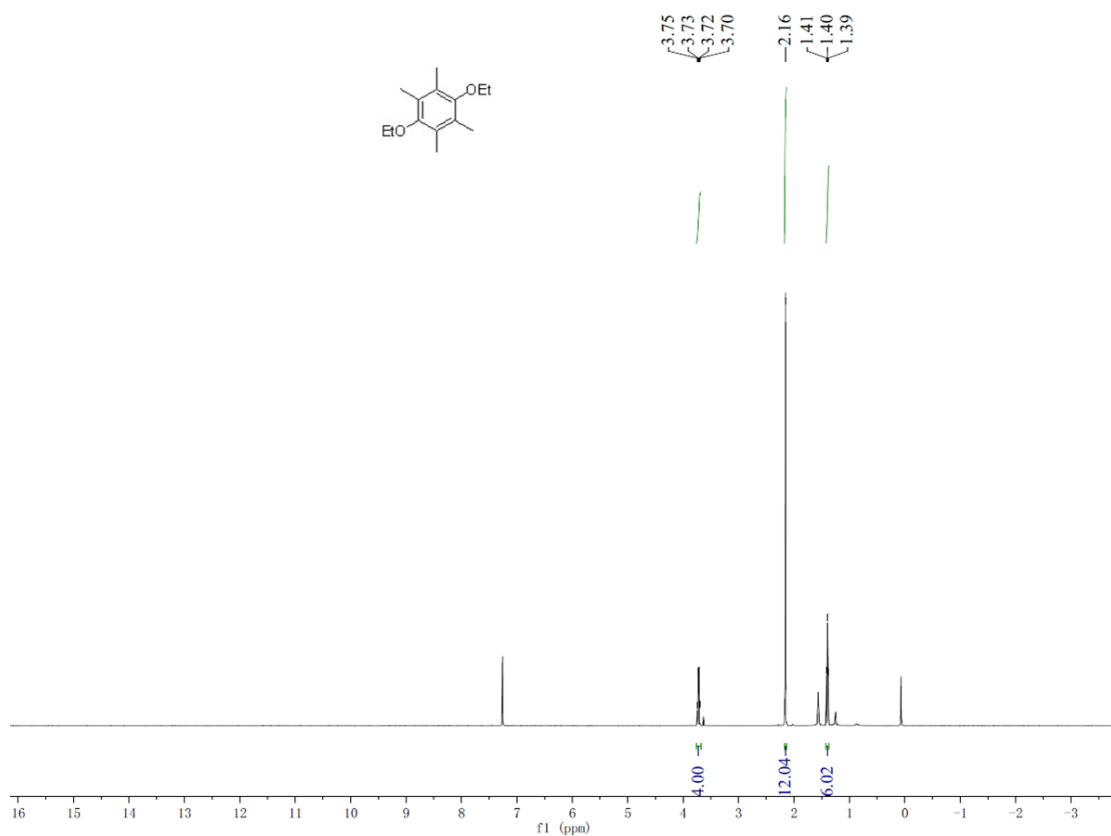
^1H spectra of product 75.



^1H spectra of product 76.



^1H and ^{13}C -NMR spectra of product 77.

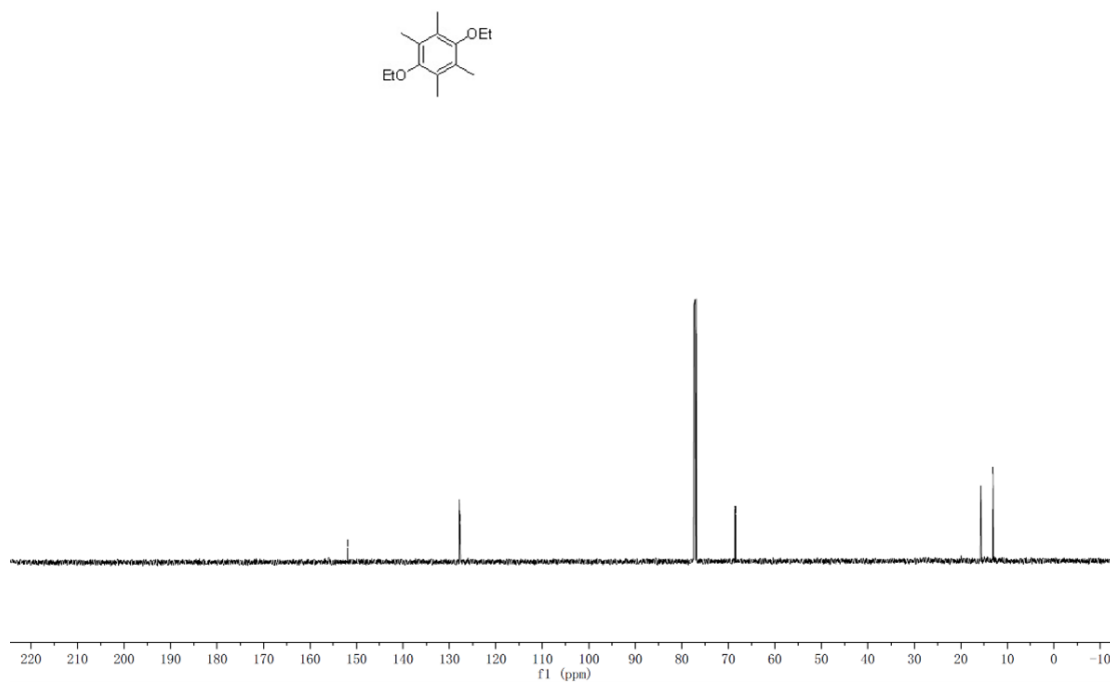


151.86

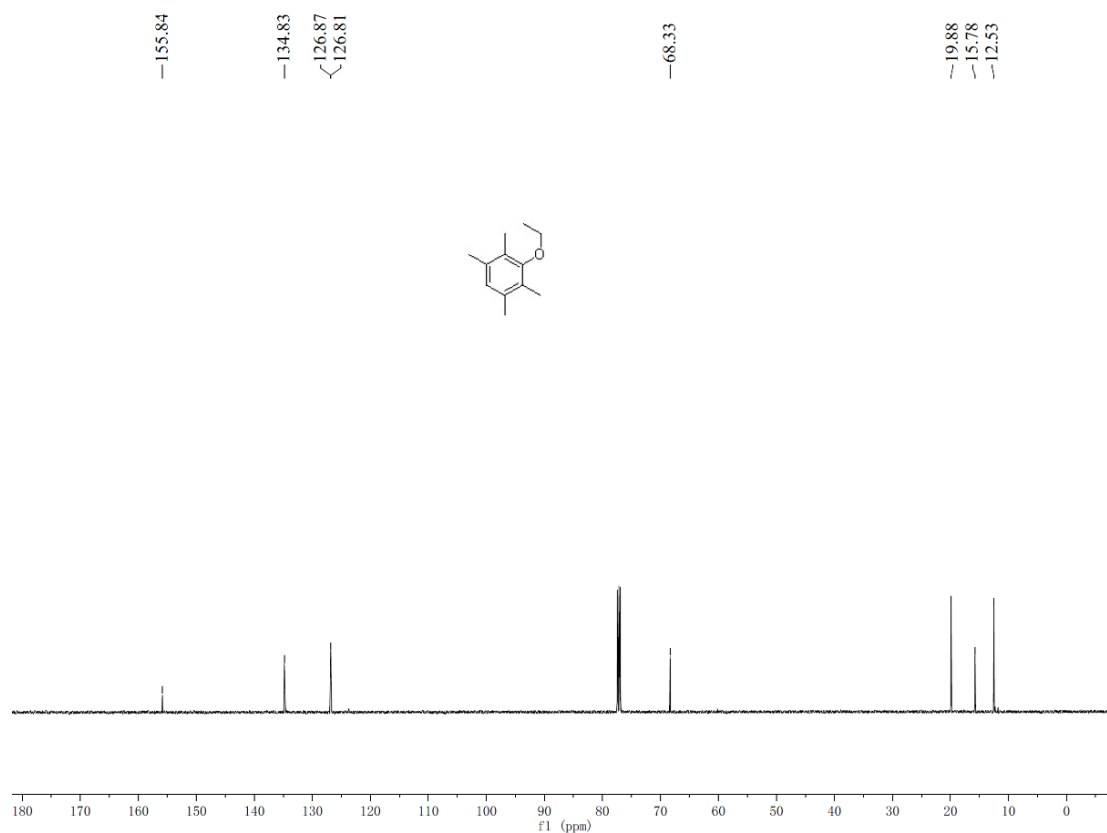
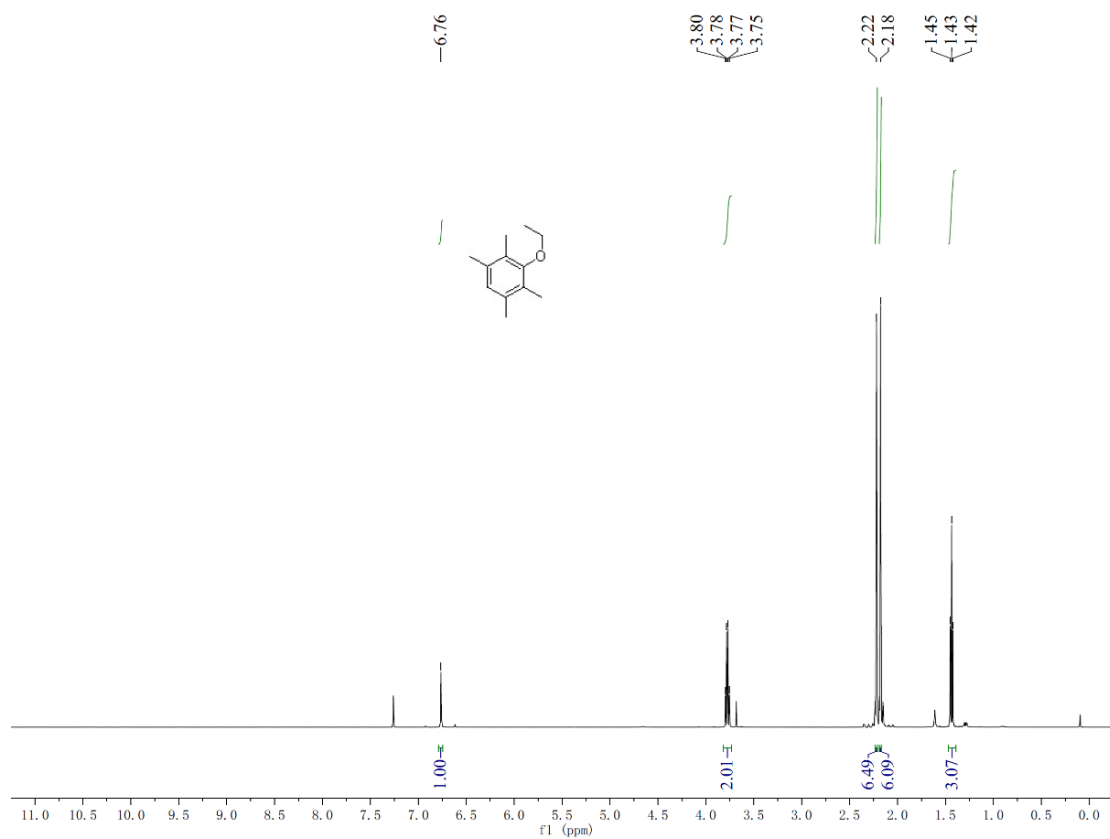
127.76

68.44

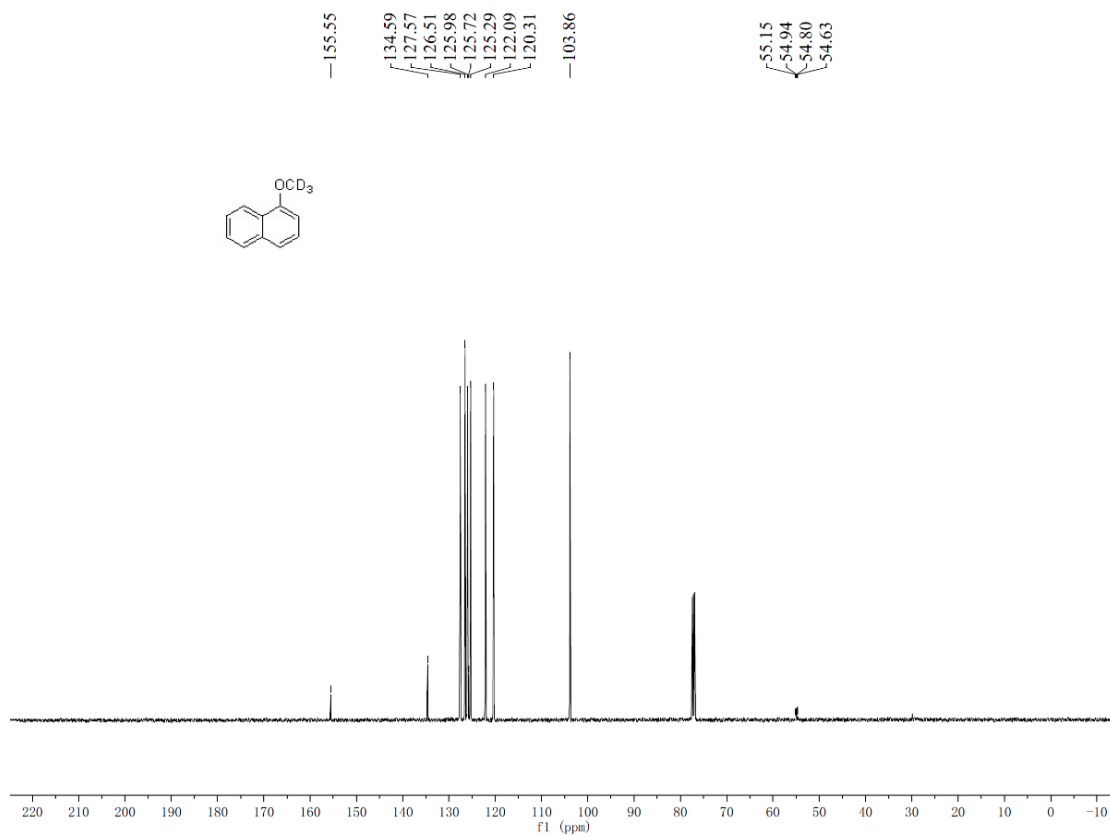
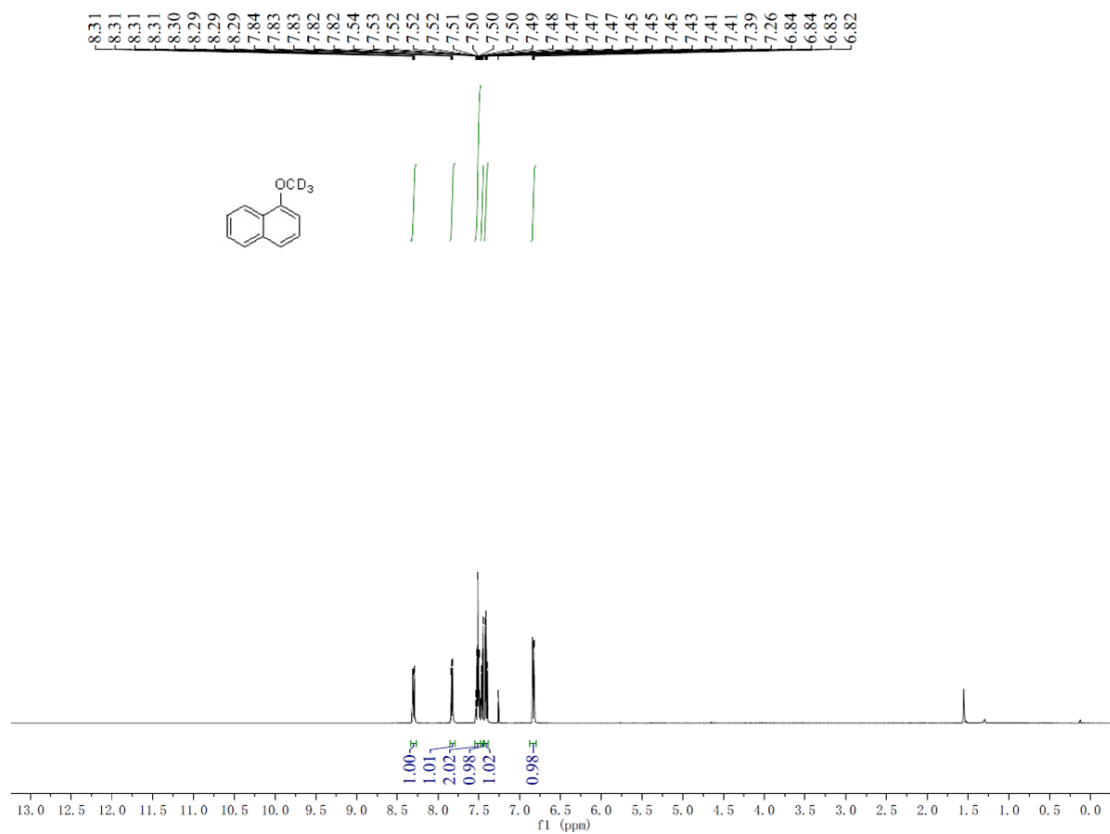
15.76
13.02



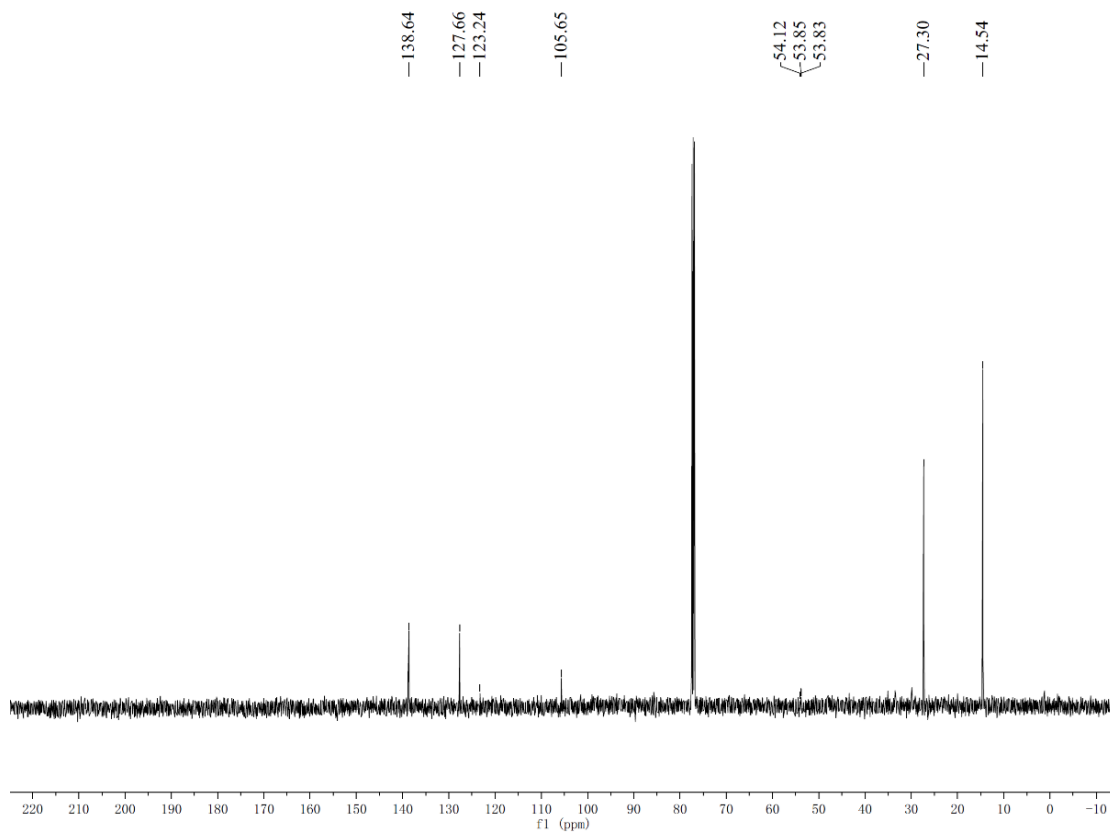
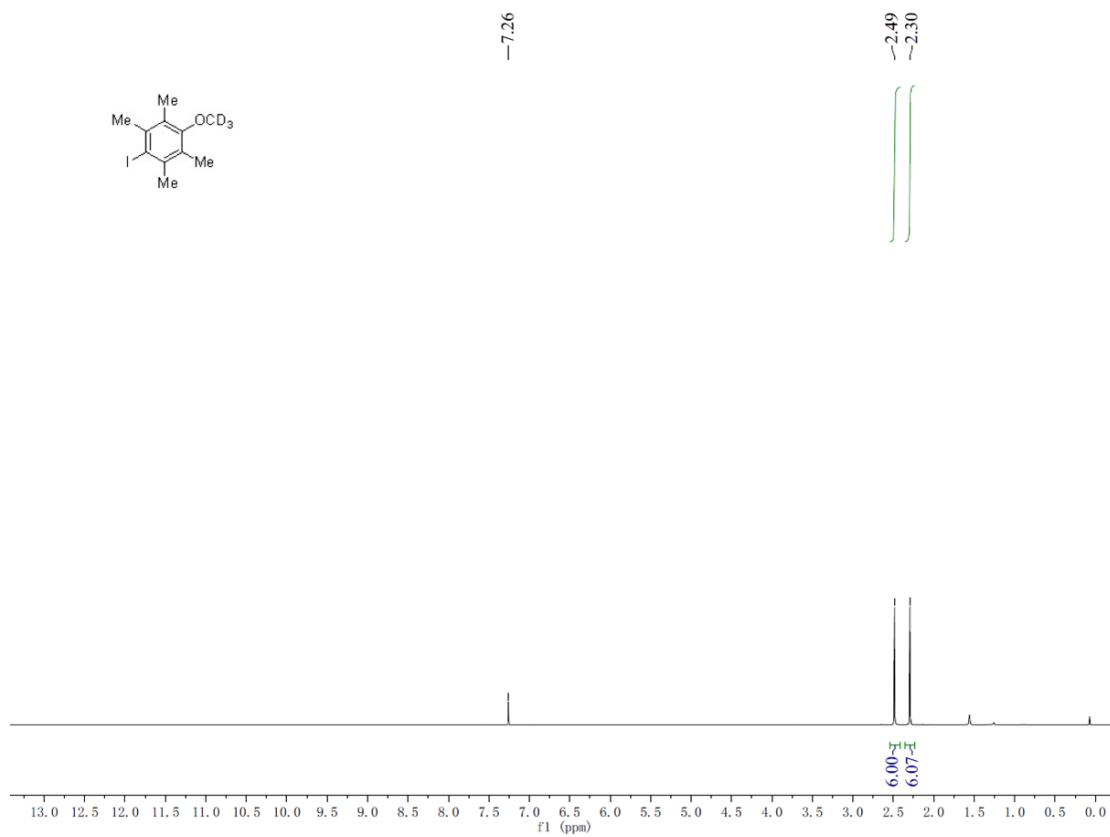
^1H and ^{13}C -NMR spectra of product 78.



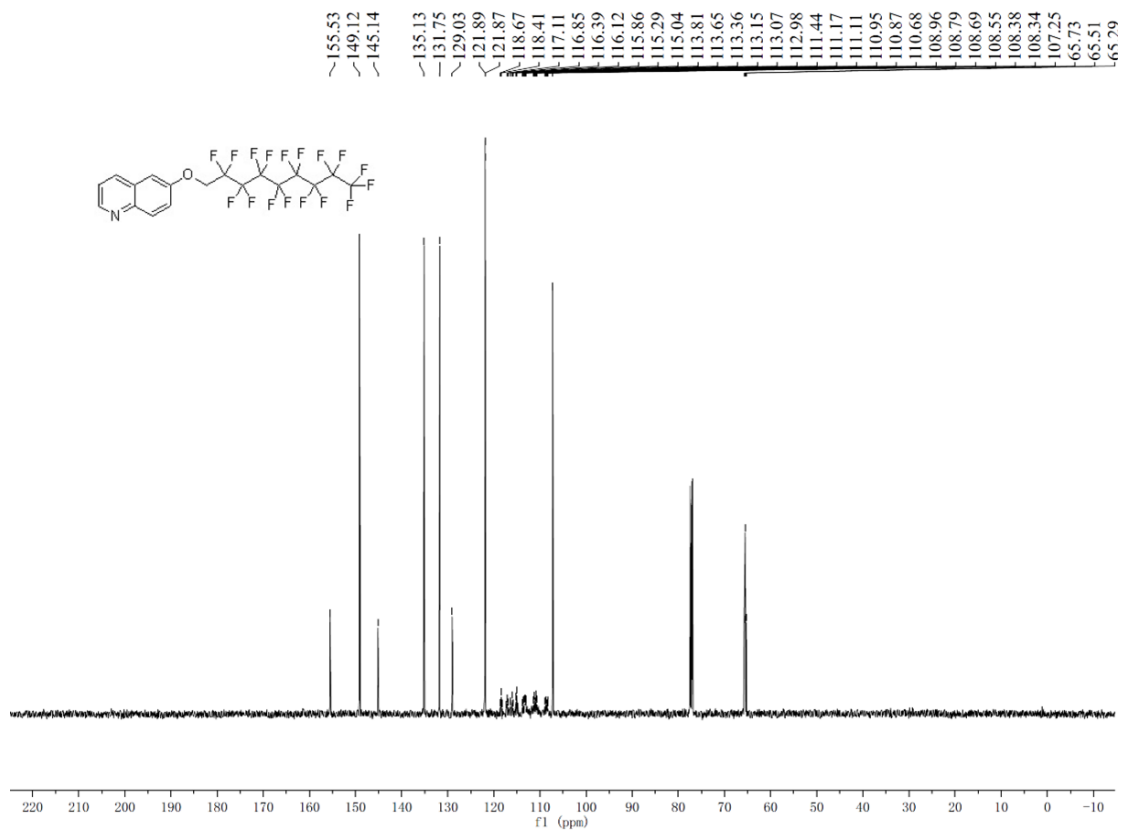
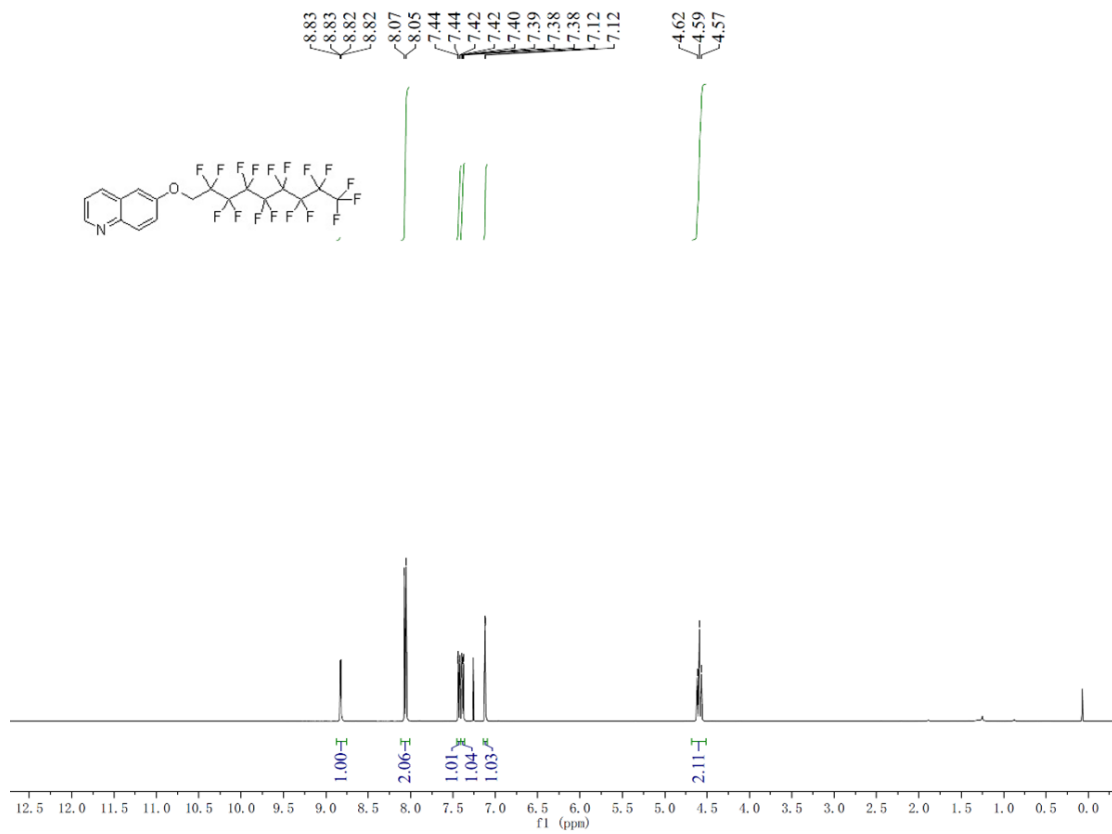
¹H and ¹³C-NMR spectra of product 79.



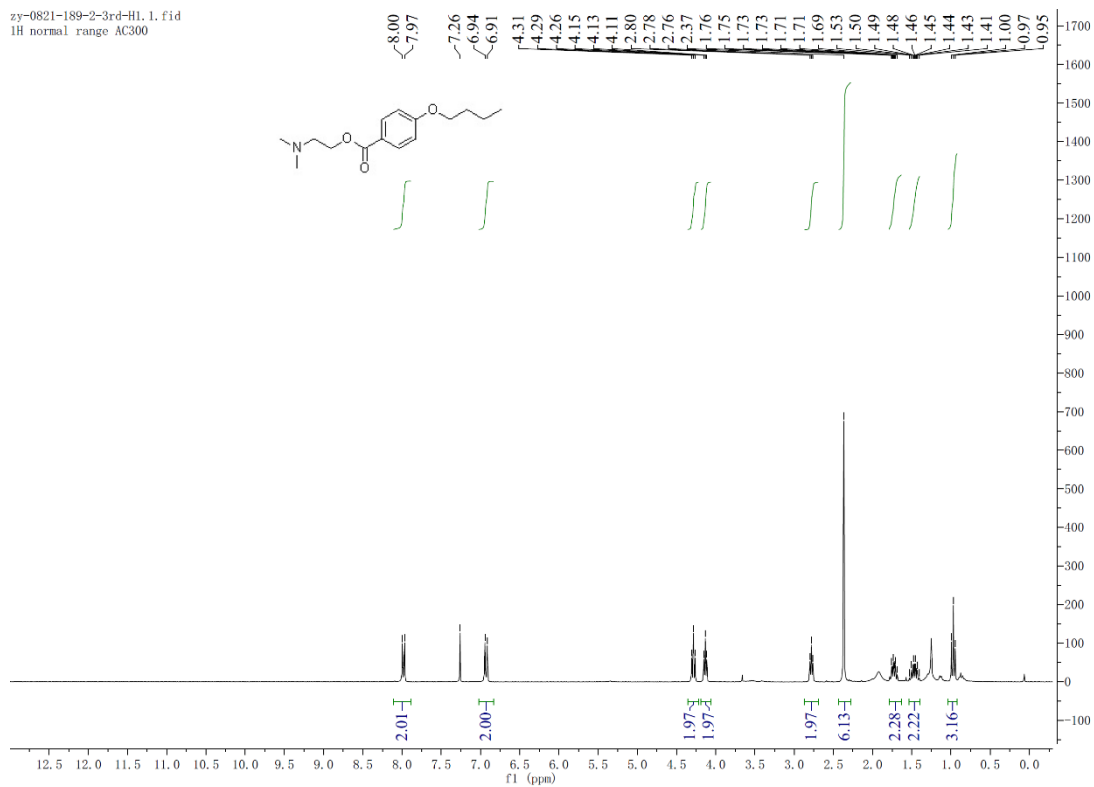
¹H and ¹³C-NMR spectra of product 80.



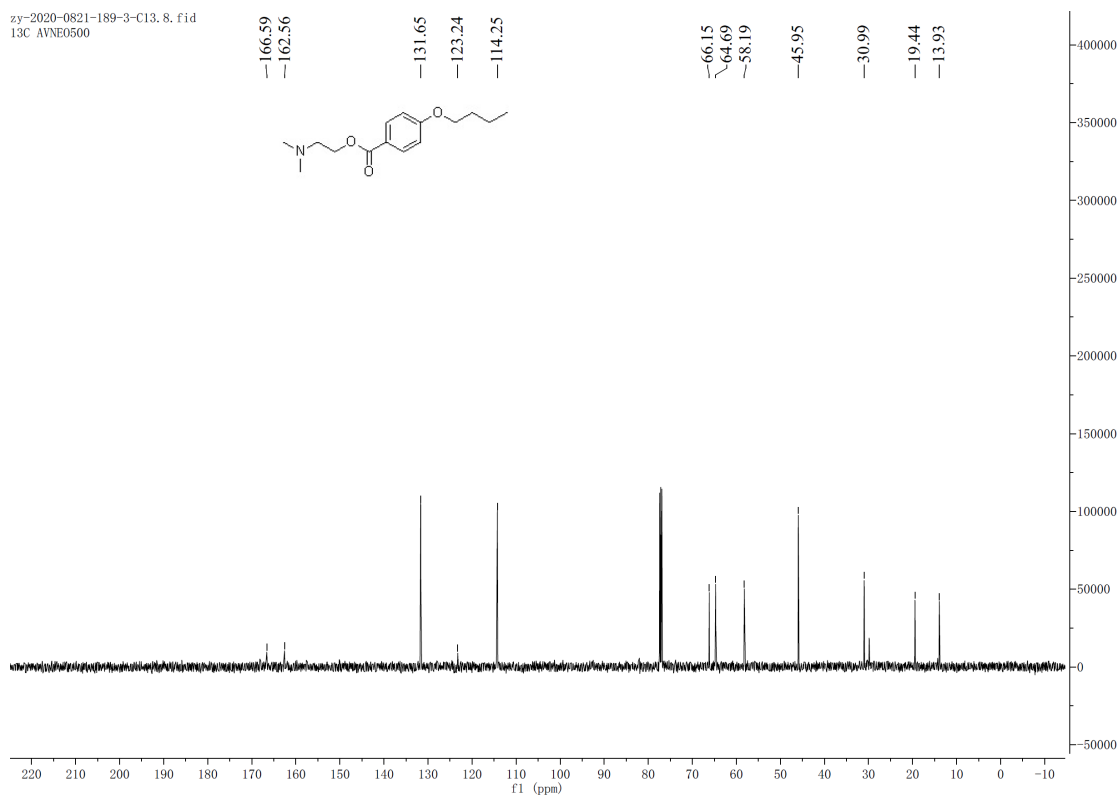
¹H and ¹³C-NMR spectra of product 81.



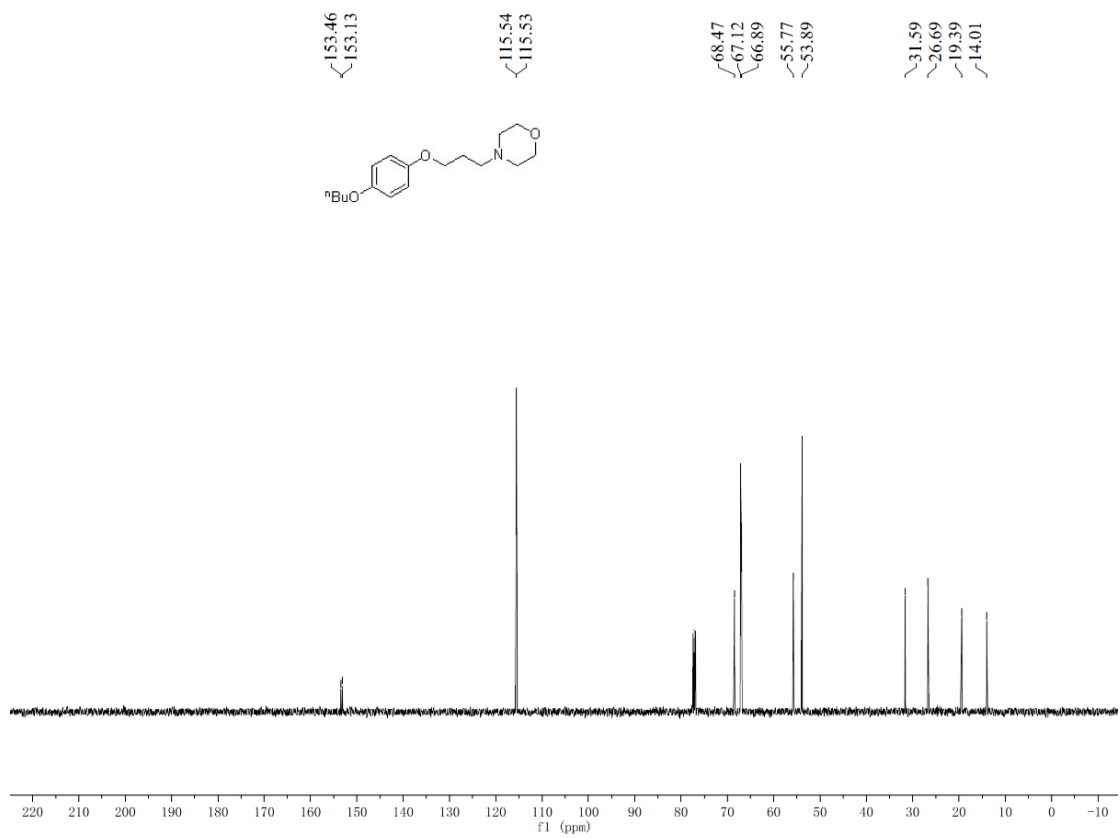
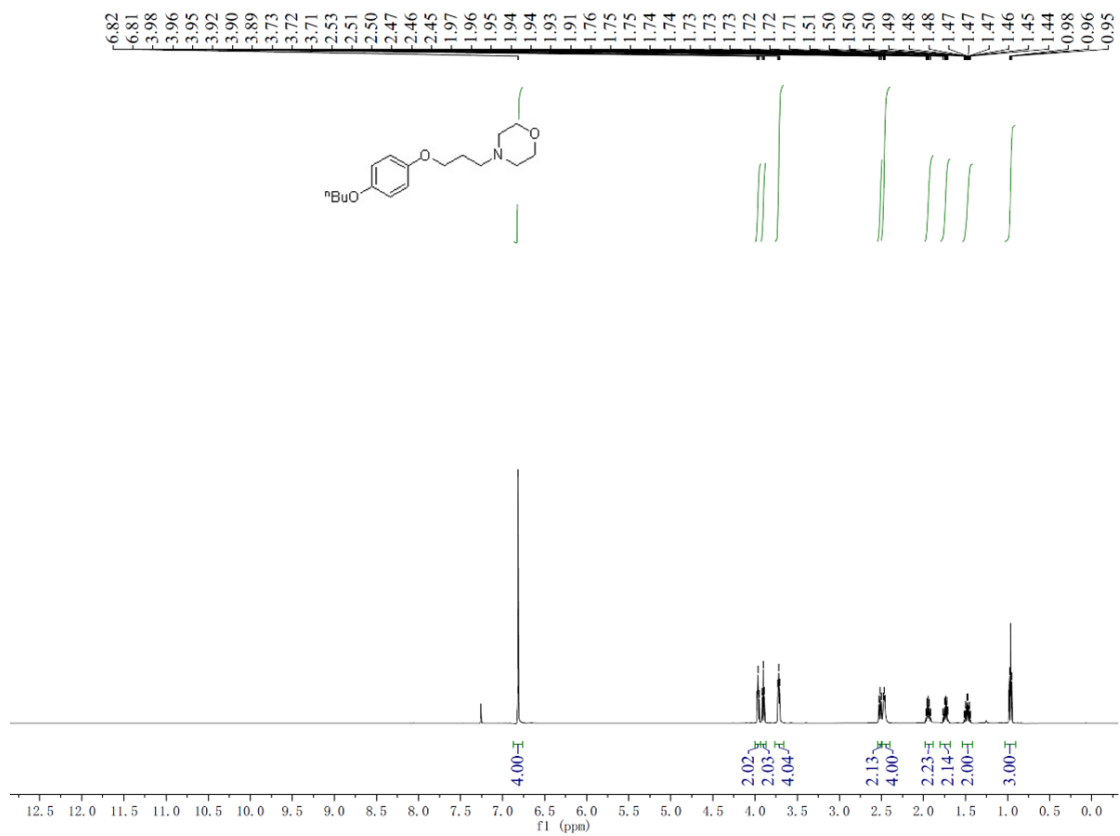
zy-0821-189-2-3rd-H1.1.fid
1H normal range AC300



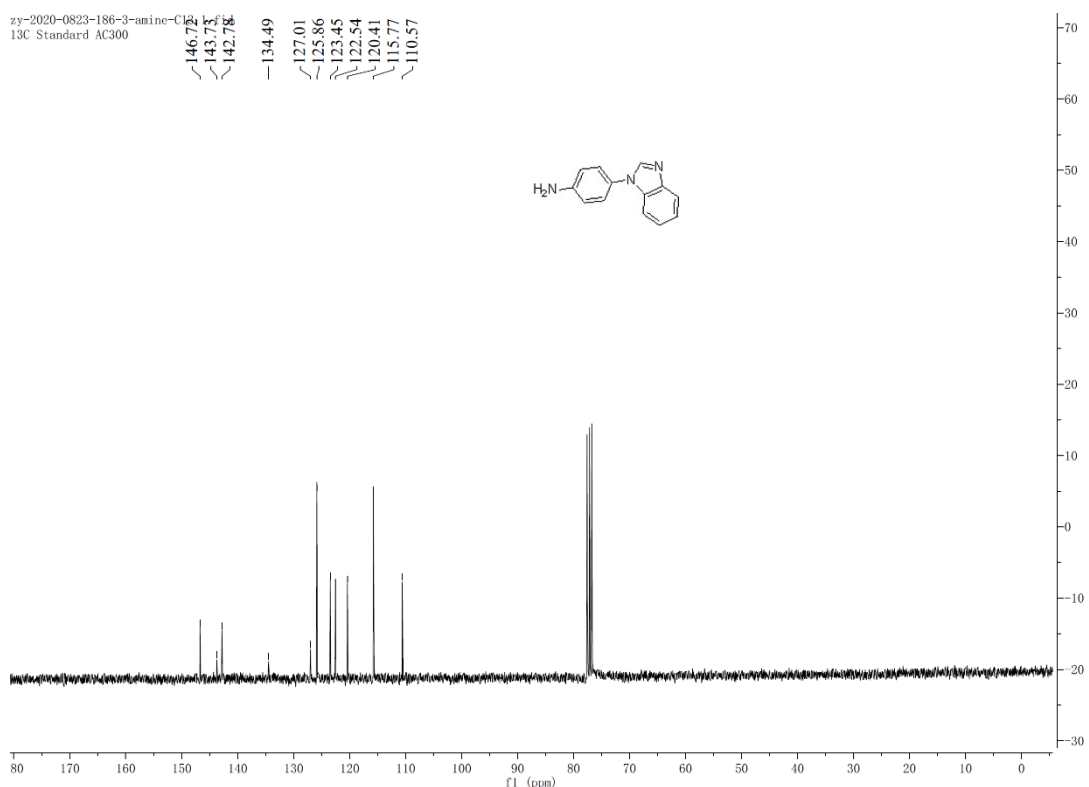
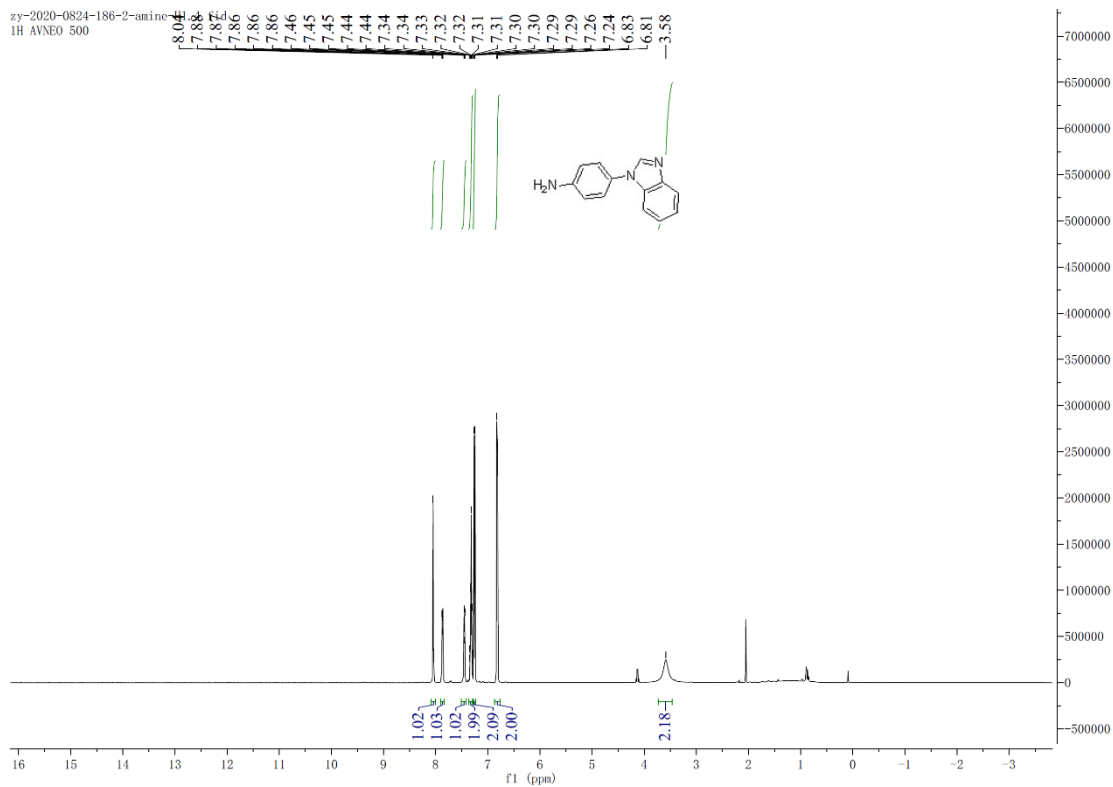
zy-2020-0821-189-3-C13.8.fid
13C AVNE0500



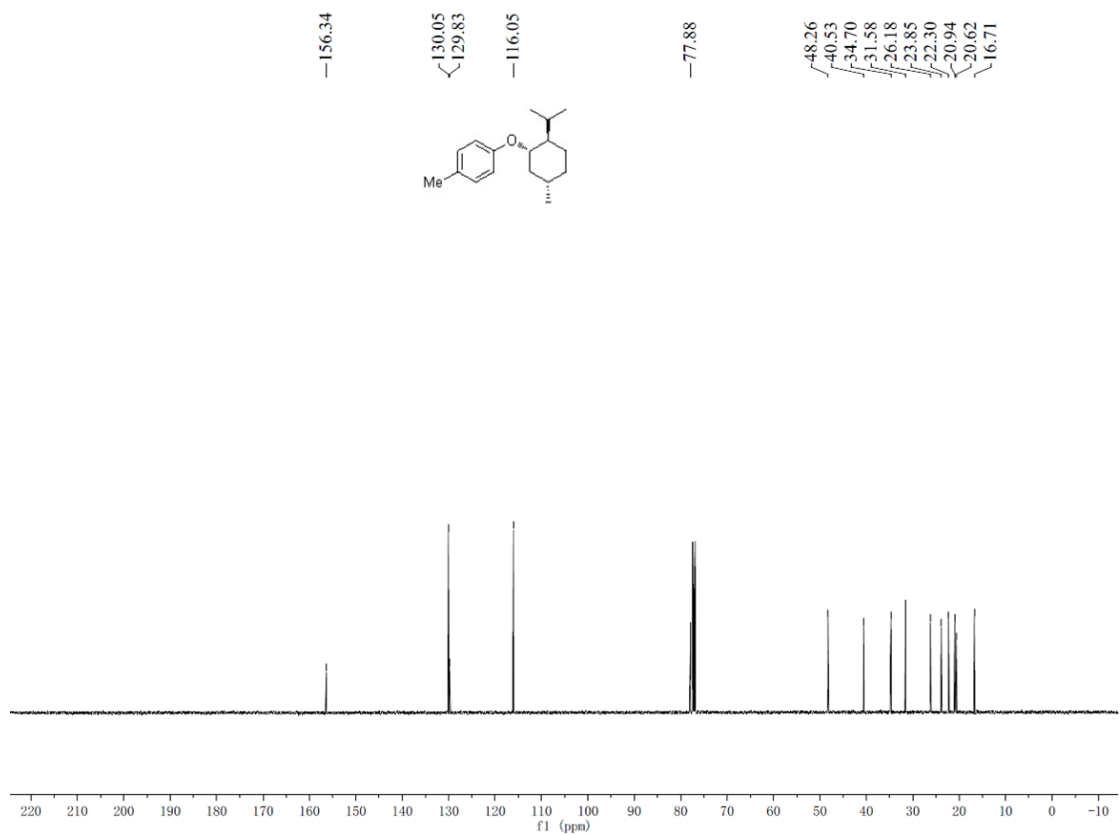
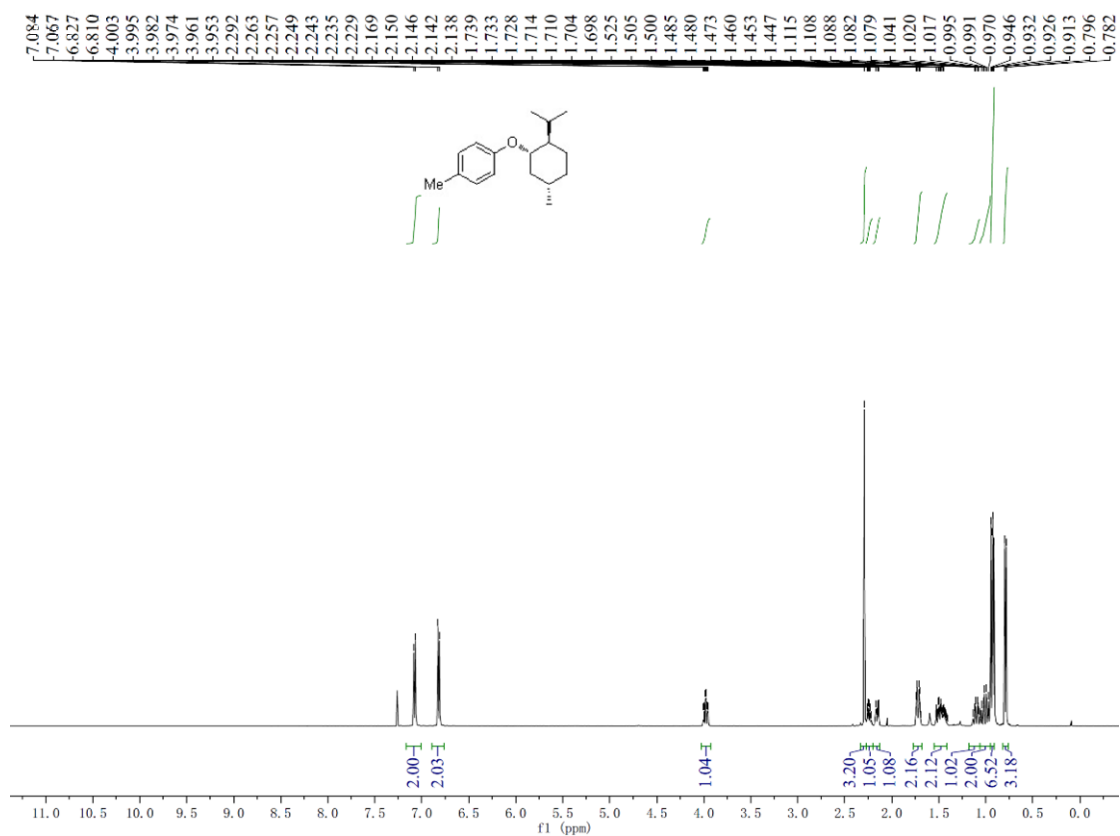
^1H and ^{13}C -NMR spectra of product 91.



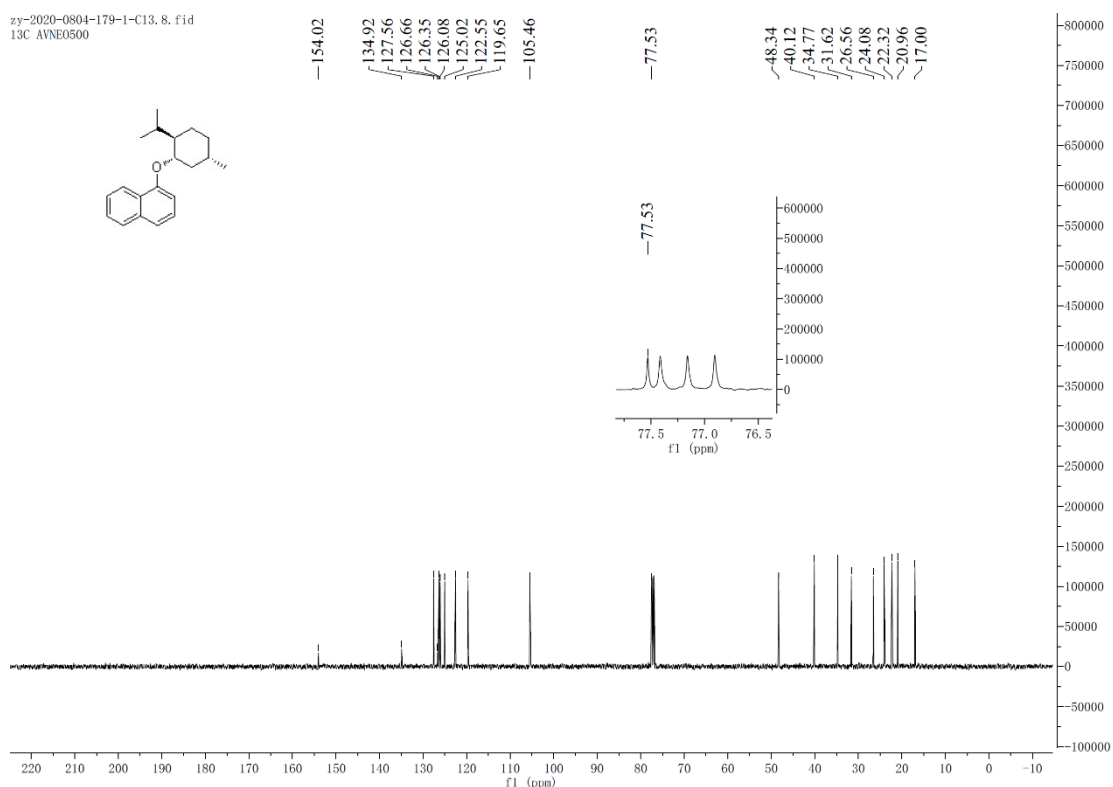
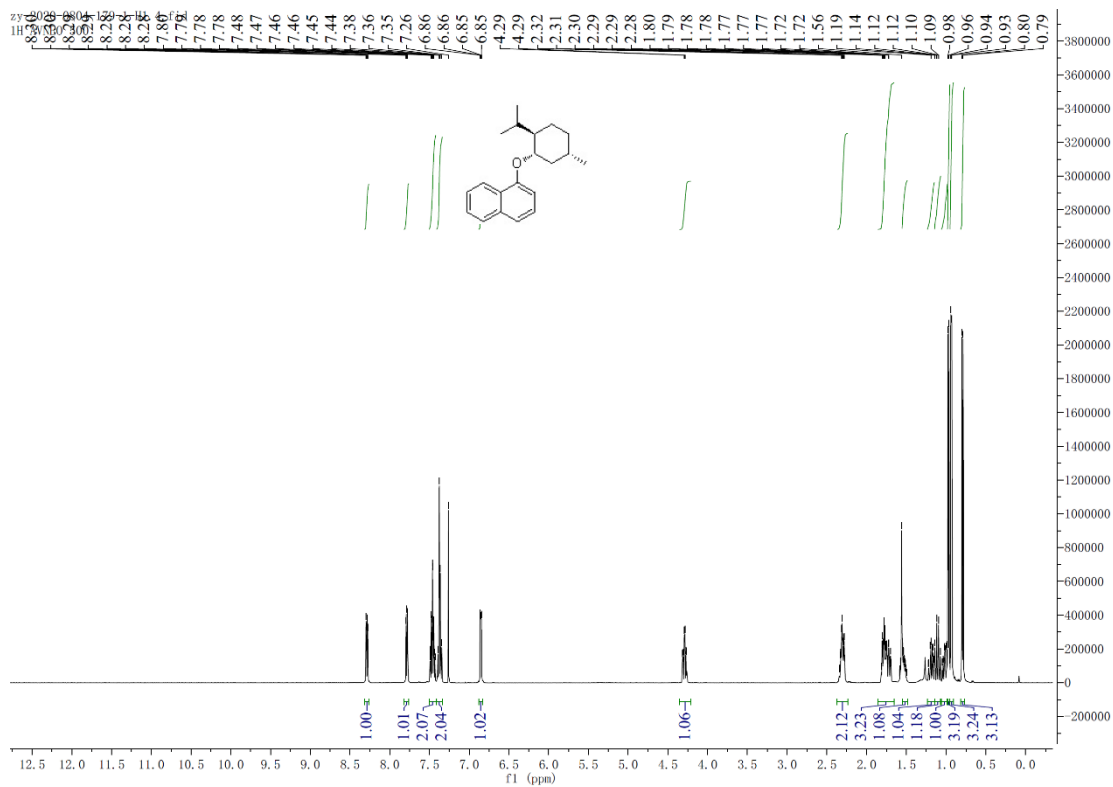
¹H and ¹³C-NMR spectra of product 92.



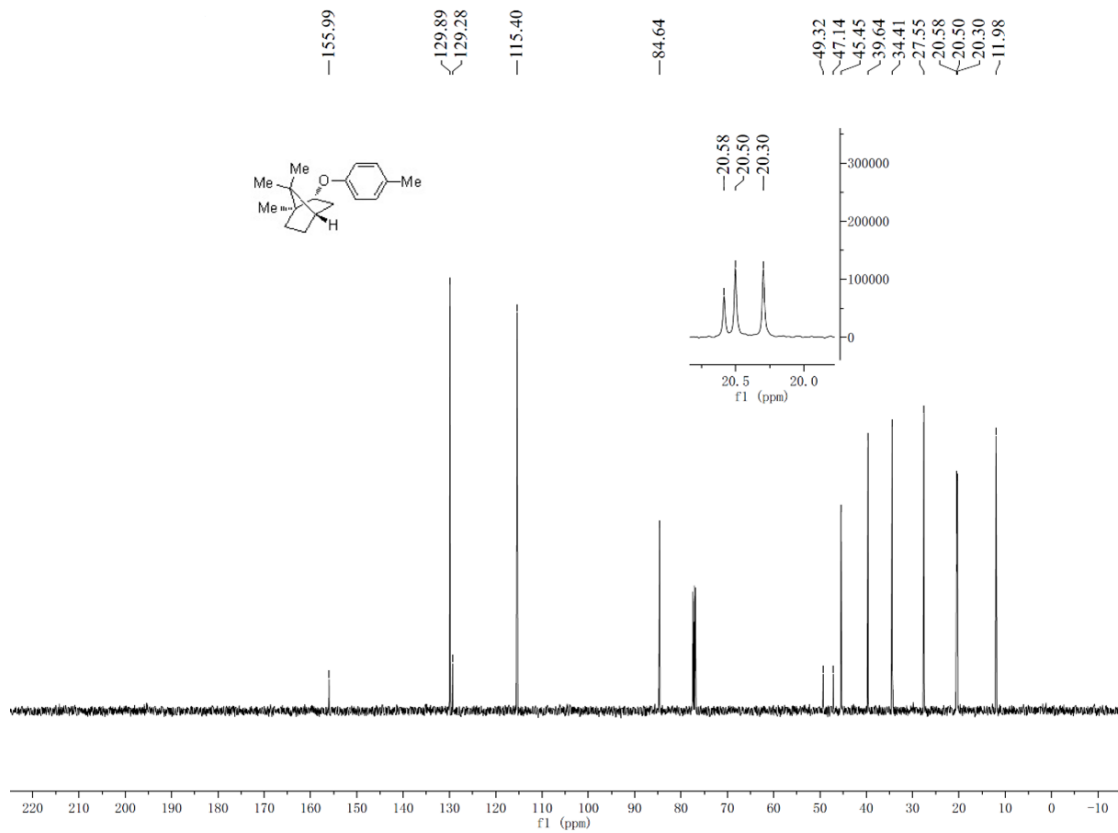
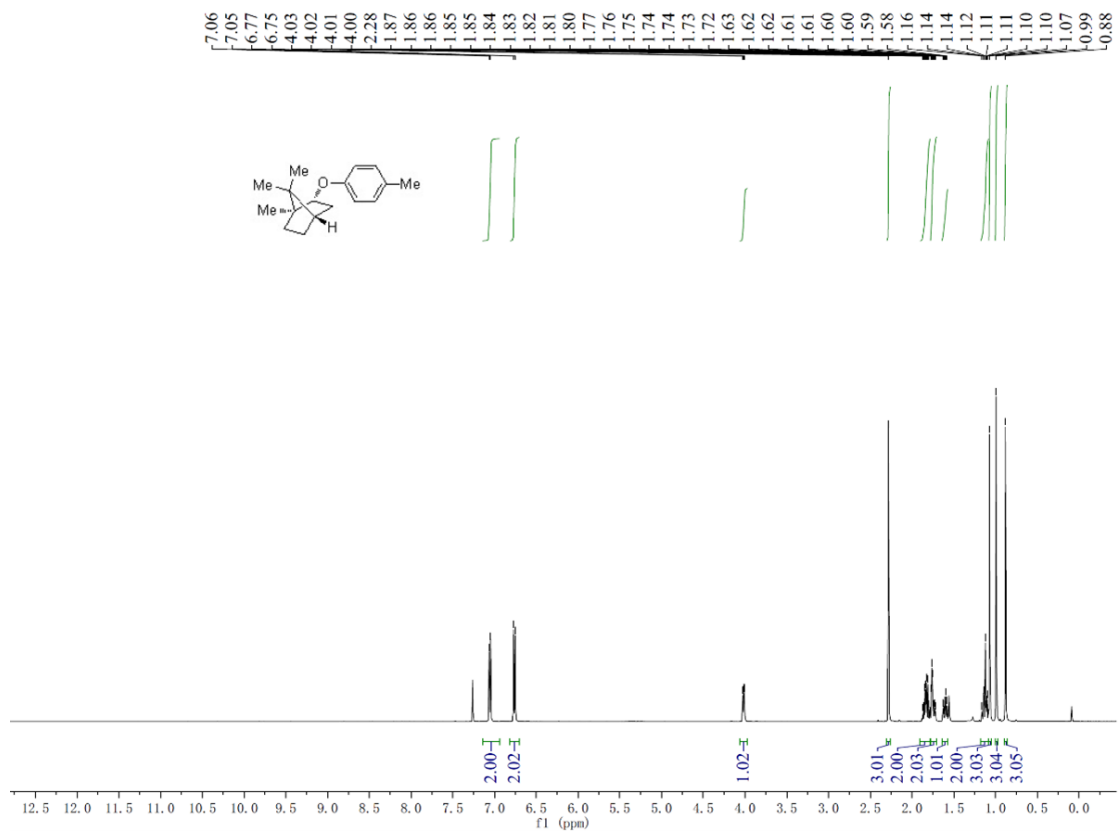
¹H and ¹³C-NMR spectra of product 93.



¹H and ¹³C-NMR spectra of product 94.

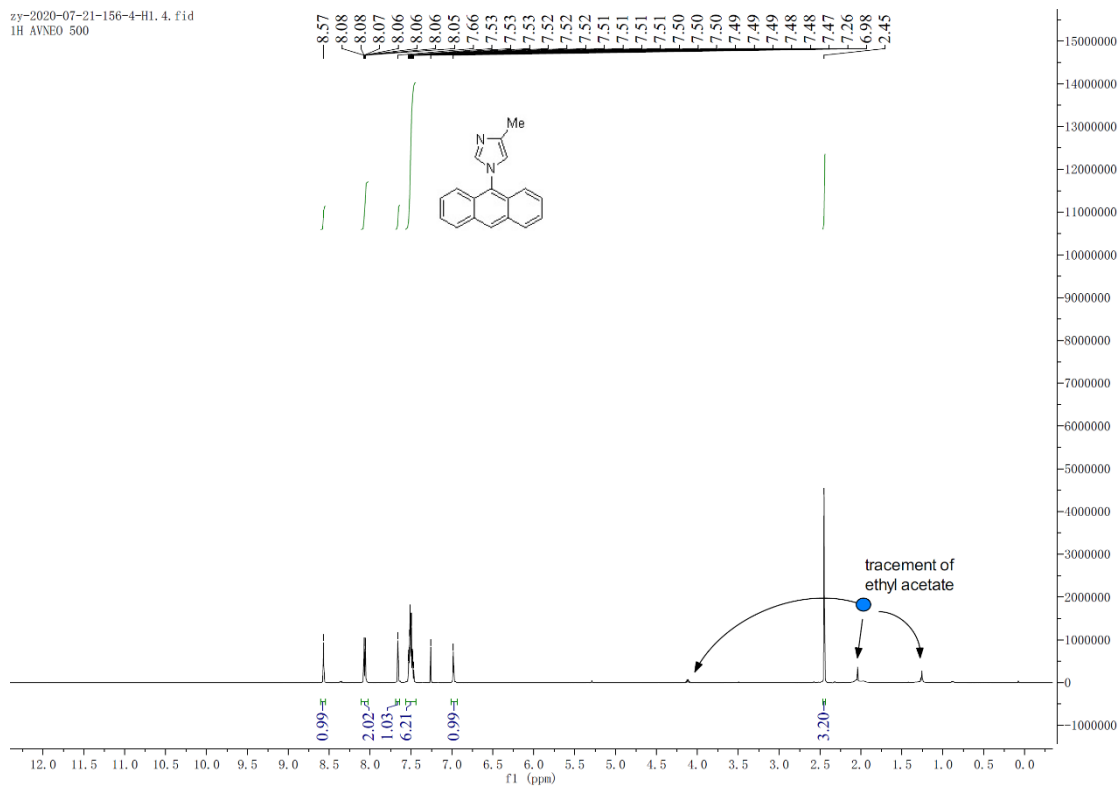


¹H and ¹³C-NMR spectra of product 95.

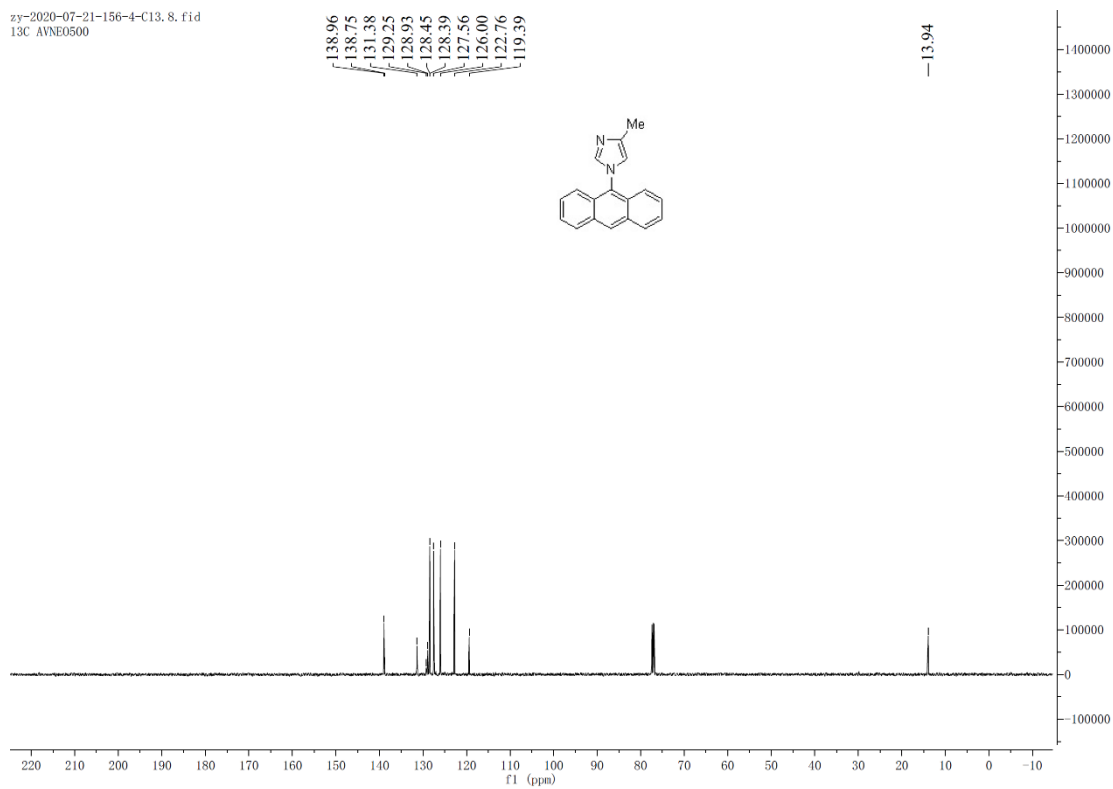


¹H and ¹³C-NMR spectra of product 96.

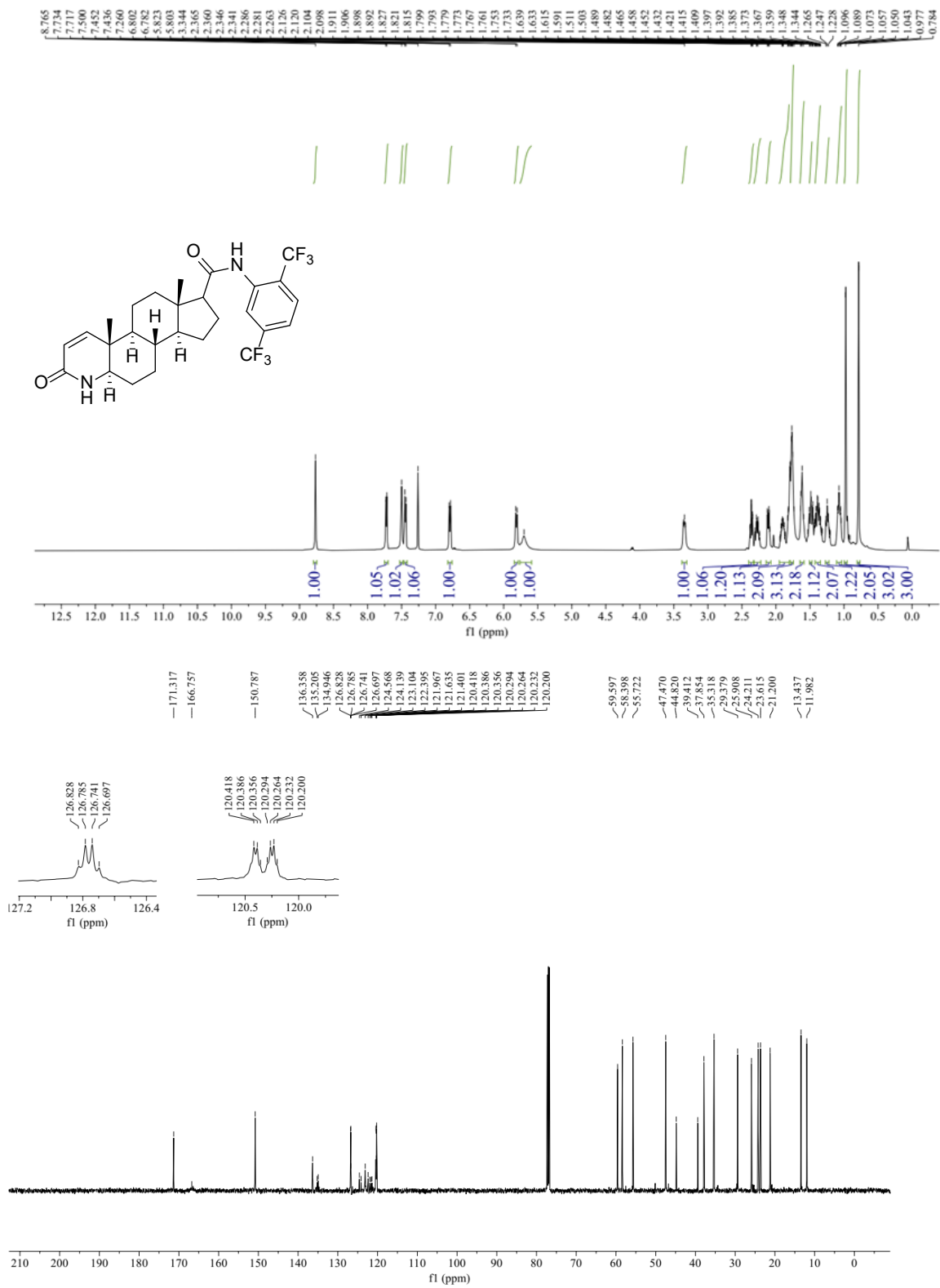
zy-2020-07-21-156-4-H1. 4. fid
1H AVNEO 500



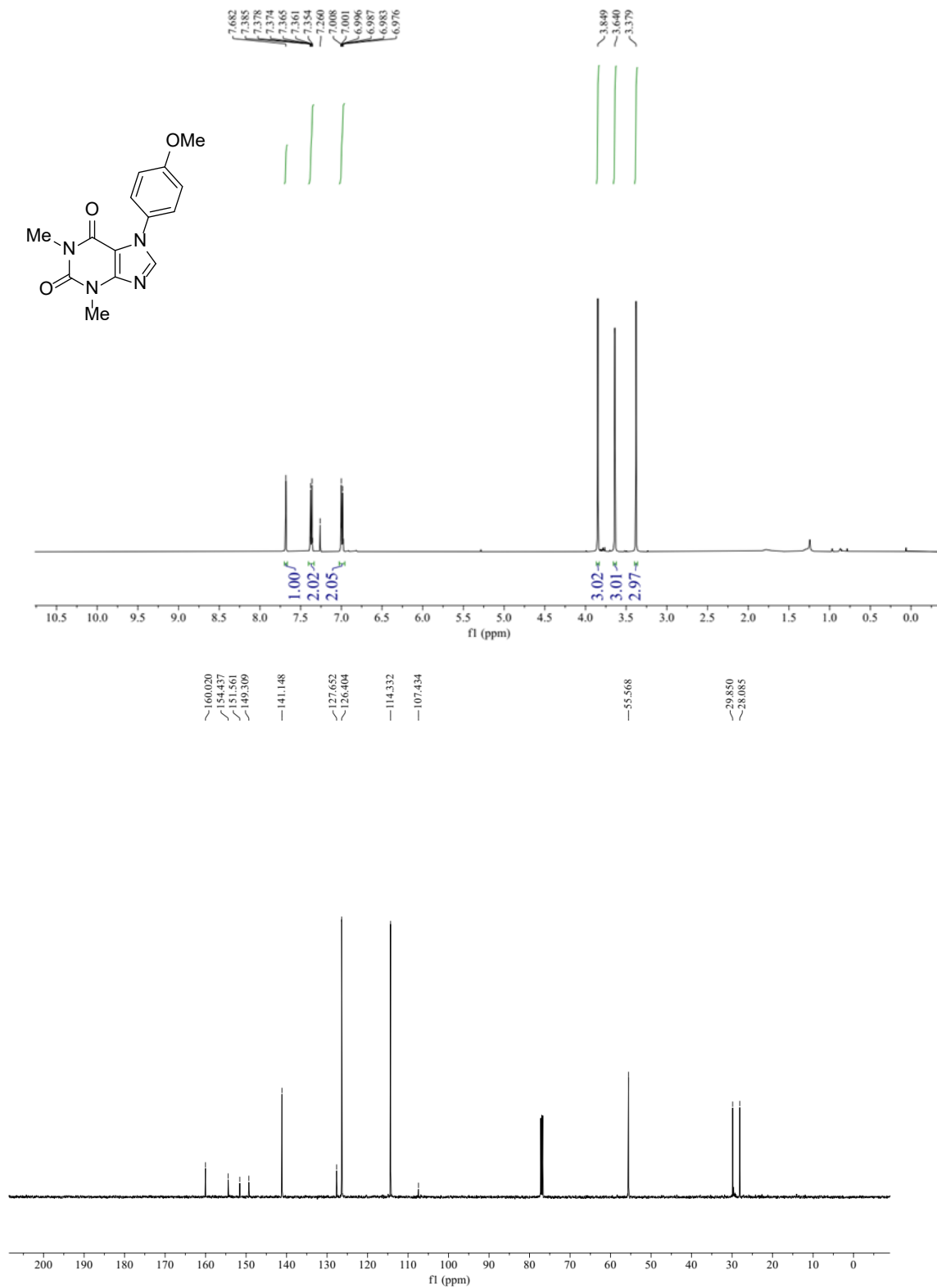
zy-2020-07-21-156-4-C13. 8. fid
13C AVNEO500



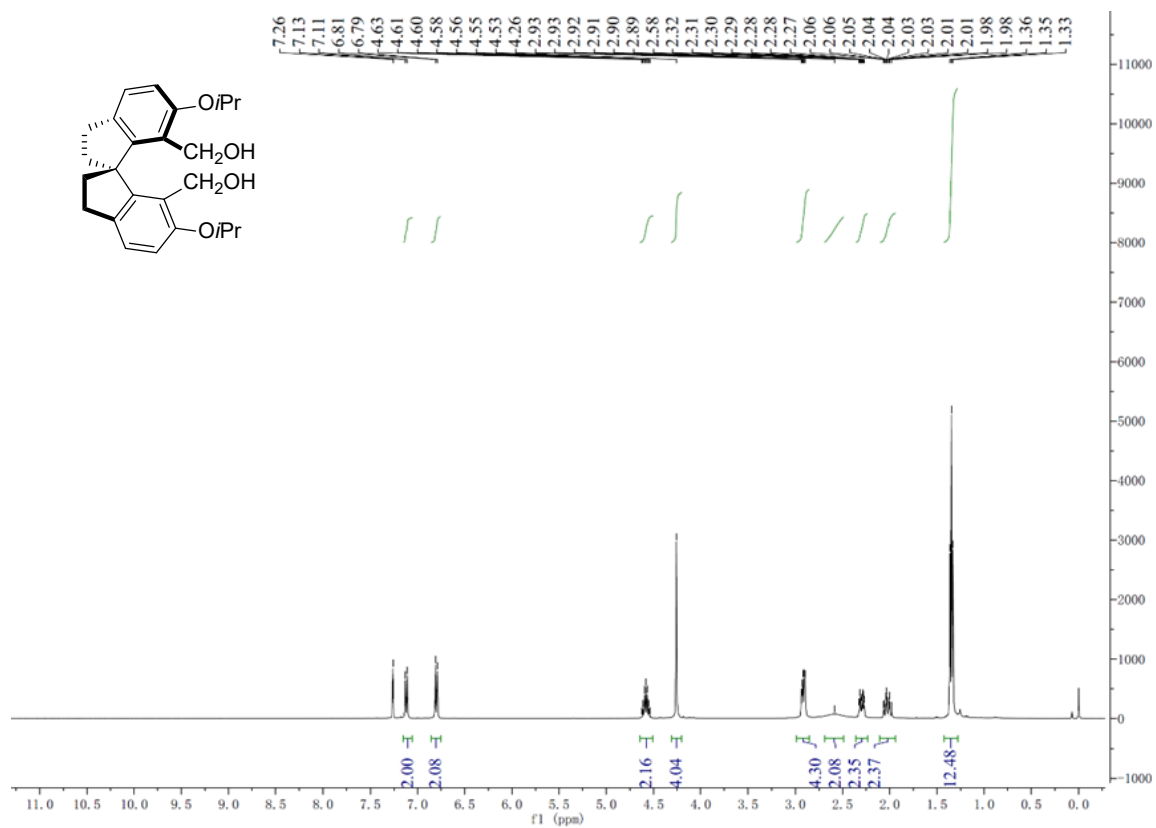
¹H and ¹³C-NMR spectra of product 97.



^1H and ^{13}C -NMR spectra of product 98.



¹H and ¹³C-NMR spectra of product 99.



¹H spectra of product 100.